Effects of age and *Pax6* deficiency on mouse limbal stem cell function

by

Panagiotis Douvaras BSc, MRes

Doctor of Philosophy

The University of Edinburgh, 2010

Author's Declaration

I hereby declare that I am the sole author of this thesis. The experiments described in this thesis are my own work, except where clearly stated otherwise. No part of this work has been submitted in support of another degree or qualification at the University of Edinburgh or any other educational institute.

Panagiotis Douvaras

February 2010

Abstract

The conventional view for corneal epithelial maintenance suggests that a stem cell population found in the limbus (at the rim of the cornea) produces daughter cells, called transient amplifying cells, which migrate centripetally. This limbal stem cell (LSC) hypothesis was recently questioned and the alternative model suggests that stem cells are present throughout the corneal epithelium. The main aims of this thesis were to investigate whether age and *Pax6* genotype affect LSC function. Previous work with X-inactivation mosaics revealed radial stripes of β-galactosidase-expressing cells in the corneal epithelium (from about 5 weeks of age), which decreased with age and were reduced in $Pax6^{+/-}$ mice (a model for aniridia, a human eye disease). The reduction in $Pax6^{+/-}$ mice could be due to either reduced LSCs function or a more coarse-grained mosaicism caused by reduced cell mixing during development. Comparison of patch sizes in $Pax6^{+/-}$ and wild-type X-inactivation mosaics showed that patches were smaller in $Pax6^{+/-}$ cornea epithelia before the initiation of stripes (3 weeks of age). This implies that stripe-number reduction is not caused by reduced cell mixing, so an effect on LSC function remained a possibility. Thus, the numbers of label-retaining cells (putative stem cells) in $Pax6^{+/-}$ were compared to controls at 15 and 30 weeks old but they were not reduced at 30 weeks or in $Pax6^{+/-}$ mice, as had been predicted. The failure to demonstrate the predicted result suggests either that the hypothesis was incorrect or the experimental approach was inappropriate. Furthermore, it was discovered that mice expressing β-galactosidase under the keratin 5 promoter produced rare stripes in the corneal epithelium, which are likely to represent clonal lineages derived from individual stem cells. Older mice demonstrated a significantly lower frequency of stripes, a result compatible with the predicted reduction of active LSC with age. $Pax6^{+/-}$ corneas were highly abnormal and stripes were not formed properly, so direct comparison was not possible. Finally, pilot experiments with conditional expression of a reporter gene revealed the successful formation of a stripe, and hence provide a plausible alternative approach to compare stripe numbers reflecting active LSCs but the method has yet to be optimised. Overall, the results suggest that LSCs are

reduced with age and support the limbal location of stem cells maintaining the corneal epithelium.

Acknowledgements

First of all, I would like to express my appreciation to my supervisors Dr. John West and Dr. Bob Hill for significant guidance on this complex project, support during the whole period I was working under their supervision, for the very interesting and fruitful discussions we had as well as for the critical revision of this thesis. Then, I would like to thank Dr. Julia Dorin and Sheila Webb for providing me with the K5-*LacZ* mice as well as Dr. Peter Hohenstein for providing me with the cell-permeable Cre recombinase plasmid and Mari Wallace for isolating and measuring the concentration of the cell-permeable Cre. Furthermore, I would like to thank Dr. Christine Mulford for helping me with the *in situ* hybridization protocol and Trudi Gillespie for my training on the confocal microscopes. A big thank you should also be addressed to all past and present members of John West's laboratory and especially Dr. Richard Mort and Dr. Thaya Ramaesh for my training on the techniques and for the excellent collaboration. Moreover, I would like to thank the personnel of the animal facilities in Little France, Western General Hospital and the Hugh Robson Building for taking so good care of my mouse colonies and for all the help they provided as well as the histology facility personnel of the HRB for the excellent collaboration and precious help with the wax embedding and processing. Lots of thanks to everyone in the HRB and especially the D-BUG for the friendly and team oriented environment they created for me. Last but not least, I would like to thank the University of Edinburgh for giving me the opportunity to study for this degree as well as the Fight for Sight organisation for the scholarship they awarded me.

Table of Contents

Author's Declaration ii
Abstract iii
Acknowledgements v
Table of Contents vi
List of Figures xi
List of Tables xiii
Abbreviations xiv
Chapter 1 General Introduction 1
1.1 THE CORNEA 1
1.1.1 Anatomy and development of the anterior ocular surface 1
1.1.2 Maintenance of the corneal epithelium 6
1.1.3 Location of corneal epithelial stem cells 8
1.2 IDENTIFICATION OF STEM CELLS 12
1.2.1 Stem Cells and nomenclature 12
1.2.2 Limbal stem cell markers 13
1.2.3 Identification of stem cell lineages 16
1.2.4 Indirect identification of LSCs 20
1.3 THE *PAX6* TRANSCRIPTION FACTOR 26
1.3.1 Regulation of eye development 26
1.3.2 *Pax6* insufficiency and aniridia 27
1.4 WORK THAT LED TO THIS PROJECT 30
1.5 Aims 32
Chapter 2 Materials & Methods 33
2.1 Animals & related work 33
2.2 BrdU administration 35
2.2.1 Intra-peritoneal (I.p.) injections 35
2.2.2 Mini-pumps 36
2.3 Tissue dissection 36
2.4 DNA extraction 36
2.5 Genotyping 37
2.6 β-galactosidase staining 39
2.7 Alkaline phosphatase staining 39

2.8 Embedding eyes in wax blocks & sectioning 40
2.9 Frozen sections 41
2.10 Neutral red & eosin counterstaining 41
2.11 Whole-mount immunofluorescence 42
2.12 Confocal imaging & photo editing 44
2.12.1 General confocal imaging 44
2.12.2 Confocal imaging for BrdU immunohistochemistry & sampling 44
2.13 H&E staining for histology 47
2.14 Keratin 5 in situ hybridization 47
2.15 Cell-permeable Cre production and purification 50
2.16 Cre activity assay 51
2.17 Measurement of cell-permeable Cre concentration 51
2.18 Cre in eye-drops 51
2.19 Tamoxifen injections 52
2.20 Statistical analysis 52
Chapter 3 Analysis of Patches in the Corneal Epithelium of X-Inactivation Mosaics 54
3.1 INTRODUCTION 54
3.1.1 Aims 57
3.2 MATERIALS & METHODS 58
3.2.1 Animals 58
3.2.2 Processing of eyes 58
3.2.3 Data collection & statistics 59
3.3 RESULTS 61
3.3.1 Comparison of patch sizes at 3 weeks of age 64
3.3.2 Growth and patch number with age 66
3.3.3 Comparison of patch lengths among different ages 69
3.3.4 Emergence of stripes in wild-type corneas 72
3.4 DISCUSSION 74
3.4.1 Evaluation of the method used 74
3.4.2 Initial mosaic pattern of randomly oriented patches 75
3.4.3 Establishment of the radial striped pattern 76
3.4.4 Direction of stripes and stem cell location 77
3.4.5 Conclusions 78

Chapter 4 Analysis of Label-retaining Cells in the Limbus of *Pax6*$^{+/-}$, *Mp*/+ and Wild-type Corneas 79
4.1 INTRODUCTION 79
4.1.1 Aims 83
4.2 MATERIALS & METHODS 84
4.2.1 Animals 84
4.2.2 Animal work 84
4.2.3 Tissue processing and staining 84
4.2.4 Confocal imaging 85
4.2.5 Data analysis of LRCs 85
4.3 RESULTS 87
4.3.1 Identification of limbus and *Pax6*$^{+/-}$ corneal abnormalities 87
4.3.2 Optimisation of BrdU labelling and chase periods 91
4.3.3 LRCs in the limbal area 95
4.3.4 LRC index 99
4.3.5 Cell density of the corneal epithelium 101
4.3.6 Location of stem cells in relation to the eye 104
4.3.7 LRCs within the cornea 107
4.3.8 LRCs in *Pax6*$^{+/-}$ heterozygotes 108
4.4 DISCUSSION 110
4.4.1 Quantitative analysis of LRCs in the limbus 110
4.4.2 Other possible shortcomings of the BrdU LRC approach 112
4.4.3 LRCs in the corneas of *Pax6*$^{+/-}$ mice 114
4.4.4 LRCs in the corneas of *Mp*/+ mice 115
4.4.5 Conclusions 116
Chapter 5 Induced Mosaicism in Reporter Mice 117
5.1 INTRODUCTION 117
5.1.1 Lineage tracing experiments 117
5.1.2 Low frequency induction of a marker 117
5.1.3 The Cre/*LoxP* system 118
5.1.4 Cre recombinase responsive to tamoxifen 120
5.1.5 Rendering Cre recombinase cell-permeable 121
5.1.6 Aims 123

5.2 MATERIALS & METHODS 124
5.2.1 Animals 124
5.2.2 Production and application of the cell-permeable Cre 125
5.2.3 Tamoxifen induced recombination in reporter mice 125
5.3 RESULTS 127
5.3.1 Cell-permeable Cre Recombinase 127
5.3.2 Tamoxifen induced reporter gene activation 133
5.4 DISCUSSION 145
5.4.1 Conclusions 149
Chapter 6 Lineage Tracing Using the *K5-LacZ* Reporter Mouse 150
6.1 INTRODUCTION 150
6.1.1 Keratin 5 150
6.1.2 Keratin 5 expression in the eye 150
6.1.3 *Pax6*$^{+/-}$ corneas 151
6.1.4 β-gal expression in the corneas of *Krt5-LacZ* mice 152
6.1.5 Aims 152
6.2 MATERIALS & METHODS 153
6.2.1 Animals 153
6.2.2 Keratin 5 in situ hybridization & immunofluorescence 153
6.2.3 β-gal staining 154
6.2.4 *Pax6* & β-gal genotyping 154
6.3 RESULTS 155
6.3.1 Keratin 5 expression in the ocular surface 155
6.3.2 β-gal staining in the ocular surface of *Krt5-LacZ/-* mice 158
6.3.3 Analysis of β-gal positive patches and stripes in the *Krt5-LacZ/-* corneal epithelium 160
6.3.4 Age-related reduction of β-gal positive stripes in *Krt5-LacZ/-* corneal epithelia 163
6.3.5 Effect of *Pax6* genotype on β-gal positive stripes in *Krt5-LacZ/-* corneal epithelia 165
6.4 DISCUSSION 168
6.4.1 Expression of *Krt5* in the ocular surface 168
6.4.2 Distribution of rare β-gal positive clones in the *Krt5-LacZ/-* corneal epithelium 168

6.4.3 β-gal positive patches in relation to age and *Pax6* genotype 169
6.4.4 Location of stem cells maintaining the corneal epithelium..... 171
6.4.5 Conclusions..... 171
Chapter 7 General Discussion..... 172
7.1 EFFECTS OF AGE AND GENOTYPE ON THE MOUSE CORNEAL EPITHELIUM AND LSC FUNCTION 172
7.1.1 Effects of Pax6 genotype on cell mixing during corneal epithelial development172
7.1.2 Identification of the limbus in the adult ocular surface..... 174
7.1.3 BrdU Label-retaining cells..... 175
7.1.4 Lineage analysis..... 178
7.1.5 The effects of age on stem cell function 182
7.1.6 The effects of *Pax6* genotype on stem cell function 185
7.2 EVALUATION OF TWO HYPOTHESES OF CORNEAL EPITHELIAL MAINTENANCE 186
7.3 FUTURE DIRECTIONS 190
Bibliography 193

List of Figures

Figure 1.1 Schematic representations of the eye and several eye structures..... 3

Figure 1.2 Schematic representation of the development of the murine eye. 4

Figure 1.3 Proposed model for the maintenance of the adult corneal epithelium..... 7

Figure 1.4 A schematic representation of the LaacZ reporter..... 17

Figure 1.5 The Cre/LoxP system for gene regulation. 19

Figure 1.6 The tetracycline-controlled switch. 25

Figure 1.7 Postnatal development of the pattern of stripes in the corneal epithelium of female X-inactivation mosaic mice. 31

Figure 2.1 Scoring area on a flattened cornea..... 46

Figure 2.2 The murine keratin 5 gene (Nucleotide BC108361)..... 49

Figure 2.3 Cell-permeable Cre transgene. 50

Figure 3.1 Diagram showing the formation of stripes on the corneal epithelium..... 56

Figure 3.2 Wax sections of adult eyes from (A & B) a wild-type and (C & D) an *Mp/+* mouse 62

Figure 3.3 β-gal positive and negative patches in the basal layer of the corneal epithelium. 63

Figure 3.4 Comparisons of patch lengths in the basal corneal epithelium of *Pax6*$^{+/-}$ or *Mp/+* mice with their respective wild-type littermates at 3 weeks of age. 65

Figure 3.5 Mean number of cells and mean number of patches in the corneal epithelium of *Pax6*$^{+/-}$ and *Mp/+* compared with their wild-type littermates at different ages. 68

Figure 3.6 Comparison of corrected mean patch length and uncorrected median patch length between *Pax6*$^{+/-}$ or *Mp/+* with their respective wild-type littermates at different ages. 71

Figure 3.7 Comparison of the mean number of patches from the periphery and the centre of the corneal epithelium of wild-type mice at different ages..... 73

Figure 4.1 Immunohistochemical detection of keratin 19 (K19) and identification of the limbus..... 88

Figure 4.2 CD31 and Keratin 19 double immunofluorescence staining in the ocular surface of wild-type (A & B) and *Pax6*$^{+/-}$ (C & D) mice. 90

Figure 4.3 Whole-mount corneas of 12-week old mice that received a single i.p. injection of BrdU and chased for different periods..... 93

Figure 4.4 Preliminary LRC experiment..... 94

Figure 4.5 LRCs in the eye of mice from the *Pax6*$^{+/-}$ (A – D) and the *Mp/+* (E – H) cross implanted with a BrdU-loaded mini-pump and chased for 10 weeks..... 96

Figure 4.6 Comparisons of LRCs per sector and per circumference in *Pax6*$^{+/-}$ (A & B) or *Mp/+* (C & D) and their respective wild-type littermates..... 98

Figure 4.7 Comparison of LRC indices per sector and per circumference in *Pax6*$^{+/-}$ (A & B) or *Mp/+* (C & D) and their respective wild-type littermates. 100

Figure 4.8 Comparisons of cell densities. 103

Figure 4.9 Distribution of LRCs in the different sectors of wild-type corneas..... 106

Figure 4.10 LRCs found in the peripheral cornea in *Pax6*$^{+/-}$ and their wild-type littermates. 107

Figure 4.11 Double immunofluorescent detection of BrdU and blood vessels in wild-type (A) and *Pax6*$^{+/-}$ (B – D) mice. 109

Figure 5.1 Gel electrophoresis of a *LoxP*-containing plasmid after Cre recombination. 128

Figure 5.2 Immunofluorescent staining to detect YFP in the ocular surface of an R26R-*YFP* mouse. 130

Figure 5.3 β-gal staining in frozen sections of livers. 130

Figure 5.4 X-gal staining of various whole-mount tissues from CAGG-Cre/ER^{TM}-*LacZ* mice. 134

Figure 5.5 Tamoxifen induced recombination in the pilot experiment. 136

Figure 5.6 Controls for AP staining in the eyes of a Z/AP mouse that never received Cre recombinase or tamoxifen. 137

Figure 5.7 Comparison of eyes from CAGG-Cre/ER^{TM}-Z/AP mice showing the effects of the mouse age when it received the tamoxifen. 140

Figure 5.8 Comparison of positive cells in the corneal epithelium of CAGG-Cre/ER^{TM}-Z/AP between different chase periods. 141

Figure 5.9 Comparison of tamoxifen dosage effects on cells in the corneal epithelium of CAGG-Cre/ER^{TM}-Z/AP mice. 142

Figure 5.10 Recombination in the corneal epithelium of *Pax6*$^{+/-}$, CAGG-Cre/ER^{TM}-Z/AP eyes. 143

Figure 6.1 Immunohistochemical detection of keratin 5 in the ocular surface of wild type mice. 155

Figure 6.2 Keratin 5 mRNA in situ hybridization on an E12.5 mouse embryo. 157

Figure 6.3 Keratin 5 mRNA in situ hybridization on the ocular surface of wild-type (A - C) and *Pax6*$^{+/-}$ (D - F) albino eyes. 157

Figure 6.4 Corneal stripes and conjunctival patches in wild-type *Krt5-LacZ* mouse eyes. . 159

Figure 6.5 Distribution of β-galactosidase-positive stripes in the corneal epithelium of *Krt5-LacZ/-* mice. 162

Figure 6.6 Comparison of stripes in the cornea (A & B) and patches in the conjunctiva (C & D) between 15 and 30 weeks old mice. 164

Figure 6.7 Patches of β-gal positive cells in the skin of *Krt5-LacZ/-* mice 165

Figure 6.8 Patches of β-gal positive cells in the ocular surface of *Pax6*$^{+/-}$ *Krt5-LacZ/-* mice. 167

Figure 7.1 Decline in stem cell functionality with age. 184

Figure 7.2 The alternative hypothesis for the maintenance of the ocular surface. 187

List of Tables

Table 2.1 Sequences of primer pairs and their annealing temperature. 38

Table 2.2 Specifications of antibodies. 43

Table 5.1 Summary of results from mice treated with cell-permeable Cre in the form of eye drops..... 132

Table 5.2 Summary of results for mice injected (i.p.) with tamoxifen. 144

Abbreviations

β-gal: β-galactosidase

AP: Alkaline phosphatase

ARK: Aniridia-related keratopathy

BrdU: 5-bromo-2′-deoxyuridine

BSA: Bovine serum albumin

CFP: Cyan fluorescent protein

CHAPS: 3-[(3-Cholamidopropyl) dimethylammonio]-1-propanesulfonate

CldU: 5-chloro-2′-deoxyuridine

DABCO: 1,4-diazobicyclooctane

DMSO: Dimethyl sulfoxide

EcR: Ecdysone receptor

EDTA: (Ethylenedinitrilo)tetraacetic acid

EdU: 5-ethynyl-2′-deoxyuridine

EGTA: Ethylene glycol-bis(2-aminoethylether)-N,N,N′,N′-tetraacetic acid

ER: Oestrogen receptor

ER^{TM}: Mutant form of oestrogen receptor activated only by tamoxifen

FACS: Fluorescence activated cell sorting

FGF: Fibroblast growth factor

GFP: Green fluorescent protein

GST: Glutathione S transferase

H&E: Haematoxylin and eosin

H_2O: Distilled water

His_6: 6 Histidines

HIV: Human immunodeficiency virus

HMG CoA: 3-hydroxy-3-methylglutaryl coenzyme A

I.p.: Intra-peritoneal

IdU: 5-iodo-2′-deoxyuridine

IPTG: Isopropyl-β-D-thiogalactopyranoside

K5: (Cyto-) keratin 5 protein

K19: (Cyto-) keratin 19 protein

Krt5: (Cyto-) keratin 5 gene or RNA

Krt19: (Cyto-) keratin 19 gene or RNA

LRC: Label-retaining cell

LSC: Limbal stem cell

MBP: Maltose binding protein

Mp: Micropinna microphthalmia gene

MTS: Membrane translocation sequence

NLS: Nuclear localization signal

PBS: Phosphate buffered saline

PBS-T: Phosphate buffered saline – Tween20

PBTX: Phosphate buffered saline – Triton X

PCR: Polymerase chain reaction

PFA: Paraformaldehyde

PI: Propidium iodide

PTD: Protein transduction domain

rtTA: Reverse tetracycline-controlled transcriptional activator

SDS: Sodium dodecyl sulfate

TAC: Transient (or transit) amplifying cell

TetO: Tetracycline operator

TM: Tamoxifen

tTA: Tetracycline-controlled transactivator

X-gal: 5-bromo-4-chloro-3-indolyl-b-D-galactopyranoside

XLacZ^{+}/Y: Genotype for H253 males

XLacZ$^{+/-}$: Genotype for hemizygous H253 females

YFP: Yellow fluorescent protein

Chapter 1
General Introduction

1.1 THE CORNEA

1.1.1 Anatomy and development of the anterior ocular surface

The cornea comprises the avascular, transparent part of the anterior surface of the eye (Fig. 1.1 A & B). The main role of this structure is to aid visual function, which is accomplished by being transparent, transmitting light and providing a refraction surface. Additionally, it protects the ocular surface from the hostile environment and represents an effective barrier to fluid transport (Boulton and Albon, 2004).

During development, the optic vesicle forms from an extension of the forebrain. Contact of the optic vesicle with the overlying surface ectoderm results in invagination of both tissues, which will create the optic cup. The inner layer of the cup will give rise to the retina whereas the outer layer will form the retinal pigment epithelium. The surface ectoderm thickens to form the lens placode, which subsequently invaginates into the optic cup and forms the lens vesicle (Fig. 1.2 A – E). After detachment of the lens vesicle from the surface ectoderm, mesenchymal cells from the neural crest, migrate into the space between the lens and the surface ectoderm (Le Douarin and Kalcheim, 1999). These mesenchymal cells will give rise to the corneal endothelium and the corneal stroma of the eye. However, there are species differences concerning the way these two tissues develop. In the avian embryo, the most well studied species for corneal development, mesenchymal cells migrate to the primary stroma, an extracellular matrix consisting of collagen fibres that already occupies the space between the lens and the surface ectoderm (Bard et al., 1975). Then these mesenchymal cells form the endothelium and the newly formed endothelium now separates the lens from the primary corneal stroma. The primary stroma is then invaded by a second wave of mesenchymal cells which, this time, give rise to the corneal stroma (Fitch et al., 1998). In humans, most of the mesenchyme cells flatten and condense to form the future corneal endothelium

(Sevel and Isaacs, 1988), while some mesenchymal cells still remain at the region between the endothelium and the surface ectoderm. These proliferate and finally they differentiate to keratocytes, the specialised cell of the corneal stroma (Cvekl and Tamm, 2004). In the mouse, by embryonic day 12, there are 4 to 7 layers of mesenchyme cells between the lens and the surface ectoderm. The number of these cells increases continuously forming more layers (Fig. 1.2 G; Haustein, 1983). These cells start to differentiate into keratocytes of the corneal stroma. The most posterior mesenchymal cells flatten and connect to each other forming a monolayer that will become the endothelium.

In the meantime, the corneal epithelium is formed by the surface ectoderm lying above the mesenchymal cells (Fig. 1.2 H; Chung et al., 1992). Extensions of the edges at the optic cup along with mesenchymal cells will finally give rise to the iris and the ciliary body (Fig. 1.2 I; Cvekl and Tamm, 2004). By the end of this process, all the layers of the adult cornea are in place. Thus, the adult mouse cornea consists of 5 layers (Fig. 1.1 C); the stratified, squamous, non-keratinised corneal epithelium, the acellular Bowman's layer, the collagen rich corneal stroma, a basal lamina called Descemet's membrane and the single layered corneal endothelium (Hay, 1979).

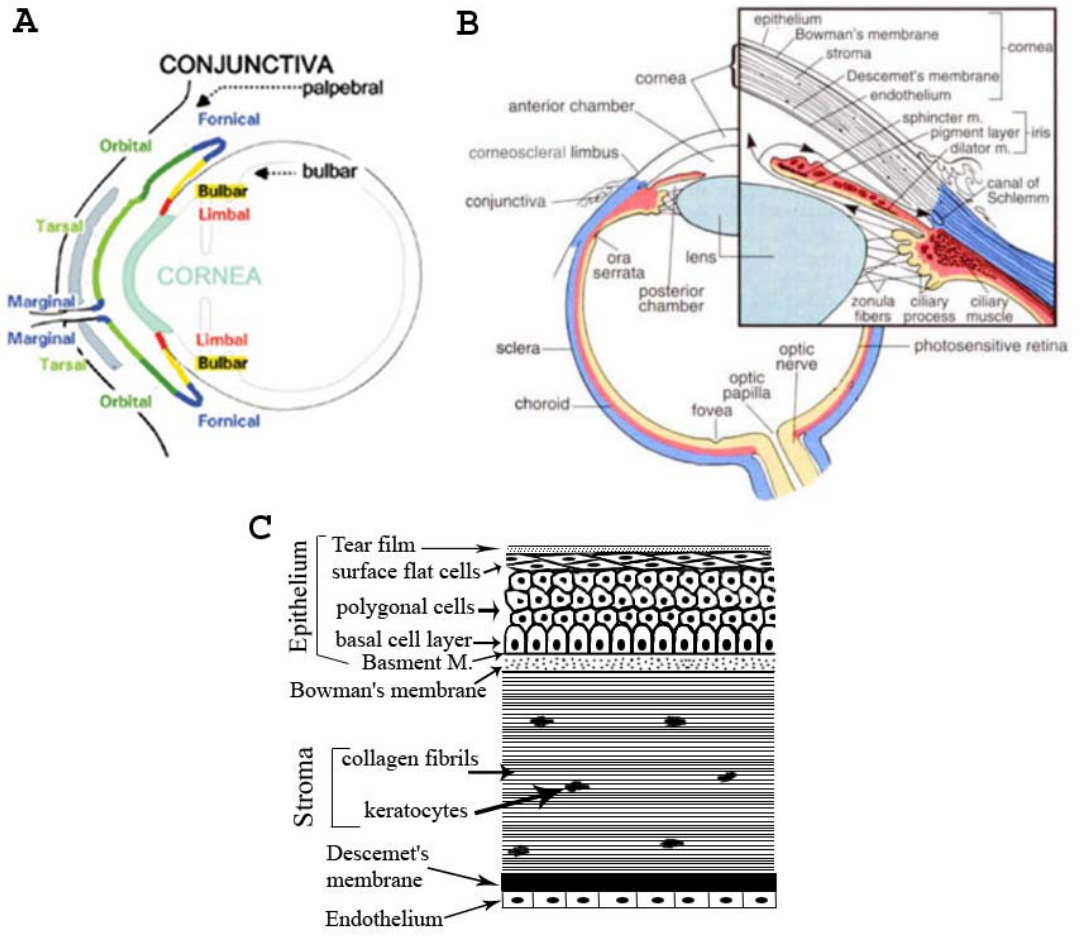

Figure 1.1 Schematic representations of the eye and several eye structures. (A) The cornea and the attached conjunctiva of the eye when eyelids are closed. (B) The different parts of the eye with a magnified image showing the anterior chamber in more detail. (C) The different layers of the cornea. Figures found on the internet at the following addresses: www.clspectrum.com/article.aspx?article=102543 ; mesentsev.fortunecity.com/columbia_2005.htm ; img242.imageshack.us/i/cornea.gif

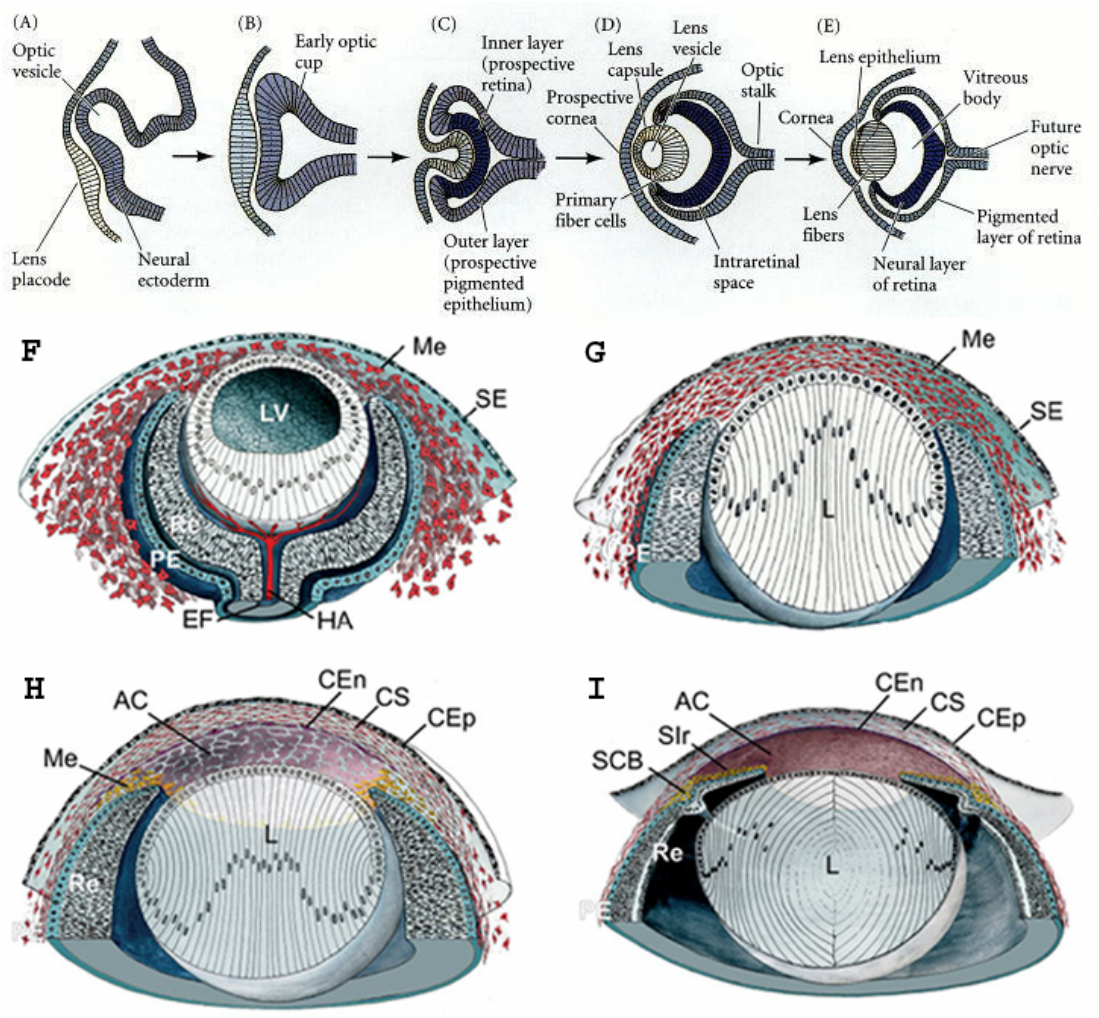

Figure 1.2 Schematic representation of the development of the murine eye. (A) At E9 the optic vesicle extends from the forebrain. (B) By E9.5 the optic vesicle forms the optic cup and the lens placode is enlarged. (C) At E10.5, the surface ectoderm invaginates. (D) At E11.5 the lens vesicle is formed. (E) At E13 the cornea develops in front of the lens. (F) At E12.5 – 13.5 the lens vesicle is developing within the optic cup and mesenchymal cells migrate between the lens and the surface ectoderm. (G) At E13.5 – 14.5 the mesenchymal cells form several flat layers. (H) At E14.5 – 15.5 mesenchyme cells begin to differentiate to keratocytes whereas the mesenchyme closest to the lens flattens and forms a monolayer that will become the corneal endothelium. The surface ectoderm covering the mesenchymal cells will become the corneal epithelium. (I) Beginning at E15.5, the optic cup enlarges, forming the iris and ciliary body. Mesenchyme cells migrate to the angle between the cornea and the anterior chamber where they differentiate into the stroma of the iris and the ciliary body. LV: lens vesicle; SE: surface epithelium; Me: mesenchymal cells; Re: retina; PE: retinal pigmented epithelium; EF: embryonic fissure; HA: hyaloid artery; L: lens; CEn: corneal endothelium; CS: corneal stroma; CEp: corneal epithelium; AC: anterior chamber; SIr: stroma of iris; SCB: ciliary body; Figure A – E from Cvekl and Piatigorsky, (1996) and F – I from Cvekl and Tamm, (2004).

In rodents, the development and maturation of the corneal epithelium continues postnatally. At birth, the eyelids are sealed and corneal epithelium consists of one or two layers of cells, until 10 days-of-age (Chung et al., 1992). Immediately after eyelid opening at two weeks of age, the corneal epithelium begins to stratify; a process, which is completed by 6 weeks-of-age in mice, when the cornea reaches its adult size and a thickness of 4-6 cell layers (Kuhlman and Resnik, 1958). The time of eyelid opening and stratification of the cornea is the period when most of the corneal epithelial cells are actively proliferating (Francesconi et al., 2000). Apart from the stratification of the epithelium, major changes in the morphology of basal cells in the corneal epithelium have been observed. Basal cells appear flattened and oval-shaped until eyelid opening when they become more rounded and at three weeks of age they finally become columnar (Chung et al., 1992).

The ocular surface is also covered by another epithelium, the conjunctival epithelium (Fig. 1.1 A) that can be divided into three regions; the palpebral, which is the part adjacent to the epidermis of the eyelid; the bulbar, which is contiguous to the cornea and the part in between these two regions, the forniceal (Nelson and Cameron, 1997). This is a two to three layer epithelium, which is in continuation with the corneal epithelium, but the two epithelia are quite different. In specific terms, the conjunctival epithelium is vascularised and is populated by goblet cells that secret mucin (Friend and Kenyon, 1987). Additionally, gene expression profiles of these two epithelia are quite distinct as well (Turner et al., 2007). The border between the corneal epithelium and the bulbar conjunctiva consists of a ring-shaped zone that is called the limbus. Limbal epithelium consists of several layers of epithelial cells and other cell types like Langerhans cells and melanocytes (in some species) but it does not harbour goblet cells.

1.1.2 Maintenance of the corneal epithelium

Tissues that lie on the outer surfaces of the body, like skin and hair, usually lose cells during normal wear and tear. The corneal epithelium also comes in to contact with the environment and cells are constantly shed from the surface of this tissue as well. The ability to replace tissue lost under normal circumstances or even after injury depends on the existence of a stem cell population that regenerates in order to maintain normal homeostasis. The thickness of the corneal epithelium remains constant throughout adulthood, in spite of continuous cell division in the basal layer and cell loss via differentiation and exfoliation. Therefore, there must be a mechanism that ensures a balance between cell production and cell loss from the tissue. Thoft and Friend were the first to propose the preservation of cell numbers in the corneal epithelium by formulating the XYZ hypothesis based on corneal wound healing experiments (Thoft and Friend, 1983). This hypothesis states that production of new cells (X) and their migration (Y) is balanced by the desquamation of corneal epithelial cells (Z) or X + Y = Z.

It has been widely accepted that the renewal of the adult corneal epithelium mass is maintained by a stem cell population in the basal limbal region that proliferates slowly unless stimulated by corneal injury (Cotsarelis et al., 1989; Davanger and Evensen, 1971). These limbal stem cells (LSCs) give rise to fast-dividing progenitor cells, the transient amplifying cells (TACs), which migrate centripetally (Buck, 1985; Kinoshita et al., 1981) entering the basal layer of the corneal epithelium, where they continue to proliferate for a limited time before their detachment from the basement membrane to become post-mitotic and more differentiated (Lehrer et al., 1998). Once these cells detach from the basement membrane, they migrate apically towards the higher squames of the corneal epithelium from where they are shed via exfoliation (Fig. 1.3; Haskjold et al., 1989). Although it is believed that TACs have a limited proliferation potential before they become terminally differentiated, they comprise the majority of proliferating cells in the corneal and limbal epithelium (Cotsarelis et al., 1989; Pellegrini et al., 1999; Schlotzer-Schrehardt and Kruse, 2005). Additionally, even in the TAC population, there is a hierarchy with more

peripherally located TACs capable of multiple divisions whereas those in the basal layer of the central cornea being able to divide only once (Lehrer et al., 1998). Furthermore, it has been reported that daughter cells in the basal corneal epithelium (TACs) are usually found near each other. This is also the case even for mitotic divisions of TACs that result in the detachment from the basal layer, where both daughter cells move together towards the upper strata of the epithelium and begin to differentiate in a synchronous manner (Beebe and Masters, 1996).

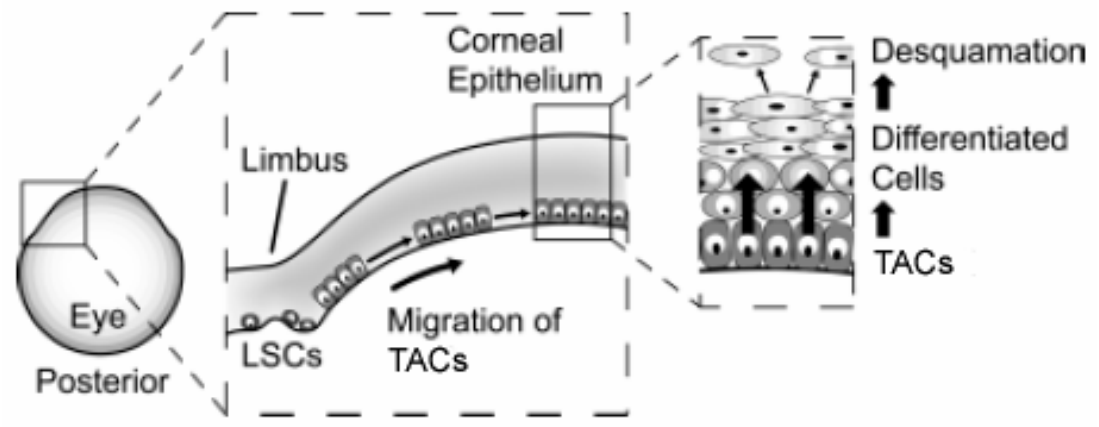

Figure 1.3 Proposed model for the maintenance of the adult corneal epithelium. Stem cells from the limbal region (LSCs) produce transient amplifying cells (TACs) that migrate centripetally towards the central cornea and then apically towards the surface of the corneal epithelium. During these migrations, they also become more differentiated (Collinson et al., 2002).

1.1.3 Location of corneal epithelial stem cells

Indications that the limbus is the corneal stem cell niche, that is the site where stem cells are located, derive from several observations. Firstly, the limbus has blood vessels in close proximity, which can supply stem cells with growth factors and other nutrients. Also, in some species the limbus has melanin pigmentation, which can provide protection from ultraviolet light and potential DNA damage. Neither of these could be present in the cornea because this would impair light transmission and refraction, the cornea's ultimate roles in vision (Boulton and Albon, 2004). In addition, the limbal epithelium consists of small cells (Romano et al., 2003) that are euchromatin-rich and have a high nucleus to cytoplasm ratio, properties that are believed to be adopted by stem cells in a variety of tissues (Chen et al., 2004). Furthermore, limbal basal cells have been shown to be less differentiated than the corneal epithelium, based on their marker expression profile like keratins or general stem cell markers (Schermer et al., 1986). The observation that most tumours originate from stem cells (Reya et al., 2001) and the fact that carcinomas in the human eye mostly originate from the limbus and rarely from corneal epithelium provides one more piece of evidence for the limbal location of the corneal stem cells.

Furthermore, based on the stem cells' unique slow cycling behaviour, in vivo studies have identified label retaining cells (LRCs) only in the peripheral cornea epithelium and specifically in the limbal zone. This approach uses long-term labelling with BrdU or radio-labelled thymidine followed by long chase periods, during which most cells dilute the label due to cell divisions but slow-cycling cells retain it (Bickenbach, 1981; Cotsarelis et al., 1989). This approach has been applied to various species (i.e. mouse, rat, rabbit and human) and is discussed in more detail in section 1.2.4. Stemness can also be assessed from cell culture experiments. Human limbal epithelium has been shown to grow better in explant cultures than the peripheral cornea (Ebato et al., 1988). Cell cultures from the human limbal region were found to yield the largest number of cell doublings prior to senescence, to have the highest ability for proliferation from an isolated state and even to produce new clones after dissociation and reseeding (Pellegrini et al., 1999). However, analogous experiments

have not been reported yet for murine corneal and limbal epithelial cells because of technical reasons discussed in section 1.2.4.

Finally, surgical removal of the limbus results in healing with non-corneal epithelium from the adjacent conjunctiva in rabbits (Huang and Tseng, 1991). If the corneal epithelium is completely destroyed along with the limbal zone, a situation that occurs in patients with chemical burns, standard cornea replacement is ineffective and only transplantation of small pieces of healthy, human limbal epithelial tissue can reconstitute the entire corneal epithelium (Kenyon and Tseng, 1989; Tseng, 1989). However, grafts that include both limbal and corneal tissue seem to be more successful than limbal grafts alone (also discussed in section 1.3.2). Taken together, the above data strongly suggest that limbus is the niche of the corneal epithelial stem cells.

Also, the observed centripetal migration of the basal cells in the corneal epithelium suggests that the source of these cells has to be in the periphery. Specifically, ink tattoos at the limbal region resulted in centripetal migration of marked cells towards the centre of the cornea (Buck, 1985). Furthermore, Nagasaki et al. used a GFP expressing mouse and was able to follow single GFP stripes on the corneas of live mice while they were extending towards the central cornea with time lapse fluorescent microscopy (Nagasaki and Zhao, 2003). Finally, X-inactivation mosaics have shown that stripes of β-galactosidase (β-gal) emerge from the limbus and they span the whole radius of the cornea after several weeks (Collinson et al., 2002; Mort et al., 2009). Interestingly, this migration of cells from the periphery to the centre of the cornea is only observed in the corneal epithelium and not in the conjunctiva. In fact, the conjunctival epithelium does not show any cell movement and stem cells renewing this epithelium are believed to be distributed throughout the tissue (Nagasaki and Zhao, 2005).

In 1971, Davanger and Evensen proposed that the structures responsible for the renewal of the corneal epithelium were the palisades of Vogt. These are subepithelial, vascularised papillae found at the limbal region of the eye between

which the epithelium projects downwards. This hypothesis was mainly based on observations of the pigmented limbus of African-American negroes' eyes where cells at the limbus have high levels of melanin (Davanger and Evensen, 1971). In 2005, the view that the palisades of Vogt were the corneal epithelial stem cell niche was challenged for the first time (Dua et al., 2005). In this report, Dua et al. identified anatomical structures at the human limbus they termed "limbal epithelial crypts". These crypts were found underneath an interpalisade ridge and were found to extend either radially into the conjunctival stroma or circumferentially along the limbus. Cells in these structures were found to be of epithelial nature and to have maximum staining for ABCG2 (a putative stem cell marker). However, in another report, Shortt et al. found projections of epithelium in between the palisades of Vogt extending into the limbal stroma, which they termed "limbal crypts" (Shortt et al. 2007). It was demonstrated, that these human limbal crypts harbour cells that are smaller in size and have a higher nuclear to cytoplasm ratio when compared to cells outside these structures, characteristics normally attributed to stem cells. Furthermore, the authors found that cells at the bottom of these crypts have higher expression of two putative stem cell markers (namely p63 and ABCG2) and when cultured they can give rise to colonies which are similar to the holoclones created by culturing stem cells. However, neither the palisades of Vogt nor structures like the limbal crypts can be found in the eyes of mice. Limbal stem cell markers are discussed in section 1.2.2 and the characteristic holoclones formed by stem cells when in culture are discussed in section 1.2.4.

Recently, Barrandon and colleagues proposed an alternative hypothesis, suggesting that the limbus only contributes cells to the corneal epithelium in response to wound healing and that during normal homeostasis the corneal epithelium is maintained by stem cells scattered throughout the corneal epithelium (Majo et al., 2008). In a careful series of experiments these authors transplanted tissues marked with a reporter transgene to the limbus of immunologically compromised mice. Transplanted limbal tissue did not produce clones of corneal epithelial cells unless the corneal epithelium was wounded. The authors concluded that although the

transplanted limbal tissue contributed to corneal repair, it did not contribute to steady state corneal maintenance during normal tissue homeostasis. Serial transplants of central cornea to limbus behaved in the same way as the transplanted limbal tissue and was interpreted as evidence that central cornea contains oligopotent stem cells which could restore both the cornea and conjunctival epithelia. They further proposed that cells in the conjunctiva and corneal epithelium responded to opposing forces that tended to expand both tissues towards each other, so they met at the limbus, which they described as ‘a zone of equilibrium’. Thus, any movement in the corneal epithelium was more likely to be centrifugal than centripetal.

The above constitute the basic principles of the newly proposed alternative hypothesis of corneal maintenance. The model is more fully discussed in relation to results reported in this thesis and other published studies in chapter 7.

1.2 IDENTIFICATION OF STEM CELLS

1.2.1 Stem Cells and nomenclature

In the last twenty years many studies have reported the existence of stem cells from a variety of adult tissues. However, the origin of these cells is in most cases assumed, rather than proven, and the actual cell lineage from which they derive is either unknown or poorly understood. In such an already complicated field, additional confusion arises from the different views on the terminology adopted by researchers regarding the characterization of stem cells, their descendants and their properties. Although previously, some criteria had been established in order to help scientists to unanimously categorize cells with various differentiation potential (Lakshmipathy and Verfaillie, 2005; Weissman, 2000), they do not take into account stem cells that normally produce only one tissue lineage, such as satellite cells that replenish the muscle fibres, or stem cells that sustain the bulk of tumours, termed cancer stem cells (Reya et al., 2001). Recently, a review by Smith in affiliation with EuroStemCell (http:/www.eurostemcell.org) was published, which provides the most accurate and up-to-date terms used in stem cell biology (Smith, 2006). According to this review, cells that have the ability to generate unaltered daughter cells and simultaneously produce daughters with different, more restricted properties are characterized as "stem cells".

The most crucial property of a stem cell is its ability to "self-renew", meaning the ability to produce identical daughter cells, which maintain the stem cell pool along with the original capacity for differentiation. The breadth of differentiation potential of a cell is called "potency" and is used to categorize cells to: "totipotent", characterizing a cell that can give rise to an entire organism (e.g. the zygote); "pluripotent", cells producing all cell types of the body, germ cells and at least some extra-embryonic cell types (e.g. embryonic stem cells; Niwa et al., 2005); "multipotent", "oligopotent" & "unipotent" refer to cells generating multiple (e.g. haematopoietic stem cells), two or more (e.g. neural stem cells) and only one (e.g. spermatogonial stem cells) lineage respectively. Furthermore, "embryonic stem

cells" are pluripotent cells that derive in vitro from the inner cell mass of a mammalian blastocyst, whereas "tissue stem cells" have limited potency to the foetal or adult tissue from which they derive from or reside in.

Finally, the term "progenitor cell" describes any dividing cell with differentiation capacity and is different from "precursor" or "ancestor" cell, terms that characterize cells without self-renewal capacity but able to contribute to tissue formation and in some cases produce tissue stem cells (Merkle et al., 2004). Self-renewal of a stem cell population is believed to be sustained due to stimuli and support of the cellular microenvironment surrounding it, which is called the "niche" (Smith, 2006; Tumbar et al., 2004).

1.2.2 Limbal stem cell markers

The development of specific markers that can identify stem cells would have an enormous impact on both basic science and the clinical use of stem cells. Examples come from haematopoietic stem cells, which is the best characterised stem cell system and for which specific membrane markers have been identified (Civin, 1992; Silvestri et al., 1992). In the field of limbal stem cells (LSCs), although several attempts have been pursued and several markers have been identified, none appears to fulfil all the criteria for LSC markers, as proposed by Pajoohesh-Ganji et al. According to these criteria, a marker should: 1) allow enrichment or isolation of cells, 2) identify LSCs in their native tissue in healthy subjects, 3) mark cells whose number remains constant throughout the life of an organism or after induction of proliferation (e.g. injury) in the long term and 4) identify fewer cells in LSC deficiency models. Isolated cells should demonstrate long term repopulation, restoration of a clear cornea, *in vitro* ability to form colonies and expression of differentiation markers in their progeny (Pajoohesh-Ganji and Stepp, 2005).

One of the more promising candidates for LSCs is the transcription factor p63, which is a member of the p53 family. This is crucial for the development of stratified epithelia since p63 knock-out mice have been demonstrated to lack epithelial structures (Yang et al., 1999). This transcription factor has been immunohistochemically localised in the basal layer of human limbus whereas the cornea was found to be negative by the authors, who claimed that p63 can distinguish putative LSCs from TACs (Pellegrini et al., 2001). Furthermore, the authors showed p63 expression in cells with high colony forming and growth potential (holoclones) whereas little or no expression was reported for cells with limited or no growth potential (mero- and para- clones respectively; see section 1.2.4). On the other hand, p63 is expressed throughout the corneal epithelium in rats (Moore et al., 2002) as well as in mice (Ramaesh et al., 2005) and, even for humans, other groups have reported the presence of p63 in the central corneal epithelium of adult eyes (Dua et al., 2003), questioning the validity of this transcription factor as LSC marker. Additionally, in another report, p63 was found to be expressed by groups of cells rather than individual cells in the human limbus, suggesting that this protein is also present in early TACs (Kim et al., 2004). More recently, a specific transcript of p63, namely ΔNp63α, has been reported to be more specific for limbal epithelial cells and hence, more likely to identify LSCs (Di Iorio et al., 2005), but these results have not been confirmed by an independent group yet.

A method that has been used to isolate putative stem cells from several tissues takes advantage of their ability to efflux the DNA binding dye Hoechst 33342. This was first observed in a Hoechst-stained bone marrow population, which showed a haematopoietic-stem-cell-rich side population after flow cytometry (Goodell et al., 1996). As it was later revealed, the ATP Binding Cassette subtype G2 (ABCG2) was the source of this phenomenon (Zhou et al., 2001) and this can also be localised to tissue sections by immunohistochemistry. This protein has also been found in many stem cell lineages like neurons (Murayama et al., 2002), muscle (Zhou et al., 2001), epithelia (Summer et al., 2003) and has thus been proposed as a universal stem cell marker (Zhou et al., 2001). Recently, this cell-membrane localised transporter was

shown to be present in human and rabbit limbal basal cells showing characteristics of stem cells (e.g. small size, induction of clones *in vitro*, slow-cycling nature etc) but it was absent from the central corneal epithelium (Budak et al., 2005; de Paiva et al., 2005). Nevertheless, the ABCG2 subpopulation probably contains but does not exclusively represent stem cells and its validity as a stem cell marker has still to be clarified (Dua et al., 2005).

Among the most recently suggested candidate molecules for LSC markers are N-cadherin (Hayashi et al., 2007) and Hes1 (Nakamura et al., 2008). Both proteins have been shown to be localised exclusively in the basal limbus of human and mouse limbus respectively, but results still await independent confirmation.

A single molecular marker able to distinguish between stem cells and other proliferating epithelial cells of the ocular surface has not yet been identified (Schlotzer-Schrehardt and Kruse, 2005). However, apart from the molecules linked to stemness, there are others that are not supposed to be expressed by stem cells. These molecules are usually associated to cells destined for differentiation and as such, stem cells are expected to be negative for them. Keratin 3 (Schermer et al., 1986) and keratin 12 (Chaloin-Dufau et al., 1990; Kurpakus et al., 1990) are examples of differentiation markers on the ocular surface, showing a similar immunostaining pattern. All layers of the human corneal epithelium and the suprabasal layer of the limbus are positive for these structural proteins, whereas they are absent from the basal limbus and the conjunctiva. However, there are some differences in the distribution of keratins across species. For example, keratin 3 was shown to be absent from the murine genome (Hesse et al., 2004), although it stains the corneal epithelium of many animals (Chaloin-Dufau et al., 1993). Furthermore, the gap junction protein connexin 43 has been reported to be absent from the limbal epithelium but present in the basal corneal epithelium and conjunctiva (Matic et al., 1997). The absence of this cell-communication-promoting molecule from the stem cell compartment of the cornea has been suggested to protect the stem cell niche. Recently, it has been demonstrated that basal limbus lacks involucrin, a structural protein of the cytosol, whilst all the cornea and the suprabasal limbus are positive

(Chen et al., 2004).

While there may never be a single unique LSC marker, in principle, all the aforementioned positive and negative markers could be combined in order to obtain a purified population of stem cells able to replenish the stem cell pool of the cornea and also able to produce corneal epithelial stem cells based on a unique LSC marker combination. However, such a combination has not yet been identified.

1.2.3 Identification of stem cell lineages

One of the fundamental characteristics of stem cells is the ability to divide either symmetrically, where both daughter cells are stem cells that replenish the stem cell pool or asymmetrically. In the latter type of division, one daughter cell will replenish the stem cell pool and the other one is destined to differentiate. So, if a stem cell is marked with a suitable permanent lineage marker, all its progeny will also be marked and all the marked cells will be clonally related. A large variety of techniques have been developed that induce the expression of a reporter gene in a limited cell population and/or for a specific time during development. These techniques include but are not limited to reporter genes being driven by tissue specific promoters and promoters that are activated in a specific developmental stage of an organism. However, in order for all the marked cells to be a single descendent clone that is derived from a single marked founder cell, the reporter gene has to be induced in a very low frequency of cells in a transgenic animal.

Such rare induction of the reporter gene has been successfully achieved with the LaacZ system (Bonnerot and Nicolas, 1993; Nicolas et al., 1996). This consists of an inactive *LacZ* reporter gene targeted to the Rosa26 locus (Fig. 1.4). The inactivation results from an internal duplication of the coding sequence of the *LacZ* gene that leads to early stop codons during translation. However, rare, stochastic intra-chromosomal (or rarely inter-chromosomal) recombination can result in *LacZ* activation marking permanently the cell where the recombination took place. If this

cell is a stem cell, it will also mark all its progeny. Interesting observations about stem cells, their niche and progeny (as well as development) have arisen from clonal analyses using this system concerning mainly stem cells of the brain (Mathis and Nicolas, 2000; Mathis and Nicolas, 2003) or melanoblasts (Wilkie et al., 2002).

Figure 1.4 A schematic representation of the LaacZ reporter. It shows the inactive form of the *LacZ* reporter due to an internal duplication that is driven by a nuclear localization signal (nls). The whole transgene is targeted to the Rosa 26 locus.

Recently, a new technique has been applied to identify clonalities in human epithelial tissues like liver, pancreas, small intestine and skin using non-pathogenic mutations in the mitochondrial DNA (mtDNA) and specifically in the cytochrome c oxidase (*COX*) gene (Fellous et al., 2009). As the authors explain, mtDNA lacks protective mechanisms and hence, mutations arise and expand stochastically. However, in order for a phenotype to be observed all or most of the mitochondria of a cell have to be mutated, a lengthy process, which is only likely to occur in relatively long-lived species in long-lasting cells of the body, like stem cells. Once a stem cell becomes biochemically deficient in *COX*, a simple enzymatic colour reaction can reveal this mutated cell as well as its progeny.

Usually, when further spatial and/or temporal control is required, the specific promoters that drive reporter gene expression are coupled with an inducible switch, making the system able to provide control over the amount of the induction by titrating the dose of the inducer as well. One of the most widely used genetic switches is the Cre/*LoxP* system, which can activate or deactivate gene expression

depending on the design of the transgenes (Fig. 1.5). As described in section 5.1, in this system the way that Cre is introduced can provide additional regulation of expression. Steroid hormone receptors are potent transcription factors that can offer gene regulation but they do have some serious drawbacks. The use of ligands or inducers to activate these receptors may also activate a small proportion of endogenous hormone receptors in the body, resulting in potential side-effects. Also, fluctuations in normal hormone levels can alter the expected transgene expression. In order to overcome some of these problems, modified versions of the hormone receptors that respond to specific agonists of the endogenous ligand have been produced (Goverdhana et al., 2005). One such example is the artificial oestrogen receptor that has been mutated to respond only to tamoxifen (Danielian et al., 1993). Fusion of Cre with the modified oestrogen receptor (Cre/ER^{TM}) results in tamoxifen-dependent Cre regulation (Badea et al., 2003). Another way to circumvent endogenous ligand-associated problems of the hormone receptors is to use non-mammalian steroid receptors, like the Ecdysone receptor (EcR), to regulate transgene expression. EcR is a steroid hormone receptor found in *Drosophila melanogaster* which is activated by ecdysteroids and they further activate genes with the ecdysone-responsive element which is uniquely found in insects (Yao et al., 1993). Additionally, the ecdysteroids have been reported not to demonstrate any apparent effect on mammalian cells in terms of toxicity and physiology (No et al., 1996).

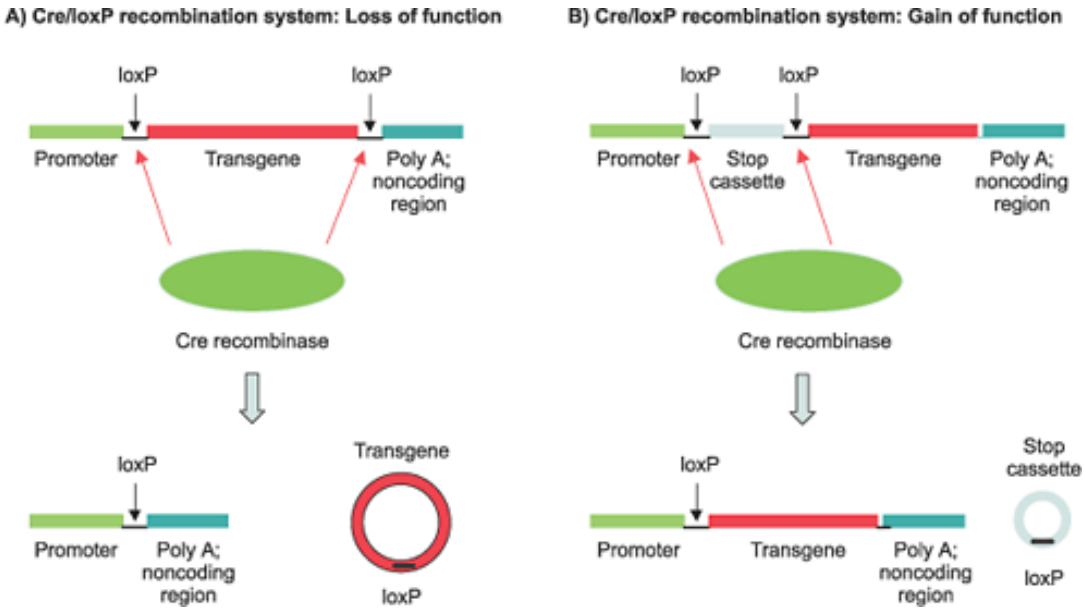

Figure 1.5 The Cre/LoxP system for gene regulation. (A) Loss of function of a gene can be achieved when *LoxP* sites flank an essential part of a gene. Cre mediated recombination excises this region leading to deactivation of the gene. (B) Gain of function is obtained when a STOP cassette is placed upstream of gene. By flanking this cassette with *LoxP* sites a switch is created that can activate gene expression in the presence of Cre recombinase, because the latter will excise the STOP cassette (Romano, 2004).

A very successful example of lineage tracing using the Cre/LoxP switch to create inducible mosaicism can be demonstrated in the case of small intestine, colon (Barker et al., 2008; Barker et al., 2007) and hair follicle (Jaks et al., 2008) stem cells. Using target genes of Wnt transcription factor, the authors selected *Lgr5* out of a pool of 80 other genes and created transgenic mice. These mice were carrying a Cre/ER^{TM} gene under the control of *Lgr5* promoter and were crossed to R26R reporter mice. The resulting offspring will have active β-gal expression in cells expressing *Lgr5* only after tamoxifen induction. Mosaic reporter expression was achieved with small doses of tamoxifen and this was demonstrated as clones of cells emanating from the base of the crypt in the case of intestine or as cells at different compartments of the hair follicle. Subsequent lineage tracing experiments in all the aforementioned tissues showed that *Lgr5* gene was expressed by stem cells since these cells could show longevity and multipotency. These two stem cell associated properties are demonstrated by the following observations. Firstly, the β-gal positive cells could maintain their respective tissues, in which they were found, for long periods of time (12 months or longer). Secondly, the authors identified many different types of cells (i.e. enterocytes, goblet cells, Paneth cells and enteroendocrine cells in the intestine and cells from all the different cell layers of the hair follicle) among the marked progeny of the *Lgr5*-expressing cells, implying that the original marked cells were multipotent.

1.2.4 Indirect identification of LSCs

Since there is no reliable marker for LSCs, alternative methods have been developed to identify these stem cells indirectly, based on general stem cell properties.

Mosaic patterns produced in mouse chimaeras and mosaics have provided indirect evidence of limbal stem cell function although they do not identify clones derived from individual stem cells as readily as the lineage markers discussed in section 1.2.3. Chimaeric mice have been produced by aggregation of LacZ-positive and

LacZ-negative eight-cell embryos (Collinson et al., 2002). These mice showed mosaicism for β-gal expression in a variety of tissues, including the eye. Adult mice (older than 10 weeks) demonstrated radial stripes of β-gal positive cells in the corneal epithelium that had sharp boundaries and spanned the whole radius from the limbus to the central cornea. An equivalent phenotype was observed in adult female X-inactivation mosaic mice (Collinson et al., 2002). These mice had a LacZ transgene in one of their X chromosomes so random X-chromosome inactivation made them obligatory mosaics for β-gal expression. (Both systems are discussed further in sections 1.4 and 3.1).

Lineages in the ocular surface have also been identified by delivering a reporter gene via a viral vector. This has effectively been performed by injecting a GFP expressing lentiviral vector in the amniotic cavity of murine embryos at embryonic stages E8 to E18 (Endo et al., 2007). GFP expressing cells, organised in radial stripes, could be identified in the cornea of adult mice (at least up to 6 months old), which supports the transduction of limbal stem cells with the lentiviral vector.

Another generally accepted property of stem cells is their ability to undergo a large number of cell divisions. This can be tested in cultures, where the ability of different cell-types can be assessed. Stem cells in culture are reported to form large clones (called holoclones) that are continuously in growth expansion and they continue to grow even when reseeded in new culture plates. Meroclones are clones of cultured cells formed from founder cells with limited growth potential and, thus, they produce clones which stop growing after they have exhausted their proliferative potential (producing terminal colonies). These cells are thought to represent TACs, which have the ability to proliferate for a small number of generations. Finally, the paraclone is formed mainly by terminally differentiated cells that do not have the ability to proliferate and hence, it is characterised by culture plates that lack cell colonies. This method was first applied to human epidermal keratinocytes and showed the three clonal types in the human epidermis (Barrandon and Green, 1987). The same technique was also successful in the human ocular surface (Pellegrini et al., 1999). According to this, only cells from limbal specimens were able to produce

holoclones, suggesting that this is the location of stem cells. Specimens from central or paracentral cornea were not able to be serially cultivated, suggesting lack of high proliferative potential of the cells occupying these areas. To date, equivalent mouse limbal and corneal epithelial cell culture experiments have not yet been performed because this has been proved technically challenging. Hazlett et al. were the first to develop a method for culturing mouse corneal epithelial cells from explants (Hazlett et al., 1996). However, these cells were only maintained short-term since they failed to subculture them beyond passage three, which is not long enough for analysis of growth potential. Later, a method to develop a stable corneal epithelial cell line from corneal-epithelial sheets was described (Kawakita et al., 2008), but it requires long culturing times (1 week for expansion to confluence plus 3 more weeks to exhaust the proliferative potential of the TACs) and an ample supply of eyes (around 200 eyes for each culture). More recently, two improved methods were reported that can maintain mouse corneal epithelial cells until passage 10 with the advantage of shorter culturing times (Kobayashi et al., 2009) or until passage 25 with longer culturing times but from single corneas (Ma et al., 2009). These techniques look very promising and will probably make the holoclone production from mouse corneal epithelial cells possible in the future, but such experiments have not been reported yet.

Early studies of epithelial tissues have revealed that a characteristic feature of their stem cells is that they divide relatively infrequently (Potten and Morris, 1988). A widely-held hypothesis is that stem cells are generally slow-cycling during normal homeostasis but they can be induced to proliferate in circumstances like injury. Thus, if all the dividing cells of a structure are labelled with a substance that gets diluted with every cell division during a subsequent chase period, stem cells will be revealed by the retention of the label after the chase period because they will have divided fewer times than TACs in the same tissue. So, the label-retaining cells (LRCs) are considered to be putative stem cells. However, it should be noted that LRCs represent only a proportion of the stem cells that reside in a tissue because only those cells that divided during the labelling period will be marked. Additionally, somatic

cells that divided during the administration of the label and then became terminally differentiated would be labelled as well and they will retain the label since they will not divide again. If these cells are still present in the tissue when the analysis is performed, they will appear as LRCs. Thymidine analogues, which are incorporated into the DNA of cells at the S-phase of the cell cycle and subsequently diluted at each cell division, are commonly used with this technique. These include ^{3}H-thymidine, BrdU, CldU, IdU and more recently EdU (whose detection is easier than that of the rest analogues because the product of the enzymatic identification is fluorescent).

The label-retaining technique has been used *in vivo* to identify the location of putative stem cells in a variety of tissues including the ocular surface. There, LRCs are predominantly found in the basal layer of the limbal epithelium, whereas the corneal epithelium is devoid of such slow-cycling cells (Cotsarelis et al., 1989; Lehrer et al., 1998; Pajoohesh-Ganji et al., 2006; Zhao et al., 2009). Also, this technique has identified cells with stem-like properties that are sequestered to wounded areas of the corneal endothelium when needed (Whikehart et al., 2005). Moreover, LRCs have been reported to reside in all major regions of the conjunctiva, namely the palpebral (Chen et al., 2003), the fornix (Wei et al., 1995) and the bulbar conjunctiva (Nagasaki and Zhao, 2005) where epithelial stem cells seem to have a uniform distribution.

Another way to identify LRCs is to label a chromatin protein rather than the DNA and then remove the source of labelled protein. Transgenic mice carrying a genetic switch that allows a chromatin protein labelled with a reporter gene to be expressed ubiquitously and then switched off would provide a suitable system. This has been successfully applied in mice expressing a histone H2B-GFP fusion protein, using the tetracycline based Tet-Off system to control the expression of H2B-GFP. In the absence of tetracycline (or doxycycline), binding of a tetracycline repressor to the tetracycline operator (TetO) sequence will inhibit the transcription of a transgene placed downstream of the TetO (Gossen et al., 1995; Kim et al., 1995) but in the Tet-Off system the switch is reverted. Fusion of the repressor with the transcription

activation domain of the Herpes simplex virus protein 16 produces a tetracycline-controlled transactivator (tTA) that in the absence of tetracycline binds to the TetO, activating the expression of the transgene rather than inhibiting it. In the presence of tetracycline (or doxycycline), the tTA is no longer able to bind to the TetO resulting in transcriptional termination of the transgene (Gossen and Bujard, 1992). This system is usually termed "Tet-Off" because the addition of tetracycline turns the expression of the transgene off (Fig. 1.6 A).

The Tet-Off system has been successfully applied to reveal slow-cycling cells (putative stem cells) in the skin of mice (Tumbar et al., 2004). This was achieved by using mice that express a fusion protein, comprising histone H2B and GFP, from a ubiquitous promoter under the control of a tetracycline-responsive element. The tTA activator was expressed in the skin from the keratin 5 promoter. In these mice H2B-GFP is always expressed in the skin unless doxycycline is administered, so the chromatin is labelled with GFP. The administration period of doxycycline is the chase period during which the more rapidly dividing skin cells will dilute the H2B-GFP to undetectable levels but H2B-GFP will be retained for longer in the more slowly cycling cells. The results from this study confirmed that H2B-GFP LRCs could indeed be used to identify stem cells in the skin. This approach has not yet been used to identify LRCs in the ocular surface but it offers some advantages over the conventional BrdU LRC approach described above and in chapter 4. One key advantage is that if tTA is expressed from a promoter that is expressed early in development, all the cells will be labelled before the chase period is started so it has the potential to identify a much higher proportion of the putative stem cells.

The Tet-Off system can be used to induce transgene expression in a variety of tissues and organs, but prolonged periods of tetracycline administration to prevent transgene expression are cumbersome for some purposes. Thus, a "Tet-On" system has also been developed (Fig. 1.6 B). Random mutagenesis of the tTA resulted in the production of a protein, called reverse tetracycline-controlled transcriptional activator (rtTA) that exhibits the reverse activity of the tTA (Gossen et al., 1995). That is, in the absence of tetracycline / doxycycline the rtTA does not bind to the

TetO and hence, the transgene is not transcribed, whereas tetracycline / doxycycline administration leads to transgene activation. Both systems have been extensively used and transgenic mice have also been produced that can easily been manipulated to express or suppress the expression of various transgenes but Tet-On has not been used to identify putative stem cells.

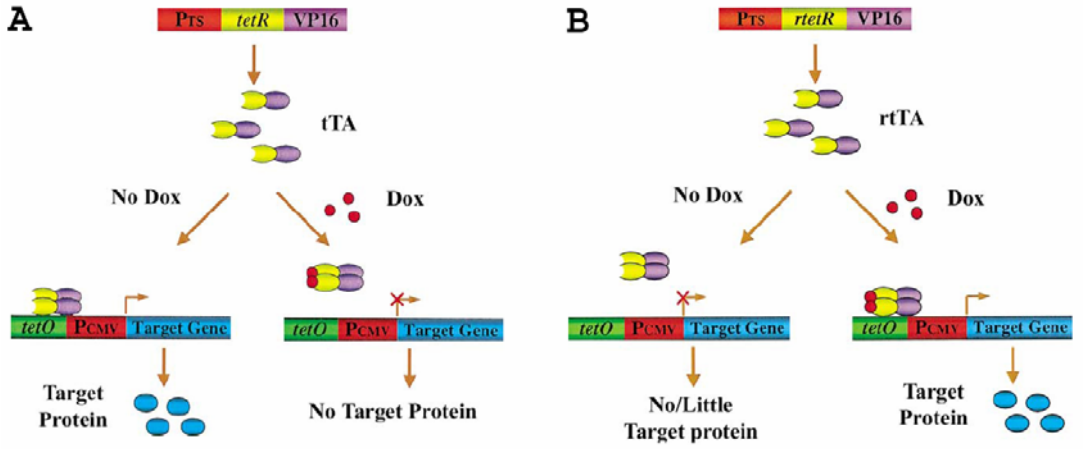

Figure 1.6 The tetracycline-controlled switch. (A) The Tet-Off system. Expression of the tTA transactivator is driven by a promoter. In the absence of doxycycline (Dox), the transactivator binds to the tetracycline operator (tetO) activating the Pcmv promoter leading to transcription and expression of the target gene. When Dox is present, tTA dislocates from tetO terminating transcription and obstructing expression of the targeted protein. (B) The Tet-On system. The reverse transactivator rtTA, driven by the tissue or cell specific promoter, does not bind to the tetO leading to ineffective transcription of the targeted gene. Addition of Dox activates the rtTA that binds to tetO and drives transcription and expression of the targeted protein. Pts: Tissue or cell specific promoter; Pcmv: cytomegalovirus promoter. Figure reproduced from Zhu et al. (2002).

1.3 THE *PAX6* TRANSCRIPTION FACTOR

1.3.1 Regulation of eye development

Pax6 encodes a highly conserved transcription factor with a conserved paired box and a paired-like homeobox DNA-binding domain (Bopp et al., 1986). The amino acid sequence is 94% identical between mammals and flies whilst even the splice sites of the gene are conserved (Quiring et al., 1994). Pax6 is known to have multiple roles in cell proliferation, adhesion, migration and signalling and is essential for the development of several tissues like the central nervous system, the endocrine glands and the eye (Simpson and Price, 2002). In mammals, *Pax6* has been found to be expressed in a variety of organs like pancreas, gut, pituitary gland, nasal structures, brain and spinal cord from early on in development (Walther and Gruss, 1991).

Specifically during eye development, *Pax6* is widely expressed in tissues that include the lens, the corneal epithelium, the iris, the ciliary body and all the layers of the retina (Grindley et al., 1995; Koroma et al., 1997) and although it is down-regulated in most eye structures after birth, expression is maintained in the corneal epithelium. The pivotal role of *Pax6* during eye development is unarguably demonstrated by the induction of ectopic eye structures in *Drosophila melanogaster*. In these misexpression experiments, *eyeless* (the *Pax6* homologue in *Drosophila*) was able to induce the development of eyes in structures like antennae, wings and legs (Halder et al., 1995). In fact the ectopic eyes on the antennae are thought to be functional since they are histologically normal, produce axons to the central nervous system and also produce an electroretinogram (Clements et al., 2008). Additionally, even the mouse *Pax6* gene has been shown capable of inducing compound eyes when expressed ectopically in *Drosophila*, whereas the *Drosophila* and the *Xenopus Pax6* can both induce retina and lens structures in *Xenopus laevis* (Chow et al., 1999; Onuma et al., 2002) showing evolutionary conservation of the gene's function in vertebrates and invertebrates. The finding that *Pax6* is adequate to induce a cascade of genes leading to eye morphogenesis in both vertebrates and invertebrates suggests that this might be a universal master control gene for eye development (Gehring, 2005).

1.3.2 *Pax6* insufficiency and aniridia

Most of the *Pax6* functional roles in different organs have been revealed through studies on mutant or transgenic mice, which lack a functional *Pax6*. Although there are various mouse lines with a null *Pax6* gene, the two most widely used mutants are $Pax6^{Sey}$ and $Pax6^{Sey\text{-}Neu}$. $Pax6^{Sey}$ is a spontaneous mutation of *Pax6* whereas $Pax6^{Sey\text{-}Neu}$ is an ethylnitrosourea-induced mutation in the same gene. Both mutations have been characterized and they comprise semi-dominant point mutations that result in the encoding of stop codons. Premature termination of transcription leads to truncated versions of the transcription factor, which is no longer functional and both strains have similar phenotypes (Hill et al., 1991).

The most obvious abnormality in homozygous $Pax6^{-/-}$ embryos is the lack of eyes and nasal cavities (Grindley et al., 1995; Hogan et al., 1986; Quinn et al., 1996). The lack of eyes in these mice has been attributed to the failure of the lens placode to develop which results in distortion and degeneration of the optic vesicle (Hogan et al., 1988; Hogan et al., 1986). Mice that lack a functional *Pax6* gene die soon after birth because the nasal malformations do not allow them to breathe while suckling (Hill et al., 1991) and they also have severe craniofacial abnormalities including anomalies in the central nervous system as the anterior neural tube fails to fuse properly (Caric et al., 1997; Hogan et al., 1988; Quinn et al., 1997; Warren and Price, 1997).

On the other hand, $Pax6^{+/-}$ mice are viable but they have several defects in their eyes, which are smaller in size than those of wild-type $Pax6^{+/+}$. $Pax6^{+/-}$ mice have hypoplastic irides and may form cataracts (Hogan et al., 1988). Other ocular abnormalities include a lens-corneal bridge and persistent hyperplastic primary vitreous whereas in the corneal stroma irregular alignment of the lamellae, vascularisation and cellular infiltration has been observed (Ramaesh et al., 2003). Moreover, the corneal epithelium has been reported to be irregular in eyes from

Pax6$^{+/-}$ mice consisting of fewer cell layers that are also fragile. Additionally, the presence of goblet cells (normally found in the conjunctiva) in the corneal epithelium of these mice has been interpreted as indication of conjunctival cell invasion into the cornea (Davis et al., 2003; Ramaesh et al., 2003). Further experiments with the *Pax6*$^{+/-}$ heterozygous mice have shown that they demonstrate disrupted clonal growth patterns and centripetal migration in the corneal epithelium (Collinson et al., 2004a) whist being more proliferative than their wild-type counterparts (Davis et al., 2003; Ramaesh et al., 2005). Some of these abnormalities may be caused by a state of continuous wounding and repair of the fragile *Pax6*$^{+/-}$ corneal epithelium (Ou et al., 2008).

In fact, the eye has been shown to be very sensitive to the dose of *Pax6*. Transgenic mice that overexpress this transcription factor also demonstrate developmental abnormalities of the eye, suggesting an extreme sensitivity of the cells within the eye to *Pax6* (Schedl et al., 1996). These authors also demonstrated that when transgenic animals overexpressing *Pax6* were mated to *Pax6*$^{+/-}$ mice, they were able to rescue the small eye phenotype and the offspring had eyes that were normal.

The *Pax6*$^{+/-}$ mouse has been reported to be an excellent model for a hereditary, human, eye disease called aniridia, since it shows an equivalent eye phenotype (Ramaesh et al., 2003). Aniridia, meaning lack of iris is a bilateral, pan-ocular disease, which is mainly characterised by variable iris hypoplasia from relatively normal iris to complete absence. Humans with heterozygous mutations in the *PAX6* gene demonstrate this phenotype, which can lead to progressive ocular surface failure and finally blindness (Glaser et al., 1992; Jordan et al., 1992; Ton et al., 1991). Apart from the iris, other parts of the eye are also affected including the optic nerve, retina, lens, anterior chamber angle and cornea. Aniridia is often associated with corneal opacification, foveal hypoplasia, cataract, optic nerve hypoplasia and macular hypoplasia (Mackman et al., 1979; Margo, 1983; Nishida et al., 1995) conditions that contribute to visual loss. Additionally, lack of Schlemm's canal and/or abnormal differentiation of the trabecular meshwork seems to be the reason why 50 -75% of patients with aniridia develop glaucoma (Nelson et al., 1984). The

various corneal changes in the aniridic patients are known altogether as aniridic keratopathy (Holland et al., 2003) or aniridia-related keratopathy (ARK; Ramaesh et al., 2003), which is usually manifested by the presence of blood vessels and goblet cells, epithelial fragility and opacity (Holland et al., 2003; Ramaesh et al., 2003). ARK occurs in the majority of patients with aniridia (about 90%) and had been characterised as the most important factor contributing to the progressive loss of vision (Mackman et al., 1979; Nelson et al., 1984). These corneal changes are manifested in puberty as an irregular peripheral epithelium but can lead to neovascularisation, fibrosis and stromal scarring. If left untreated, patients will finally develop, ulcers, recurrent erosions and eventually blindness (Holland et al., 2003).

The underlying processes of the described abnormalities in ARK are poorly understood but are traditionally attributed to LSC deficiency (Mackman et al., 1979; Nishida et al., 1995). However, since a definite LSC marker has yet to be identified, a LSC deficiency in the case of aniridia cannot be demonstrated directly. One of the most convincing pieces of evidence for LSC deficiency comes from the clinical treatment of patients suffering from aniridia. Treatment by surgical transplantation of healthy limbal tissue or ex-vivo expanded LSC grafts have been shown to have a better success rate than corneal transplants alone (Holland et al., 2003), suggesting that LSC deficiency is involved but there are no studies addressing this issue directly. On the other hand, patients transplanted with both limbal and corneal tissue tend to have an even better outcome.

1.4 WORK THAT LED TO THIS PROJECT

Previous investigations of the laboratory were based on analyses of variegated patterns of a reporter gene in mosaic mouse models. These mosaics were either chimaeras, produced by aggregation of two 8-cell embryos, one of which was carrying a *LacZ* reporter gene, or female mice that carried a *LacZ* reporter gene on the X chromosome, which is subjected to random inactivation. Careful examination of corneas from mice younger than 5 weeks of age revealed that the cornea demonstrates a speckled pattern of randomly oriented patches (Fig. 1.7 A). At 5 weeks, the first organised stripes of β-galactosidase (β-gal) positive cells appear in the limbal region (Fig. 1.7 B & G) and by the age of 8 weeks the whole pattern has resolved to such stripes with sharp boundaries that span the whole radius of the corneal epithelium (Fig. 1.7 D & H). The identified radial stripes are believed to reflect cohorts of clonally related corneal epithelial cells migrating inwards from LSCs surrounding them. In both models the expression of β-gal was qualitatively identical, proving that stripes are not artefacts created by the system used.

Corneal epithelial clone numbers were estimated (because a stripe could be composed of more clones with the same phenotype) from the observed stripes. This analysis resulted in two key observations. Firstly, the number of LSC clones declined with age in wild-type mice and secondly, *Pax6*$^{+/-}$ mosaics have fewer clones when compared to wild-type and *Pax6*$^{+/-}$ cells are underrepresented in the corneal epithelium of chimaeras (Collinson et al., 2004a; Collinson et al., 2002; Mort et al., 2009). These suggest that LSC deficiency contributes to corneal deterioration in *Pax6*$^{+/-}$ mice and the age effect could be relevant to the progressive nature of the deterioration. However, these observations on functional LSC clones do not indicate whether the number of functional LSCs is also affected. The number of functional LSC clones is not the same as the number of functional LSCs because individual LSCs may be randomly distributed or clustered in clonal units and the sizes of the clonal units may vary with age or genotype. (For further details see section 3.1).

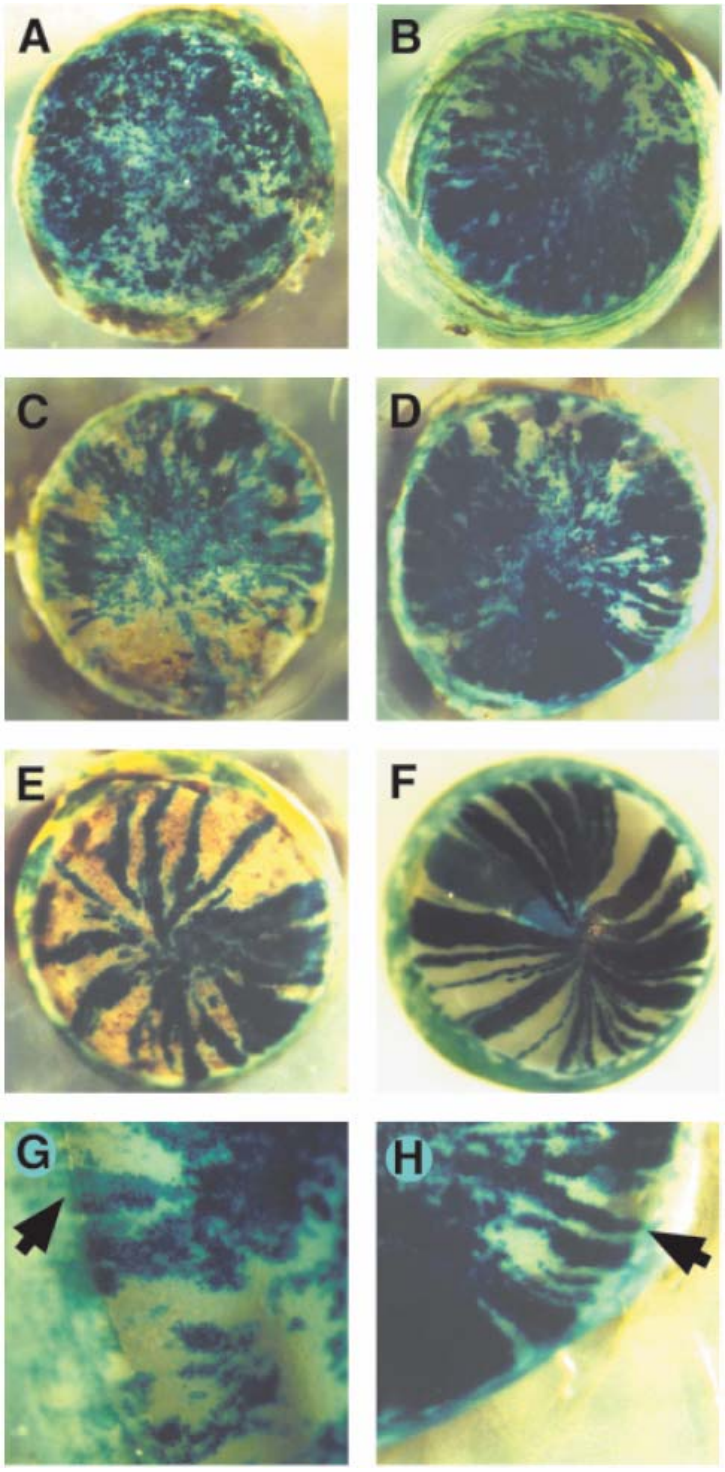

Figure 1.7 Postnatal development of the pattern of stripes in the corneal epithelium of female X-inactivation mosaic mice. Corneas from different individuals are shown at 3 weeks (A), 5 weeks (B & G), 7 weeks (C), 8 weeks (D & H), 10 weeks (E) and 20 weeks (F). G: Detail of periphery of 5-week-old cornea showing nascent stripe emerging from the limbal region (arrow). H: Detail of D showing stripe (arrow) passing from limbal region to centre of corneal epithelium (Collinson et al., 2002).

1.5 Aims

The main aim of this project was to compare the number of functional LSCs in the murine limbus in wild-type and *Pax6*$^{+/-}$ mice at different ages in order to investigate the following two hypotheses:

a) Heterozygous Pax6 mice have fewer functional LSCs than wild-type mice

b) The number of functional LSCs declines with age

First, in chapter 3, the mosaic patterns in young wild-type and *Pax6*$^{+/-}$ X-inactivation mosaics were compared before the stripes were formed to investigate an alternative explanation of why the corrected stripe number was lower in adult *Pax6*$^{+/-}$ than wild-type X-inactivation mosaics.

In chapters 4 – 6, wild-type mice at different ages and *Pax6*$^{+/-}$ mice were compared using a BrdU-label retaining cell approach and two lineage analysis approaches to test the two hypotheses outlined above.

The ultimate goal of the project was to determine whether stem cell deficiency contributes to the progressive corneal deterioration that occurs in the *Pax6*$^{+/-}$ mouse model of ARK.

Chapter 2
Materials & Methods

All consumables were purchased from Sigma (Poole, UK) and procedures were carried out at room temperature, unless stated otherwise.

2.1 Animals & related work

Mice were maintained in animal facilities of the College of Medicine and Veterinary Medicine, University of Edinburgh and the MRC Human Genetics Unit, Edinburgh. Animal work was performed in accordance with institutional guidelines and UK Home Office regulations. Regulated procedures were carried out under Dr John West's Home Office Project Licence PPL 60/3635.

The H253 transgenic mouse is a reporter line carrying an *nLacZ* gene under the control of the ubiquitously expressed, housekeeping gene 3-hydroxy-3-methylglutaryl coenzyme A reductase (HMG CoA) promoter on the X chromosome (Tan et al., 1993). Crosses between H253 males (genotype abbreviated to $XLacZ^{+}$/Y) and inbred CBA/Ca females produce hemizygous $XLacZ^{+/-}$ females, which are mosaics for the *LacZ* reporter gene expression because of random X chromosome inactivation.

Krt5-LacZ transgenic mice, expressing a β-galactosidase (β-gal) reporter gene under the control of the human keratin 5 (*Krt5*) promoter were produced in Dr Julia Dorin's laboratory (MRC Human Genetics Unit, Edinburgh) as described below. These mice were maintained by crossing hemizygous *Krt5-LacZ/-* mice to wild-type C57BL/6 or (C57BL/6×CBA/Ca)F1 hybrid mice.

The Z/AP transgenic mouse line carries a *LacZ* gene between two *LoxP* sites followed by an alkaline phosphatase (AP) gene downstream and the transgene is under the control of the constitutively active pCAGG promoter sequence (Lobe et al., 1999). In the absence of Cre recombinase activity, the *LacZ* gene is expressed ubiquitously but, in the presence of Cre recombinase, expression of *LacZ* is replaced by expression of alkaline phosphatase. This line was provided by Dr John Mason and Dr Vassiliki Fotaki (Centre for Integrative Physiology, University of Edinburgh) and maintained on an outbred CD1 background.

CAGG-Cre/ER^{TM} transgenic mice produce the Cre/ER fusion protein ubiquitously, under the control of the CAGG promoter (Hayashi and McMahon, 2002). Cre/ER comprises Cre recombinase fused to a mutant form of oestrogen receptor (ER^{TM}), so Cre is only active when Tamoxifen (TM) binds to the ER domain and Cre/ER is translocated to the nucleus. The line was provided by Dr. Peter Hohenstein (MRC Human Genetics Unit, Edinburgh) and was maintained on a partially congenic C57BL/6 background (4 generations).

Two *Pax6*$^{+/-}$ mouse lines, carrying the *Pax6*^{Sey} and *Pax6*$^{Sey\text{-}Neu}$ mutations respectively, were used for experiments. The original *Pax6*^{Sey} (small eye) mutation is a spontaneous mutation (Hill et al., 1991; Roberts, 1967) but most experiments used the *Pax6*$^{Sey\text{-}Neu}$ (small eye, Neuherberg), ethylnitrosourea-induced mutation, (Favor and Neuhauser-Klaus, 2000; Hill et al., 1991). Both alleles produce non-functional truncated proteins, so are effectively *Pax6* null alleles. Congenic CBA-*Pax6*$^{Sey\text{-}Neu/+}$ mice were maintained by crossing *Pax6*$^{Sey\text{-}Neu/+}$ to inbred CBA/Ca mice, which were obtained from the Biological Research Facility at Little France Phase 1 (BRF-LF1), University of Edinburgh. *Pax6*$^{Sey\text{-}Neu/+}$ were distinguished from wild-type littermates by eye size and their genotypes were confirmed by polymerase chain reaction (PCR) genotyping (Collinson et al., 2000; Quinn et al., 1996). *Pax6*$^{Sey/+}$ mice, maintained on an outbred CD1 genetic background, were provided by Dr. Dirk A. Kleinjan (MRC Human Genetics Unit, Edinburgh).

The partially congenic CBA/Ca-*Mp* line has an uncharacterised mutation (*Mp*, micropinna microphthalmia) that was induced by irradiation (Phipps and Sullenger, 1964) and *Mp*/+ mice have small eyes and small ears. Although, the gene had not been mapped when this project was started, the region of chromosome 2 to which the *Pax6* gene maps had been excluded (Prof. Ian Jackson, MRC Human Genetics Unit, Edinburgh, personal communication), so *Mp*/+ mice were used as controls for the small size of $Pax6^{+/-}$ eyes. Recent unpublished work has shown that *Mp* involves a rearrangement of chromosome 18 that includes both *Fbn2* (fibrillin 2) and *Isoc1* (isochorimatase domain containing 1). *Mp/Mp* homozygotes and *Mp*/+ heterozygotes have intracellular inclusions that may be attributable to abnormalities of the endoplasmic reticulum and impaired protein transport (Dr. Joe Ranger, MRC Human Genetics Unit, Edinburgh, personal communication). *Mp*/+ mice were provided by Prof. Ian Jackson (MRC Human Genetics Unit, Edinburgh) on a mixed genetic background and crossed to inbred CBA/Ca mice for 5 generations before being used in experiments. The mice were maintained as a partially congenic stock on an inbred CBA/Ca genetic background. Crosses between CBA/Ca-*Mp*/+ and CBA/Ca mice produced both wild-type (+/+) and *Mp*/+ but they were easily distinguished by phenotype.

Various crosses between the above lines were used to produce the appropriate offspring for the experiments as described in the individual experimental chapters.

2.2 BrdU administration

2.2.1 Intra-peritoneal (I.p.) injections

For i.p. injections, BrdU was dissolved (10 mg/ml) in isotonic saline (0.9% w/v) at 60 ^{o}C until a clear solution was produced and aliquots of 1 ml were immediately frozen and stored at -20 ^{o}C. 0.2 ml of the BrdU solution was injected into the peritoneal cavity of mice by an experienced technician, who had the appropriate Home Office personal licence.

2.2.2 Mini-pumps

A 50 mg/ml BrdU solution was prepared as above and 0.1 ml was loaded into an ALZET micro-osmotic pump 1007D [Charles River UK Ltd.], according to manufacturer's instructions. This mini-pump delivers 0.5 µl/h of the solution constantly for 1 week. An experienced technician, who had the appropriate Home Office personal licence, surgically implanted the pump into an anaesthetised mouse by creating a small incision on the back of the mouse and sealing the wound with a clip. After the 7-day administration period, the clips and pump were removed and the wound was closed again with clips, which were removed 7 days later. The mouse was sacrificed 10 weeks after the end of the 7-day administration period.

2.3 Tissue dissection

Mice were culled by a schedule 1 procedure, usually by transferring them to a jar containing a lethal dose of a volatile anaesthetic or by cervical dislocation. Eyes were removed with forceps, along with part of the conjunctiva and the optic nerve. Other tissues, including ear, liver, lung, heart, kidney and small intestine were also dissected for some experiments. Tissues were then placed in bijoux tubes containing PBS at 4 ^{o}C and processed as soon as possible. When required, the tip of the tail (about 3 cm) was also removed during dissection for PCR genotyping. This tissue was placed directly into 1.5 ml tubes and stored at -20 ^{o}C.

2.4 DNA extraction

Tail-tips or ear-clips (which were usually stored at -20^{o}C) were put in 1.5 ml tubes containing 0.5 ml of quick lysis buffer (100 mM Tris-HCl pH: 8.5, 5 mM EDTA, 0.2% w/v SDS and 200 mM NaCl). 100 µg of proteinase K was added and the sample was incubated at 55 ^{o}C overnight. The sample was then mixed using a vortex and any remaining undigested tissue (hair, bones etc) was removed by a brief spin in

a microcentrifuge for 5 min and the supernatant was transferred into a new tube. 0.5 ml of isopropanol was added and the tube was shaken well to mix and precipitate DNA. After letting the mixture settle for 20 min, precipitated DNA was collected by centrifuging (13,000 rpm) for 10 min and the supernatant was discarded. 70% v/v ethanol was added to wash the DNA, the sample was centrifuged for 5 min, the supernatant was discarded and the sample was left to air-dry for 20 min. Finally, the pellet was dissolved in TE (10 mM Tris-HCl pH8, 1 mM EDTA) or H_2O and stored at -20 ^{o}C.

2.5 Genotyping

PCR reactions were carried out by adding 1 µl DNA, 200 ng of each primer (Table 2.1), 200 µM dNTPs [Invitrogen], 1x reaction buffer and 1 U Taq DNA polymerase [Roche] to a final volume of 50 µl. Targeted sequences were then amplified in a Hybaid Omn-E thermocycler by an initial incubation at 95 ^{o}C for 5 min and 40 cycles of the following program: incubation at 95 ^{o}C for 1 min, 1 min at the primer specific temperature (Table 2.1) and 1 min extension at 72 ^{o}C. This was followed by a final step of 5 min incubation at 72 ^{o}C.

Table 2.1 Sequences of primer pairs and their annealing temperature. The sequence in bold is the T7 polymerase binding site. F: forward primer, R: reverse primer.

Gene Name	5′ → 3′ Sequence	Annealing Temperature
Pax6-Sey-Neu F	GCAACACTCCTAGTCACATTCC	57.5°C
Pax6-Sey-Neu R	ATGGAACCTGATGTGAAGGAGG	
Pax6-Sey F	TTAGGAAGGCTTTGTGGAGGC	56.5°C
Pax6-Sey R	CTTTCTCCAGAGCCTCAATCTG	
LacZ F	GTGACTACCTACGGGTAACA	60°C
LacZ R	ATTCATTGGCACCATGCCGT	
Krt5 F	GTCAAGGAGGCATGAGCTTC	61°C
Krt5 R	**GTAATACGACTCACTATAGGG** - AGGTGGGTATCTGGGTAGGG	

For *LacZ* and *Krt5* genotyping, 20 µl of the PCR products were mixed with 5 µl of 6x DNA loading buffer (0.25% w/v bromophenol blue, 15% w/v Ficoll 400) and the mixture was subjected to electrophoresis in a 2% w/v agarose [BMA] gel containing 1xTBE (45 mM Tris, 45 mM Boric acid, 10 mM EDTA) and SYBR Safe [Invitrogen] to help the visualisation of the DNA fragments. Electrophoresis was performed at 100 V for 1 hour and DNA bands were visualized under 320 nm UV light.

The presence of the *Pax6*^{Sey} *or Pax6*$^{Sey\text{-}Neu}$ mutation was determined by restriction enzyme digestion and gel electrophoresis (Collinson et al., 2000; Quinn et al., 1996). 10 µl of PCR product was incubated with 2 µl of 10x buffer and 5 U of restriction enzyme, that is HindII [Roche] (for *Pax6*$^{Sey\text{-}Neu}$) or DdeI [Roche] (for *Pax6*^{Sey}), in a total volume of 20 µl. Enzymatic digestion was carried out at 37°C for 5-18 hours. 4 µl of 6x DNA loading buffer (0.25% w/v bromophenol blue, 15% w/v Ficoll 400) was then added to each tube and the DNA fragments were subjected to gel electrophoresis in a 3% w/v NuSieve GTG [Lonza] + 1% w/v normal agarose

[BMA] gel containing 1x TBE and SYBR Safe [Invitrogen] to visualize DNA. Electrophoresis was performed at 100 V for 1-2 hours and DNA bands were visualized under 320 nm UV light. DNA from *Pax6*$^{Sey\text{-}Neu/+}$ mice produces 3 bands of 223, 141 and 82 bp whereas *Pax6*$^{+/+}$ mice show only one band at 223 bp. *Pax6*$^{Sey/+}$ DNA produces 3 bands at 199, 180 and 19 bp whereas *Pax6*$^{+/+}$ produces a 199 and an 83 bp band.

2.6 β-galactosidase staining

As described elsewhere (Collinson et al., 2002), directly after dissection, eyes were fixed in glutaraldehyde fix solution (0.1 M Na phosphate, 5 mM EGTA pH: 7.3, 2 mM $MgCl_2$ and 0.2% w/v glutaraldehyde) for 2 hours and then washed in X-gal wash buffer (0.1 M Na phosphate, 2 mM $MgCl_2$, 0.01% v/v sodium deoxycholic acid and 2% v/v IGEPAL) 3 times for 20 min. X-gal staining solution (0.1 M Na phosphate, 5 mM potassium ferrocyanide, 5 mM potassium ferricyanide, 0.01% v/v sodium deoxycholic acid, 2% v/v IGEPAL, 2 mM $MgCl_2$ and 1 mg/ml X-gal (5-bromo-4-chloro-3-indolyl-b-D-galactopyranoside) [Bioline]) was then applied to tissues at 37°C overnight. Once the desired degree of staining was achieved, tissues were washed in PBS 3 times for 10 min and post-fixed in 4% w/v PFA in PBS for 2 hours at 4 ^{o}C. Tissues were then washed in PBS, dehydrated through ethanol grade series in isotonic saline (0% v/v, 50% v/v, 70% v/v) and stored in 70% v/v ethanol at 4 ^{o}C. Calibrated digital images were captured with a Nikon Coolpix 995 digital camera mounted on a Wild M5A dissecting microscope.

2.7 Alkaline phosphatase staining

Dissected eyes were punctured at the posterior of the eye with a 23G, 25 mm hypodermic needle [BD Microlance] in order to help reagents to reach the interior of the eye. Eyes were then fixed in glutaraldehyde fix solution (0.1 M Na phosphate, 5

mM EGTA pH: 7.3, 2 mM $MgCl_2$ and 0.2% w/v glutaraldehyde) for 2 hours and then washed twice with PBS for 20 min. Eyes have endogenous alkaline phosphatase activity which has to be abolished. So, eyes were incubated in PBS at 70 ^{o}C for 30 min. Then, samples were washed with AP wash solution (0.1 M Tris-Base pH 9.5, 0.1 M NaCl, 10 mM $MgCl_2$) 3 times for 20 min. BM Purple [Roche] staining solution was then applied to tissues usually overnight. Tissues were washed in PBS 3 times for 10 min and post-fixed in 4% w/v PFA in PBS for 2 hours at 4 ^{o}C. Finally, eyes were washed in PBS, dehydrated through a graded series of ethanol in isotonic saline (0% v/v, 50% v/v, 70% v/v) and stored in 70% v/v ethanol at 4 ^{o}C. Calibrated digital images were captured with a Nikon Coolpix 995 digital camera mounted on a Wild M5A dissecting microscope.

2.8 Embedding eyes in wax blocks & sectioning

Fixed eyes were stored in 70% v/v ethanol at 4 ^{o}C. Before wax embedding, eyeballs were cleared of adjacent tissue (optic nerve, muscle etc) and a cross-shaped cut was made at the posterior part of the eye. The lens was removed through the cut to avoid damaging the microtome blade. Eyes were then put into cassettes and were processed through a routine histological protocol by the histology service lab. Briefly, eyes were dehydrated further by placing them in 85% v/v, 95% v/v and 3 times in 100% v/v ethanol solutions for 15 minutes in each and were dipped in xylene twice for 15 minutes and stored in xylene overnight. For xylene to be displaced, eyes were placed in embedding wax at 60 ^{o}C for 1 hour followed by 2 hours incubation in fresh embedding wax. Wax blocks were created after placing the eyes in wax for a third time, orienting them for longitudinal sections and cooling them. Solid wax blocks containing whole eyes were sectioned in 7 μm thick sections with a Leica Jung Biocut 2035 microtome. Finally, sections were mounted on standard microscope slides by floating them on warm water at 45 °C and slides were air-dried in an incubator at 37 ^{o}C for at least 12 hours.

2.9 Frozen sections

After fixed eyes were washed in PBS, the tissue was cleared with glycerol [Fisher Scientific] in solutions of increasing concentrations (30% v/v, 50% v/v & 80% v/v in PBS) and stored in 80% v/v glycerol in PBS at 4 ^{o}C. Eyes were then re-hydrated in decreasing glycerol concentration solutions and they were washed in PBS 3 times for 15 minutes. Eyeballs were then cleared of adjacent tissue (optic nerve, muscle etc) and a cross-shaped cut was made at the posterior part of the eye. The lens was removed through the cut to avoid damaging the cryostat blade. Tissues were then placed in Peel-A-Way Embedding (Truncated - T8) Molds [Polysciences, Inc] containing Lamb OCT embedding medium [Raymond Lamb Ltd] and they were properly orientated. Dry ice was used to snap freeze the tissues, which were then stored at -20 ^{o}C. Eyes were sectioned with a Leica CM1900 cryostat at 10 μm thickness and sections were placed on polysine microscope slides [VWR].

2.10 Neutral red & eosin counterstaining

Sections of eyes that were stained for β-gal expression in X-gal (section 2.6) were counterstained with 1% w/v neutral red [BDH] (staining nuclei red) and eosin [Surgipath; No.01600] (staining cytoplasm pink) to help the visualization of nuclei and cytoplasm of the observed cells. Sections were de-waxed in Histoclear II [Raymond A Lamb] twice for 5 min and then dipped in 95% v/v ethanol for 1 min and in eosin solution [Surgipath] for 20 sec. Afterwards, slides were rinsed in tap water and counterstained with 1% w/v neutral red (in 1.48 mM acetate buffer pH: 4.8) for 6 min. After rinsing with distilled H_2O, sections were dehydrated through a series of ethanol solutions of increasing concentrations (70% v/v, 95% v/v, 100% v/v). Finally, slides were immersed in xylene twice for 1 min and cover-slipped using DPX [BDH] as mounting medium.

2.11 Whole-mount immunofluorescence

The method used for whole-mount immunofluorescence was adapted from a published protocol (Pal-Ghosh et al., 2004). Dissected eyes were fixed in 4 methanol : 1 DMSO for at least 2 hours at -20 ^{o}C. This fixative is preferred for immunofluorescence staining because, unlike its aldehyde counterparts, it does not create crosslinks between proteins. Thus, it does not need a harsh antigen retrieval step with high temperature, which could damage the structure of the cornea.

Fixed eyeballs were rehydrated through a methanol gradient with consecutively lower methanol concentrations in PBS (70% v/v, 50% v/v, 30% v/v), 30 min in each. Then eyes were washed in PBS for 30 min and the corneal button was dissected from the eye along with the limbus and some conjunctiva, discarding the posterior part of the eye and the lens. Additionally, attention was given to removing as much of the iris, ciliary body and trabecular meshwork as possible because leaving any of these tissues may result in fluorescent light absorption. Corneas were then washed in PBS for 30 min and, only for BrdU immunohistochemistry, a 15 min incubation with 2N HCl at 37 ^{o}C was performed at this point to denature the DNA. Corneal buttons were placed in freshly prepared blocking serum (1% v/v Goat Serum, 1% w/v BSA in PBS containing 0.02% v/v Tween_20) for 2-3 hours and incubated with the primary antibody (or antibodies, in double-labelling experiments) at 4 ^{o}C overnight (for primary antibody specifications and dilutions see Table 2.2). The next day, samples were washed 5 times for 1 hour each in PBS-T (PBS containing 0.02% v/v Tween_20), placed in blocking serum for 2 hours and incubated with the secondary antibody/ies at 4 ^{o}C overnight. The following day, corneas were washed in PBS-T 6 times for 45 min each and counterstained with nuclear counter-stain solution (0.1% v/v TO-PRO3 iodide [Invitrogen] and 10 μg/ml RNase A in PBS-T) for 15 min at 37 ^{o}C. After washing briefly in H_2O (3 times for 5 min) corneas were flattened with radial cuts and mounted on a microscope slide with Mowiol 4-88 Reagent [Calbiochem] containing 2.5% w/v DABCO (1,4-diazobicyclooctane).

For the double immunofluorescent labelling of the corneal buttons for BrdU and blood vessels, a different protocol was followed because both the anti-BrdU and the anti-CD31 antibodies were raised in the same host (rat; see Table 2.2). The amendments of this protocol are detailed in chapter 4, section 4.2.3.

Table 2.2 Specifications of antibodies. Details concerning primary and secondary antibodies used for immunohistochemistry with a fluorescent end-point.

Antibody	Host	Dilution	Source
Ki67	Rabbit	1/200	Abcam
Keratin 5	Rabbit	1/100	Abcam
Keratin 19	Rabbit	1/100	LifeSpan Biosciences
BrdU	Rat	1/750	Abcam
GFP	Rabbit	1/750	Abcam
CD31	Rat	1/50	BD Pharmingen
Alexa 488 Anti-Rat IgG	Goat	1/200	Invitrogen
Alexa 488 Anti-Rabbit IgG	Goat	1/400	Invitrogen
Alexa 568 Anti-Rat IgG	Goat	1/750	Invitrogen

2.12 Confocal imaging & photo editing

2.12.1 General confocal imaging

In order to image whole-mount corneas stained with fluorescent conjugated antibodies, overlapping Z-stacks were obtained with a Leica TCS-NT confocal microscope using the appropriate lasers and filters. The whole width of the corneal epithelium was imaged with sequential scans whenever more than one laser was used to avoid cross-talk between different laser channels. Stacks were obtained consisting of 4 – 8 optical sections in 1024x1024 pixel resolution, and each section was averaged 4 times for every channel. Each stack was then compiled using the free Leica Confocal Software (LCS Lite; Version 2051347a) and projected to a single image based on maximum intensity of each voxel. If overlapping photos were taken from the same cornea, images were imported to ImageJ (a public domain Java image processing program) and the whole cornea was re-assembled using the MosaicJ plug-in. For imaging the cell packing density of the corneal epithelium, single images rather than Z-stacks were obtained, with a x40 oil-immersion objective. Each image was averaged 6 times and 1024x1024 pixel resolution images were acquired.

2.12.2 Confocal imaging for BrdU immunohistochemistry & sampling

For BrdU whole mount immunohistochemistry, corneal buttons had already been dissected and flattened with 8 (for wild-type and *Pax6*$^{+/-}$) or 4 (for *Mp*/+) radial cuts. Eight or four Z-stack images were obtained per eye (1 at each sector) consisting of 5 – 6 optical sections in 2 – 3 μm intervals. Z-stack images always included the limbus and they were taken in a clockwise direction with a Zeiss LSM510 CLSM confocal microscope using a x20 lens. Images were acquired after sequential scans for the two channels (568 for BrdU & 645 for TO-PRO3) at 1024x1024 pixel resolution and the microscope stage was rotated so that the limbus was always in the middle of the

image (Fig. 2.1). Individual photographs were then compiled using the Zeiss LSM Image Browser software (version 4.2.0.121) and projected to a single image based on maximum intensities. Thresholding was then performed in ImageJ based on particle sizes of 150 – 5000 voxels (to include nuclei of 3 – 15 μm in diameter). Finally, images were imported to Adobe Photoshop 7.0 [Adobe Systems Inc] where a 340x200 μm size box was placed on top of the limbus and BrdU-positive nuclei were counted. Fluorescent spots that were outside the size range for BrdU-positive nuclei were not included in the analysis.

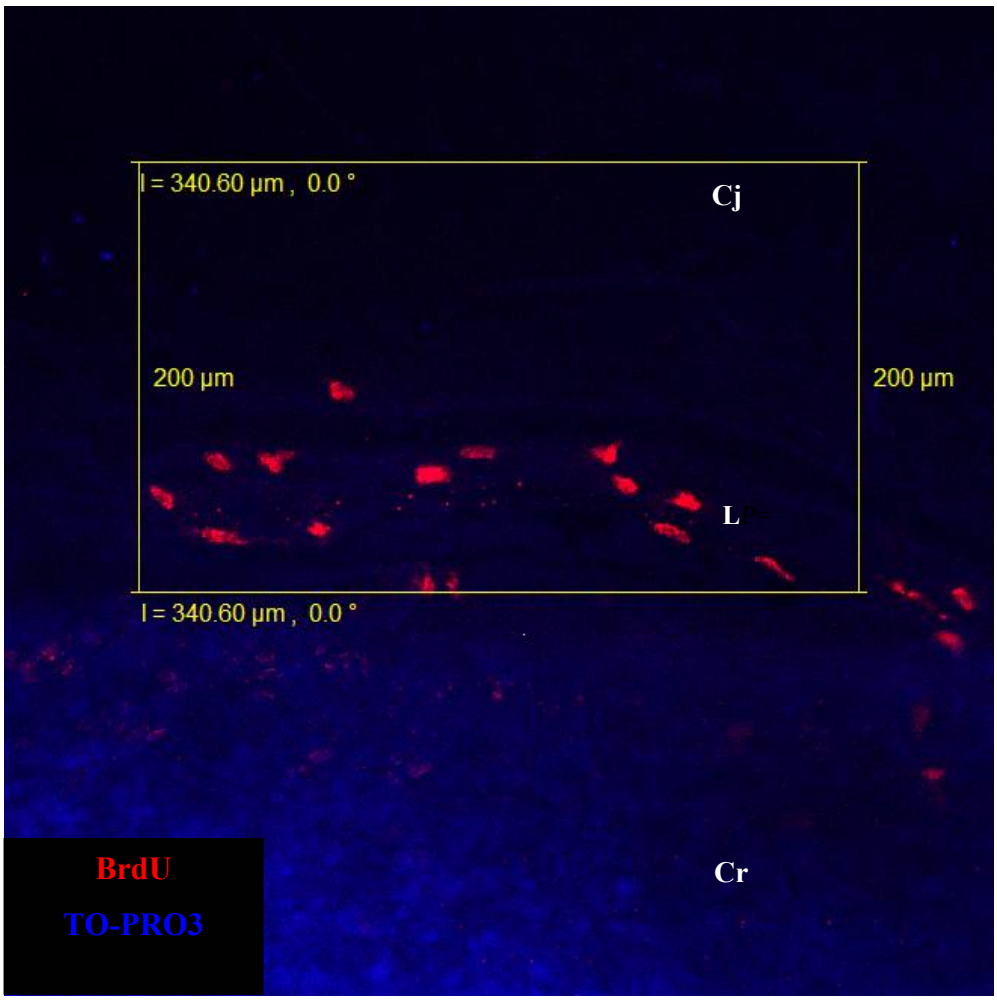

Figure 2.1 Scoring area on a flattened cornea. A representative image showing a sector of a flattened cornea, including BrdU label-retaining cells (Red) in the limbus, with the counting box placed on it. Pixel resolution 1024x1024; Cj: Conjunctiva; L: Limbus; Cr: Cornea.

2.13 H&E staining for histology

Haematoxylin and eosin (H&E) staining was performed on wax sections to aid the identification of cells and their nuclei during histological examination of *Mp/+* mutant eyes. Sections were de-waxed by placing slides into Histoclear II twice for 10 min. Re-hydration of sections was performed by dipping slides twice for 5 min in solutions containing consecutively lower ethanol concentration (100% v/v, 70% v/v) and then placing them in PBS twice for 5 min. Slides were then rinsed in tap water and stained in haematoxylin [Vector] for 2 min. After rinsing slides in tap water, they were immersed 10 times in acid rinse solution (2 ml glacial acidic acid in 98 ml distilled H_2O) followed by 10 dips in tap water. Slides were then incubated in bluing solution (1.5 ml NH_4OH in 98.5 ml 70% v/v ethanol) for 2 min, dipped 10 times in tap water, immersed in eosin solution for 30 sec and washed in tap water. Sections were dehydrated by briefly dipping slides in increasing ethanol-concentration solutions (70% v/v, 80% v/v, 95% v/v, 100% v/v). Finally, slides were immersed in xylene twice for 2 min and cover-slipped using DPX as mounting medium.

2.14 Keratin 5 in situ hybridization

The protocol used was a modified version of a published one (Christiansen et al., 1995). The cDNA template of the probe was produced by PCR amplification of a 404 bp fragment of the *Krt5* gene (Nucleotide BC108361; Fig. 2.2) using primers shown in Fig. 2.2. The reverse primer also contained the additional sequence "GTAATACGACTCACTATAGGG" for T7 RNA polymerase binding (Table 2.1). The DIG-labelled riboprobe was produced after transcribing 10 µl PCR product with 5 U T7 RNA polymerase [Roche], DIG RNA labelling mixture [Roche], appropriate buffer and 40 U RNasin Ribonuclease Inhibitor [Promega] in a 50 µl reaction volume. The reaction took place at 37 ^{o}C for 2 hours and the probe was precipitated after NaOAc and ethanol mixing over dry ice. Tissues that had been dissected in cold PBS, fixed in 4% w/v PFA overnight at 4 ^{o}C and stored in methanol at –20 ^{o}C were

re-hydrated by a methanol/PBTX series for 10 min each. Then they were treated with 20 μg/ml Proteinase K for 20 min, re-fixed in 0.2% v/v glutaraldehyde/4% w/v PFA and placed in pre-hybridisation mix (50% v/v formamide, 5x SSC, 2% w/v Boehringer blocking powder [Roche], 0.1% v/v Triton X-100, 0.5% w/v CHAPS, 50 μg/ml yeast RNA, 5 mM EDTA and 50 μg/ml heparin) at 65 ^{o}C for 24 hours. Then they were incubated with hybridisation mix (pre-hybridisation mix containing 1 μg/ml of the probe) at 65 ^{o}C overnight. After 2-hour-washings with decreasing SSC concentration and 0.1% w/v CHAPS at 65^{o}C, tissues were blocked with 10% v/v sheep serum and 2% w/v BSA solution for 2 hours and sheep anti-digoxigenin-AP Fab fragments were applied overnight at 4 ^{o}C. Finally, tissues were washed for at least 24 hours in TBTX (50 mM Tris-Base pH 7.5, 150 mM NaCl, 0.1% v/v Triton X-100) and colour was developed after incubation with BM Purple [Roche] for 8 hours.

Figure 2.2 The murine keratin 5 gene (Nucleotide BC108361). The 9 coloured sequences indicate the 9 exons of the gene and arrows are placed above the complimentary sequence of each primer used to make the keratin 5 probe. (See also Table 2.1)

2.15 Cell-permeable Cre production and purification

A vector encoding the Cre recombinase fused with a His-tag, an HIV-TAT sequence and a nuclear localization signal (NLS) as protein transduction domains (Peitz et al., 2002) was kindly provided by Dr. Peter Hohenstein (MRC Human Genetics Unit, Edinburgh). It has been reported that these domains increase cellular uptake of the Cre recombinase protein in cultured cells (Peitz et al., 2002; Lin et al., 2004). *Escherichia coli* bacteria of the strain BL21(De3) pLysS [Promega] were transformed and over-expression of the protein was induced with 0.1 mg/ml isopropyl-β-D-thiogalactopyranoside (IPTG) at 25 ^{o}C for 2 hours. Cells were then harvested by centrifugation and frozen in dry ice. Finally, the protein was purified with the QIA*express* Ni-NTA Fast Start Kit [Qiagen] following the protocol for purification of His-tagged recombinant proteins under native conditions according to the manufacturer's instructions.

Figure 2.3 Cell-permeable Cre transgene. A graphical representation of the sequences fused to Cre recombinase to aid cell intake. His: Histidine Tag; TAT: HIV basic TAT peptide; NLS: Nuclear localization signal.

2.16 Cre activity assay

Cre recombinase activity was checked *in vitro* on a linearized plox2+ [New England Biolabs] DNA plasmid, which contains a *LoxP* site 350 bp from each end. In the presence of Cre recombinase a 850 bp fragment is excised and the plasmid becomes circular. The assay was performed in 25 μl reactions containing 2.5 μl of buffer, 1 μl of 125 ng/μl plasmid DNA, 0.5 μl Cre produced in the laboratory and 21 μl H_2O. Commercially available Cre recombinase [New England Biolabs] was used as positive control and a reaction without Cre was used as the negative control. The mixture was then incubated at 37 ^{o}C for 30 min to activate the enzyme. Cre was then deactivated by a 10 min incubation at 70 ^{o}C. Products were then loaded on a 0.8% w/v agarose gel containing ethidium bromide, electrophoresed at 100 V for 1 hour and DNA was visualized under UV light.

2.17 Measurement of cell-permeable Cre concentration

Cell-permeable Cre concentration was measured with Protein Assay Kit [Bio-Rad] according to manufacturer's instructions. For this Bradford-based method, BSA was used as standard and absorption was measured with a Jen Way 6505 UV/Vis. spectrophotometer set to 595 nm. After plotting the standard curve, the concentration of the Cre protein was measured by comparing its absorbance measurements to the standard curve. Two different batches of the cell-permeable Cre were produced and their concentrations were measured as 120 μg/ml and 750 μg/ml, respectively.

2.18 Cre in eye-drops

Purified cell-permeable Cre in various concentrations was used in the form of eye-drops to induce *in vivo* recombination in the eye of reporter mice (e.g. Z/AP mice).

Mice were either restrained manually or anaesthetised with Hypnorm/Hypnovel [Pfizer] mixture and 5 – 25 μl of the cell-permeable Cre were applied directly onto the corneas in 1 – 5 μl volume per minute. In a different set of experiments, mice were anaesthetised with ketamine/medetomidine [Pfizer] mixture and proparacaine [Pfizer] was applied to the corneas 15 minutes later to dry the eye out and permit the Cre solution to penetrate the cornea, which was applied 5 minutes later at a rate of 1 – 5 μl per minute. Finally, mice were injected with atipamezole [Pfizer] to reverse the anaesthetic.

2.19 Tamoxifen injections

Tamoxifen was dissolved at 10 mg/ml or 50 mg/ml concentrations in corn oil and a Diagenode Bioruptor sonicator was used to dissolve it completely. Several different volumes of tamoxifen solution were injected intraperitoneally into mice expressing both the Cre/ER^{TM} and Z/AP transgenes (section 2.1), with average weights of 25 – 30 gr. Mice were then left for different periods of time (chasing period), during which time the cells with Cre-mediated *LoxP* sites in the cornea should be shed, so that only cells that were produced by a limbal stem cell with recombined *LoxP* sites should be identifiable in the corneal epithelium as expressing the alkaline phosphatase reporter transgene.

2.20 Statistical analysis

Statistical tests were performed using Microsoft Office Excel 2002 SP3 [Microsoft] and the statistical packages StatView 5.0 [SAS Institute Inc] and SigmaStat 3.1 [Systat software Inc.]. The Kolmogorov–Smirnov normality test (SigmaStat 3.1) was used to check whether data fitted a normal distribution to help decide which statistical test to use. Parametric tests were used to compare normally distributed data. Specifically, t-tests were used for pairwise comparisons using Excel and more

than two sets of data were compared with ANOVA test followed by Bonferroni/Dunn post-hoc tests for the statistically significant comparisons, available on the StatView statistical package. If at least one of the data sets under comparison were shown to have non-normally distributed data, non-parametric tests instead of parametric were used, because the latter assume that data are normally distributed. If that was the case, comparisons between two sets of data were performed with Mann-Whitney U-tests whereas comparisons of more than two data sets were performed using the Kruskal-Wallis test followed by pairwise Mann-Whitney U-tests for the significantly different comparisons. Both tests are available on StatView. Finally, all graphs were made in Excel and although the error bars are always 95% confidence intervals, in the text, the data are summarised as mean ± standard error of the mean.

Chapter 3
Analysis of Patches in the Corneal Epithelium of X-Inactivation Mosaics

3.1 INTRODUCTION

It is widely known that one of the two copies of the X chromosome present in female mammals is inactivated in order to compensate for gene dosage. This inactivation event is random in placental mammals like mice and humans and it was first proposed by Mary F. Lyon in 1961 (Lyon, 1961). Tam et al. produced transgenic mice that express nucleus-localized β-gal under the constitutive promoter of the housekeeping gene HMG-Co A (3-hydroxy-3-methylglutaryl coenzyme A) reductase in order to identify cell fates in mouse embryos by transplantation (Tam and Tan, 1992). However, the transgene integrated in a region of the X chromosome and was subjected to X-chromosome inactivation (Tan et al., 1993) in females, creating "X-chromosome inactivation mosaics". Such mosaics have previously been used to visualize cell lineages and cell migration in a wide variety of cell populations like Purkinje cells (Baader et al., 1996), cells in the murine retina (Reese et al., 1999), cerebral cortex (Tan et al., 1995) and adrenals (Morley et al., 2004).

In an attempt to visualize cell lineages and migration pathways in the corneal epithelium, previous work of the laboratory had utilized X-inactivation mosaics and $LacZ^{-} \leftrightarrow LacZ^{+}$ chimaeras which were produced by aggregating eight-cell ROSA26$LacZ^{+/+}$ embryos and $LacZ^{-/-}$ embryos (Collinson et al., 2002). Results from both techniques have shown that corneal maturation continues well into adult life of the mouse. Specifically, it was demonstrated that until 5 weeks of age, mosaicism in the corneal epithelium appeared as a random, speckled pattern of blue and white patches. At 5 weeks of age, the first evidence of stripe formation appeared at the periphery of the corneal epithelium, suggesting that LSCs are active at this stage of

development (Collinson et al., 2002). At 8 weeks of age, the first stripes reached the middle of the cornea and hence, stripes which extended throughout the whole radius of the cornea could be observed. After the establishment of the stripy pattern, variation in stripe number (corrected for the effects of differences in the percentage of β-gal positive cells) can be used to compare limbal stem cell function in different groups. For example, the corrected stripe number was found to decline with age, suggesting that stem cell function also declined with age (Mort et al., 2009). The observed stripe number was corrected because the stripe widths and stripe numbers are affected by the proportions of β-gal positive and β-gal negative cells, so comparisons of the uncorrected, observed stripe number may be misleading. That is, if two or more stripes of cells with the same phenotype (e.g. β-gal positive) are adjacent to each other, they will be mistakenly counted as one stripe. The correction removes variability in the number of stripes that is attributed to variation in the proportion of β-gal positive cells in the corneal epithelium and allows comparison of corneas with different proportions of β-gal positive cells (West et al., 1997; Collinson et al., 2002; Mort et al., 2009).

Chimaeras and X-inactivation mosaics were also used to track migration of corneal epithelial cells in *Pax6*$^{+/-}$ mice (Collinson et al., 2004a). Both methods showed that *Pax6*$^{+/-}$ and their wild-type littermates demonstrate the same speckled pattern of blue and white cells at 3 weeks of age which then resolves to a stripy pattern. Analysis of corrected patch sizes in intact corneas from 3 weeks old X-inactivation mosaics suggested that patches were larger in *Pax6*$^{+/-}$ than in wild-type corneas. Although this kind of analysis might be inaccurate if mosaic patterns in different epithelial layers were not perfectly aligned at this age, abnormalities were clear in older *Pax6*$^{+/-}$ corneas. After stripes were fully established, around 12 weeks of age, corneas of *Pax6*$^{+/-}$, X-inactivation mosaics showed a disorganized stripy pattern and the corrected stripe number was reduced, even after taking into account the smaller eye size of these mice. This abnormal cell migration was shown to be rescued in *Pax6*$^{+/-}$, *LacZ*$^{+}$ ↔ *Pax6*$^{+/+}$, *LacZ*$^{-}$ chimaeras, revealing a non-autonomous function of *Pax6*, but *Pax6*$^{+/-}$ cells contributed less to the corneal epithelium than to other tissues

that did not express *Pax6*, suggesting that *Pax6*$^{+/-}$ stem cells were deficient.

The finding that corrected stripe numbers in the corneal epithelium were lower in *Pax6*$^{+/-}$ mice and in older mice may indicate that LSCs are reduced in number or show reduced function. However, the reduced corrected stripe number in *Pax6*$^{+/-}$ corneas could also be explained by an alternative hypothesis (Fig. 3.1). Specifically, if during development there was less cell mixing in the ocular surface of *Pax6*$^{+/-}$ mice, mosaicism in the limbal epithelium would be more coarse-grained than in wild type mice. In this case, clonally related LSCs would be more likely to be adjacent to each other, producing larger and fewer stripes in the mature corneal epithelium.

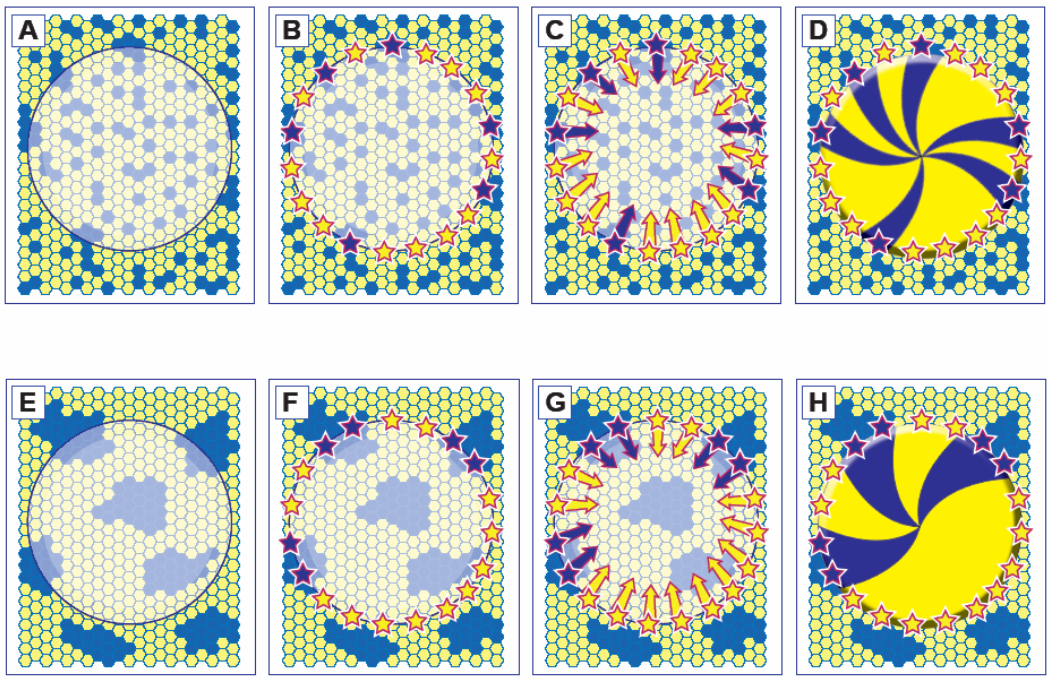

Figure 3.1 Diagram showing the formation of stripes on the corneal epithelium. Schematic representation of the alternative hypothesis to explain the higher corrected stripe numbers in wild-type corneal epithelium (A - D) than in *Pax6*$^{+/-}$ (E - H). (A & E) Mosaicism in the ocular surface. (B & F) Stem cell specification in the limbal epithelium. (C & G) Limbal stem cell activation. (D & H) Tissue maintenance. Stars and arrows represent limbal stem cells and their progeny respectively. Figure from Mort et al. (2009).

3.1.1 Aims

The first aim of this chapter was to investigate if there is any difference in cell mixing between *Pax6*$^{+/-}$ and wild-type corneal epithelia by comparing the size of the patches in the ocular surface before the emergence of the stripes. If the corneal epithelium in *Pax6*$^{+/-}$ is more coarse-grained than in wild-type mice, it would provide a developmental explanation for the observed lower corrected stripe number in *Pax6*$^{+/-}$ eyes that would not imply an impairment of LSC function (Fig. 3.1 E – H). The second aim was to compare patterns and timing of stripe formation in *Pax6*$^{+/-}$ and wild-type mice before the initiation of stripes (3 weeks), while the first stripes appear (6 weeks) and after the first stripes reach the centre of the cornea (10 weeks).

3.2 MATERIALS & METHODS

3.2.1 Animals

For the experiments described in this chapter, X-inactivation mosaics were used, which were produced by crossing hemizygous *XLacZ*$^{+}$/Y, H253 males to *Pax6*$^{Sey\text{-}Neu/+}$ mice. Female offspring were obligatory *XLacZ*$^{+/-}$, X-inactivation mosaics, of which 50% were wild-type and 50% were *Pax6*$^{Sey\text{-}Neu/+}$. Furthermore, in order to control for the small eye size of the *Pax6*$^{+/-}$ mice, hemizygous *XLacZ*$^{+}$/Y, H253 males were also crossed to *Mp*/+ females and results from *Mp*/+ *XLacZ*$^{+/-}$ X-inactivation mosaics were compared to their wild-type *XLacZ*$^{+/-}$ littermates. The different female genotypes produced by each cross were distinguished by PCR, as described in section 2.5 (for more information about the parental mouse lines see section 2.1).

3.2.2 Processing of eyes

Eyes from X-inactivation mosaic females were dissected and stained for β-gal activity (see sections 2.3 & 2.6). Then they were embedded in wax, sectioned with a microtome at 7μm thickness and mounted on slides (see section 2.8). The slide with sections closest to the middle of the cornea was then counterstained with Neutral Red (stains nuclei red) and Eosin (stains cytoplasm pink), to help the counting of β-gal positive cells at the basal layer of the corneal epithelium, and mounted with DPX (see section 2.10).

3.2.3 Data collection & statistics

Slides were checked under a microscope for eye abnormalities and the section from the middle of the cornea was then identified. The overall appearance of β-gal negative cells on each section was evaluated, because there was usually some leakiness of the β-gal staining outside the nucleus in the basal cells (Fig. 3.2), probably because of the embedding procedure. Cells in the basal layer of the corneal epithelium were scored as blue or red, depending on the expression of β-gal, under the microscope with a x40 objective. All basal cells were scored across the diameter of the corneal epithelium and the numbers of cells in alternate β-gal positive and β-gal negative patches were recorded in a spreadsheet. The total number of basal cells across the corneal diameter, the total number of patches and the % β-gal positive cells were calculated, along with the number of patches, mean patch length and median patch length, which were calculated separately for the β-gal positive and β-gal negative cell populations.

The rationale for making all these measurements is based on the hypothesis that if daughter cells of a dividing corneal epithelial cell stay together, they will form a "coherent clone" of either β-gal positive or β-gal negative cells, depending on the genotype of the dividing cell. The sizes and the numbers of the different coherent clones in the dividing (basal) layer of the corneal epithelium will depend on the extent of cell mixing during corneal development. The sizes of the patches will depend on both the size of the coherent clones and the percentage of β-gal positive cells. For one-dimensional strings of β-gal positive and β-gal negative cells, the number of β-gal positive coherent clones per patch of β-gal positive cells can be estimated as $1/(1-p)$, where p is the proportion of β-gal positive cells (Roach, 1968; West, 1976). Thus, the mean patch length was corrected by dividing it by the function $1/(1-p)$, to derive a 'corrected mean patch length'. This provides a measure for comparing patch sizes among mosaics which have different percentages of β-gal positive cells (West et al., 1997). An alternative measure that has been suggested (Schmidt et al., 1986) for comparing patch lengths is the uncorrected median patch

length when calculated for the minority cell population (e.g. the patches of β-gal negative cells when the β-gal positive cells comprise more than 50% of the tissue under examination). So both the uncorrected median patch length for the minority cell type and the corrected mean patch lengths for the β-gal-positive cells were calculated.

Statistical analysis was performed as described in section 2.20. Most of the data were compared with non-parametric tests because they were found to have at least one set with non-normally distributed data. The only comparison with data normally distributed was for the mean number of patches between the periphery and the centre of the wild-type corneal epithelium at different ages. For these pairwise comparisons, t-tests were performed using Excel.

3.3 RESULTS

H253 male mice were crossed to *Pax6*$^{Sey\text{-}Neu/+}$ females to produce *Pax6*$^{Sey\text{-}Neu/+}$ and wild-type *XLacZ*$^{+/-}$, X-inactivation mosaics. In a separate experiment, H253 males were crossed to *Mp*/+ females to produce *Mp*/+ and wild-type *XLacZ*$^{+/-}$, X-inactivation mosaics. As mentioned before (see section 2.1), the *Mp* mice were used as controls for eye size, since they have small eyes like the *Pax6*$^{+/-}$ whist the *Pax6* gene has no mutations. Histological examination also showed that *Mp*/+ mice had normal corneas (Fig 3.2). Both *Pax6*$^{+/-}$ and *Mp*/+ X-inactivation mosaics along with their wild-type littermates were culled at 3, 6 and 10 weeks of age. Data from the 3 weeks old mice were used to test for differences in the extent of cell mixing between *Pax6*$^{+/-}$ and wild-type mice before the stripes emerge. The other age groups were used to compare the time when β-gal positive stripes were formed in the corneas of mutant mice and their wild-type littermates.

Eyes from 5 or more (n= 5 – 9) animals at each age and genotype were used and only one eye per animal was scored. Nuclei in the central section of each eye (Fig. 3.3) in the basal layer of the corneal epithelium were counted and recorded as blue (β-gal positive) or red (β-gal negative) across the diameter of the cornea.

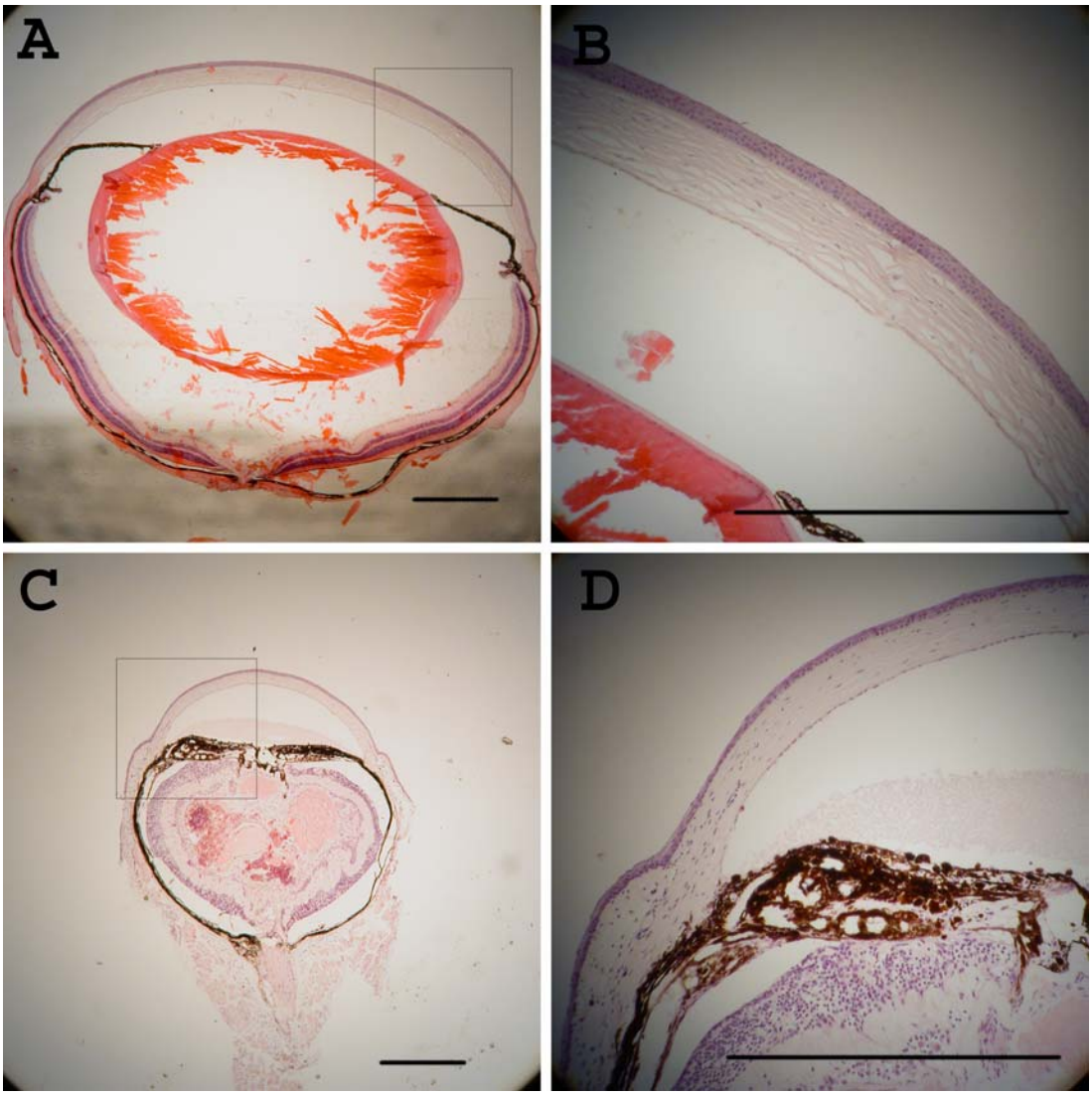

Figure 3.2 Wax sections of adult eyes from (A & B) a wild-type and (C & D) an *Mp*/+ mouse. It is evident that *Mp*/+ eyes are a lot smaller than the wild type eyes and have many abnormalities in the lens and the retina but the corneal epithelium seems normal. The abnormal appearance of the wild-type lens in (A & B) is a technical artefact. The lens has shattered during sectioning, so much of it is missing. B & D are higher magnifications of the areas indicated by squares in A & C respectively. Sections were H&E stained. Scale bars are 1 mm.

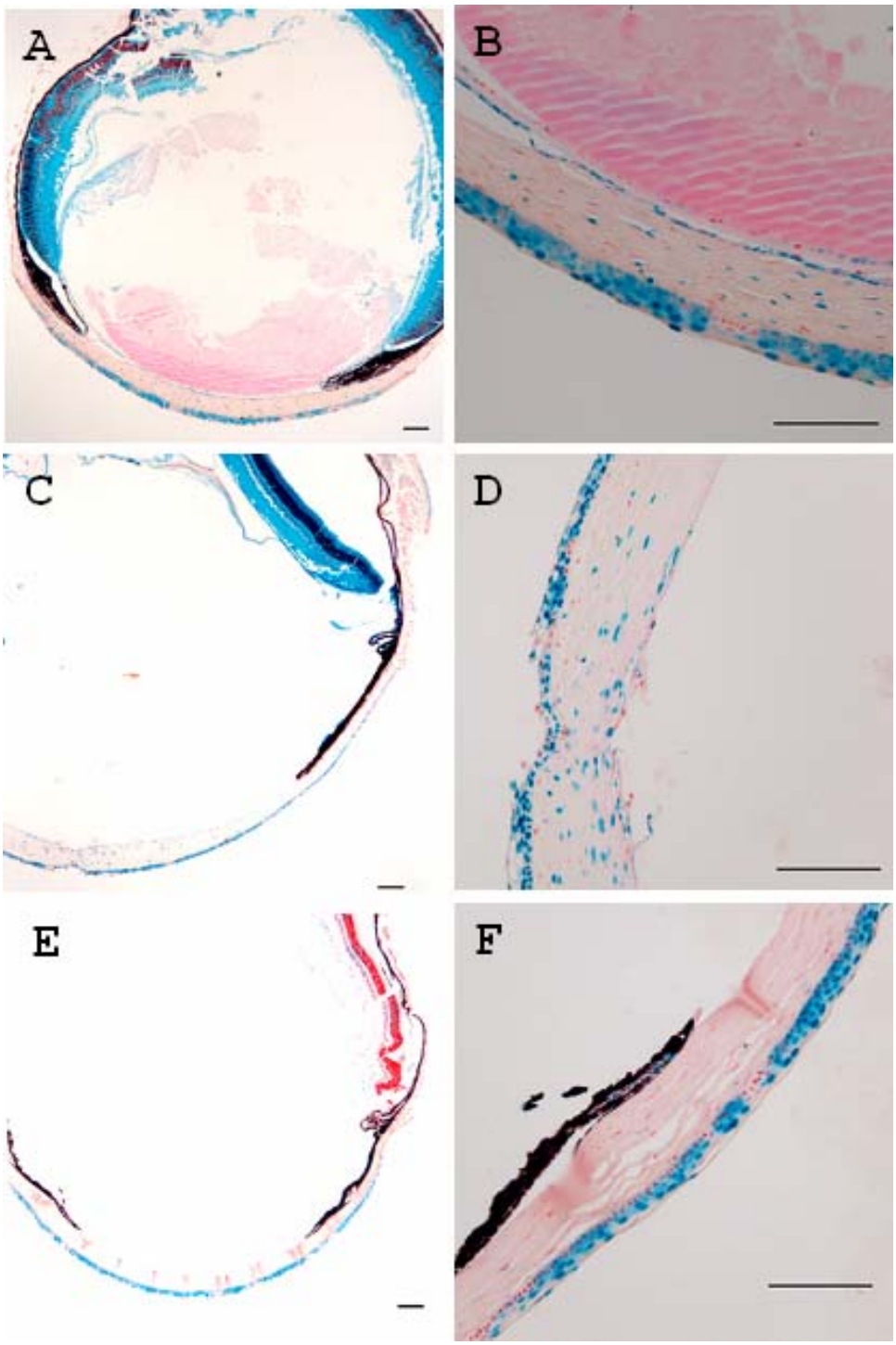

Figure 3.3 β-gal positive and negative patches in the basal layer of the corneal epithelium. Representative images from middle sections of *Mp/+* (A & B), *Pax6*$^{+/-}$ (C & D) and wild-type (E & F) *XLacZ*$^{+/-}$ X-inactivation mosaic eyes from 3-week old mice, demonstrating blue and red nuclei in the corneal epithelium. (B, D & F) High magnification versions of the images shown in (A), (C) & (E) respectively. Eyes were X-gal stained for β-galactosidase activity and counterstained with Neutral Red and Eosin. Scale bars are 0.1 mm.

3.3.1 Comparison of patch sizes at 3 weeks of age

To test whether the speckled mosaic pattern was more coarse grained in the *Pax6*$^{+/-}$ corneal epithelium than in wild-type controls, before the corneal epithelial stripes emerged, the corrected mean patch lengths and the uncorrected median patch length in the basal corneal epithelium were compared by Mann-Whitney U-tests for *Pax6*$^{+/-}$ and wild-type X-inactivation mosaic eyes at 3 weeks. Contrary to what was predicted by the alternative hypothesis (Fig. 3.1), the corrected mean patch length (calculated for the β-gal positive cells) in 3-week old mice (Fig. 3.4 A) was smaller, not greater in the basal corneal epithelial layer in *Pax6*$^{+/-}$ (n=6; mean ± standard error of the mean = 2.04±0.17 cells) than in wild-type mice (n=6) from the same cross (2.79±0.15 cells) and this difference was statistically significant by Mann-Whitney U-test (P=0.016). Fig. 3.4 B shows a similar difference that was observed for the median patch lengths (calculated for the minority cell population) for *Pax6*$^{+/-}$ (1.83±0.31) compared to wild-type corneas (3.00±0.37; P=0.044). This shows that before the emergence of the stripes, the mosaic pattern is not more coarse-grained in *Pax6*$^{+/-}$ corneal epithelium. If anything, cells are more finely mixed, which might reflect reduced cell adhesion between *Pax6*$^{+/-}$ cells. This implies that the reduced number of corrected stripes reported for adult *Pax6*$^{+/-}$ *XLacZ*$^{+/-}$, X-inactivation mosaics is not a result of reduced cell mixing during development.

On the other hand, comparison of *Mp/+* (n=7) and wild-type (n=7) corneas from the same cross showed no significant differences for either the corrected mean patch length (3.24±0.23 for *Mp/+* and 4.23±0.83 for wild-type; Fig. 3.4 C) or the uncorrected median patch length (3.71±0.42 for *Mp/+* and 4.50±0.81 for wild-type; Fig. 3.4 D). This control result suggests that the observed difference in patch size between *Pax6*$^{+/-}$ and wild-type animals at 3 weeks is not affected by the small size of the eyes in *Pax6*$^{+/-}$ mice.

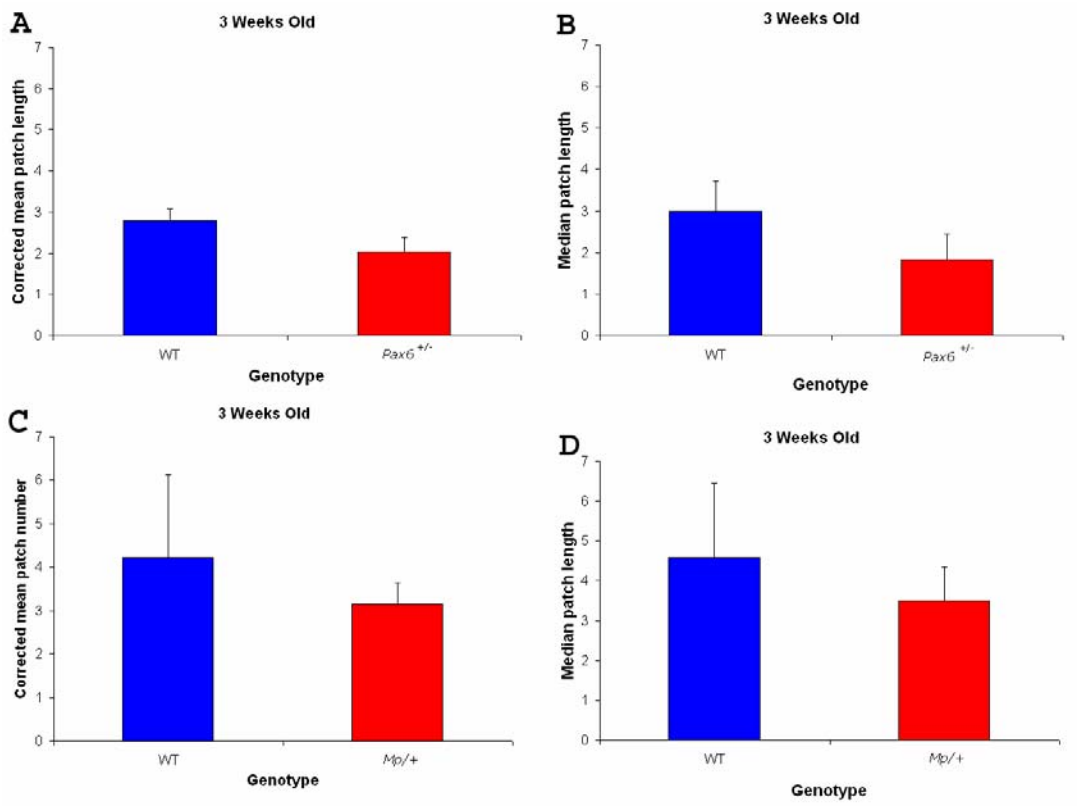

Figure 3.4 Comparisons of patch lengths in the basal corneal epithelium of *Pax6*$^{+/-}$ or *Mp*/+ mice with their respective wild-type littermates at 3 weeks of age. (A & B) The corrected mean patch length and uncorrected median patch length in wild-type corneas are both larger than in *Pax6*$^{+/-}$. This suggests there is a more finely mixed speckled mosaic pattern in *Pax6*$^{+/-}$ eyes before the emergence of stripes. (C & D) No statistically significant difference could be observed between *Mp*/+ and wild-type animals for either corrected or median patch lengths in eyes from 3 weeks old *XLacZ*$^{+/-}$, X-inactivation mosaics. Patch length units are in cell numbers.

3.3.2 Growth and patch number with age

Under normal circumstances, the eye is still growing during the age range under examination for these experiments. So, as shown in Fig. 3.5 A & C, the number of cells across the diameter of the eye increased with age for both groups of wild-type eyes. These overall increases were statistically significant by Kruskal-Wallis test (P=0.001 and P=0.003 respectively). Kruskal-Wallis tests were followed by Mann-Whitney U-tests, which showed that cell numbers differed significantly for all the pairwise age combinations for the wild-type corneas from both crosses. The same was true for the *Pax6*$^{+/-}$ eyes, where a significant overall increase in total basal cell number (P=0.003) was followed by significant differences between all age combinations. *Mp*/+ eyes, on the other hand, did not demonstrate any significant growth over the age range examined in this project (P=0.419). This is in accordance with the consistently very small size of these eyes at all ages.

Also, as the eye increases in size, the overall mean number of patches decreases significantly (P=0.047) in wild-type corneal epithelia in the cross shown in Fig 3.5 B. This, result implies that patch numbers decrease while cell numbers are increasing and so demonstrates the establishment of the stripy pattern, as it replaces the random "speckled" mosaic. The subsequent Mann-Whitney U-tests revealed that the only significant difference was between 3 and 10 week old corneas (P=0.025). Although there is also a tendency for a decrease in the mean number of patches for the *Pax6*$^{+/-}$ eyes, Kruskal-Wallis test showed that there was no overall significant difference in the mean number of patches (P=0.483). This suggests that in the *Pax6*$^{+/-}$ eyes although the eye continues to grow, stripe formation either fails or is less pronounced in the corneal epithelium of these mice. The mean number of patches in the *Mp/+* cross was maximal at 6 weeks for both the wild-type and the *Mp/+* corneas (Fig. 3.5 D). The reason why this differed from the distribution of the wild-type eyes in the *Pax6*$^{+/-}$ cross (Fig. 3.5 B) is unclear and these experiments would have to be repeated before conclusions were drawn. One possibility is that, as mentioned in section 2.1,

although *Pax6*$^{+/-}$ mice are congenic on the CBA/Ca genetic background, mice from the *Mp/+* colony are only partially congenic (five generations of backcrosses) and the different background might be responsible for such discrepancies. However, after statistical analysis, the differences in the mean number of patches among ages were found not to be significant for the wild-type eyes (P=0.215). On the other hand, the mean number of patches in the *Mp/+* corneas differs significantly across ages (P=0.003). The subsequent Mann-Whitney U-tests demonstrated a significant decrease between 3 and 10 weeks old eyes (P=0.004), as well as between 6 and 10 weeks old (P=0.009). The increase in patch numbers between 3 and 6 weeks old *Mp/+* mice was not quite significant (P=0.051).

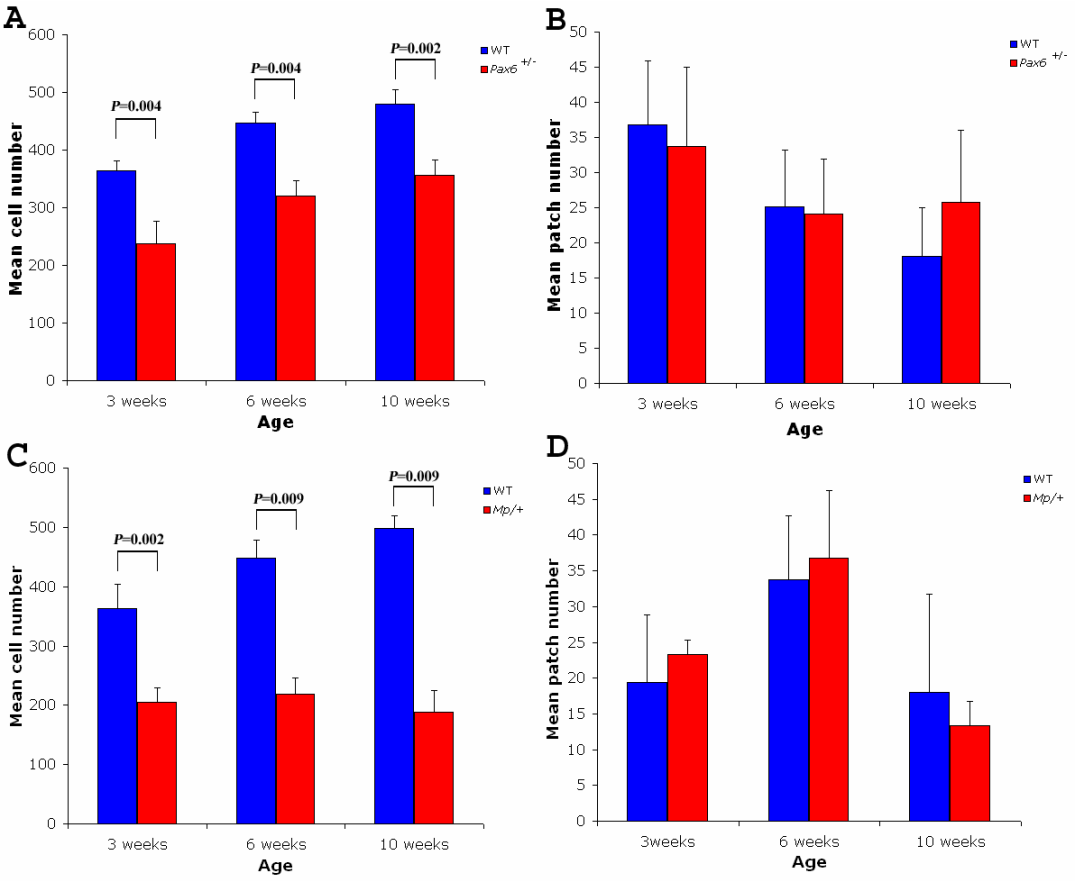

Figure 3.5 Mean number of cells and mean number of patches in the corneal epithelium of *Pax6*$^{+/-}$ and *Mp/+* compared with their wild-type littermates at different ages. (A & B) In wild-type animals the mean number of cells increases significantly with age (*P*=0.001) whilst the mean number of patches decreases (*P*=0.047), consistent with the establishment and elongation of stripes. In *Pax6*$^{+/-}$ eyes, although the corneas continue to grow (*P*=0.003), there is no significant difference in the patch number. (C & D) Cell numbers across the basal layer of the corneal epithelium increase significantly across ages only for the wild-type group (*P*=0.003) while patch numbers do not differ significantly. Conversely, in *Mp/+* the number of cells does not change significantly with age whilst patch numbers differ among ages, overall (*P*=0.003). Significant pairwise comparisons between genotypes are shown in the figure and pairwise comparisons for the same genotype at different ages are discussed in the text.

3.3.3 Comparison of patch lengths among different ages

To test when the pattern of mosaic patches was replaced by stripes, apart from the total cell and patch number that have already been presented (section 3.3.2), the corrected mean patch lengths and uncorrected median patch lengths were also compared at three ages for two genotypes from each of two genetic crosses, producing respectively *Pax6*$^{+/-}$ and *Mp/+* mice (Fig 3.6). As discussed before, stripes are expected to emerge around 5 weeks of age (see section 3.1). The Kruskal-Wallis test revealed a significant change in corrected mean patch length with age for *Pax6*$^{+/-}$ (P=0.003) and their wild-type littermates as well (P=0.016; Fig. 3.6 A). Pairwise comparisons showed a significant increase in the corrected mean patch lengths between 3 and 6 weeks old for both *Pax6*$^{+/-}$ (n=6; P=0.004) and their wild-type littermates (n=6; P=0.010). The same was true for comparisons between 3 and 10 weeks of age (P=0.004 and P=0.013 for *Pax6*$^{+/-}$ and wild-type eyes respectively). This result can be explained by the emergence of a stripy pattern in the corneal epithelium of both genotypes, as radial stripes would be aligned approximately parallel to the plane of section for the middle section. However, there was a trend for a further increase in the corrected mean patch length for the wild-type eyes at 10 weeks (n=9; although not statistically significant) but not in eyes from the *Pax6*$^{+/-}$ mice (n=6; Fig. 3.6 A). This discrepancy between *Pax6*$^{+/-}$ and their wild-type littermates is consistent with the mean patch number data presented previously and suggests that in wild-type eyes, the stripes continue to grow until they reach the centre of the eye at 10 weeks old whereas, in *Pax6*$^{+/-}$ eyes, although the patches are getting bigger the stripy pattern is disrupted. These results are in accordance with 2-dimensional mosaic patterns seen in whole-mount corneas (Collinson et al., 2004a; Collinson et al., 2002).

In the *Mp/+* cross, the corrected mean patch length differed significantly with age for both *Mp/+* and their wild-type littermates (P=0.007 and P=0.032 respectively; Fig. 3.6 C). Pairwise comparisons with Mann-Whitney U-tests reveal significant increases in the corrected mean patch length for both genotypes between 3 and 10 weeks (P=0.012 for *Mp/+* and P=0.019 for wild-type), similar to the observations for

the *Pax6*$^{+/-}$ cross. Additionally, for the *Mp*/+ there is also significant difference between 6 and 10 weeks old mice (*P*=0.009), whereas in wild-type mice the trend for an increase was not significant because the corrected patch length appeared quite variable at 10 weeks (Fig. 3.6 C). This suggests that although *Mp*/+ corneas do not appear to grow between 3 and 10 weeks (Fig. 3.5 C), they demonstrate the same pattern of stripe formation as that seen in the corneal epithelium of wild-type eyes, implying that eye-size is not affecting the observed corrected mean patch length.

Results for the uncorrected median patch length showed similar trends to the corrected mean patch length for both crosses (Fig. 3.6 B & D). Specifically, median patch lengths for the mutant corneas from both crosses were found to differ significantly with age (*P*=0.037 for *Pax6*$^{+/-}$ and *P*=0.017 for *Mp*/+). As in the case of corrected mean patch length, significant increases in median patch length were found between 3 and 10 weeks old corneas (*P*=0.020) as well as between 3 and 6 weeks old (*P*=0.037) *Pax6*$^{+/-}$ and for the *Mp*/+ between 3 and 10 (*P*=0.017) and between 6 and 10 weeks of age (*P*=0.019). However, although the median patch lengths, like the corrected mean patch lengths, increased with age in the wild-type animals from both crosses the trends for median patch lengths were not significantly different.

Comparisons between genotypes showed that at 3 weeks the corrected mean patch length and the median patch length were significantly lower for *Pax6*$^{+/-}$ than wild-type corneas (Fig 3.6 A & B), as discussed in section 3.3.1 (Fig 3.4 A & B). While there were no comparable significant differences between *Mp*/+ and wild-type corneas at 3 weeks both the corrected mean patch length and the median patch length were significantly lower in *Mp*/+ than wild-type corneas at 6 weeks. This coincides with the unexplained peak in patch numbers at 6 weeks that is mentioned above.

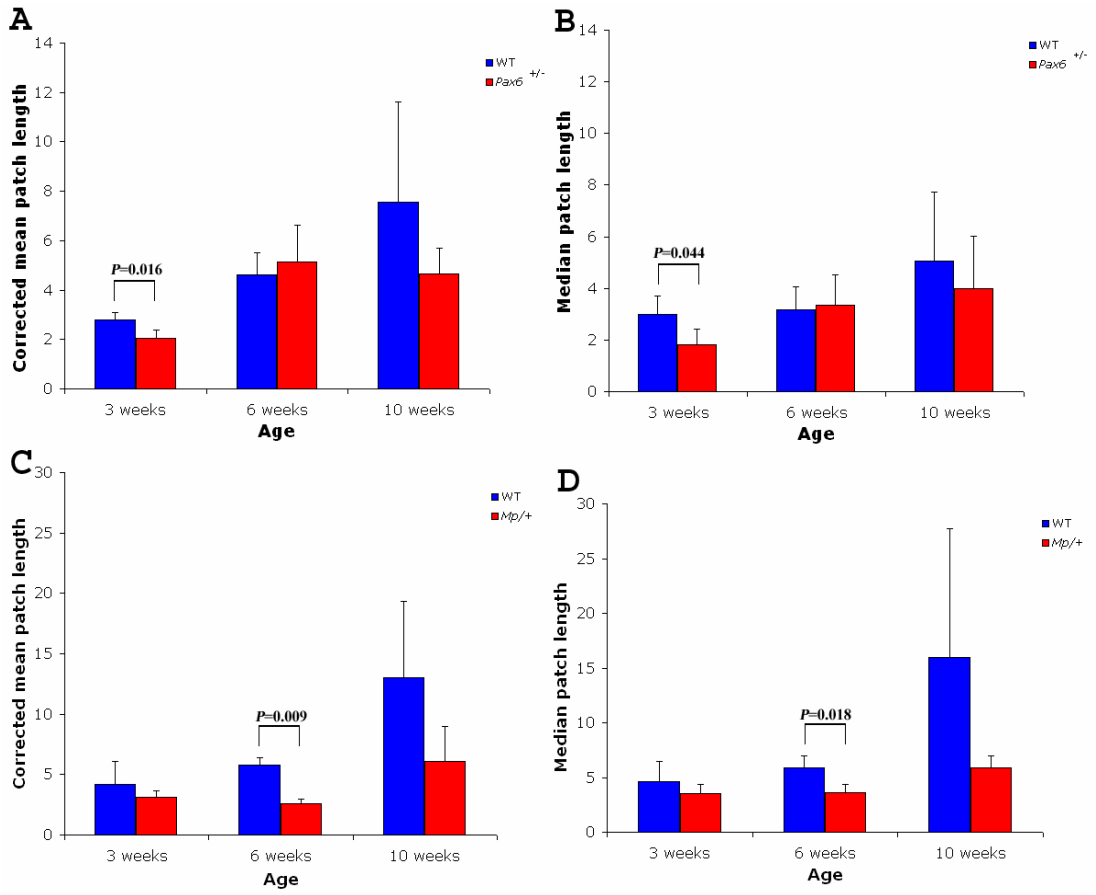

Figure 3.6 Comparison of corrected mean patch length and uncorrected median patch length between *Pax6*$^{+/-}$ or *Mp*/+ with their respective wild-type littermates at different ages. (A) There is a significant overall increase in corrected mean patch length with age for both *Pax6*$^{+/-}$ (*P*=0.003) and wild-type corneas (*P*=0.016). However, trends show that the increase is sustained until 10 weeks of age only for the wild-type eyes and not for the *Pax6*$^{+/-}$. (B) Although the trends show a general increase in median patch length for both genotypes, only *Pax6*$^{+/-}$ were found to change significantly (*P*=0.037). (C) There is a significant increase in corrected mean patch length with age for both *Mp*/+ (*P*=0.007) and their wild-type littermates (*P*=0.032) suggesting that *Mp*/+ behave like their wild-type counterparts. (D) Again, although trends show an increase in median patch length, only *Mp*/+ eyes were found to change significantly with age (*P*=0.022). Significant pairwise comparisons between genotypes are shown in the figure and pairwise comparisons for the same genotype at different ages are discussed in the text. Patch length units are in cell numbers.

3.3.4 Emergence of stripes in wild-type corneas

If a decrease in the number of patches indicates the formation of stripes, the direction of stripes (centrifugal or centripetal) in wild-type eyes can be predicted by checking if the number of patches decreases first in the centre of the cornea and then continues at the periphery or vice versa. Thus, cells at the basal layer of each wild-type eye from the cross between *Pax6*$^{+/-}$ and wild-type mice were counted and then divided into 4 regions. Patches found in region numbers 1 and 4 were considered to belong at the periphery of the corneas whereas those in regions 2 and 3 represent centrally located patches. The total, uncorrected, mean patch number for these regions of each eye was calculated including both β-gal-positive and β-gal-negative patches and plotted (Fig. 3.7). Since data were found to be normally distributed, t-tests were used to address pairwise statistically significant differences. As shown below in Figure 3.7, the number of patches in the periphery was found to be significantly reduced between 3 and 6 weeks of age (P=0.014) and between 3 and 10 weeks (P=0.003). In the centre, the statistically significant decrease is only between 3 and 10 weeks of age (P=0.026), suggesting a delay in the reduction of patch number at the centre of the corneal epithelium. These data provide indirect evidence that stripes emerge in a centripetal direction, supporting the limbal location of the stem cells responsible for renewing the corneal epithelium.

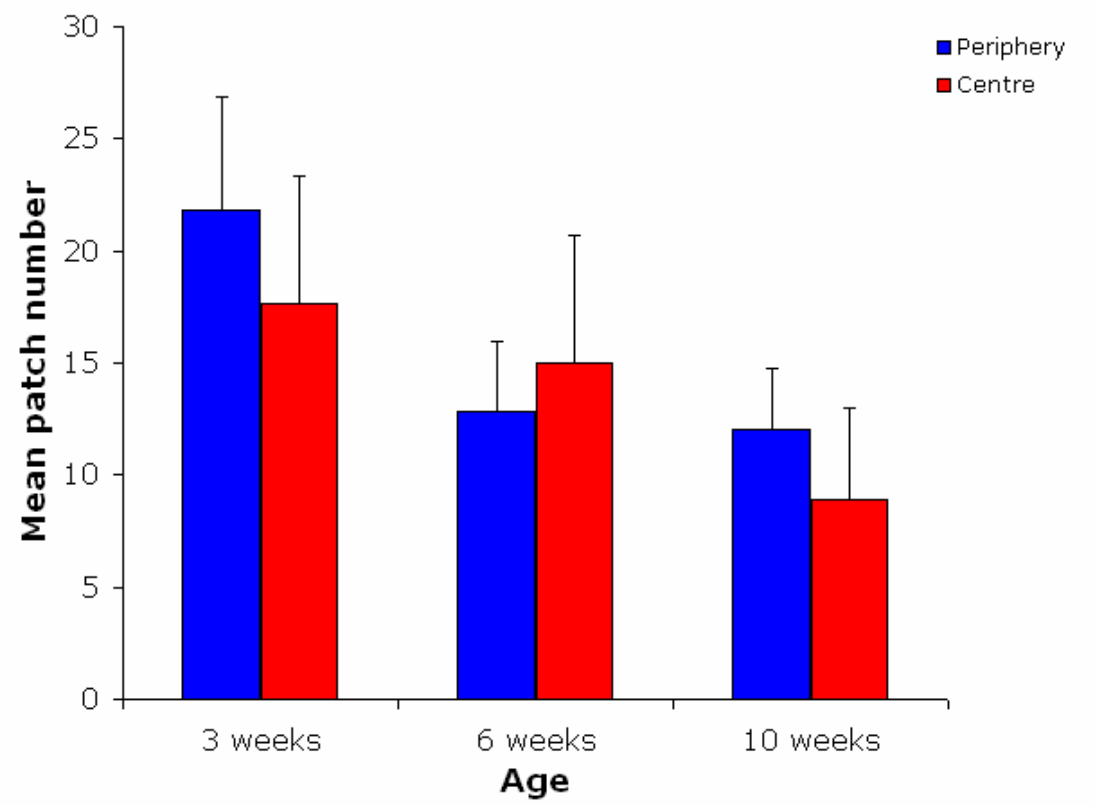

Figure 3.7 Comparison of the mean number of patches from the periphery and the centre of the corneal epithelium of wild-type mice at different ages. A decrease in the mean number of patches is evident from 3 weeks of age in the periphery whereas a statistically significant decrease for the centre of the corneal epithelium can only be observed at 10 weeks old eyes, suggesting centripetal movement of stripes. Pairwise comparisons were performed with t-tests since data were normally distributed.

3.4 DISCUSSION

3.4.1 Evaluation of the method used

Previous observations of the emergence of stripes in corneas were made from intact eyes, which might confuse the stripy pattern because observations are made through multiple layers of epithelial cells. As stripes are probably formed first in the continuously dividing basal layer, for a short period of time the remains of the immature, speckled pattern will still be present in the suprabasal layers, obscuring the underlying emerging stripes. In addition, corneas from both the *Pax6*$^{+/-}$ and *Mp/+* mutant eyes appeared to also have β-gal positive cells in the stroma (Fig. 3.3), which could interfere with the interpretation of the epithelial pattern. The appearance of β-gal positive cells in the stroma of the mutant eyes can probably be attributed (at least for the *Pax6*$^{+/-}$ mice) to the fact that corneas are thinner and more fragile probably resulting in better penetration of the X-gal stain reaching the lower parts of the cornea including the stroma. Abnormalities in the *Mp/+* eyes might result in analogous alterations of corneal properties, allowing the stain to reach even the corneal endothelium (Fig. 3.3 A). However, defects in *Mp/+* corneas have yet to be evaluated. By using sections of X-gal stained eyes, all layers of the cornea are revealed separately making it possible to focus only in the basal layer without interference of the other parts of the eye.

On the other hand, the major drawback of the technique used was the diffusion of the X-gal stain outside the nucleus of β-gal positive cells. The cellular compartment where the enzyme was localised could not be distinguished, so it is not clear whether it leaked out of the cell. If so, this might result in an overestimation of the β-gal positive percentage in the cornea. Thus, an overall evaluation of the β-gal staining was essential before counting every time a new cornea was observed under the microscope. As mentioned before, the observed diffusion probably occurred during the processing of the previously stained eye for embedding in wax. Since this kind of evaluation is subjective and could vary between individuals, an alternative method would be to obtain frozen sections of the eye. Pilot experiments using frozen, X-gal

stained and fixed eyes embedded in OCT (using the protocol described in section 2.9) showed poor histology of the tissue and often the corneal epithelium was not intact or became separated from the rest of the eye. This was attributed to the embedding medium and the fact that the eye was already fixed. It might have been possible to obtain better results, with sections from fresh tissue embedded in a medium that shows better penetration (e.g. 15% w/v sucrose and 7% w/v gelatine in PBS) and then stain the sections with X-gal, but this was not attempted. Nevertheless, despite some technical problems, the results obtained were largely consistent with the predicted time of stripe emergence.

3.4.2 Initial mosaic pattern of randomly oriented patches

As mentioned before, previous published data of the laboratory have shown an age-related decrease in the corrected stripe number around the circumference of the corneal epithelium of adult *Pax6*$^{+/-}$ mice. This could reflect the existence of fewer LSCs or less active LSCs maintaining the corneal epithelium in these mice. On the other hand, such a reduction could also be a result of a developmental difference between wild-type and *Pax6*$^{+/-}$ corneas. For example, if there was less cell-mixing in the corneal epithelium of the mutant mice, there would be fewer but larger patches and hence, a more coarse-grained, "speckled" pattern of randomly oriented patches would be present before the establishment of the stripes in the ocular surface, resulting in a decreased corrected mean stripe number identified by the analysis (Fig. 3.1). By comparing *Pax6*$^{+/-}$ and wild-type littermates at 3 weeks of age, data for both the corrected mean length and the uncorrected median length of patches across the corneal diameter revealed significantly larger patches in the corneal epithelium of wild-type mice rather than in *Pax6*$^{+/-}$ (Fig. 3.4 A & B). Additionally, when patch lengths in *Mp*/+ corneas were similarly compared to wild-type littermates (Fig. 3.4 C & D) at the same age, no statistically significant difference could be identified, suggesting that small eye-size is not critically affecting the results. The above results support the idea that in the ocular surface of adult *Pax6*$^{+/-}$ mice, the lower corrected

mean stripe number around the circumference is more likely to reflect a defect in the LSCs maintaining the corneal epithelium than a more clumped distribution of β-gal positive and β-gal negative LSCs (shown in Fig. 3.1). The difference in the distribution of the patch number in the wild-type eyes between the two crosses (*Pax6*$^{+/-}$ and *Mp*/+) might be attributed to the different genetic backgrounds of the mice since *Pax6*$^{+/-}$ are congenic on CBA/Ca genetic background whereas *Mp*/+ mice are only partially congenic on this background with backcrosses for five generations (for details on the background of parental mouse lines see section 2.1).

3.4.3 Establishment of the radial striped pattern

As stripes emerge and displace the randomly-oriented, speckled mosaic pattern of the immature corneal epithelium of the X-inactivation mosaics, the patches are expected to become longer and their numbers to decrease. Consistent with the above prediction, as the wild-type corneas got older and bigger (Fig. 3.5 A & C), the mean patch number decreased (Fig. 3.5 B & D), whilst the corrected mean patch length and the uncorrected median patch length increased (Fig. 3.6). Specifically, the first significant difference between ages can be identified in the corrected mean patch length between 3 and 6 week old corneas. The same is true for the *Pax6*$^{+/-}$ corneas, which show a significant increase in patch length between these two ages. This means that up to 6 weeks of age the corneal epithelium of *Pax6*$^{+/-}$ behaves in a comparable way to the wild-type one and LSCs are probably activated at the correct time and produce their progeny.

However, things differ dramatically at older ages. In the wild-type, the corrected mean patch length continues to increase and the mean number of patches decreases further at 10 weeks of age (although these differences did not reach statistical significance) but in the *Pax6*$^{+/-}$ mice both the corrected mean patch length (Fig. 3.6 A) and the mean number of patches (Fig. 3.5 B) stay unchanged between 6 and 10 weeks of age. This suggests that in the *Pax6*$^{+/-}$ corneas, although the timing of the

emergence of stripes appears normal, the pattern does not resolve to a complete stripy pattern, at least not by 10 weeks of age, the latest age group examined in this experiment. These findings are consistent with previously published observations (e.g. 9 week old eye illustrated in Fig. 1L of (Collinson et al., 2004a)) showing that the pattern in the corneal epithelium of *Pax6*$^{+/-}$ is disorganized. One possibility is that in the *Pax6*$^{+/-}$ corneas, a defect in the LSCs results in corneas that do not fully mature, since the size, the mean patch number and the corrected patch length of these *Pax6*$^{+/-}$ eyes at 10 weeks of age stay almost the same as those from 6 week old *Pax6*$^{+/-}$ mice.

3.4.4 Direction of stripes and stem cell location

In order to determine the direction of stripe-extension as they emerge and displace the random, speckled pattern of the corneal epithelium in wild-type animals, the number of patches across the diameter was compared at the periphery and centre in the middle section of the cornea (Fig. 3.7). Consistent with the initiation and elongation of stripes, the mean number of patches decreased with age. Interestingly, for the periphery of the corneal epithelium, the reduction was obvious from the comparison between 3 and 6 weeks of age and also, reduced further so that it continued to be significant between 3 and 10 weeks of age. However, for the centre of the epithelium, a significant reduction could only be observed between 3 and 10 weeks of age, revealing that stripes reach this area later than the periphery. This result is consistent with previous observations from intact mouse eyes (Collinson et al., 2002). As mentioned before, the previous study implied that stripes in the corneal epithelium extend towards the centre of the cornea because the formation of stripes was firstly seen at the periphery at 5 weeks of age, whereas the first stripes spanning the whole radius of the cornea were only seen at the age of 8 weeks. Conversely, by showing that a reduction of patch numbers in the centre of the corneal epithelium is taking place later than in the periphery, a more objective confirmation of the above result is provided, showing that stripes move towards the centre of the corneal

epithelium. Additionally, this analysis provides further support for the limbal location of stem cells maintaining the corneal epithelium, which is discussed in more detail in Chapter 7.

3.4.5 Conclusions

The observation that the mosaic pattern was not more coarse-grained in *Pax6*$^{+/-}$ than wild-type X-inactivation mosaics before the stripes emerged provides evidence against the possibility that differences in cell mixing during development cause the larger stripe widths in adult *Pax6*$^{+/-}$ corneas. This observation is consistent with the alternative interpretation that the larger adult stripes in *Pax6*$^{+/-}$ corneas are a result of differences in LSC function between *Pax6*$^{+/-}$ and wild-type mice. Additional observations support previous suggestions that the initial speckled mosaic pattern is replaced by stripes and that the stripes emerge from the periphery of the cornea by 6 weeks and extend towards the centre.

Chapter 4
Analysis of Label-retaining Cells in the Limbus of *Pax6*$^{+/-}$, *Mp*/+ and Wild-type Corneas

4.1 INTRODUCTION

Observations from studies in epithelia from skin and small intestine of irradiated mice have led to the concept that the relative cell-cycle lengths of cells in the basal layer of an epithelium may be indicative of their "stemness" (Potten and Morris, 1988). Specifically, slow cycling cells are considered to be putative stem cells, able to produce two kinds of daughter cells. One that will continue to be a stem cell and hence, it will replenish the stem cell pool, and a second one, which divides more frequently but is further down the differentiation pathway, the transit or transient amplifying cell (TAC) that is destined to undergo terminal differentiation after a few cell divisions.

A method to label stem cells has been developed, which takes advantage of their slow cycling properties (Bickenbach, 1981). This method involves the application of an artificially produced thymidine analogue, which gets incorporated into the DNA of cells that are currently undergoing division, irrespective of the cell's "stemness". In order for the label to be incorporated into stem cells, administration should take place when stem cells are expected to be active. Long administration periods of the label (e.g. longer than the average cell cycle of the stem cell, if known) can achieve successful labelling of stem cells, as long as the stem cell divides during this period. After exposing the animal to the thymidine analogue for a certain period of time, the label is chased, or in other words, the animal is left for several weeks without any further manipulation. This is a crucial step of the procedure during which every cell division leads to the dilution of the incorporated label since there will not be any artificial thymidine in the tissue environment and normal thymidine will be

incorporated into the newly synthesised DNA strands. So, after a few cell divisions, the label will be diluted to undetectable levels in the somatic cells, whereas stem cells, on the other hand, will retain the label due to their slow cycling nature and hence these cells are termed label-retaining cells (LRCs).

The first applications of the LRC technique were performed by using ^{3}H-thymidine and cells were then visualised by autoradiography. Although this label can be detected after more cell divisions than other types of labels introduced more recently, and so it provides higher sensitivity, it has certain limitations. These include the inconvenience of handling radioactivity, the time-consuming development of the autoradiography and the poor solubility of ^{3}H-thymidine, which limits its administration via drinking water (Jecker et al., 1997). Consequently, ^{3}H-thymidine has largely been replaced by synthetic nucleosides like BrdU, CldU and IdU, which have become the most widely used thymidine analogues for this purpose. After their incorporation into the cellular DNA, these nucleosides can be detected with specific antibodies following a classic immunohistochemistry protocol. However, immunological detection is not that sensitive and hence, the label gets diluted to undetectable levels after 2-3 cell divisions (Braun et al., 2003).

Furthermore, irrespective of the thymidine analogue used, complete labelling of all the proliferative cells should not be assumed because none of the known protocols provide such high labelling (Bickenbach et al., 1986). Additionally, the LRC population is not a purified population and by no means should it be considered as the whole adult stem cell population of a tissue but rather as a population of cells enriched in stem cells (Bickenbach, 1981; Braun and Watt, 2004; Cotsarelis et al., 1989). For example, cells that divided for the last time before their terminal differentiation while the label was available will take up the label and they will retain it. Conversely, stem cells that were not in S phase of their cell cycle while the label was administered, a relatively common phenomenon considering their slow-cycling nature, will not have incorporated any label into their DNA and thus they will not be marked.

The LRC technique has been applied in various tissues in order to study the location of the adult stem cells and/or the numbers of putative stem cells responsible for the maintenance of the respective tissue including the epidermis (Braun et al., 2003), hair follicles (Cotsarelis et al., 1990), the small intestine (Potten et al., 2002), liver (Li et al., 2009), haematopoietic system (van der Wath et al., 2009), adipose tissue (Staszkiewicz et al., 2009), brain (Golmohammadi et al., 2008), endometrium (Chan and Gargett, 2006) and kidney (Maeshima et al., 2003).

LRCs in the anterior part of the eye were among the earliest to be identified. Cotsarelis et al. were the first to inject mice consecutively with ^{3}H-thymidine and check the cornea for LRCs (Cotsarelis et al., 1989). They found that LRCs were absent from the central corneal epithelium but were enriched in the limbus, a finding that, among others, was used to support the limbal location of stem cells maintaining the corneal epithelium. Later studies have confirmed these findings using BrdU as label and administering it either by osmotic mini-pumps (Lehrer et al., 1998) or by multiple injections (Pajoohesh-Ganji et al., 2006; Zhao et al., 2009). Additionally, the two latter studies obtained quantitative data for label retention and both reported asymmetric distribution of LRCs around the mouse limbal circumference. In more detail, Pajoohesh-Ganji et al (2006) found LRCs to consist 0.94 – 3.6% of the total cells in the basal layer of the mouse limbal epithelium and their distribution to be higher in the superior and the inferior part of the limbal circumference rather than the nasal and the temporal ones. Zhao et al (2009) on the other hand, estimated the percentage of the slow-cycling cells in the mouse basal limbus to be 4.2% of the total number of cells (a figure very close to the estimate by Pajoohesh-Ganji et al) but the distribution of the LRCs was found to be higher in the superior and temporal part of the limbal circumference rather than the inferior and nasal part. Both studies emphasised that the number of LRCs was an estimate of the slow cycling cells in the limbus and that *in vivo* the number of these cells should be higher. The discrepancies in the differential distribution of LRCs around the limbal circumference were attributed to the different strain of mice used by the two studies and/or to the difference in the length of the chase period the studies adopted in order to identify

LRCs (Zhao et al., 2009).

A crucial step in the immunohistochemistry protocol used to identify DNA strands that have incorporated a thymidine analogue is the denaturation of the DNA, so that the antibody will be able to reach the synthetic nucleoside. This procedure is fatal for the cells and thus isolation and further handling of the cells (e.g. fluorescence activated cell sorting (FACS) of labelled cells) is not possible. In an attempt to overcome the requirement for harsh denaturating conditions that could degrade the tissue, a new method using 5-ethynyl-2′-deoxyuridine (EdU) as a label has been developed (Buck et al., 2008). The EdU thymidine analogue can be detected via the reaction of the ethynyl group with a fluorescent-azide probe in a copper-catalyzed reaction. This technique has been successfully applied for proliferation studies in cultured cells as well as in mouse tissues and has also been used in live cell imaging proving that cells are viable after the staining (Salic and Mitchison, 2008). Additionally, adipose tissue derived stem cells were labelled with EdU and transplanted in the mouse, proving its suitability for long term tracking (Lin et al., 2009) but this analogue has not been applied for labelling slow-cycling cells yet.

Recently, a new way to label all the cells in an experimental animal and then reveal the LRC in a specific tissue by allowing a chase period has been developed (Tumbar et al., 2004). This consists of mice expressing a histone H2B protein fused to GFP (Kanda et al., 1998) ubiquitously, under the control of a tetracycline-responsive element. These mice are then crossed to mice carrying a tissue specific driven VP16 transgene (tetracycline repressor; Diamond et al., 2000). In the absence of tetracycline, GFP is expressed in all cells of the animal but when it is administered, GFP expression is turned off in the tissue that the repressor is expressed. Continuous administration of tetracycline for several weeks will make somatic cells dilute the GFP via cell division whereas stem cells will retain the label (rendering them LRCs) due to their infrequent divisions. It is clear that since histone H2B is expressed from early in development and continues to be expressed in all cells for their whole life, almost every single cell will be labelled. This results in marking almost every stem cell as well, irrespective of how frequently they divide. Finally, the most important

advantage of using this method for label-retention experiments is that LRCs are still alive after their identification and thus, they can be isolated with FACS and they can further be processed. For example, this can identify in what way their transcription profile differs from the somatic cells of the tissue, they can be cultured in order to assess their potential in terms of cell divisions and/or multipotency, or they can even be transplanted either to wild-type animals (to follow their migration and their progeny) or to disease models (to check if they are beneficial).

These label-retaining cell approaches have proved suitable for identifying putative stem cells and the BrdU method has already been used to identify LRCs as putative stem cells in the mouse limbus (Lehrer et al., 1998; Pajoohesh-Ganji et al., 2006; Zhao et al., 2009). This, therefore, offers a suitable approach for comparing the number of active putative stem cells at different ages and in different mouse genotypes.

4.1.1 Aims

The first aim of this chapter was identify a structural characteristic that would indicate the location of the limbus, the border between the conjunctival and the corneal epithelium, in whole-mount preparations of wild-type and *Pax6*$^{+/-}$ mouse eyes. This involved staining for known markers that are uniquely present in one of the two epithelia. The second aim was to identify the location of putative stem cells and compare their numbers in wild type and *Pax6*$^{+/-}$ mice as well as between young and old adult mice. This was pursued by using the BrdU-LRC technique, which identifies cells with infrequent divisions that will predominantly be stem cells. This was to test whether the numbers of LRCs (putative stem cells) was reduced in *Pax6*$^{+/-}$ or older mice.

4.2 MATERIALS & METHODS

4.2.1 Animals

For experiments described in this chapter *Pax6*$^{Sey\text{-}Neu/+}$ and *Mp*/+ colonies were used (for further details see section 2.1). Both colonies produce 50% wild-type animals and 50% animals heterozygous for the *Pax6*$^{Sey\text{-}Neu}$ and *Mp* mutation respectively.

4.2.2 Animal work

Offspring were selected based on phenotypic characteristics (both mutant mice have small eyes) and they were implanted with an osmotic mini-pump loaded with BrdU (see section 2.2). After a week of BrdU administration the mini-pump was removed and the mouse was sacrificed after an additional specific time period called the chase period (time which allows the BrdU to be diluted in most somatic cells but allows BrdU to be retained in the slow cycling putative stem cells). Eyes from wild-type CBA/Ca mice that had received an i.p. injection of BrdU and were sacrificed 4 hours later were used as positive controls whereas negative controls consisted of eyes from wild-type CBA/Ca mice that never received BrdU in any form. Mice were phenotyped by eye size and tail tips were also taken from the *Pax6*$^{+/-}$ mice to confirm their genotypes by PCR (see sections 2.4 & 2.5).

4.2.3 Tissue processing and staining

Eyes were dissected (see section 2.3) and prepared for whole-mount immunofluorescent staining (see section 2.11) for BrdU, K19 and/or blood vessels (with CD31 antibody). However, when double-labelling specifically for BrdU and CD31 (a membrane protein found in endothelial cells as well as peripheral leukocytes and platelets that is used for labelling blood vessels), a longer protocol

was used because both primary antibodies were raised in rats (Table 2.2). Specifically, the primary antibody for BrdU was applied first and it was left at 4 ^{o}C overnight. The next day, samples were washed 5 times for 1 hour each in PBS-T, placed in blocking serum for 2 hours and incubated with the secondary Alexa 488 Anti-Rat IgG antibody at 4 ^{o}C overnight. The following day, corneas were washed in PBS-T 6 times for 45 min each, blocked with freshly prepared blocking serum for 2 hours and incubated with the second primary antibody specific for blood vessels at 4 ^{o}C overnight. Next, samples were washed 5 times for 1 hour in PBS-T, placed in blocking serum for 2 hours and incubated with the secondary Alexa 568 Anti-Rat IgG antibody at 4 ^{o}C overnight. Finally, corneas were washed in PBS-T 6 times for 45 min each, counterstained and mounted on slides as the normal protocol indicates. Tail tips were also taken from the *Pax6*$^{+/-}$ mice to confirm their genotypes by PCR (see sections 2.4 & 2.5).

4.2.4 Confocal imaging

A confocal microscope was used to obtain photos from eyes stained by immunofluorescence. For staining involving K19, blood vessels or cell density measurements, imaging was performed as described in section 2.12.1. For BrdU imaging and sampling of the area where LRCs were counted, a specific confocal setup was used (see section 2.12.2).

4.2.5 Data analysis of LRCs

After obtaining images stained for BrdU, LRCs were counted as described before (section 2.12.2). Although every *Pax6*$^{+/-}$ or wild-type corneal button was flattened with 8 radial cuts creating 8 sectors and hence, 8 sampling areas, due to technical difficulties (e.g. tissue folding produced while flattening the corneal button on a slide or unidentifiable limbal areas due to extensive abnormalities of the *Pax6*$^{+/-}$ cornea),

some corneas ended up with less than 8 LRCs measurements. Furthermore, due to the very small eye size of the *Mp/+* mice, only 4 cuts were made and 4 measurements were taken from equal sampling areas. In order to normalise for equal number of counts per eye, a mean number of LRCs per sector was calculated.

A second normalisation was also considered necessary since there were variable differences found between each staining experiment. Every staining run always had at least one eye from each of the two ages and genotypes compared in the experiment. Thus, a weighted total number of LRCs found in all eyes stained in each run was calculated and then a "LRC index" was calculated by expressing the number of LRCs found in each sector as percentages of the weighted total number of LRCs per run. To accommodate staining runs with unequal number of eyes in each group, this weighted total was calculated as the total of the average LRC numbers for each of the four groups in the same experimental run. This is explained more fully in section 4.3.4.

Furthermore, wild-type, *Pax6*$^{+/-}$ and *Mp/+* eyes were quite different in size. In order to correct for such discrepancies, the circumference of each eye was measured by obtaining 3 different diameter measurements of the flattened eye. The mean of these measurements was used to calculate the circumference in millimetres according to the formula $C = \pi d$, where C is the circumference, π is the constant 3.141 and d is the diameter. Then, the mean number of LRCs per sampling area was multiplied by the circumference and divided by 0.34, which is the length of the box used for sampling in millimetres (see section 2.12.2), producing an estimate of the number of LRCs in a 200 µm wide ring around the whole circumference of the eye.

The distribution of all the data sets were checked for normality as described in section 2.20. All data were found to be normally distributed, so data were compared by ANOVA and statistically significant differences were followed by pairwise t tests.

4.3 RESULTS

Pax6$^{+/-}$ mice were crossed to CBA/Ca and the offspring (50% *Pax6*$^{+/-}$ and 50% wild-type) was used for this experiment. Additionally, in an independent experiment *Mp/+* mice and wild-type littermates were used as additional controls. *Mp/+* mice have small eyes but their genetic defect does not affect the *Pax6* gene and they have a histologically normal appearing corneal epithelium (see section 2.1).

4.3.1 Identification of limbus and *Pax6*$^{+/-}$ corneal abnormalities

In order to count the LRCs, first the limbal area had to be reliably identified. Keratin 19 (K19) is an intermediate filament protein that is localised in the limbus and the conjunctiva of the mouse, but it is absent from the corneal epithelium (Yoshida et al., 2006). As shown in figure 4.1 A, K19 immunohistochemistry was successful in revealing the boundary between the limbus and the cornea in wild-type eyes. This coincided with a structure that looked like a tissue crease (arrows in Fig. 4.1). This crease must be an artefact resulted from the flattened corneal button, since the limbus usually forms a "dent" in the intact eye ball (e.g. see Fig. 6.3 C in chapter 6). However, K19 staining was dramatically different in the *Pax6*$^{+/-}$ eye (Fig. 4.1 B). This keratin was found all over the whole anterior of the *Pax6*$^{+/-}$ eye, having a patchy distribution in the corneal epithelium, even in the centre of this tissue. Nevertheless, the crease indicating the limbus was identifiable in this tissue as well, although it was not as obvious as in the wild-type corneal button. Additionally, double immunofluorescence identifying BrdU and K19 in the same wild-type cornea revealed that LRCs are indeed localised in the limbus rather than the corneal epithelium, as shown in figure 4.1 C.

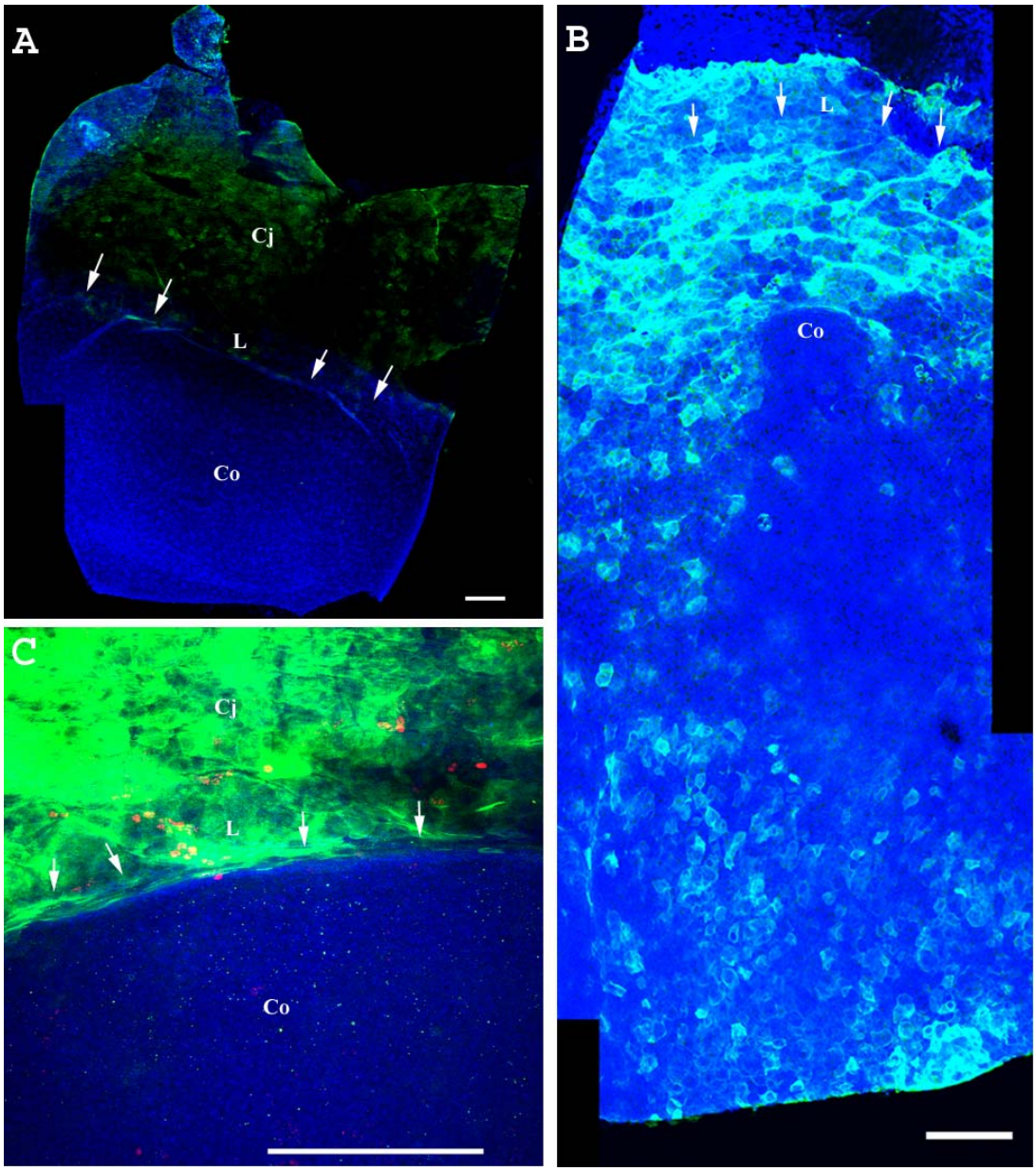

Figure 4.1 Immunohistochemical detection of keratin 19 (K19) and identification of the limbus. Whole-mount corneas of (A) a wild-type and (B) a *Pax6*$^{+/-}$ mouse. In the wild-type eye K19 staining is restricted to the conjunctiva and limbus whereas in the *Pax6*$^{+/-}$ eye K19 staining is also present in the corneal epithelium. (C) Double immunofluorescent staining for BrdU and K19 of a cornea from a wild-type mouse injected with BrdU. (This mouse had been injected with BrdU and chased for only 3 weeks. Some red BrdU-labelled cells are present in the cornea as well as the limbus). Arrows show the crease of the tissue indicating the limbus. L: Limbus; Co: Cornea; Cj: Conjunctiva; Green: K19; Red: BrdU; Blue: TO-PRO3 iodide nuclear counterstain. Scale bars are 0.2 mm.

Another characteristic that differentiates the conjunctival and the limbal epithelium from the corneal one is the existence of blood vessels in the limbus but not the cornea. In order to confirm with another independent marker the location of limbus, double, immunofluorescent labelling for CD31 (identifying blood vessels) and K19 was performed. As demonstrated in figure 4.2 A & B, in the wild-type eye, blood vessels were restricted to the conjunctiva and the limbus along with K19. However, in *Pax6*$^{+/-}$ eyes blood vessels were shown to be growing into the cornea and K19 was present even in the central cornea (Fig. 4.2 C & D). These abnormalities may reflect incursion of the conjunctiva into the corneal epithelium (conjunctivalisation of the cornea) in *Pax6*$^{+/-}$ mice and *PAX6*$^{+/-}$ humans, reported by several labs (Davis et al., 2003; Nishida et al., 1995; Ramaesh et al., 2003).

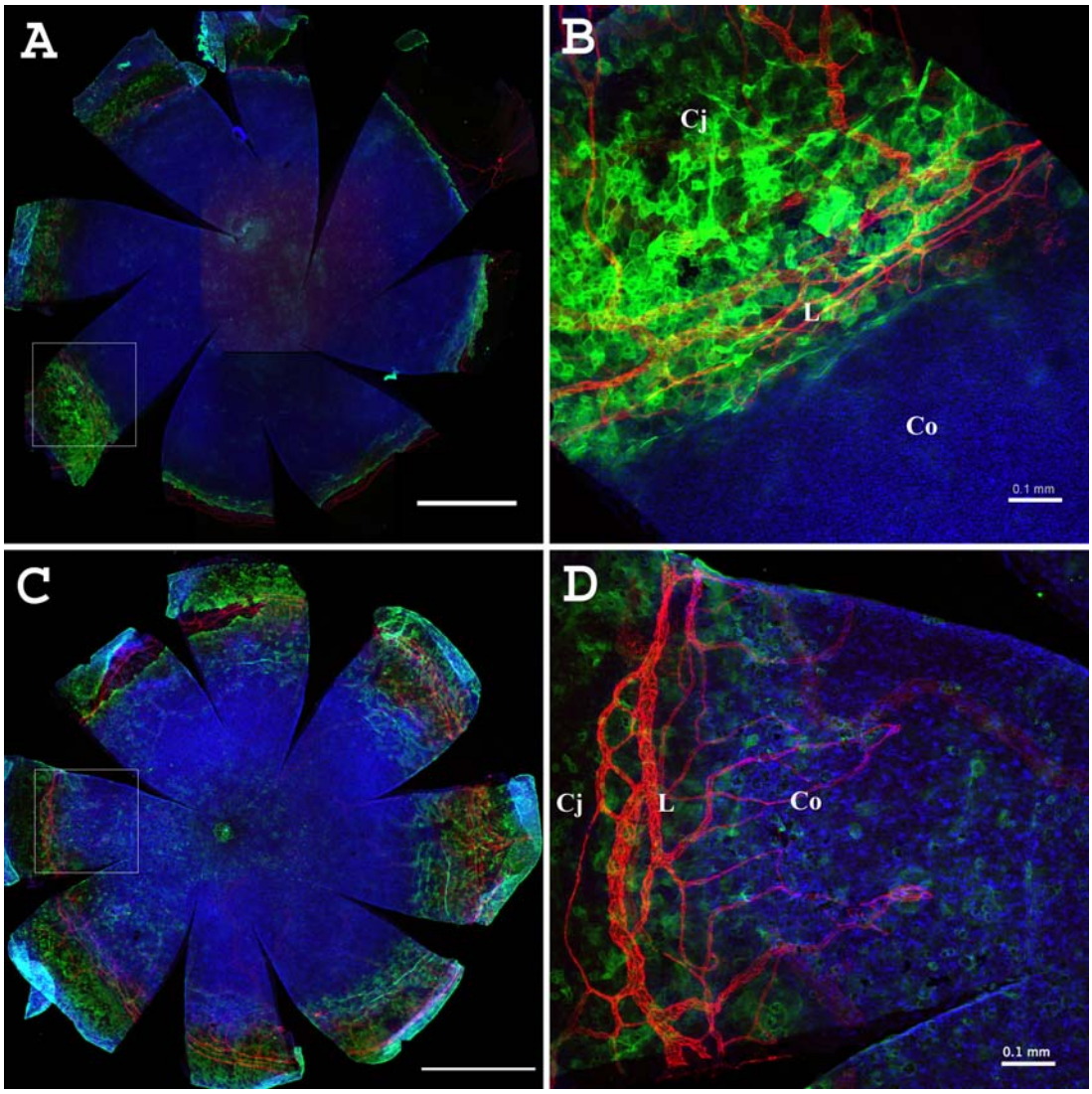

Figure 4.2 CD31 and Keratin 19 double immunofluorescence staining in the ocular surface of wild-type (A & B) and *Pax6*$^{+/-}$ (C & D) mice. B & D are higher magnification images from the areas indicated by a square in A & C respectively. Although in wild-type corneas both blood vessels and keratin 19 are present only in conjunctiva and limbus, in the *Pax6*$^{+/-}$ mice they both extend into the corneal epithelium. L: Limbus; Co: Cornea; Cj: Conjunctiva; Red: CD31; Green: K19; Blue: TO-PRO3 iodide nuclear counterstain. Scale bars are 1 mm unless otherwise stated.

4.3.2 Optimisation of BrdU labelling and chase periods

In a preliminary technical control experiment, wild-type, 12 week old mice were each given a single i.p. injection delivering 0.2 ml of 10 mg/ml BrdU and animals were left for 1, 3, 6 and 10 weeks for the BrdU to be diluted from the somatic cells. As shown in Figure 4.3, up to 6 weeks of age there were some cells in the central corneal epithelium (somatic cells) that were still retaining the label. At 10 weeks of age, most of the LRCs were restricted to the limbus but there were very few labelled cells altogether. This showed that it would probably be necessary to label for a longer period of time in order to label sufficient slow cycling cells and implied that the chase period would have to be more than 6 weeks.

To optimise BrdU labelling and chase periods in order to identify LRCs, osmotic mini-pumps loaded with 0.1 ml of 50 mg/ml BrdU were implanted in the peritoneal cavities of mice, delivering 0.5 µl/h of the solution constantly for 1 week. In this way, a higher amount of BrdU was administered and critically, the solution was administered for longer compared to the single i.p. injection. Eight adult, 15-week old mice (4 *Pax6*$^{+/-}$ and 4 wild-type) were used for optimization of the technique and they were sacrificed 0, 4, 8 and 12 weeks after the end of the administration period (Fig. 4.4). Some 30-week old mice were also implanted with a BrdU-loaded mini-pump and chased for the same period of time. Technical problems prevented a full set of data from being produced for 30 weeks, but results were similar to those produced by the mice implanted at 15 weeks of age (data not shown). As demonstrated in figure 4.4 A – D, for wild-type eyes, there was a gradual reduction of labelled cells in the cornea with increasing chase periods. However, the eye from the 4 week chase (Fig. 4.4 B) unexpectedly showed very few labelled cells and these were restricted to the limbus. This presumably reflects a problem with the specific mouse/implantation because in the eye that was chased for 8 weeks (Fig. 4.4 C), we can still identify labelled cells in the cornea, although there were very few of them.

For the *Pax6*$^{+/-}$ eyes, the first two chase periods revealed a lot of labelled cells in the central and peripheral cornea (Fig. 4.4 E & F). However, even with the longest chase period (12 weeks; Fig. 4.4 H) there were some labelled cells in the cornea, which additionally, were appearing to be organised in a pattern that resembled the in-growth of blood vessels seen with the CD31 immunostaining (Fig. 4.2 D). In the literature, different chase periods have been used for different amounts of BrdU administration. From a combination of results from this preliminary experiment and published results, 10 weeks was considered to be the optimal chase period for the main experiments. More recently, Zhao et al. (2009) used a similar chase period (9 – 11 weeks). Although they administered BrdU in the form of consecutive i.p. injections, the total amount was similar to that provided by the mini-pump.

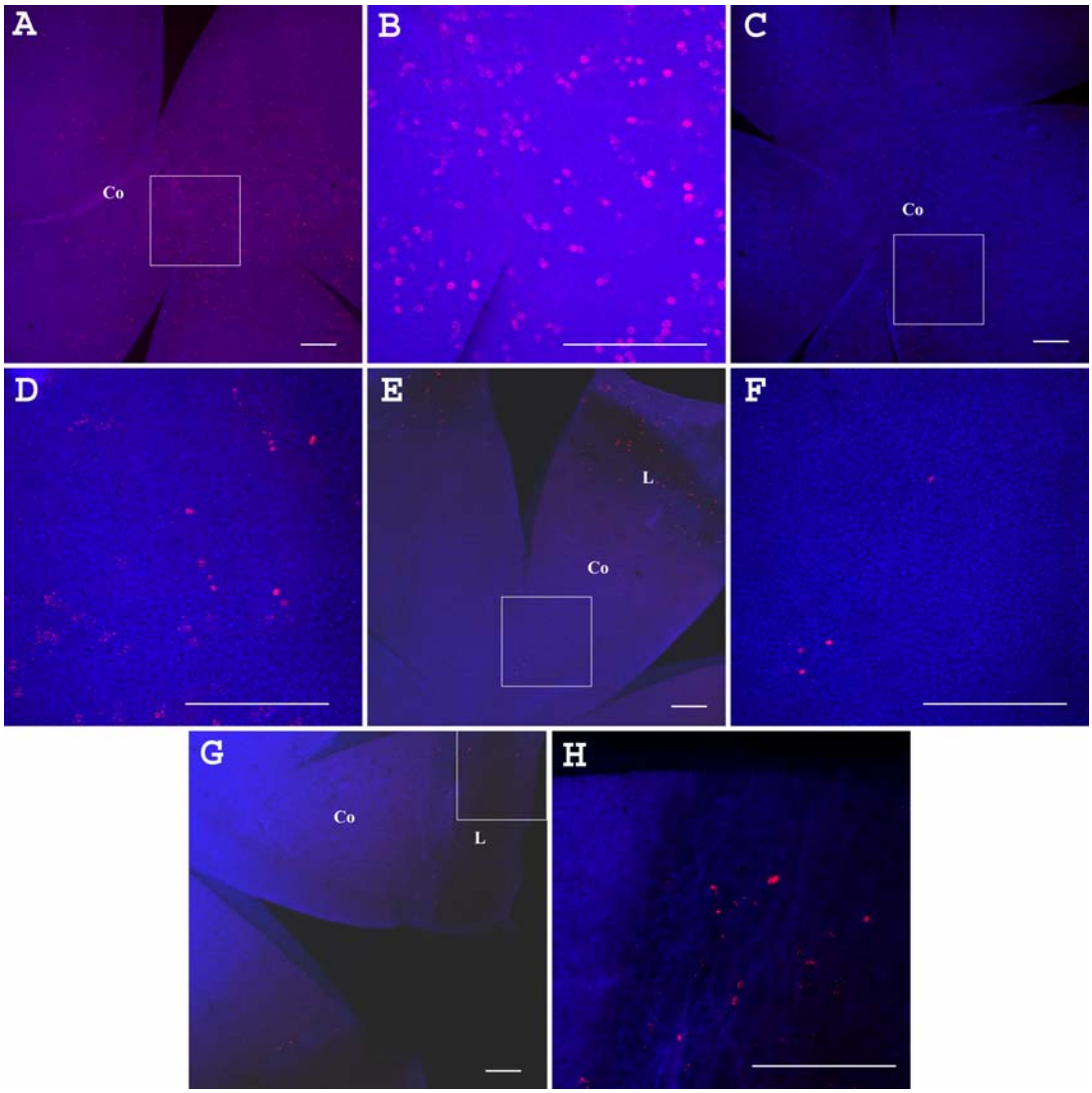

Figure 4.3 Whole-mount corneas of 12-week old mice that received a single i.p. injection of BrdU and chased for different periods. (A & B) 1 week chase. (C & D) 3 weeks chase. (E & F) 6 weeks chase. (G & H) 10 weeks chase. B, D, F & H are magnified versions of the areas indicated by a square in A, C, E & G respectively. L: Limbus; Co: Cornea; Red: BrdU; Blue: TO-PRO3 iodide counterstain. Scale bars are 0.2 mm.

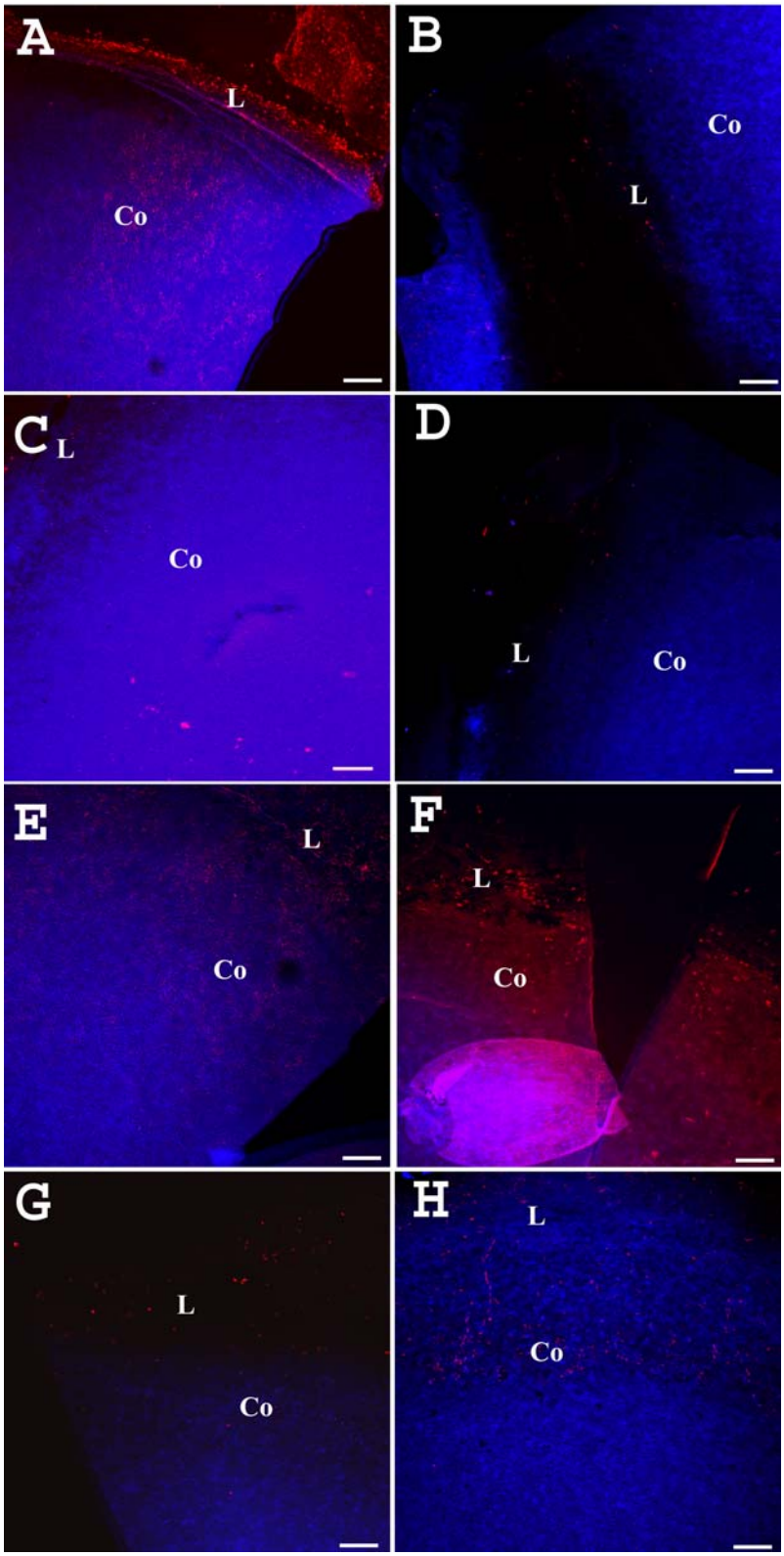

Figure 4.4 Preliminary LRC experiment. Whole mount corneas of 15-week old wild-type (A – D) and *Pax6*$^{+/-}$ (E – H) mice that were implanted with a BrdU-loaded mini-pump for 1 week and chased for various periods. (A & E) 0 weeks chase. (B & F) 4 weeks chase. (C & G) 8 weeks chase. (D & H) 12 weeks chase. L: Limbus; Co: Cornea; Red: BrdU; Blue: TO-PRO3 iodide counterstain. Scale bars are 0.1 mm.

4.3.3 LRCs in the limbal area

The original plan was to implant a BrdU-loaded mini-pump into at least 20 mice at 15 weeks of age and 20 at 30 weeks, half of which would have been *Pax6*$^{+/-}$ and the rest would have been their wild-type littermates. The selection of mice to be implanted with mini-pumps was performed based on the small size of the *Pax6*$^{+/-}$ eyes and their genotypes were checked by PCR at the time of analysis. However, in some cases the phenotype proved misleading, so the final number of mice per group was 14 *Pax6*$^{+/-}$ mice implanted at 15 weeks old, 8 wild-type mice implanted at the same age, 9 *Pax6*$^{+/-}$ mice implanted at 30 weeks of age and 11 wild-type mice at 30 weeks. Furthermore, due to technical difficulties and the corrections that were applied to the data (see section 4.2.5) not all eyes could be included in the final analysis. Although the number of eyes in each group differed, it was always higher than 12.

In an independent experiment 5 mice at each age and genotype group from the *Mp/+* colony were implanted with a mini-pump. The *Mp* genetic defect had not been characterised at the time of the experiment, so no PCR method was available for genotyping these mice. So, again the selection of mice was based on the small eye size of the mice but *Mp/+* eyes are very small making the phenotypic appearance both reliable and adequate for genotypic evaluation. Thus, in this experiment there were measurements for 10 eyes in each age and genotype group.

Representative images for all ages and genotypes are shown in Figure 4.5. In wild-type eyes from both crosses, LRCs were restricted in the limbal area. In the *Pax6*$^{+/-}$ eyes, however, more LRCs could be identified overall and additionally, they were not usually confined to the limbus. Also, in *Pax6*$^{+/-}$ corneas the anti-BrdU antibody identified some “particles” that were smaller than normal nuclei and not nuclear-localised (Fig. 4.5 B & D). The *Mp/+* eyes seemed to have even more LRCs than *Pax6*$^{+/-}$ eyes, but they were almost exclusively found in the limbus rather than extending into the cornea.

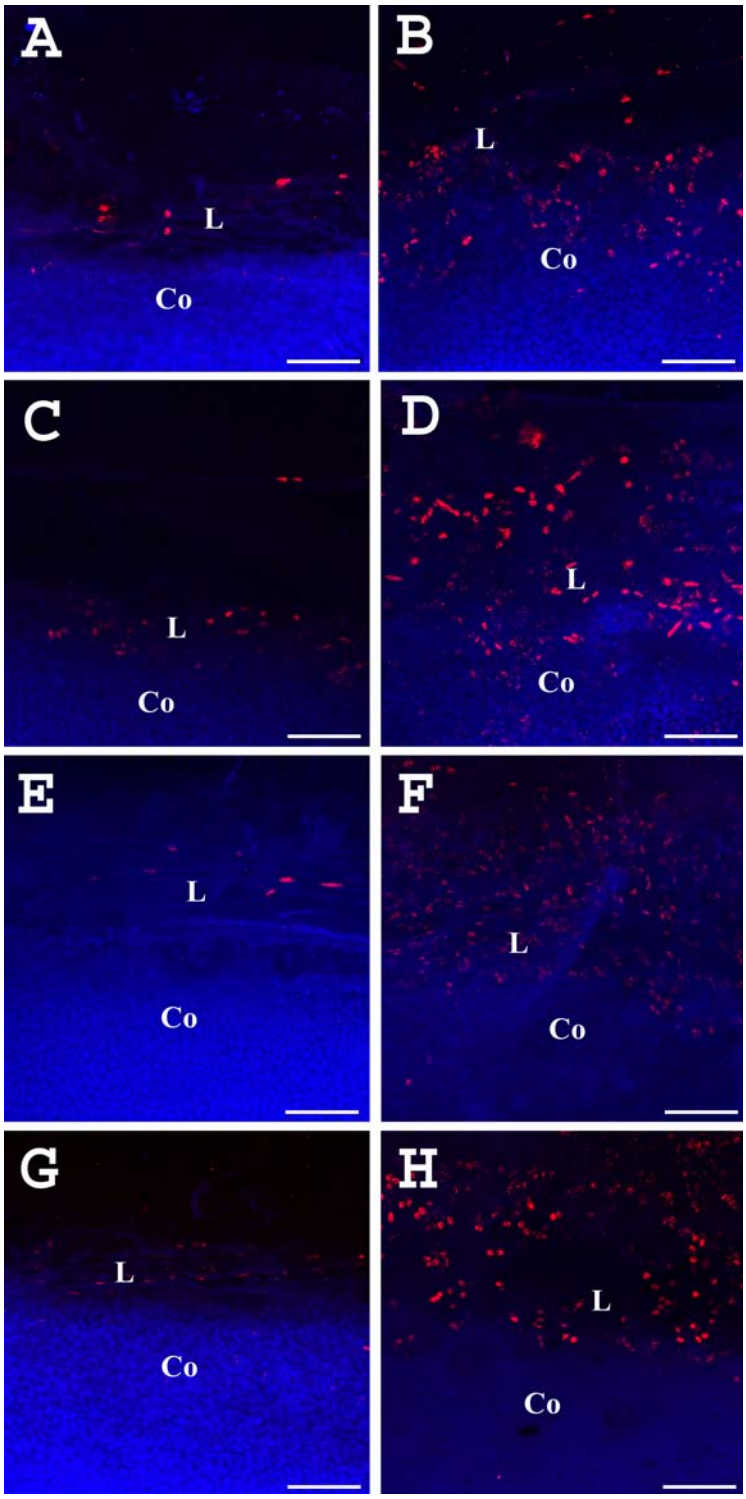

Figure 4.5 LRCs in the eye of mice from the *Pax6*$^{+/-}$ (A – D) and the *Mp*/+ (E – H) cross implanted with a BrdU-loaded mini-pump and chased for 10 weeks. (A) 15 weeks old wild type. (B) 15 weeks old *Pax6*$^{+/-}$. (C) 30 weeks old wild-type. (D) 30 weeks old *Pax6*$^{+/-}$. (E) 15 weeks old wild-type. (F) 15 weeks old *Mp*/+. (G) 30 weeks old wild-type. (H) 30 weeks old *Mp*/+. L: Limbus; Co: Cornea; Red: BrdU; Blue: TO-PRO3 iodide counterstain. Scale bars are 0.1 mm.

Statistical analysis showed that the mean number of LRCs in the limbal region did not differ significantly between *Pax6*$^{+/-}$ and their wild-type littermates at either of the ages tested. In addition, although the prediction was that the number of LRCs and thus the LSCs would be decreased with age and in *Pax6*$^{+/-}$ mice, the trends pointed towards the opposite direction for the genotype comparisons (Fig. 4.6 A). Next, the numbers of LRCs were corrected for the circumference. Since *Pax6*$^{+/-}$ eyes are smaller in size, this could have an effect in the proportion of the corneal area that was imaged. So, the circumference was calculated from measurements of the flattened cornea, and this was used to predict the number of LRCs within a 200 μm wide annulus throughout the whole limbal circumference. However, even after applying this correction the numbers were still not statistically significant and the genotype related trends (Fig. 4.6 B) were opposite to what was predicted (i.e. there was a non-significant trend for *Pax6*$^{+/-}$ eyes to have more LRCs in the limbus than wild-type eyes).

Interestingly, comparisons of *Mp/+* and their wild-type littermates, showed significant differences between genotypes for LRCs per sector with *Mp/+* eyes having more LRCs than wild-type (ANOVA: $P<0.0001$) but not between ages (Fig. 4.6 C). This was quite surprising because, as mentioned in section 2.1, *Mp/+* mice were included in the experiment as wild-type controls with very small eye size, for comparison with the small *Pax6*$^{+/-}$ eyes. Histological observations showed that the corneal epithelium of *Mp/+* mice appeared normal (Fig. 3.2). However, *Mp/+* eyes appeared to have more LRCs in the limbal region than their wild-type littermates and even more LRCs than the *Pax6*$^{+/-}$ mice. This was also true after correcting LRC numbers for the very small eye size these mice have, as described above. As demonstrated in Figure 4.6 D, there were more LRCs per circumference in the *Mp/+* eyes than the wild-type littermates with larger eyes (ANOVA: $P=0.0016$).

Finally, the numbers of LRC per sector and per circumference did not differ significantly ($P>0.4$) between the wild-type eyes in the two experiments (Fig. 4.6), showing consistency between the different experiments. LRC indices for wild-type eyes, on the other hand, were not compared because this normalisation takes into

account the numbers of LRCs in the mutant eyes as well and this was higher for the *Mp*/+ eyes than the *Pax6*$^{+/-}$ eyes.

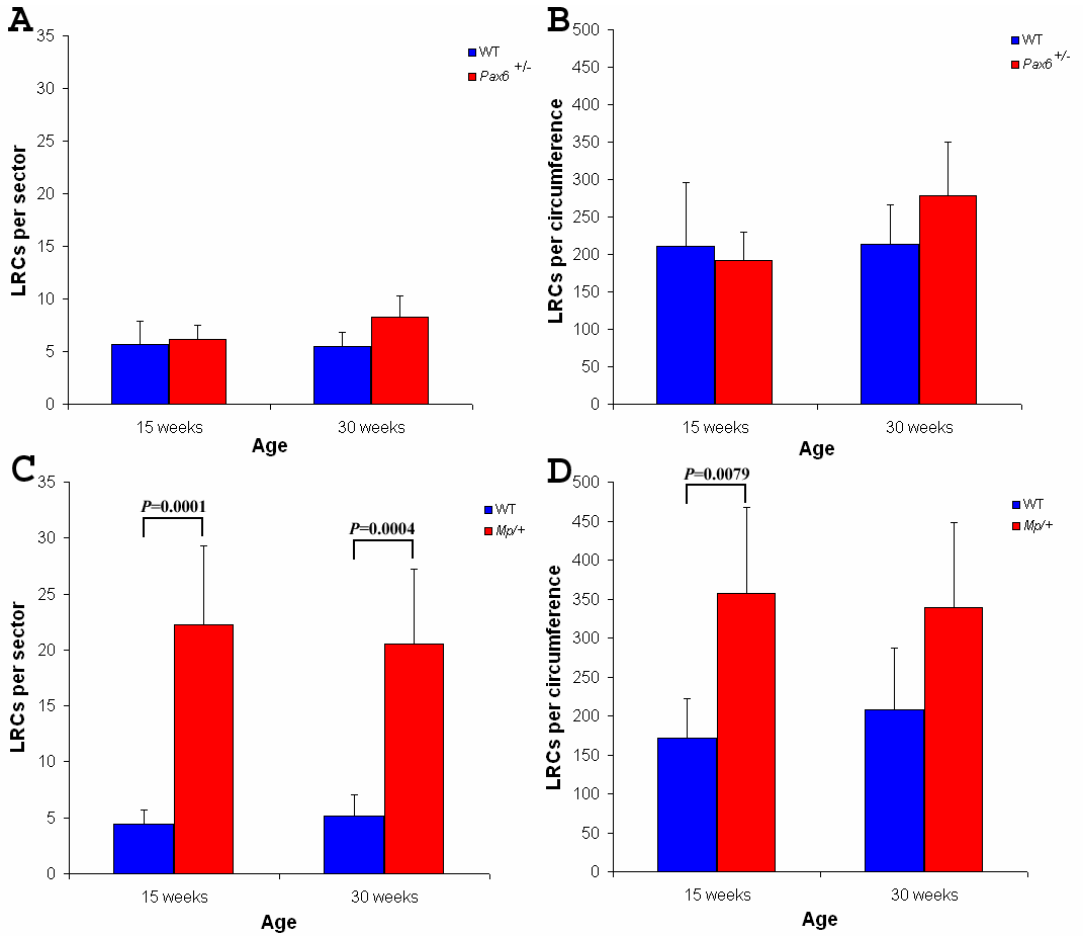

Figure 4.6 Comparisons of LRCs per sector and per circumference in *Pax6*$^{+/-}$ (A & B) or *Mp*/+ (C & D) and their respective wild-type littermates. (A & B) Numbers of eyes are 13 for 15 weeks old wild-type, 23 for 15 weeks old *Pax6*$^{+/-}$, 20 for 30 weeks old wild-type and 17 for 30 weeks old *Pax6*$^{+/-}$. (C & D) Numbers of eyes are 5 for each age and for each genotype. If 2-way ANOVAs identified significant differences among groups this was followed by pairwise comparisons by t-tests. Only statistically significant pairwise differences with t test are shown.

4.3.4 LRC index

One technical concern was the large variability in the number of LRCs found in different immunohistochemistry experiments, resulting in large standard errors. Big differences were also found in the total number of LRCs for each experiment. In order to correct for these discrepancies between immunohistochemistry experiments, a "LRC index" was calculated for each eye. This was done by calculating a weighted total number of LRCs for each experiment (which was the total of the average LRC numbers for each of the four groups in the same run) and then expressing the number of LRCs per sector as percentages of this weighted total. Runs that did not have at least one eye per age and per genotype group were excluded from the analysis. Also, for runs that had more than one eye per group (genotype-age combination), the mean number of LRCs per sector was averaged for each group before calculating the weighted total number of LRCs per run. The same normalization was also performed on data corrected for differences in the limbal circumference.

As demonstrated in Figure 4.7 A & B, the results were not different from the previous analysis. For comparisons between *Pax6*$^{+/-}$ and their wild-type littermates, *Pax6*$^{+/-}$ had more LRCs per experimental run, although the difference between genotypes was barely significant (ANOVA: P=0.0452). For corrected data, the LRC index per circumference was not significantly different between the groups under examination.

In the *Mp/+* versus wild-type littermates comparisons (Fig. 4.7 C), results were still statistically highly significantly different between genotypes for LRC index per sector (ANOVA: P<0.0001) with the LRC index significantly higher in *Mp/+* for both ages tested. The same could be observed for the LRC index in these mice for the data corrected for differences in limbal circumference (ANOVA: P=0.0006; Fig. 4.7 D).

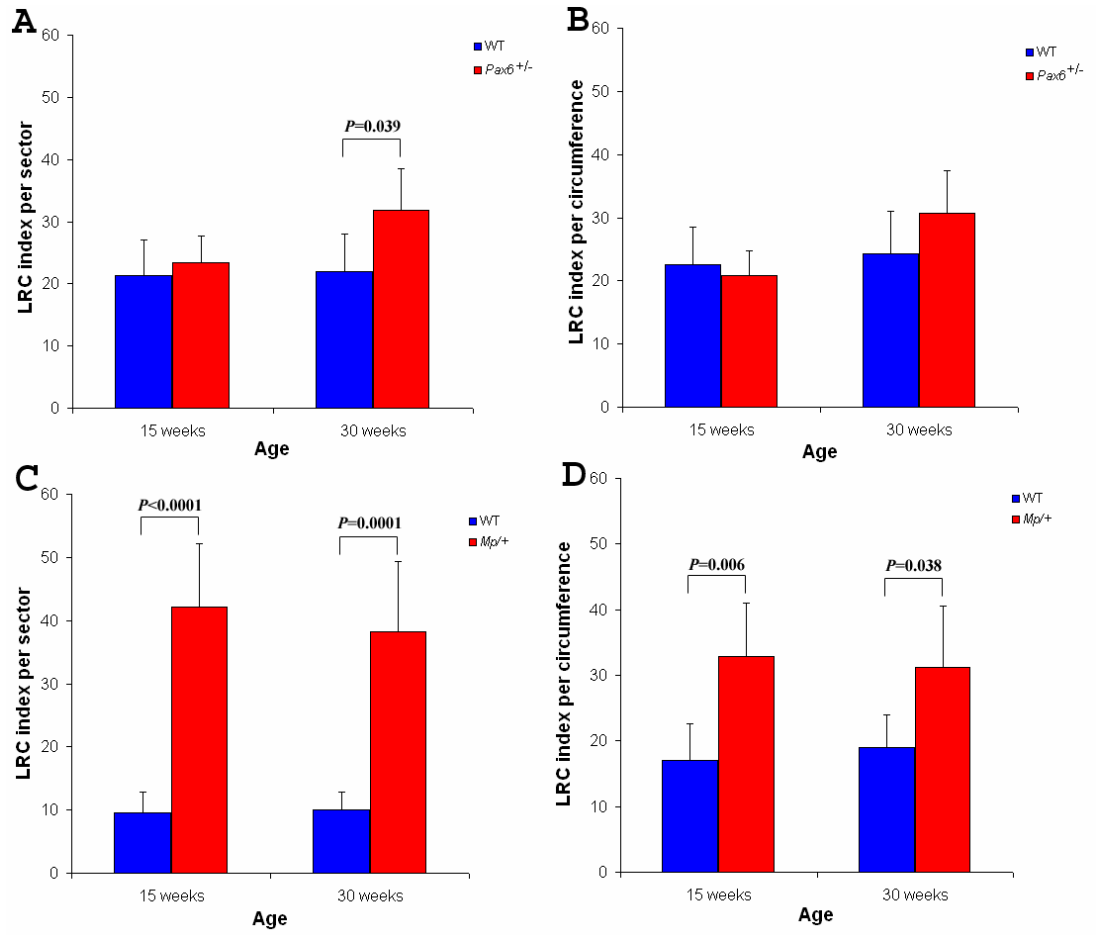

Figure 4.7 Comparison of LRC indices per sector and per circumference in *Pax6*$^{+/-}$ (A & B) or *Mp*/+ (C & D) and their respective wild-type littermates. (A & B) Numbers of eyes are 12 for 15 weeks old wild-type, 16 for 15 weeks old *Pax6*$^{+/-}$, 15 for 30 weeks old wild-type and 14 for 30 weeks old *Pax6*$^{+/-}$. (C & D) Numbers of eyes are 5 for each age and for each genotype. If 2-way ANOVAs identified significant differences among groups this was followed by pairwise comparisons by t-tests. Only statistically significant pairwise differences with t test are shown.

4.3.5 Cell density of the corneal epithelium

The frequencies of LRCs were estimated from counts of labelled cells in a defined area rather than from separate counts of labelled and unlabelled cells. If the cell density varied with age or genotype this could affect the results. It proved difficult to count unlabelled cells in the limbus because the underlying area, where the ciliary body is located, interfered with the fluorescence, so cell densities were estimated in the cornea. Preliminary observations were made from one eye at each of the 15 & 30 week old *Pax6*$^{+/-}$ and wild-type littermates groups, which were counterstained with propidium iodide (PI). These eyes were imaged with a x20 objective. Cells in a 300 x 300 μm sized box (Fig. 4.8 A) were counted from three peripheral areas and a central one for every eye and their numbers were compared. As shown in Figure 4.8 C, mean numbers were very similar for peripheral and central cornea.

Cell densities were then compared in the central cornea from images used for the analysis of LRCs. The cell density in the corneal epithelium was estimated from 3 eyes from each genotype (*Pax6*$^{+/-}$ & wild-type littermates and *Mp/+* & wild-type littermates) and from each age. In order to have truly representative eyes from each group, the selected eyes were those whose limbal circumference was closer to the mean circumference of the respective group. Single images were obtained from flattened corneas counterstained with TO-PRO3 iodide using a confocal microscope equipped with a x40 oil-immersion objective for clearer results. Three regions from the corneal epithelium of each eye were imaged and the nuclei were counted in a region defined by a 150 x 150 μm sized box (Fig. 4.8 B). In a blind manner, an independent person placed the box on the images using Adobe Photoshop 7.0 and the nuclei were counted with ImageJ.

As shown in Figures 4.8 D & E, wild-type eyes from both the *Pax6*$^{+/-}$ and the *Mp/+* crosses tended to have more densely packed cells when compared to either *Pax6*$^{+/-}$ or *Mp/+* but significant differences between genotypes were only detected for *Mp/+* and their wild-type littermates (ANOVA: P=0.020). If cell densities in the cornea are representative of those in the limbus, these results imply that the higher frequency of

LRCs per unit area in *Mp/+* eyes when compared to wild-type controls was not a result of higher cell density in the *Mp/+* ocular surface. Similarly, the trend towards more LRCs per unit area in *Pax6*$^{+/-}$ eyes than in wild-type controls was not a result of higher cell density in the *Pax6*$^{+/-}$ ocular surface.

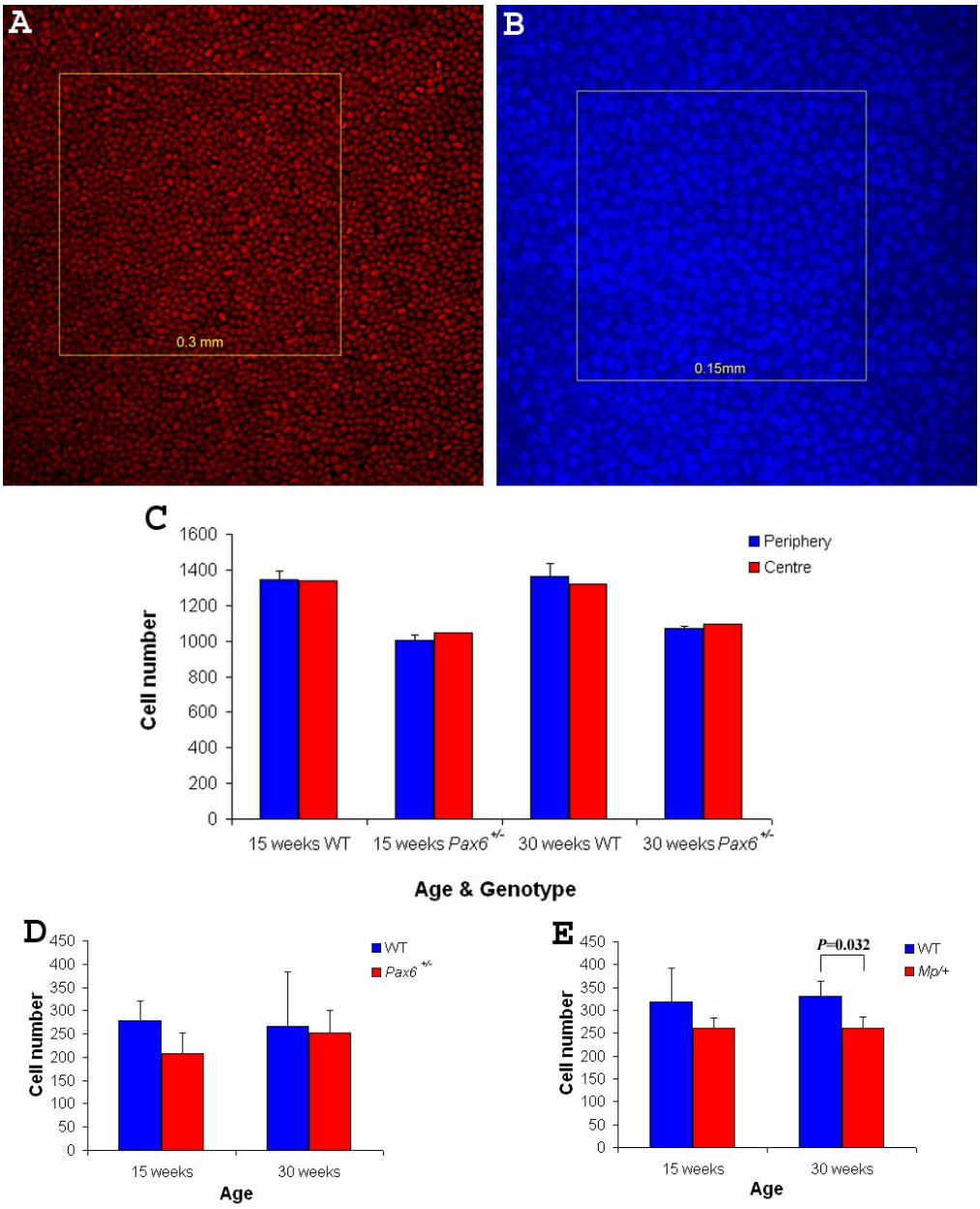

Figure 4.8 Comparisons of cell densities. (A) Image from the periphery of a PI stained cornea indicating the sampling area. (B) Image from the periphery of a TO-PRO3 iodide stained cornea indicating the sampling area. (C) Preliminary data showing the mean of the three measurements from the periphery and the number of cells from the centre of the PI corneas in *Pax6*$^{+/-}$ and wild-type mice. Cell densities were similar between the periphery and the centre of the corneal epithelium. (D) Cell density measurements in *Pax6*$^{+/-}$ and their wild-type littermates. (E) Cell density measurements in *Mp/+* and their wild-type measurements. Wild-type eyes seem to have more densely packed cells when compared to either of the mutant ones, but differences were statistically significant only for the *Mp/+* mice. If 2-way ANOVAs identified significant differences among groups this was followed by pairwise comparisons by t-tests. Only significant pairwise comparisons with t test are showing.

4.3.6 Location of stem cells in relation to the eye

As mentioned in the introduction (section 4.1), there are at least two publications (Pajoohesh-Ganji et al., 2006; Zhao et al., 2009) that have reported a difference in the frequency of LSCs in relation to different locations around the eye (nasal, temporal, inferior or superior limbus) where LRCs seemed to be enriched. Both studies identified two quadrants of the eye harbouring statistically more LRCs than the other two, namely superior & inferior regions in the first and superior & temporal regions in the latter. In order to test for such a difference each eye has to be marked in a way that after immunohistochemistry it would be easy to relate the hallmark with the original orientation of the eye. Although this experiment was not designed to check for such a difference, the fact that the sectors of each cornea were always imaged in a clockwise manner allows a limited investigation of spatial differences in LSC frequency around the circumference. This was achieved for wild-type eyes in the following way: The LRCs in every sector were expressed as percentages of the total number of LRCs found in all the sectors of the eye. Then, the sector with the highest percentage of LRCs was identified and was considered as sector number 1. The rest of the sectors were then arranged after sector 1 but always keeping the order by which the sectors were imaged originally. If two parts of the limbus were enriched in LRCs, after arranging the sectors as described before, the graphs should show two peaks. One would be in sector 1 because this is the sector that we manually picked to be the one having the highest number of LRCs. The other peak should be in sector 5 if superior & inferior parts are enriched in LRCs or in either of sectors 3 and 7 if superior and temporal are having the most LRCs (Fig. 4.9 A).

Analysis of data revealed that there was no significant difference amongst sectors 2 – 8 either when all the eyes were considered together (Fig. 4.9 B & C) or when left and right eyes were considered separately (Figure 4.9 D – G). This is not consistent with the hypothesis that the proportion of LRCs is higher in the superior and inferior regions than the other two regions because there was no evidence for more LRCs in position 5 (opposite position 1) rather than in positions 2 – 4 or 6 – 8. However, our analysis does not adequately test whether the superior & temporal regions had more

LSCS than inferior and nasal regions because if this was the case the highest frequencies after position 1 could be either position 3 or 7, depending on whether left or right eyes were analysed and whether results for superior or temporal were designated as position 1.

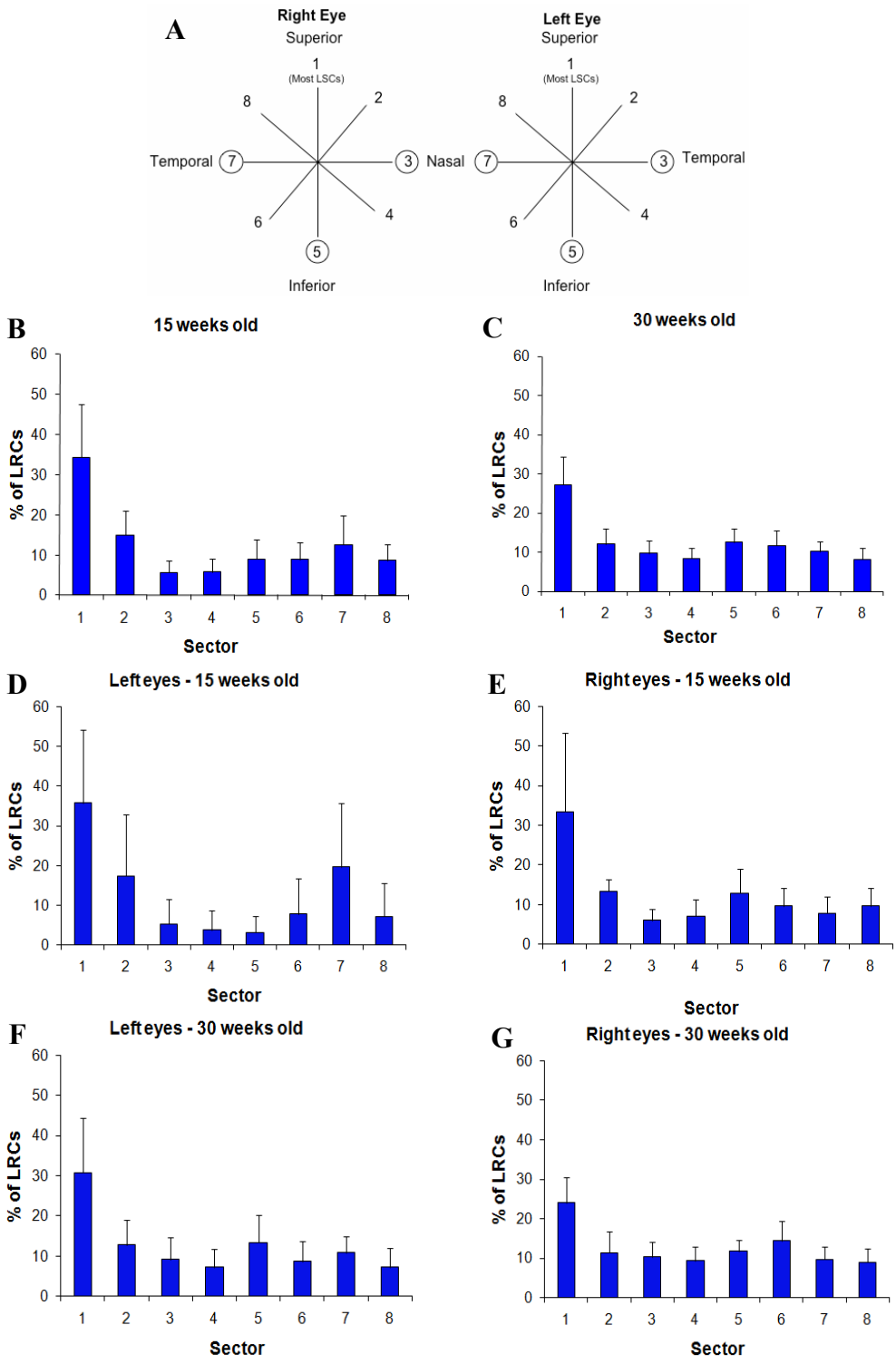

Figure 4.9 Distribution of LRCs in the different sectors of wild-type corneas. (A) Diagram showing the numbering of the sectors in relations to the different eye parts. Sector 1 was designated as the sector with the most LSCs but this need not be the superior section (as shown). Other sectors were numbered clockwise from sector 1. (B) 15-week old left and right eyes (N=10). (C) 30-week old left and right eyes (N=15), (D) 15-week old left eyes (N=4), (E) 15-week old right eyes (N=6), (F) 30-week old left eyes (N=7), (G) 30-week old right eyes (N=8). 1-way ANOVAs showed no differences among sectors 2 – 8 for any of the groups shown.

4.3.7 LRCs within the cornea

Although the box that was placed on the confocal images in order to count the LRCs in the limbus, there were some cases where some LRCs were found to be in the cornea rather than the limbus, especially in the *Pax6*$^{+/-}$ eyes. As shown in Figure 4.10, these cells were counted and plotted. There was a significant difference between LRC numbers below the limbus for *Pax6*$^{+/-}$ and their wild-type littermates (ANOVA: P=0.0007) for both ages checked.

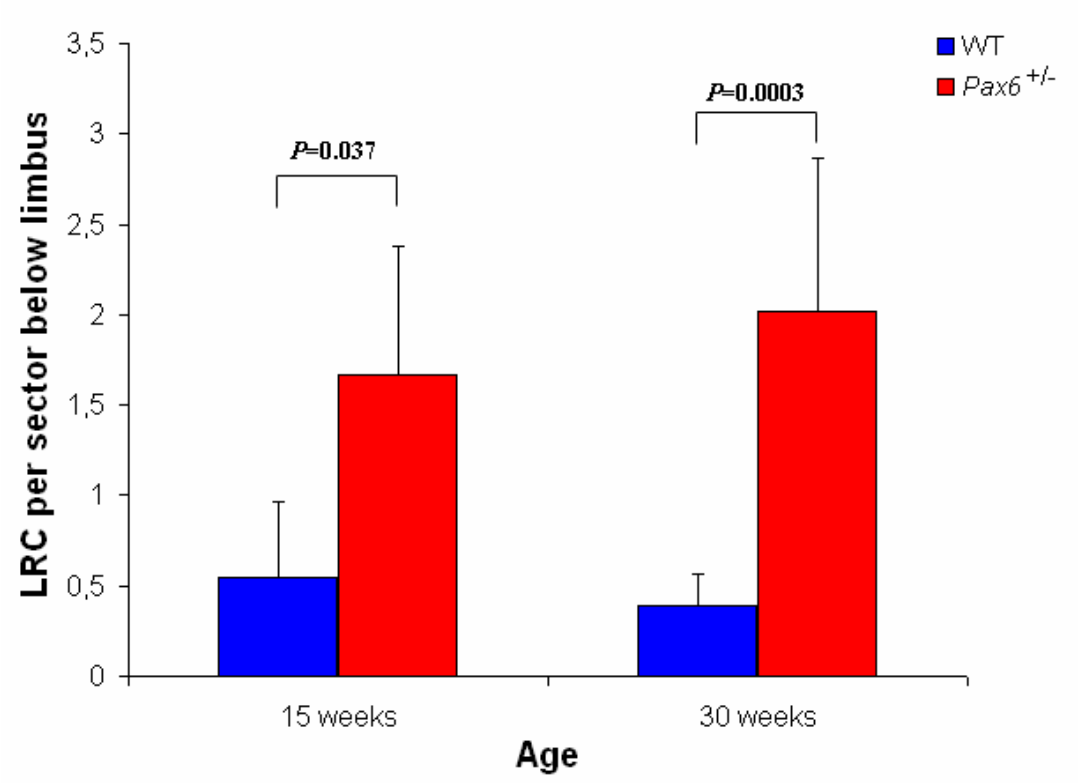

Figure 4.10 LRCs found in the peripheral cornea in *Pax6*$^{+/-}$ and their wild-type littermates. In this analysis, 12 wild-type eyes and 22 *Pax6*$^{+/-}$ from 15 weeks old mice were included, whereas 19 wild-type and 15 *Pax6*$^{+/-}$ from 30 weeks old mice were compared. *Pax6*$^{+/-}$ eyes had consistently more LRCs below the limbus (i.e. in the cornea) than their wild- type counterparts, in both ages. Only significant pairwise comparisons, by t-tests, are shown.

4.3.8 LRCs in *Pax6*$^{+/-}$ heterozygotes

The identification of LRCs in the corneal epithelium of *Pax6*$^{+/-}$ eyes in conjunction to the observation that blood vessels invade the corneal epithelium in *Pax6*$^{+/-}$ mice (Fig. 4.2) prompted a study to localise both LRCs and blood vessels in the same samples. Some eyes from the mice that had been implanted with a mini-pump loaded with BrdU (see section 2.2.2) at the age of 15 weeks were double-stained for BrdU and CD31. However, as mentioned before (section 4.2.3), a slightly different protocol was used for this double immunofluorescence staining since both primary antibodies were raised in rats. Because of the way that these corneas were stained, BrdU positive cells were positive for both secondary antibodies and thus they appear as yellow (Fig. 4.11) instead of green (Alexa 488 stains green). Blood vessels on the other hand were red because after the anti-CD31 antibody only the Alexa 568 secondary antibody was applied.

Wild type (Fig. 4.11 A) and *Pax6*$^{+/-}$ (Fig. 4.11 B – D) eyes from 15 weeks old mice were implanted with BrdU-loaded mini-pumps at the age of 15 weeks, double labelled for BrdU (yellow) and blood vessels (red) whilst TO-PRO3 iodide (blue) was used as counterstain. As expected, blood vessels in the wild-type eye were restricted to the limbal area whereas in the *Pax6*$^{+/-}$ eye they were present even in the central cornea (compare Fig. 4.11 A to C & D). Interestingly, the distribution of LRCs was the same as the blood vessels (they were restricted to the limbus of the wild-type eyes but present in both the limbus and cornea of the *Pax6*$^{+/-}$ eyes). In fact, as the arrows in Figure 4.11 show, LRCs were usually found on top of the blood vessels. Unfortunately, this technique cannot reveal if BrdU staining co-localizes with the blood vessels because, according to the protocol followed, BrdU positive cells will always be yellow. However, this finding suggests that, at least in the *Pax6*$^{+/-}$ eyes, BrdU-LRCs are not all LSCs (further discussed in section 4.4.3).

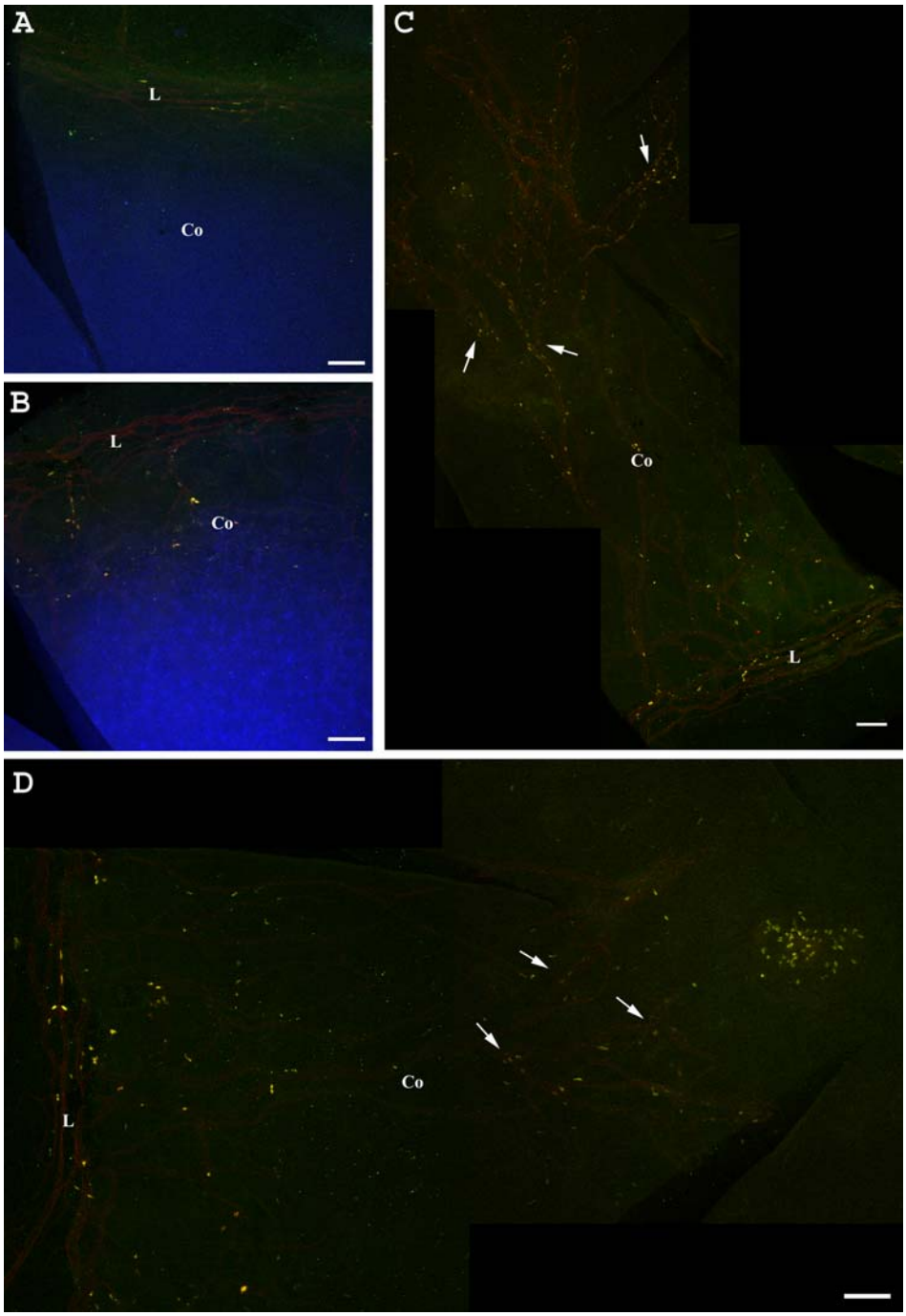

Figure 4.11 Double immunofluorescent detection of BrdU and blood vessels in wild-type (A) and *Pax6*$^{+/-}$ (B – D) mice. (A) Wild-type flattened cornea showing BrdU-retaining cells and blood vessels in the limbus. (B) *Pax6*$^{+/-}$ flattened cornea demonstrating blood vessel in-growth and BrdU-labelled cells in the cornea. (C & D) Montages of *Pax6*$^{+/-}$ flattened corneas showing blood vessels and BrdU-positive cells even in the centre of the cornea. Arrows show blood vessels with adjacent BrdU-positive cells. For demonstration purposes the counterstain channel was deactivated. L: Limbus; Co: Cornea; Yellow: BrdU; Red: CD31; Blue: TO-PRO3 iodide counterstain. Scale bars are 0.1 mm.

4.4 DISCUSSION

The border between the cornea and the conjunctiva comprises a region called the limbus. By applying different markers successfully, a structural artefact was revealed and was used to identify the limbus in the consequent experiments. In wild-type eyes, this was a well defined ridge that has also been reported by others (Pajoohesh-Ganji et al., 2004). The detection of conjunctival markers and blood vessels also provided some useful findings concerning the abnormal phenotype of *Pax6*$^{+/-}$ eyes. Both CD31 and K19 positive cells were found to be present in the cornea of these mice. This finding confirms previously published data on the possible intrusion of conjunctiva into the *Pax6*$^{+/-}$ cornea (Davis et al., 2003; Nishida et al., 1995; Ramaesh et al., 2003). Specifically, it has been suggested that in the absence of limbal stem cells or if the whole limbus is destroyed, conjunctival cells invade the cornea, in an attempt to repair the tissue which results in corneal opacity since the reconstituted cornea is no longer transparent (Kruse et al., 1990).

4.4.1 Quantitative analysis of LRCs in the limbus

LRCs in wild-type and *Mp/+* mice were almost all confined to the limbus. This is consistent with the conventional view that the adult corneal epithelium is maintained by stem cells in the limbus. However, the quantitative results from the LRCs technique failed to support either of the hypotheses being tested. First, there was no evidence that older wild-type mice had fewer active stem cells than younger mice because they did not have fewer label retaining cells. Second, there was no evidence that *Pax6*$^{+/-}$ mice had fewer active stem cells than age-matched wild-type mice because they did not have fewer label retaining cells. This implies that either the hypotheses are incorrect or the LRC method that was used was not appropriate for quantifying the number of putative active LSCs.

In addition, the number of LRCs may not be proportional to the number of putative active LSCs if the kinetics of cell renewal among the compared groups (15 weeks versus 30 weeks or wild-type and *Pax6*$^{+/-}$) was different. The success of the LRC technique is highly dependent on the cell cycle length since both the rate of BrdU uptake and the time required for somatic cells to dilute the incorporated label will depend on the division rate of the cells under investigation. If the rates of corneal epithelial renewal differed between young and old animals or between *Pax6*$^{+/-}$ and wild-type mice, this could result in labelling different proportions of the cells. In addition, differential renewal would also result in cells diluting the label at different times. However, at least in wild-type mice, no difference has been found in the incorporation of ^{3}H-thymidine in any part of the corneal epithelium (either central or peripheral) for mice between one month and one year of age (Gao et al., 1993) and thus the renewal rate should be equivalent throughout the corneal epithelium for these ages. These results, although performed with a different label, are probably applicable to the BrdU labelling as well, since the way both thymidine analogues enter the cells and label them is the same. However for the *Pax6*$^{+/-}$ eyes it has been shown that there is more proliferation in the basal layer of the corneal epithelium compared to wild-type mice (Davis et al., 2003; Ramaesh et al., 2005). On the other hand, even if there is differential cell renewal, the amount of LRCs could, at least in theory, be the same. That is because the technique reflects a tight equilibrium; higher proliferation will mean higher labelling index but at the same time, cells will dilute the label faster. Thus, the proportion of LRCs could end up being the same even in circumstances where there are differences in the rate of cell renewal (e.g. different ages or genotypes for the same tissue). However, these issues have to be further investigated and are probably depending on the properties of the tissue under investigation as well.

In principle, the failure to identify fewer LRCs in older and *Pax6*$^{+/-}$ mice could be explained if the cell packing density was affected by age and genotype, because there would be different numbers of cells per sampling area. However, cell density measurements suggest that the predicted differences in LRC numbers were not

masked by differences in cell packing. The cell density did not change with age and the non-significant trends towards slightly lower cell densities in *Pax6*$^{+/-}$ and *Mp/+* corneas means that the proportion of cells that were LRCs is unlikely to be lower than estimated. However, it is acknowledged that the estimates for cell density were not perfect and should only be considered as approximate estimates of cell packing densities. Images for analysis were taken from either the peripheral or central cornea instead of the limbus. Although it was shown that there are not large differences between the density in the peripheral and the central cornea, this does not rule out the possibility that the limbus has different cell density. Furthermore, imaging was performed on whole-mount eyes and the whole depth of the corneal epithelium and consequently all its layers were examined under the confocal microscope and an image from a single optical section was obtained. However, different layers of the cornea are known to have cells arranged in different densities and the width of the cornea at which the image was taken could not be determined confidently for all the eyes examined. For these reasons, the cell density estimates were not used to apply a further correction to the estimates of the relative LRC numbers.

4.4.2 Other possible shortcomings of the BrdU LRC approach

Recent studies have suggested that extreme caution is necessary when interpreting results from some types of experiments using thymidine analogues to label cells. These concerns are mainly raised by studies where cells were marked with such labels and then were transplanted in host tissue (Burns et al., 2006; Coyne et al., 2006). Both studies found that the distribution of the thymidine analogue in the host tissue was identical irrespective of whether dead or alive cells carrying the label were used for transplantation. This surprising finding was even observed 12 weeks after the operation (Coyne et al., 2006). This result was obtained by labelling cells and then killing them by either freeze-thaw lysis or microwave irradiation before transplanting them. The exact mechanism by which the surrounding tissue takes up the label is not yet clear, but it is presumed to involve death of the labelled cells. The

labelled oligonucleosides of the dying cells could be processed by endogenous DNase and recycled for incorporation to other dividing cells or to cells undergoing DNA repair (Burns et al., 2006). Another potential means by which label can be transferred is by activated macrophages, which can phagocytose labelled cells or their remnants, thereby labelling themselves. In fact, a study was recently published that showed 10 – 20 % of BrdU labelled cells were taken up by activated macrophages in an *in vitro* model of inflammation (Pawelczyk et al., 2008). The same group also published an *in vivo* study showing that 5 – 15 % of the label can be transferred, especially in a localized area of inflammation and angiogenesis (Pawelczyk et al., 2009).

Extensive cell death is likely to occur in the *Pax6*$^{+/-}$ corneal epithelium since it has been shown to be more fragile than the normal corneal epithelium (Ramaesh et al., 2003), possibly contributing to its continuous state of wound-healing (Ou et al., 2008). These findings suggest that the corneal epithelium of the *Pax6*$^{+/-}$ eyes is a place of inflammation. Additionally, vascularisation of the peripheral epithelium is one of the main characteristics of the *Pax6*$^{+/-}$ corneas. The evidence for vascularisation, extensive inflammation and cell death in *Pax6*$^{+/-}$ corneas could mean that some BrdU may be released extracellularly or transferred between cells. The detection of extracellular or cytoplasmatic BrdU in the *Pax6*$^{+/-}$ eyes (Fig. 4.5 B & D) is consistent with this possibility. If BrdU transfer between cells is extensive in *Pax6*$^{+/-}$ mice, it may obscure differences in the relative numbers of LSCs in the limbus of *Pax6*$^{+/-}$ and their wild-type littermates. Also, doubts have been raised to whether the BrdU-LRC technique can provide a reliable estimate of the number of active stem cells in the limbus.

4.4.3 LRCs in the corneas of *Pax6*$^{+/-}$ mice

It was clear that in *Pax6*$^{+/-}$ mice LRC were detected in the cornea as well as the limbus. This suggests either that stem cells that maintain the corneal epithelium are present in both the limbus and cornea of *Pax6*$^{+/-}$ mice or that some of LRCs are not putative stem cells. To evaluate this second possibility it is necessary to consider what cell types could be identified as LRCs.

Some of the LRCs in the cornea of *Pax6*$^{+/-}$ mice were seen to be organised in elongated groups, appearing to follow blood vessels in the cornea. In fact, when double immunodetection of BrdU and CD31 (marking endothelial cells of the blood vessels) was performed, LRCs were found to be at least in very close proximity to blood vessels, although the protocol used could not address their co-localisation. One possible explanation of the corneal LRCs in *Pax6*$^{+/-}$ mice is that they reflect cells that are produced during vascularisation of the *Pax6*$^{+/-}$ cornea, which occurs as part of a range of corneal abnormalities that cause progressive corneal deterioration in *Pax6*$^{+/-}$ mice (Ramaesh et al., 2003). Thus, if BrdU is present in the eyes of these mice while new blood vessels are formed, it will be incorporated into dividing cells in the growing vasculature, which then differentiate and stop dividing, so will retain the label. In principle, differences in the degree of vascularisation in the limbus of young and old mice might mask an age-related reduction in LRCs in the limbus. However, since new blood vessels should not be actively formed in healthy adult eyes, cells from the blood vessels are not expected to be labelled.

Also, as discussed above in section 4.4.2, some of these labelled cells could be macrophages that infiltrated into the tissue from the growing blood vessels in the cornea of *Pax6*$^{+/-}$ eyes, phagocytosed the remaining of labelled corneal epithelial cells and hence they appeared labelled. Activated macrophages have been reported to act in a similar way both *in vitro* (Pawelczyk et al., 2008) and *in vivo* (Pawelczyk et al., 2009). Additionally, a small proportion of the labelled cells, even in the wild-type limbal epithelium, could be Langerhans cells, which have been recently identified to be present in the limbus and to have a slow-cycling nature (Chen et al., 2007).

Conversely, it is also possible that the LRCs in the *Pax6*$^{+/-}$ cornea are indeed stem cells. There are several published studies that have reported a close relationship between LRCs and blood vessels in different tissues and cell environments like the endometrium (Chan and Gargett, 2006), dental pulp (Shi and Gronthos, 2003), adipose tissue (Staszkiewicz et al., 2009), neural cells (Shen et al., 2004), endothelial cells (Kiel et al., 2005). Such reports have led to the hypothesis that some stem cells can be transferred via blood circulation from places like the bone marrow, to a variety of tissues where they adopt a new cell fate that is determined by their new environment.

On balance it seems more likely that the LRCs in the *Pax6*$^{+/-}$ corneas are not all putative stem cells and many are likely to be differentiated cells of the corneal vasculature which forms in *Pax6*$^{+/-}$ corneas but not in wild-type corneas.

4.4.4 LRCs in the corneas of *Mp*/+ mice

Interestingly, *Mp*/+ mice showed a higher LRC index than their wild-type littermates. *Mp*/+ mice were used as an additional control because of their small eye size, which was not attributable to a *Pax6*-defect and they had a histologically normal corneal epithelium. However, it has subsequently become clear that this mutation causes a range of eye defects so, with hindsight, it was a poor choice as a control.

It is now known that *Mp* involves a rearrangement of a region of chromosome 18 and *Mp*/+ heterozygotes have intracellular inclusions that may be attributable to abnormalities of the endoplasmic reticulum and impaired protein transport (Dr. Joe Rainger, MRC Human Genetics Unit, Edinburgh, personal communication). In *Mp*/+ heterozygotes the lens appears to deteriorate with age (data not shown). One possibility is that corneal homeostasis is affected as a secondary consequence of abnormalities in other eye tissues some of which arise after birth. Further work will be needed to characterise aspects of corneal epithelial maintenance (cell proliferation

and apoptosis) in *Mp/+* mice before the LRC results can be interpreted.

4.4.5 Conclusions

LRCs in wild-type and *Mp/+* mice were almost all confined to the limbus, which supports the conventional view that the adult corneal epithelium is maintained by stem cells in the limbus. In contrast, LRCs in *Pax6*$^{+/-}$ eyes extended from the limbus into the cornea and these may represent terminally differentiated cells rather than putative stem cells. Quantitative analysis showed no significant differences in LRC numbers in wild-type mice at 15 and 30 weeks or between age-matched *Pax6*$^{+/-}$ and wild-type mice. This suggests either that the numbers of active putative stem cells did not differ between these groups (so failing to support the hypotheses that active stem cell numbers declined with age and were depleted in *Pax6*$^{+/-}$ mice) or that quantitative analysis of LRCs is not a suitable means of comparing the numbers of active putative stem cells in different groups.

Chapter 5
Induced Mosaicism in Reporter Mice

5.1 INTRODUCTION

5.1.1 Lineage tracing experiments

Lineage tracing is a general term that describes the various methods for marking mitotically active cells and retrospectively tracing their migration and/or progeny. The need to visualize developmental lineages and cell movement has prompted scientists to explore various methods for labelling cells for many years. Thus, there are techniques as simple as injecting tissues with a dye (e.g. India ink) which cells can phagocytose to provide a means of analysing the migration of the marked cells (Buck, 1985). More sophisticated techniques include using molecularly manipulated retroviruses to deliver a reporter gene to certain cells to determine the fate of the infected cells and their progeny (Frank and Sanes, 1991).

5.1.2 Low frequency induction of a marker

Tracing of specific lineages often requires the introduction of the marker in a defined cell population. Transgenic animals are often produced that express a molecular marker (e.g. reporter gene) under the control of a tissue- or cell-specific promoter. In this way only cells in which the promoter is active express the marker. Furthermore, if the time of marker expression has to be regulated i.e. at a specific time frame during development of transgenic animals, conditional expression of the reporter can be achieved by promoters responsive to a variety of physiological or artificial stimuli like heat shock, metal ions, interferons, steroids (reviewed by Goverdhana et al., 2005) or any possible combination of the above providing a wide variety of regulation. However, this will not provide a lineage marker unless the transgene is

designed to ensure that the transgene is expressed in all the daughter cells regardless of their developmental fates, as discussed below.

In some cases, the induction of the reporter has to be rare, so that the marked progeny is a result of a single marked cell. Rare genetically marked clones of cells have been identified in different tissues by a method that involves the production of transgenic animals that carry a *LacZ* gene, which is inactive due to an internal duplication (Nicolas et al., 1996). Stochastic homologous intra- or (rarely) inter-chromosomal recombination re-establishes the open reading frame resulting in the successful marking of cells and their progeny (Bonnerot and Nicolas, 1993). This system has successfully been applied to identify stem cells or pools of progenitors based on the clonal relationships of their progeny in a variety of tissues including the myotome (Nicolas et al., 1996), the central nervous system (Mathis and Nicolas, 2000) and the cerebellum (Mathis and Nicolas, 2003).

One drawback of the cell lineage marking system described above is that the rare recombination events that restore *LacZ* activity are stochastic. Thus, there is a lack of either spatial or temporal control of transgene expression and marked clones can be initiated throughout development in every tissue. The Cre/*LoxP* transgenic system, on the other hand, can produce rare marked clones in specific tissues and/or at specific times depending on the regulatory elements introduced, offering advantages over the systems described before.

5.1.3 The Cre/*LoxP* system

The Cre/*LoxP* system is naturally found in bacteriophage P1 and serves a critical role in the viral life cycle, especially for its integration to the host's genome (Sternberg and Hamilton, 1981). The two components that comprise this system are *LoxP*, a 34 bp sequence on the phage DNA and Cre, a 35 kDa DNA binding protein encoded by the phage that catalyses the recombination between two *LoxP* sites. These two components appear to be sufficient for successful recombination, whereas the form

of the DNA substrate containing the two *LoxP* sites (e.g. linear, supercoiled etc) is not critical (Abremski and Hoess, 1984). Cre recombinase makes specific complexes with the *LoxP* sites and the intermediate DNA sequence either becomes inverted, if the *LoxP* sites are in opposite directions, or it is excised in a circular form, if the *LoxP* sites are orientated in the same way as direct repeats (Abremski and Hoess, 1984).

Cre/*LoxP* technology has been successfully applied to analysis in the mouse mainly because it provides a means to conditionally remove or activate gene function. Both applications are based on the ability of Cre recombinase to precisely excise DNA regions between two *LoxP* sites (floxed region: flanked by *LoxP* sites). If the *LoxP* sites are in the same orientation, flanking an essential part of the gene, Cre mediated recombination will remove this region leading to gene deactivation. In the case of gene activation, *LoxP* sites must be similarly orientated and flank a DNA sequence that prevents the expression of the gene downstream (often called a STOP cassette). Excision of this functional barrier will result in switching the gene activity on (Fig. 1.5). This technology, in combination with other transgenic technology, has resulted in successful cell lineage tracing by producing Cre dependent reporter mouse strains that express the respective reporter gene ubiquitously after the activation of the Cre recombinase. Specifically, genes like *LacZ* (Soriano, 1999) or *YFP* and CFP (Srinivas et al., 2001) preceded by a *LoxP* flanked (floxed) transcriptional termination sequence have been targeted to the ROSA26 locus in transgenic animals. An alternative variation is the development of the Z/AP reporter strain where the floxed *LacZ* gene is followed by an alkaline phosphatase reporter gene (Lobe et al., 1999). Here, all cells are express the *LacZ* unless Cre is introduced in the system in which case recombination is excises *LacZ*, activating the alkaline phosphatase expression.

5.1.4 Cre recombinase responsive to tamoxifen

Conditional alterations of the genome depend on the production of various Cre expressing transgenic mice that have the ability to regulate the tissue or the timing in which the alteration is taking place. This regulation is achieved by inserting the Cre recombinase gene under the control of several different promoters, an ongoing effort of many different groups around the world. Also, attempts are made towards the production of transgenic mouse strains where Cre activity is induced by the administration of exogenous substances. In one such approach, Cre was effectively activated by administering the animal with tamoxifen, an oestrogen-receptor antagonist (Badea et al., 2003). This was achieved by creating a gene that encodes a fusion protein between Cre recombinase and a mutant form of the ligand-binding domain of oestrogen receptor (ER^{TM}). Under normal circumstances, the mutant oestrogen receptor fails to bind its natural ligand, but it is responsive to tamoxifen (Danielian et al., 1993). This fusion protein is sequestered in the cytoplasm of the cell where oestrogen receptor is usually found and hence, prevents nuclear Cre mediated *LoxP* recombination. When tamoxifen is administered, it enters the cell and binds to the ER^{TM} domain of the fusion protein, which then moves to the nucleus where Cre mediated recombination takes place (Mattioni et al., 1994).

This method is not restricted only to adult mice since experiments have also been conducted on pregnant females and showed that tamoxifen can induce recombination in the developing embryo as well and in a dose dependent manner (Danielian et al., 1998). Transgenic animals that ubiquitously express the Cre/ER^{TM} fusion protein have been produced by inserting the gene under the control of the constitutively active CAGG promoter (a chimaeric promoter of the cytomegalovirus immediate-early enhancer and the chicken β-actin promoter/enhancer; Hayashi and McMahon, 2002). However, as pointed out by the authors, there are two issues with this approach. First, the tamoxifen related toxicity, which seems to be dose dependent. The observed lethality of the mice that received tamoxifen, is attributed to the hormonal disruption that this oestrogen-like steroid can cause in the interactions between the foetus and the mother when administered in high concentrations (Sadek

and Bell, 1996). Second, spontaneous sporadic recombination in the absence of tamoxifen was detected to be less than 0.1% in 9.5dpc embryos, but it was higher in later stages. This "leakiness" was more pronounced in the cerebellum, kidney, lung and liver, as judged by X-gal staining of sections from these tissues. Interestingly, the latter feature of these mice can be used for clonal analysis since the tamoxifen independent recombination occurs very infrequently so that it can provide a means to study rare recombination events in very few cells and follow their progeny and/or migration (Hayashi and McMahon, 2002).

5.1.5 Rendering Cre recombinase cell-permeable

As mentioned above, Cre recombinase delivery can be a limiting factor of the conditional mutagenesis since it usually requires excessive mouse breeding, which is expensive and time consuming, and/or the administration of reagents with toxic side effects. Additionally, the leakiness of the Cre/ER^{TM} system and its activation before the desired induction can be a disadvantage when tight regulation of the recombination event is crucial. In an attempt to deliver biologically active Cre recombinase into mammalian cells, protein transduction technology has been implemented. This technology fuses specific peptides or protein fragments, called protein transduction domains (PTDs), with proteins in order to modify their biophysical properties, especially with respect to their cellular uptake (reviewed by Hawiger, 1999). In terms of rendering Cre recombinase permeable to cells, three different PTDs were fused to a nuclear localisation signal (NLS) carrying Cre that also contained a membrane translocation sequence (MTS) from the Kaposi fibroblast growth factor (FGF) and their efficiency was compared. These PTDs were a glutathione S transferase (GST), a maltose binding protein (MBP) and a six histidines (His_6) tag (Jo et al., 2001). The best results concerning yield, solubility, *in vitro* activity, localization and activity in cells was achieved with a Cre fused with a His_6 tag, NLS and MTS. Cell permeable Cre efficiency was also tested by administering it in the form of i.p. injection in R26R-*LacZ* mice (which have a floxed

STOP cassette upstream of *LacZ*) and this showed recombination in a variety of tissues including brain, heart, kidney, lung, spleen and liver. On the other hand, a comparative study between a hydrophobic peptide from the Kaposi FGF and a basic peptide from the TAT gene of the human immunodeficiency virus (HIV), which has successfully been used to render β-gal cell permeable (Schwarze et al., 1999) was conducted (Peitz et al., 2002). These peptides were fused independently as PTDs to a His-NLS-Cre recombinase and their transduction efficiencies were compared. This study showed that His-TAT-NLS-Cre was the most efficient in terms of protein transduction and *LoxP* recombination in culture cells. However, the authors failed to reproduce the previously mentioned recombination in mice irrespectively of the cell permeable Cre they used (even with the His-NLS-Cre-FGF which is similar to the one used by Jo et al.). Finally, Ruley and his colleagues tested a few more combinations of PTDs on the Cre recombinase and concluded that NLS, His_6 and TAT enhances cellular uptake and in their hands His-NLS-Cre showed the best results concerning activity, solubility and yield of the protein, although they did not use the aforementioned His_6-TAT-NLS-Cre construct (Lin et al., 2004).

An alternative application of Cre dependent recombination is the administration of the cell-permeable Cre directly into the tissue of interest. Ambati et al. achieved successful recombination in the mouse cornea, by applying a cell permeable Cre (consisting of His_6-NLS-Cre) as eye drops directly into the eyes of R26R-*LacZ* mice. They also used this Cre in mice with a floxed VEGF receptor gene (flt-1) and proved that blood vessels were growing in corneas treated with cell-permeable Cre as a result of knocking out flt-1 activity via recombination (Ambati et al., 2006).

5.1.6 Aims

The aim of this chapter was to mark few stem cells and their TACs by inducing rare recombination of *LoxP* sites that flank a reporter gene. Since all their progeny would also be labelled by this permanent DNA alteration, clones of cells expressing the reporter gene were expected to be detected in the corneal epithelium. If the conventional limbal stem cell hypothesis is correct, these clones should appear as stripes and the number of these stripes should be proportional to the number of active LSC in the mice. Thus, by comparing stripe numbers in the corneal epithelium of wild-type and *Pax6*$^{+/-}$ mice and between young and old adult mice, it should be possible to assess the possibility that LSCs are depleted in the *Pax6*$^{+/-}$ heterozygotes and in older mice.

The plan was to induce *LoxP* recombination first by applying cell permeable Cre recombinase in the form of eye drops directly on the eyes of reporter mouse lines. Rare recombination could then be achieved by titrating the concentration of the cell permeable Cre recombinase that is applied. In a second approach, the aim was to cross reporter mice with CAGG-Cre/ER^{TM} mice and inject their double positive progeny with tamoxifen. Then by titrating the dose of tamoxifen it should be possible to produce rare recombination that will allow clonal analysis of the stem cell progeny.

5.2 MATERIALS & METHODS

5.2.1 Animals

Several mouse strains were used for these experiments in an attempt to find a good reporter mouse line. Apart from the Z/AP, CAGG-Cre/ER^{TM} and *Pax6*$^{Sey\text{-}Neu}$ mice, which have already been described (section 2.1), R26R-*LacZ* and R26R-*YFP* mouse lines were also checked for reporter gene expression. Both lines have a reporter gene (β-gal and yellow fluorescent protein respectively) targeted to the Rosa26 locus for ubiquitous expression but also a floxed STOP cassette upstream, which obstructs expression of the reporter gene under normal circumstances. However, when Cre is introduced in this system, it recombines the two *LoxP* sites flanking the STOP cassette. This results in the excision of the STOP sequence and the subsequent ubiquitous activation of the reporter gene.

However, the main experiments were performed on mice carrying the Z/AP transgene. For these, Z/AP mice were mated to CAGG-Cre/ER^{TM} and since both colonies were heterozygous for the transgenes, the offspring were: 25% Z/AP positive and CAGG-Cre/ER^{TM} positive, 25% Z/AP positive and CAGG-Cre/ER^{TM} negative, 25% Z/AP negative and CAGG-Cre/ER^{TM} positive, 25% Z/AP negative and CAGG-Cre/ER^{TM} negative. Only mice positive for both transgenes were used for the experiments described in this chapter. Mice positive for both transgenes were also crossed to *Pax6*$^{Sey\text{-}Neu/+}$ mice to produce mice positive for both transgenes and also heterozygous for the *Pax6*$^{Sey\text{-}Neu}$ mutation (1/8). Mice from the above colonies were genotyped by Paul Devenney (MRC Human Genetics Unit, Edinburgh) from DNA extracted from ear clips.

5.2.2 Production and application of the cell-permeable Cre

The plasmid expressing the cell-permeable Cre was multiplied in bacteria and purified as described before (section 2.15). Cell-permeable Cre recombinase activity was compared to commercially available Cre in vitro as detailed in section 2.16 and its concentration was measured based on a Bradford method (see section 2.17). Cell-permeable Cre was also applied in live ES cells from R26R-*LacZ* mice, where it was found able to activate β-gal at least once (work performed by Dr. Peter Hohenstein's group, MRC Human Genetics Unit, Edinburgh).

Furthermore, experiments with the cell-permeable Cre in the form of eye-drops were conducted on live reporter mice (namely the Z/AP, R26R-*LacZ* & R26R-*YFP*) in order to topically activate, in the eye, the reporter gene these mice are carrying (detailed in section 2.18). Two batches of cell-permeable Cre were used with different concentrations (120 ng/μl and 750 ng/μl). 5 – 25 μl were applied directly onto the corneas in 1 – 5 μl aliquots, allowing 1 minute between aliquots. Thus, the final dose of Cre in μg is shown in the Results section. Mice were sacrificed and their eyes were dissected (section 2.3) and stained according to the mouse strain. Z/AP mice were stained for alkaline phosphatase (section 2.7), R26R-*LacZ* mice were stained for β-gal activity (section 2.6) and R26R-*YFP* were either checked directly under a fluorescent microscope fitted with a YFP filter or they were stained for YFP using the immunofluorescence protocol described before with the GFP antibody which also recognises YFP (see section 2.11 and Table 2.2).

5.2.3 Tamoxifen induced recombination in reporter mice

A different way to introduce Cre recombinase into the reporter mice is to mate these mice with CAGG-Cre/ER^{TM} mice, which carry an inactive form of Cre that gets activated once tamoxifen is administered. Z/AP and R26R-*LacZ* mice were mated to CAGG-Cre/ER^{TM} mice and offspring positive for either of the reporter genes (Z/AP or β-galactosidase respectively) and the Cre/ER^{TM} transgene received an i.p.

injection of tamoxifen. Tamoxifen was dissolved at either 10 mg/ml or 50 mg/ml in corn oil and several different volumes of the solution were injected intraperitoneally (see section 2.19). The final dose of tamoxifen in mg is shown in the Results section and the typical weight of the treated mice was 25 – 30 g. After culling the mice, their eyes were dissected (section 2.3) and stained for alkaline phosphatase (section 2.7) or β-gal activity (section 2.6) respectively.

5.3 RESULTS

As mentioned in the aims section (5.1.6), these experiments were designed to achieve induction of the reporter gene in a very small number of stem cells (ideally only one). After the induction, mice were culled at various time points, allowing sufficient time to elapse for the recombination event to occur and also allow the terminally differentiated cells to be desquamated from the cornea. Initially, cells throughout the whole cornea should be labelled because the treatment is not specific for a selected population. By allowing time for the transient amplifying cells and the terminally differentiated cells to be desquamated from the cornea, only the progeny of marked stem cells should be identified in the cornea, since the activation via recombination is a permanent DNA change leading to the production of clones of cells that constantly express the reporter gene.

5.3.1 Cell-permeable Cre Recombinase

As mentioned previously (section 5.2.2), bacteria were transformed with a cell-permeable Cre-containing plasmid and were induced to over-express the protein, which was then isolated and purified. An *in vitro* assay based on the ability to recombine a plasmid containing two *LoxP* sites was established to measure the enzymatic activity of the cell-permeable Cre (Fig. 5.1). The linear plasmid (Fig. 5.1 L7) after incubation with the Cre recombinase, which recombined the two *LoxP* sites, appeared circularised (Fig. 5.1 L1 - L3). Furthermore, the activity of the enzyme was demonstrated in cells by treating ES cell-cultures, which showed that the enzyme could indeed enter into mammalian cells and recombine *LoxP* sites in their nuclei. These culture experiments were performed by Dr. Peter Hohenstein's group (MRC Human Genetics Unit, Edinburgh). These successful preliminary *in vitro* results prompted the *in vivo* assessment of the enzymatic activity of cell-permeable Cre in transgenic mice with constructs containing *LoxP* sites.

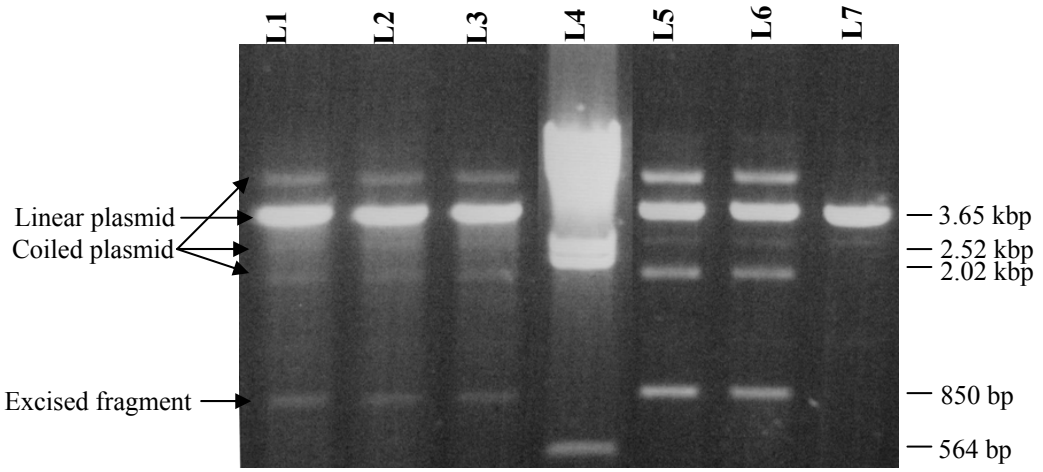

Figure 5.1 Gel electrophoresis of a *LoxP*-containing plasmid after Cre recombination. A 0.8% w/v agarose gel containing reactions of the plox2+ plasmid after incubation with different concentrations of Cre recombinase. Lanes L 1 – 3: Treatments with cell-permeable Cre at concentrations 1.6 ng/µl, 1.2 ng/µl and 0.96 ng/µl; L 4: HindIII digested λ DNA marker; L 5: 1.8 ng/µl commercially available Cre recombinase; L 6: 3.6 ng/µl commercially available Cre recombinase; L 7: Linear plox2+ plasmid in the absence of cell-permeable Cre. It is evident that after recombination at least 3 more DNA bands appear on the gel, demonstrating the different super-coiled states of the circularised plasmid.

The technique has already been successful in eyes of R262R-*LacZ* mice, by direct topical application (Ambati et al., 2006), resulting in β-gal activation in corneal epithelia. Thus, based on these protocols, the cell-permeable Cre was applied as a solution in the form of eye drops to check several reporter mouse lines for reporter gene activation. R26R-*LacZ*, R26R-*YFP* and Z/AP adult mice at different ages (ranging from 11 – 40 weeks) were anaesthetised and received eye-drops containing different amounts of cell-permeable Cre (to give final doses of 1.2 – 18.75 µg). Eye drops were applied directly to one eye whereas the other one was left untreated and was used as a negative control. Mice were then culled either after a few (2 – 6) days, to allow the recombination event to occur, or after several (5 – 20) weeks, to allow time for normal corneal cells to be desquamated. Eyes were then checked for reporter

gene activation but no activity could be detected apart from one single occasion of an R26R-*YFP* mouse (Fig. 5.2). The eyes of this mouse were stained with an anti-GFP antibody, which also recognises YFP, and the treated cornea showed a high frequency of YFP-stained cells. However, as demonstrated in Figure 5.2 B, the untreated eye also showed YFP staining, which was equivalent to the treated one, so this result could not be trusted.

In a final attempt to induce *LoxP* recombination with cell-permeable Cre, a 24-week-old R26R-*LacZ* mouse was treated more than once. It received 2.2 μg of the Cre in eye drops and 9 weeks later it received another 3.8 μg in eye drops and 190 μg of Cre in the form of an i.p. injection. This mouse was sacrificed 5 days later but again recombination and subsequent reporter gene activation could not be detected in the eye. A sample of the liver was also removed from this mouse along with the eyes, to check for β-gal activity in an independent tissue, since the cell permeable Cre was injected i.p. Although this tissue confirmed the absence of recombination, it also proved the tight regulation of the reporter gene, since the tissue was completely negative (Fig. 5.3).

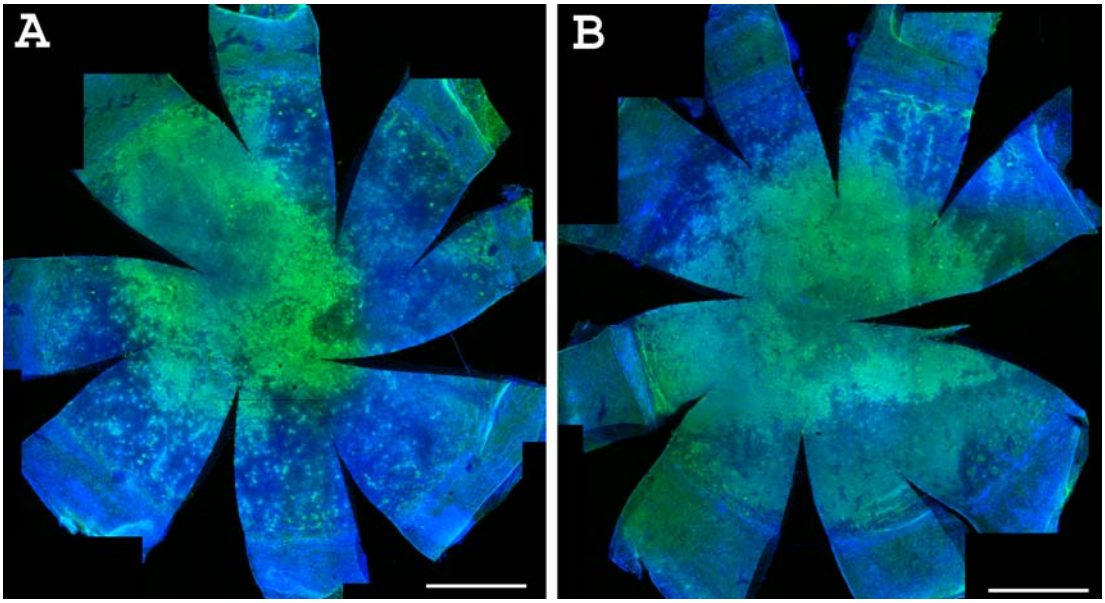

Figure 5.2 Immunofluorescent staining to detect YFP in the ocular surface of an R26R-*YFP* mouse. This 35-week old mouse received 9 mg of cell-permeable Cre in the left eye (A) whereas the right one (B) was left untreated and it was sacrificed 5 days later. YFP was detected with a GFP-specific antibody that also recognises YFP. Green: YFP; Blue: TO-PRO3 iodide counterstain. Scale bars are 1 mm.

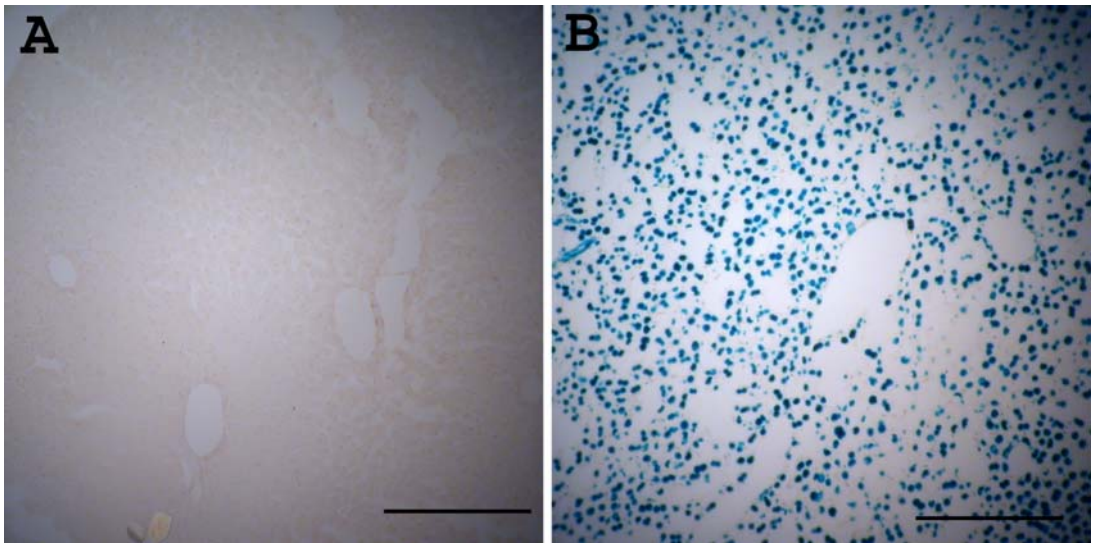

Figure 5.3 β-gal staining in frozen sections of livers. (A) Liver from an R26R-*LacZ* mouse that received cell-permeable Cre twice as eye-drops and once as i.p. injection. (B) Liver from a homozygous female H253 transgenic mouse, which expressed an X-linked *LacZ* transgene ubiquitously (positive control). Both tissues were stained with X-gal and counterstained with neutral red. Scale bars are 0.2 mm.

In order to improve the chances of success, Dr John West and I sought advice from Professor Jayakrishna Ambati (University of Kentucky) who was the corresponding author of the study where cell-permeable Cre in eye drops was successful in recombining *LoxP* sites in corneal epithelial cells (Ambati et al., 2006). He advised us to add an additional step to my protocol. This involved applying a topical anaesthetic (proparacaine) to the corneas. This step was not for anaesthetic purposes as the mice were already treated with a general anaesthetic. It was designed to dry the cornea and reduce the intercellular barriers to allow the solution to penetrate the cornea. This additional step was added to a revised protocol, which was developed in consultation with Jane Gebbie (a senior veterinary surgeon in Biological Services, University of Edinburgh). Adult (11 – 24 weeks old) R26R-*LacZ* and Z/AP mice under general anaesthesia, received proparacaine as eye drops and after drying the eyes out, eye drops containing a final dose of 4.5 – 7.5 μg of the cell-permeable Cre were applied. Mice were sacrificed just 2 – 6 days later allowing time only for the recombination to occur because the main purpose of these experiments was to prove that the cell-permeable Cre could induce recombination *in vivo*. None of the mice showed any staining in the eye and so the cell-permeable Cre experiments were aborted.

All the mice that received cell-permeable Cre in the form of eye-drops, their age, the chasing period and the outcome of the staining are summarised in Table 5.1.

Table 5.1 Summary of results from mice treated with cell-permeable Cre in the form of eye drops. Only one eye from each mouse was treated with cell-permeable Cre. Most R26R-*YFP* mice were checked under a fluorescent microscope whereas one was stained with an antibody first. The asterisk (*) indicates an R26R-*LacZ* mouse that received 2.16µg of cell permeable Cre and 9 weeks later received another 3.75µg in eye drops followed by 192µg of cell-permeable Cre as a single i.p. injection and was sacrificed 5 weeks later. † Liver, ovaries and ocular surface tissues were examined. The lower part of the table includes mice that were also treated with proparacaine before the application of the cell-permeable Cre. The dose of Cre is shown as the final dose in µg. This is because two different batches of the enzyme were used with different concentrations, so volumes were adjusted accordingly.

Reporter strain	Cre (µg)	Age (weeks)	Chase	Outcome
R26R-*YFP*	6	35	2 days	- (Fluorescence)
	7.5	15	4 days	- (Fluorescence)
	7.5	15	4 days	- (Fluorescence)
	9	35	5 days	Both eyes positive (antibody staining)
Z/AP	5.625	25	6 days	-
R26R-*LacZ*	1.2	15	3 days	-
	1.2	15	5 weeks	-
	3.6	15	5 weeks	-
	3.75	30	5 days	-
	3.75	40	20 weeks	-
	7.5	18	2 days	-
	7.5	30	5 days	-
	18.75	24	2 days	-
	* 2.16 / 3.75 + 192 i.p.	24	9 weeks / 5 weeks	All tissues† negative
Reporter strain	**Proparacaine & Cre (µg)**	**Age (weeks)**	**Chase**	**Outcome**
Z/AP	3.75	11	6 days	-
	5.625	11	6 days	-
R26R-*LacZ*	4.5	24	2 days	-
	7.5	24	2 days	-

5.3.2 Tamoxifen induced reporter gene activation

The successful published use of the cell-permeable Cre recombinase (Ambati et al., 2006) could not be confirmed in my hands, so the alternative way to introduce Cre recombinase in the reporter mice was tried. This involved tamoxifen activation of Cre, which in turn activates the reporter gene in mice with both a transgene carrying the conditional form of Cre recombinase (Cre/ER^{TM}) and a reporter transgene. As mentioned before, the Cre/ER^{TM} transgene is known to show some leakiness in certain tissues, especially in the liver and the brain (Hayashi and McMahon, 2002). If the Cre/ER^{TM} was leaky in the cornea, the small amount of the reporter gene expressed might be enough to mark a very small number of stem cells producing rare clones in the form of marked patches or stripes. Since no study checking for such leakiness in the ocular surface was known, eyes and several other tissues (namely liver, lung, heart, kidney and small intestine) were checked for leaky expression. Four mice carrying both the reporter gene and the Cre/ER^{TM} transgene were checked for leakiness as whole-mounts (two at 8 and two at 15 weeks of age from a cross between the CAGG-Cre/ER^{TM} and R26R-*LacZ* mice). Although eyes were negative for β-gal activity, most of the other tissues that were checked from these mice were found to have a considerable proportion of stained cells (Fig. 5.4) at both ages.

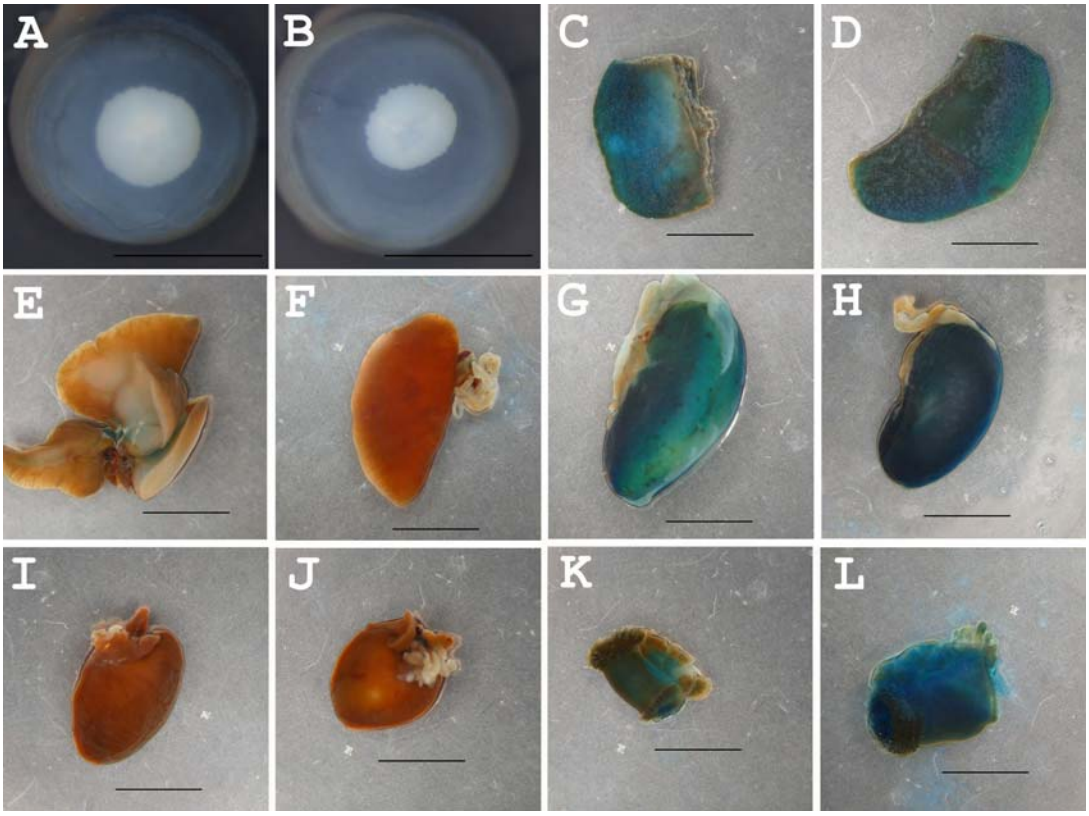

Figure 5.4 X-gal staining of various whole-mount tissues from CAGG-Cre/ER^{TM}-*LacZ* mice. (A & B) Eye, (C & D) liver, (E & F) lung, (G & H) kidney, (I & J) heart and (K & L) small intestine from two 15 weeks old mice. Most of the tissues show leaky expression of the reporter gene without the administration of tamoxifen. Scale bars are 2 mm.

The leakiness of the CAGG-Cre/ER^{TM} mice was not beneficial since it was not present in the eye. So, reporter gene activation had to be induced by the administration of tamoxifen. Pilot experiments were conducted by crossing CAGG-Cre/ER^{TM} mice to both R26R-*LacZ* and Z/AP mice to identify any possible differences in the reporter mouse lines. Offspring at various ages (8 to 35 weeks old), positive for both the Cre/ER^{TM} transgene as well as the reporter gene (β-gal or alkaline phosphatase respectively), received 10 mg of tamoxifen dissolved in corn oil in the form of a single i.p. injection. Mice were sacrificed 3 and 8 days later, to allow the recombination event to occur and a small piece of the liver was also dissected and stained whole-mount with X-gal along with the eyes. Three days after the administration of tamoxifen, the liver samples from both reporter lines were positive (Fig. 5.5 C & F), but no reporter gene activity was detected in the eyes (Fig. 5.5 A, B, D & E) apart from a few scattered cells in the conjunctiva (Fig. 5.5 A & B).

However, 8 days after the tamoxifen injection (Fig. 5.5 G – J), there was a dramatic change in reporter gene expression. Alkaline phosphatase positive cells could be detected all over the cornea and additionally, a stripe was observed in the corneal epithelium of one CAGG-Cre/ER^{TM}-Z/AP mouse (Fig. 5.5 J). Unfortunately, the CAGG-Cre/ER^{TM}-R26R-*LacZ* mouse died one day before it was due to be analysed. However, the eyes were stained anyway and they both appeared positive for β-gal activity in the corneal epithelium. These findings could be the result from tissue decay, since the mouse had been dead for 24 hours, and/or due to cells been lysed as the body was stored in -20 ^{o}C. Hence, the CAGG-Cre/ER^{TM}-Z/AP reporter mice were chosen for further experiments. Also, as controls in Figure 5.6 show, alkaline phosphatase was very specific with no background staining.

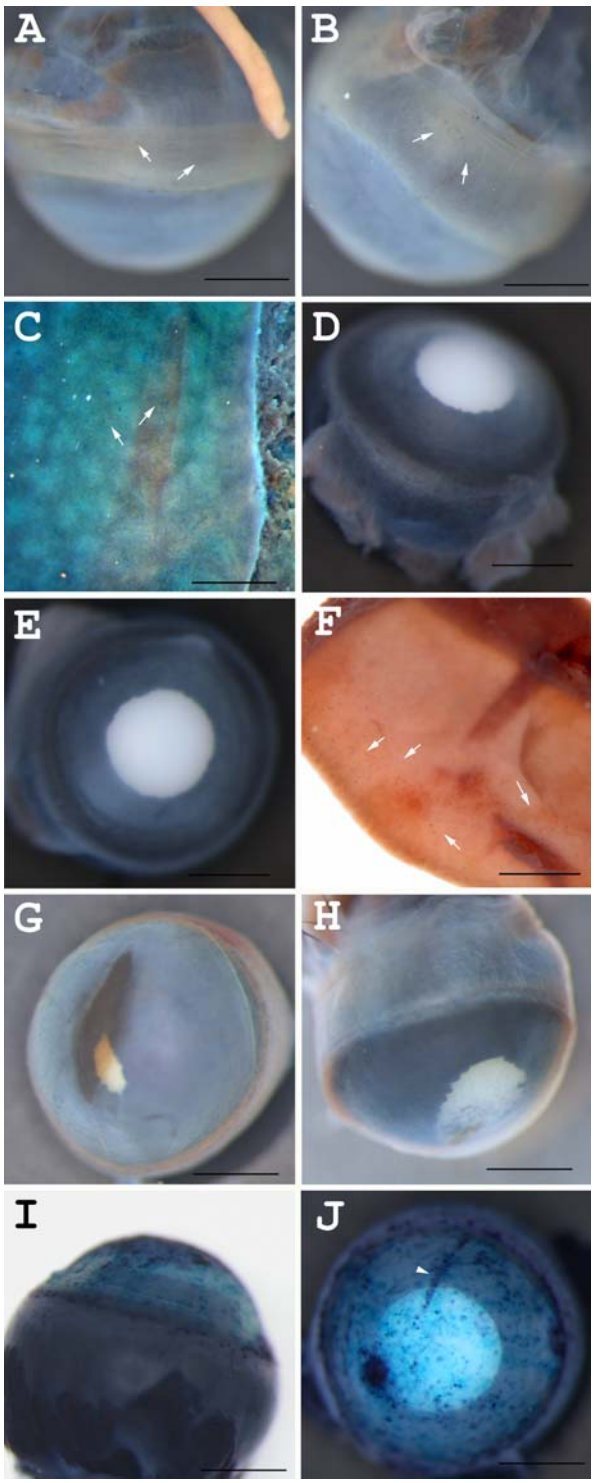

Figure 5.5 Tamoxifen induced recombination in the pilot experiment. Samples shown are whole-mount ocular (A – B & G – H) and liver (C) tissues from CAGG-Cre/ER^{TM}-R26R-*LacZ* and ocular (D – E & I – J) and liver (F) tissues from CAGG-Cre/ER^{TM}-Z/AP mice. Mice were sacrificed 3 (A – F) and 8 (G – J) days after the i.p. injection with 10 mg tamoxifen. Arrows show scattered recombined cells that express the respective reporter gene. The arrow head in J shows a stripe of alkaline phosphatase positive cells in the corneal epithelium. Scale bars are 1 mm.

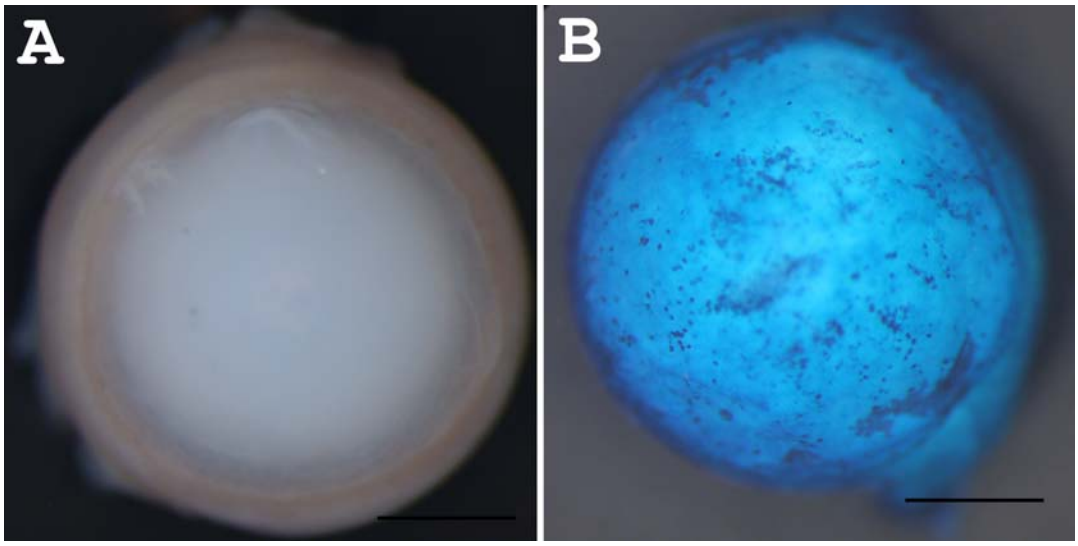

Figure 5.6 Controls for AP staining in the eyes of a Z/AP mouse that never received Cre recombinase or tamoxifen. (A) Negative control eye from the Z/AP mouse that was stained for alkaline phosphatase (AP) following the normal protocol. (B) Positive control eye from the Z/AP mouse for which the endogenous AP deactivation step was omitted.

As rare induction of the reporter gene was needed in order to obtain rare stripes or other clones derived from stem cells in the corneal epithelium, the dose of tamoxifen was varied. Unfortunately, in one experiment where the mice were given a single injection of 10 mg tamoxifen a high proportion of animals either became sick and so were culled or died before the date of analysis. This was the same dose used for the mouse that died in the pilot experiment and overall one of two R26R-*LacZ*, seven of fourteen CAGG-Cre/ER^{TM}-Z/AP and nine of eleven *Pax6*$^{+/-}$, CAGG-Cre/ER^{TM}-Z/AP mice either became sick or died. Consequently, in other experiments the dose of tamoxifen was either reduced or the dose was split between several injections. All 8 mice that received a lower dose of tamoxifen (1 – 5 mg) and all 4 mice that received a total of 15 mg, split into three doses of 5 mg per day, on 3 consecutive days survived.

Mice at several different ages were injected because it has been proposed that LSCs are more active in younger animals and thus there are more chances to observe the progeny of a recombined active LSC. Finally animals were chased for longer periods than in the pilot experiments because the corneal epithelium had to be cleared of the marked somatic cells that were not produced by LSC in which the Cre-mediated *LoxP* recombination took place. No combination of age, chase period and concentration of tamoxifen resulted in the production of a stripe like that observed in the pilot experiments (Fig. 5.5 J). The tamoxifen-induced recombination was observed as spots or patches of reporter gene expression in the corneal epithelium. However, recombination in the cornea was found to depend on the age of the mouse, the chase period and the amount of the administered tamoxifen, as judged by the degree of staining.

As shown in Fig. 5.7, younger mice generally achieved higher levels of recombination compared to older ones that were injected with the same amount of tamoxifen and left for the same chase period. However, the pattern of positive cells in older animals appeared to be more organised in radial-like arrays of small patches rather than the more randomly oriented speckled mosaic patterns seen in younger animals. A differential frequency of marked cells could indicate differences either in the labelling efficiency or in age-related cell turnover. Discontinuous radial arrays and the way in which they might arise are considered further in the discussion. Also, longer chase periods resulted in less staining in the corneal epithelium (Fig. 5.8). This would not be predicted if the stained cells were produced by stem cells but is expected if they are produced by TAC because corneal epithelial cells are eventually desquamated from the cornea and if longer times are allowed, more labelled cells will be shed from the cornea and will not be replenished unless a stem cell is labelled. Furthermore, recombination was found to be dependent to the dose of the administered tamoxifen (Fig. 5.9). Even when the dose of tamoxifen was split into three daily i.p. injections with a total dose higher than the highest single injection, more cells with an activated reporter gene were identified in the corneal epithelium, although mice were treated at the same age and chased for the same amount of time.

There were too few *Pax6*$^{+/-}$, CAGG-Cre/ER^{TM}-Z/AP mice for a meaningful comparison of stripe production in *Pax6*$^{+/-}$ and wild-type CAGG-Cre/ER^{TM}-Z/AP mice. However, two *Pax6*$^{+/-}$, CAGG-Cre/ER^{TM}-Z/AP mice were injected with 10 mg of tamoxifen and chased for 9 weeks (Fig. 5.10). These mice showed abnormal corneas and very few positive cells in the corneal epithelium, compared to those found in *Pax6*$^{+/+}$, CAGG-Cre/ER^{TM}-Z/AP mice.

All reporter mice that were injected with tamoxifen, their ages, the chase periods, the tissues checked and the outcome of the staining are summarised in Table 5.2.

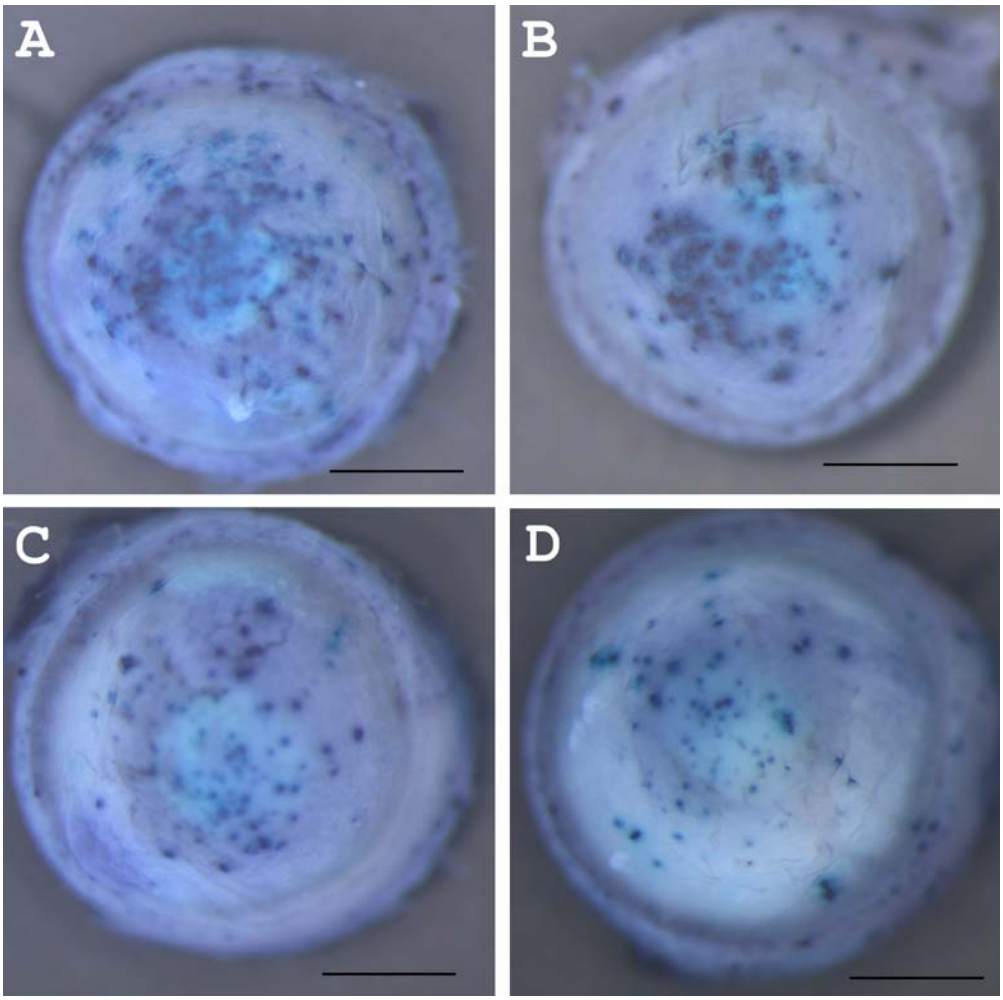

Figure 5.7 Comparison of eyes from CAGG-Cre/ER^{TM}-Z/AP mice showing the effects of the mouse age when it received the tamoxifen. (A & B) 5 weeks old and (C & D) 12 weeks old mice with 7 (A & C) or 9 (B & D) weeks chase. All mice received a single i.p. injection of 10 mg tamoxifen. Scale bars are 1 mm.

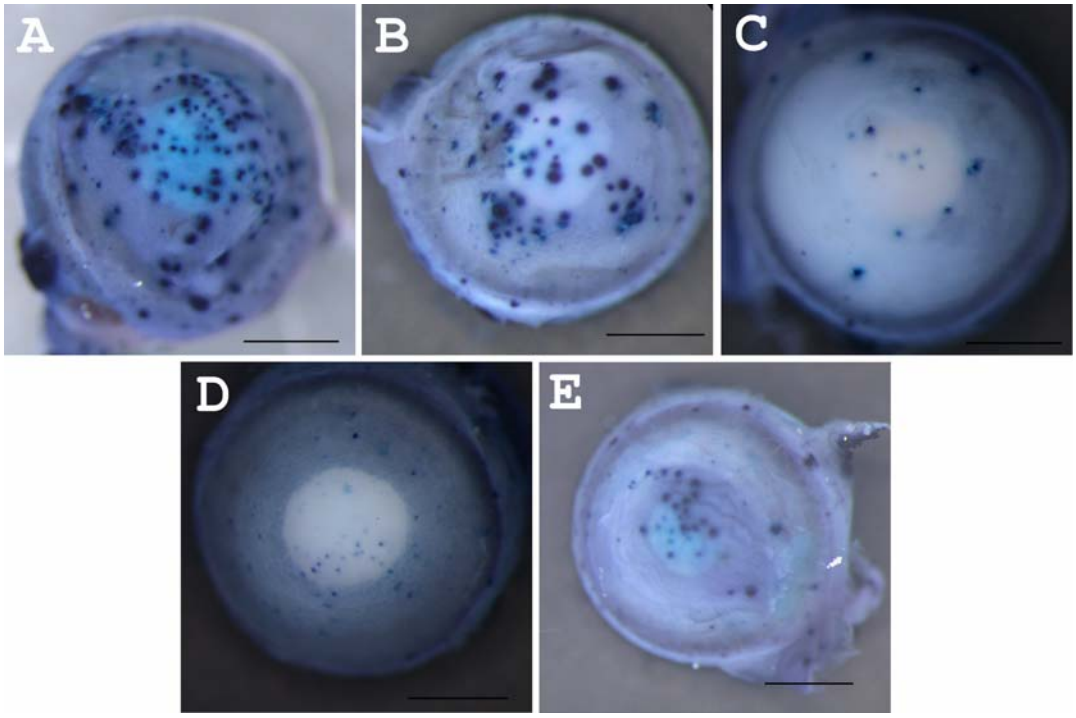

Figure 5.8 Comparison of positive cells in the corneal epithelium of CAGG-Cre/ER^{TM}-Z/AP between different chase periods. (A – C) 5 weeks old mice with 3 (A), 5 (B) and 7 (C) weeks chase. (D – E) 8 weeks old mice with 3 (D) and 7 (E) weeks chase. All mice received a single i.p. injection of 5 mg tamoxifen. Scale bars are 1 mm.

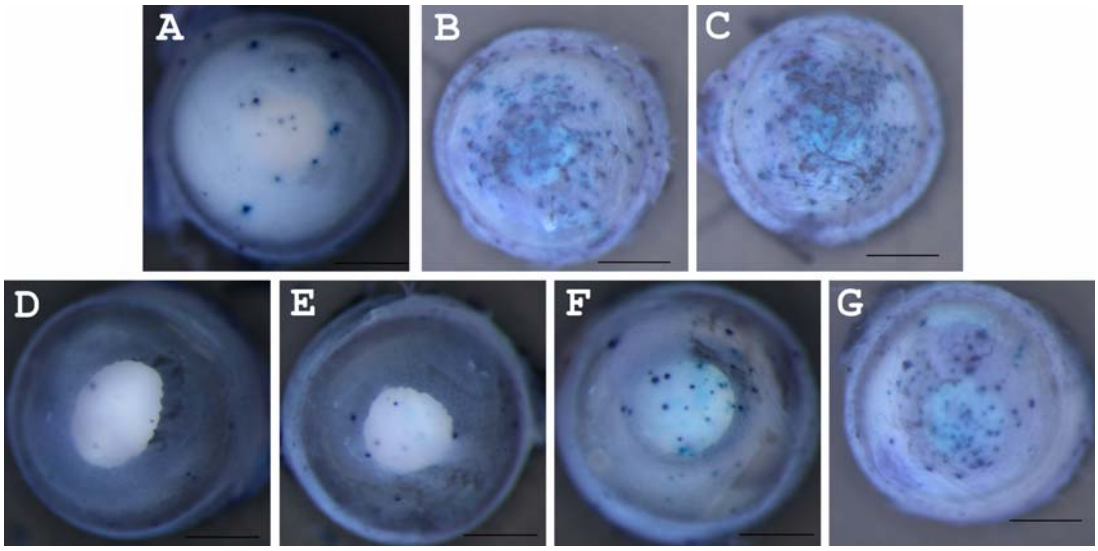

Figure 5.9 Comparison of tamoxifen dosage effects on cells in the corneal epithelium of CAGG-Cre/ER^{TM}-Z/AP mice. (A – C) 5 weeks old mice that received 5 mg (A) and 10 mg (B) of tamoxifen as a single i.p. injection or 15 mg (C) of tamoxifen split into 3 i.p. injections with 5 mg each, for 3 days (one injection per day). (D – G) 12 weeks old mice that received a single i.p. injection of 1 mg (D), 2 mg (E), 5 mg (F) and 10 mg (G) of tamoxifen. All mice were chased for 6 or 7 weeks. Scale bars are 1 mm.

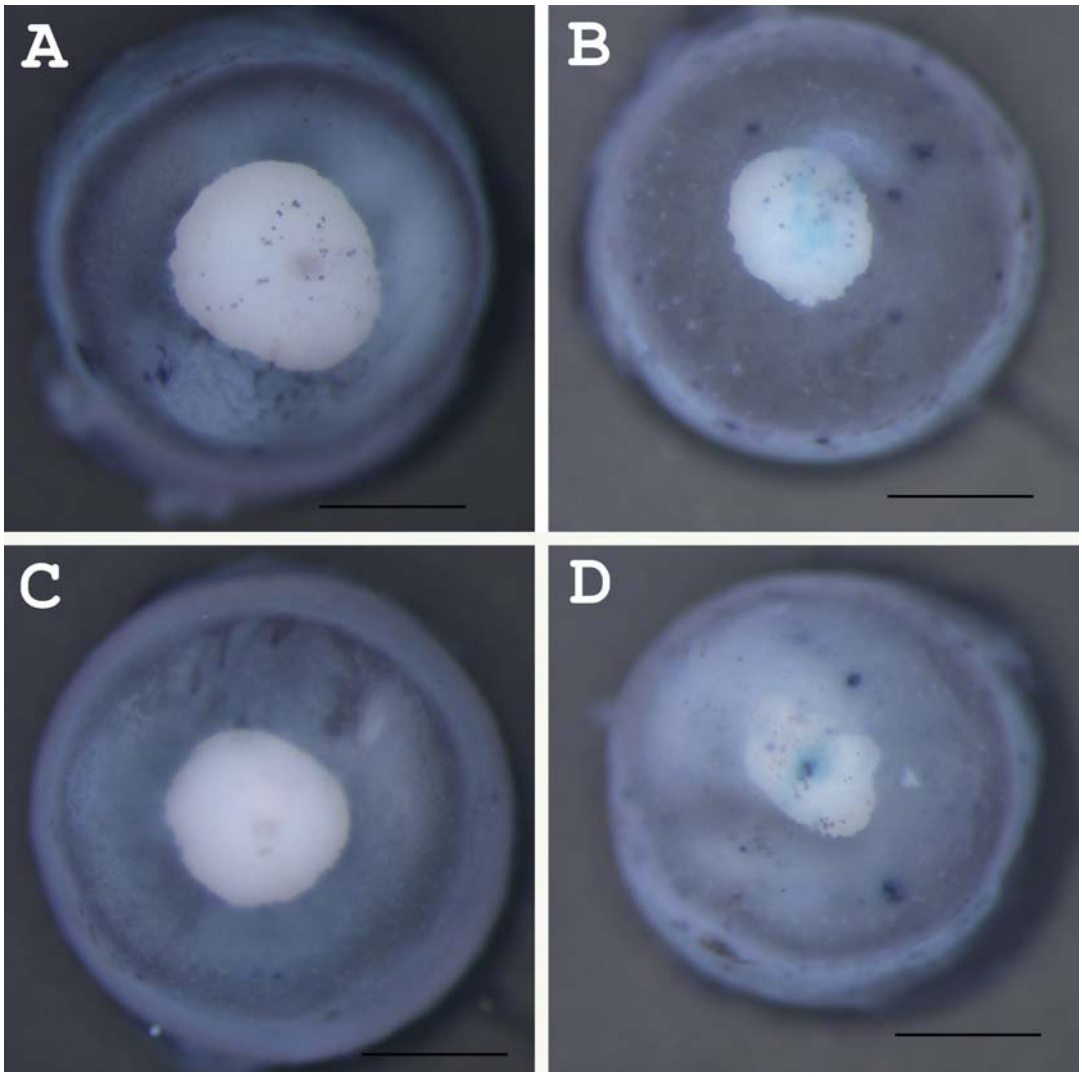

Figure 5.10 Recombination in the corneal epithelium of *Pax6*$^{+/-}$, CAGG-Cre/ER^{TM}-Z/AP eyes. Mice were 9 weeks old, received 10 mg of tamoxifen as a single i.p. injection and they were chased for 9 weeks. Scale bars are 1 mm.

Table 5.2 Summary of results for mice injected (i.p.) with tamoxifen. Mice that did not receive any tamoxifen were used for checking leaky expression of the reporter gene and are indicated with "-" in the TM field. "3 i.p." indicates the animals that received 3 i.p. injections with 5 mg tamoxifen each for 3 days (one per day). The dose of tamoxifen is shown as final dose in mg. TM: Tamoxifen.

Reporter Strain	TM (mg)	Age (weeks)	Chase	Tissue	Outcome
CAGG-Cre/ER^{TM}-R26R-*LacZ*	-	8	-	Eye	Negative
	-	8	-	Eye	Negative
	-	15	-	Eye Liver Lung Heart Kidney S. Intestine	Negative Positive Few positive cells Mostly negative Positive Positive
	-	15	-	Eye Liver Lung Heart Kidney S. Intestine	Negative Positive Few positive cells Mostly negative Positive Positive
	10	36	3 days	Eye Liver	Few conjunctival Positive cells
	10	20	8 days	Eye	Positive cornea
CAGG-Cre/ER^{TM}-Z/AP	1	12	6 weeks	Eye	Positive cornea
	2	12	6 weeks	Eye	Positive cornea
	5	5	3 weeks	Eye	Positive cornea
	5	5	5 weeks	Eye	Positive cornea
	5	5	7 weeks	Eye	Positive cornea
	5	8	3 weeks	Eye	Positive cornea
	5	8	7 weeks	Eye	Positive cornea
	5	12	6 weeks	Eye	Positive cornea
	10	5	7 weeks	Eye	Positive cornea
	10	5	9 weeks	Eye	Positive cornea
	10	8	3 days	Eye	Negative
	10	8	8 days	Eye	Positive cornea (stripe)
	10	12	7 weeks	Eye	Positive cornea
	10	12	7 weeks	Eye	Positive cornea
	10	12	9 weeks	Eye	Positive cornea
	15 (3 i.p.)	6	6 weeks	Eye	Positive cornea
	15 (3 i.p.)	6	6 weeks	Eye	Positive cornea
	15 (3 i.p.)	6	8 weeks	Eye	Positive cornea
	15 (3 i.p.)	6	8 weeks	Eye	Positive cornea
Pax6$^{+/-}$, CAGG-Cre/ER^{TM}-Z/AP	10	9	9 weeks	Eye	Few corneal cells
	10	9	9 weeks	Eye	Few corneal cells

5.4 DISCUSSION

Cell-permeable Cre induced recombination was successfully performed *in vitro* and in cultures. Although it seemed very promising, recombination could not be induced in live animals. The most probable reason is that the corneal barrier could not be overcome. On the other hand, a different cell permeable Cre might have been more efficient in recombining cells in live animals and specifically in the cornea. The only published report, where a cell permeable Cre successfully recombined *LoxP* sites in corneal cells of mice, used a cell-permeable Cre with different PTDs from the Cre used in the experiments described in this chapter (Ambati et al., 2006). The difference was that Ambati et al. used a Cre without the basic HIV-TAT peptide. The reason why a cell permeable Cre carrying the HIV-TAT was used in this project was because this construct had been found more efficient in recombining *LoxP* sites when compared to the Cre lacking this peptide, at least in cultured cells (Lin et al., 2004; Peitz et al., 2002) and also because the construct was readily available. However, by adding this peptide, the final cell permeable Cre protein will be occupying more space compared to the Cre lacking this extra sequence, a property that might have been critical for protein entrance to the cells of the corneal epithelium. Additionally, cells in the ocular surface may be less efficient in absorbing substances (e.g. by showing low rate of endocytosis, if any) when compared to cells in culture. This would not be surprising, because one role of the cells in this tissue is to prevent harmful substances from the environment to enter into the eye. To further the complexity of this matter, different cell permeable Cre constructs have worked with different rates of success in different laboratories. Specifically, Peitz et al. (2002) reported that neither of the cell permeable Cre constructs (with and without the HIV-TAT sequence) were able to induce recombination when injected intraperitoneally in mice, whereas Jo et al. (2001) achieved recombination in a variety of tissues after i.p. injections of their Cre (without the TAT sequence) in mice.

The reported leaky expression of the reporter gene in mice crossed with the CAGG-Cre/ER^{TM} mice was confirmed in both strains of reporter mice (namely R26R-*LacZ* and Z/AP mice). Several tissues showed widespread expression of the reporter gene

without the introduction of tamoxifen, in accordance to the published studies (Hayashi and McMahon, 2002). However, leakiness could not be detected in the eyes of the four mice that were checked (Fig. 5.4). Of course the possibility that spontaneous recombination in the absence of tamoxifen is taking place in the eye as well but in a very low frequency could not be ruled out because of the small number of eyes that were checked. Larger number of eyes might prove that leakiness is indeed taking place in the eye, but to evaluate this system in this study, tamoxifen had to be used to try to induce recombination of *LoxP* sites in limbal stem cells, in order to produce clonal stripes of cells in the corneal epithelium positive for reporter gene expression. However, since no positive cells were observed in the limbus and not all limbal cells are stem cells that are able to produce daughter cells in the cornea, the number of eyes required would probably make reliance on leaky expression unrealistic.

After administering tamoxifen as single i.p. injections *LoxP* site recombination was obtained in corneal cells but in almost all cases the pattern comprised a series of spots rather than radial stripes. If the conventional LSC hypothesis is correct, and stem cells in the limbus produce transient amplifying cells that migrate centripetally towards the centre of the cornea, it would be expected that the induction of the reporter gene in a limbal stem cell would produce radial stripes of cells if the chase period was long enough. Previous estimates of the rate of cell movement in the corneal epithelium suggest that a stripe spanning the whole corneal radius should be visible with chase periods of only a few weeks in mice that were at least 5 weeks old (Collinson et al., 2002). The only one eye that produced the expected stripy organisation of cells positive for the reporter gene in the corneal epithelium was observed in the pilot experiment (Fig. 5.5 J). The mouse was injected with tamoxifen at the age of 8 weeks but the chase period was only 8 days. A complete radial stripe would probably take more than 8 days to form, so this stripe could have been initiated by leaky Cre expression in the limbus earlier than the tamoxifen injection at 8 weeks of age.

However, a radial stripe was not demonstrated again in any of the mice tested with

chase periods of 3 – 9 weeks and at ages of 5 – 12 weeks. Instead, the predominant pattern of reporter transgene expression was a speckled pattern of spots or randomly orientated patches. If the hypothesis for the limbal location of the stem cells responsible for corneal maintenance is correct, it seems likely that these spots reflect small clones produced by the action of Cre recombinase in the corneal epithelium rather than the limbal stem cells themselves. Alternatively, the spots might have been produced by marked LSCs but in a discontinuous manner. This discontinuity could be explained if LSCs are organised in clusters around the limbal circumference, as it has already been suggested (Kawakita et al., 2009; Schlotzer-Schrehardt and Kruse, 2005) and each cluster acts as a functional unit to maintain a sector of the cornea. If the LSCs in the cluster were functioning one at a time to replenish the same corneal sector, marking of a single LSC of a cluster would result in discontinuous patches of labelled corneal cells that would probably be aligned radially, since they originate from the same cluster. In fact, there were cases where the spots appeared to be aligned in radial arrays (Fig. 5.7 D & 5.8 D). Alternatively, these arrays might reflect either non-coherent clones of cells descended from a single progenitor (such as an early TAC) or they may reflect activation of reporter gene expression in separate TACs along the same unlabelled radial coherent clone. The absence of radial coherent clones may simply reflect the small number of target limbal stem cells relative to the number of corneal epithelial cells.

On the other hand, the fact that the marked corneal cells were able to produce progeny that persisted on the cornea for at least 9 weeks might suggest the existence of a cell population with long-term progenitor properties that resides in the corneal epithelium. This possibility is consistent with the model of corneal maintenance by stem cells in the corneal epithelium recently suggested by Majo et al. (2008). If this hypothesis is correct, TACs should move relatively little (since there are stem cells scattered throughout the whole cornea) but the movement should be towards the limbus, as the authors propose this to be a zone of equillibrium where cells of the expanding conjunctival and corneal epithelia meet (Majo et al., 2008; section 7.2). Superficially, the observed pattern of spots seems to fit the expectations of the

corneal stem cell hypothesis. However, if the patterns represented clonal derivatives of true stem cells, it would be expected that long chase periods (e.g. 9 weeks) would result in some movement of the TACs that would have been manifested as elongated patches of marked cells instead of rounded spots. Additionally, if the movement of the stem cell progeny was so small that 9 weeks of chase period was not adequate to demonstrate elongated patches, at least the comparison of chase periods (Fig. 5.8) should have demonstrated larger spots for longer chase periods, which clearly is not the case. In fact, less staining was observed for longer chase periods. Thus, it seems more likely that the staining patterns were mostly the result of labelling TACs in the corneal epithelium rather than true stem cells.

In the pilot experiment that produced the radial stripe in the corneal epithelium, a high dose of tamoxifen was used (10 mg) for mice of approximately 25 – 30 gr body weight. As it has already been reported, high doses of tamoxifen can result in death due to toxicity (Hayashi and McMahon, 2002; Sadek and Bell, 1996) and the minimum effective dose of tamoxifen is close to the toxic dose. In the experiments described in this chapter, a single injection of 10 mg of tamoxifen was sometimes tolerated but sometimes proved toxic. Lower doses (1 – 5 mg) and split doses (3 x 5 mg) were always tolerated. Mice that received a lower dose of tamoxifen were useful for evaluating a dose-response relationship because a rare induction of reporter gene expression in the corneal epithelium was required. Although the expression of the reporter gene in these mice showed a dose response up to a maximum of 3 x 5 mg tamoxifen (Fig. 5.9), none of the corneas had a continuous stripe of positive cells like the one observed in the animal that received the 10 mg of tamoxifen (Fig. 5.5 J).

If it had been possible to treat more mice with multiple injections and their chase period was optimised, clones of cells might have been produced by labelled stem cells. If the conventional limbal stem cell hypothesis is correct, more stripes might have been produced from infrequent *LoxP* recombination in LSCs that activate the reporter transgene and form a clone of marked cells extending into the corneal epithelium organised as a stripe. Unfortunately, there was insufficient time to explore these possibilities.

Another consideration is that the frequency of *LoxP* recombination may be relatively low in LSCs, especially if they become quiescent like stem cells in the haematopoietic lineage (reviewed by Lin, 2002). As discussed in chapter 3, previous studies have suggested that LSCs must be established by the age of 5 weeks, when the first stripes appear in the corneal epithelium of X-inactivation mosaics (Collinson et al., 2002). Thus, the LSCs will already be established by the time tamoxifen was administered (5 – 12 weeks of age). In order to tackle this, it might be better to administer multiple injections of tamoxifen to mice younger than 5 weeks old or to pregnant females. CAGG-Cre/ER^{TM} mice have been shown to be responsive to tamoxifen even during development, since injecting pregnant females resulted in successful recombination in the embryo (Danielian et al., 1998). In this way, there should be higher chance of expressing the reporter gene by recombination of *LoxP* sites in stem cells while they are still active and this might result in a stripe of positive cells in the corneal epithelium of postnatal mice. Also, if clusters of stem cells maintain the same sector of the cornea, earlier treatment is more likely to label all the cells in a cluster as they may be clonally related and produced during foetal development.

5.4.1 Conclusions

Treatment of Z/AP reporter mice with cell permeable Cre recombinase in eye drops failed to produce any alkaline phosphatase expression in the corneal epithelium. However, treatment of CAGG-Cre/ER^{TM}- Z/AP reporter mice with tamoxifen successfully induced alkaline phosphatase expression in the corneal epithelium. Although only one radial stripe was produced in the corneal epithelium, the system seems promising and given more time it may be possible to optimise the protocol to produce radial stripes or other clones of cells produced by labelled stem cells more consistently. If so, this should provide a suitable system for comparing stem cell activity in different groups of mice.

Chapter 6
Lineage Tracing Using the *K5-LacZ* Reporter Mouse

6.1 INTRODUCTION

6.1.1 Keratin 5

Keratin 5 (K5) is a basic, type II keratin with a molecular weight of 58kDa, which is found in basal epithelial layer of the skin and most stratified epithelial tissues including the conjunctival and limbal epithelia (Byrne and Fuchs, 1993). In humans, the gene is found on chromosome 12 at the q12-q13 region whereas its murine ortholog is located on chromosome 15 at 58.79cM. This cytokeratin forms obligatory heteropolymers with keratin 14 to create the intermediate filament cytoskeleton of all basal, mitotically active keratinocytes in the skin (Nelson and Sun, 1983).

6.1.2 Keratin 5 expression in the eye

In humans the adult basal epithelium of the ocular surface, expresses the K5/K14 pair in the more undifferentiated cells whereas the K3/K12 pair is expressed in the suprabasal corneal epithelium, where more differentiated cells are located (Schermer et al., 1986). In the mouse, however, the expression pattern is different. K12 is expressed in the suprabasal corneal epithelium during development, but in adulthood, K12 can be found in all cell-layers of the murine cornea (Kurpakus et al., 1994). Furthermore, although immunochemistry studies have identified K3 protein in the ocular surface of many species including human, rabbit, dog and cow, it could not be detected in the mouse (Chaloin-Dufau et al., 1993) a fact that was recently explained in an *in silico* study that showed that a K3 gene is absent from the genome of the mouse (Hesse et al., 2004).

Expression of the keratin 5 gene (*Krt5*) in the cornea has been more controversial. In humans, immunohistochemistry revealed the presence of K5 protein in the basal layers of conjunctival and limbal epithelium but the corneal epithelium was either negative or contained a few positive cells (Schlotzer-Schrehardt and Kruse, 2005). Similar findings have been reported for bovine eyes, where K5 protein was immunohistochemically detected in the basal limbal epithelium and at low levels in the peripheral corneal epithelium but the central epithelium was negative (Zhao et al., 2008). Lu et al. found *Krt5* to be expressed in the corneal surface by RT-PCR whilst they also identified it immunologically in the basal layer of the corneal epithelium (Lu et al., 2006). Bryne et al. on the other hand, conducted experiments with truncated forms of the human *KRT5* promoter, which showed that the *Krt5* gene encoding K5 is expressed in the conjunctiva and limbus but no reporter gene expression could be detected in the corneal epithelium, notwithstanding the immunostaining for K5 that identified the protein in the corneal epithelium (Byrne and Fuchs, 1993). Persistence of K5 in the corneal epithelium has been attributed to the extreme stability of keratins, especially when in filament networks (Byrne and Fuchs, 1993; Lersch et al., 1989) as it is in cells exported from the limbus to the corneal epithelium.

6.1.3 *Pax6*$^{+/-}$ corneas

As discussed in chapter 1, mice heterozygous for the *Pax6* transcription factor can be used as a model for human aniridia. Their eye size is small and corneas demonstrate equal abnormalities to the human disease including a thinner, fragile epithelium, blood vessel in-growth and conjunctivalisation. With all these abnormal features present, it is highly possible for the epithelial cells to also have an altered keratin expression pattern.

6.1.4 β-gal expression in the corneas of *Krt5-LacZ* mice

While exploring options for marking limbal stem cells at a low frequency (discussed in chapter 5) it was discovered that *Krt5-LacZ* transgenic mice (in which the human *KRT5* promoter drives *LacZ* expression) spontaneously showed the required low-grade mosaic *β-gal* expression pattern in the conjunctiva and limbus and this sometimes extended to the corneal epithelium. The experiments reported in this chapter were designed to investigate whether this *Krt5-LacZ* system is likely to provide an alternative means of comparing LSC function in different groups of mice.

6.1.5 Aims

The first aim of this study was to compare the endogenous expression of *Krt5* and the reporter *Krt5-LacZ* transgene in the ocular surface of the adult mouse. The second aim was to compare the frequency of clone numbers in different groups of *Krt5-LacZ* mice to investigate the possibilities that the number of active stem cells were reduced in older mice and $Pax6^{+/-}$ mice. This approach is based on the prediction that the number of rare β-gal positive clones should be proportional to the number of active stem cells.

6.2 MATERIALS & METHODS

6.2.1 Animals

For the experiments described in this chapter, the *Krt5-LacZ* mice were used and they were crossed to both *Pax6*$^{+/-}$ mouse lines (see section 2.1). Since both mouse lines were heterozygotes, the offspring could have been hemizygous for the *LacZ* transgene and heterozygous for the *Pax6* mutation, hemizygous for the reporter and wild-type for *Pax6*, heterozygous for *Pax6* without the reporter or homozygotes for wild-type *Pax6* alleles without the reporter. Only mice with the first two genotypes were useful for the analyses.

In addition, for the in situ hybridization, albino mice were used to aid the visualization of *Krt5* expression. These were CD1 mice that were used as wild-type controls and *Pax6*$^{+/-}$ on an outbred Swiss albino genetic background.

6.2.2 Keratin 5 in situ hybridization & immunofluorescence

In situ hybridisation to *Krt5* was carried out as described in section 2.14, with the invaluable help of Dr. Christine Mulford (MRC Human Genetics Unit, Edinburgh). Alkaline phosphatase was the final end point, which stains the tissue blue-purple. Immunofluorescence with rabbit anti-Keratin 5 primary antibody and Alexa 488 goat anti-rabbit IgG secondary antibody (Table 2.2) was used for protein identification as described in section 2.11.

6.2.3 β-gal staining

Eyes from *Krt5-LacZ/-*, *Pax6*$^{+/+}$ and *Krt5-LacZ/-*, *Pax6*$^{+/-}$ mice were dissected and stained with X-gal (see section 2.3 & 2.6). Then patches of β-gal positive cells were evaluated and measured under a dissecting microscope.

Some eyes with β-gal positive clones were embedded in wax, sectioned and counterstained (see sections 2.8 & 2.10) for histological examination.

6.2.4 *Pax6* & β-gal genotyping

In order to identify the genotype of the mice, a tail tip was obtained from the mice, DNA was extracted and the genotype was identified by PCR and subsequent restriction enzyme digestion (see sections 2.4 & 2.5).

6.3 RESULTS

6.3.1 Keratin 5 expression in the ocular surface

In order to test whether presence of K5 protein in the corneal epithelium was a consequence of persistence of a stable protein synthesised in corneal progenitor cells in the limbus (stem cells and/or early TACs) rather than gene expression in the cornea itself, immunohistochemistry and RNA *in situ* hybridisation for *Krt5* were compared in wild-type mice at 15 and 30 weeks of age. Immunohistochemistry for K5 in adult whole-mount eyes showed that this protein was present in virtually all conjunctival and most limbal cells but had a much more patchy distribution in the corneal epithelium (Fig. 6.1). Consistent age-related differences in K5 immunohistochemical staining could not been seen between wild-type eyes at 15 and 30 weeks of age (n=4). Although there was variation in the degree of staining, the staining of 30 week old corneas was either similar to that at 15 weeks or sometimes more extensive, like the example shown in Fig. 6.1.

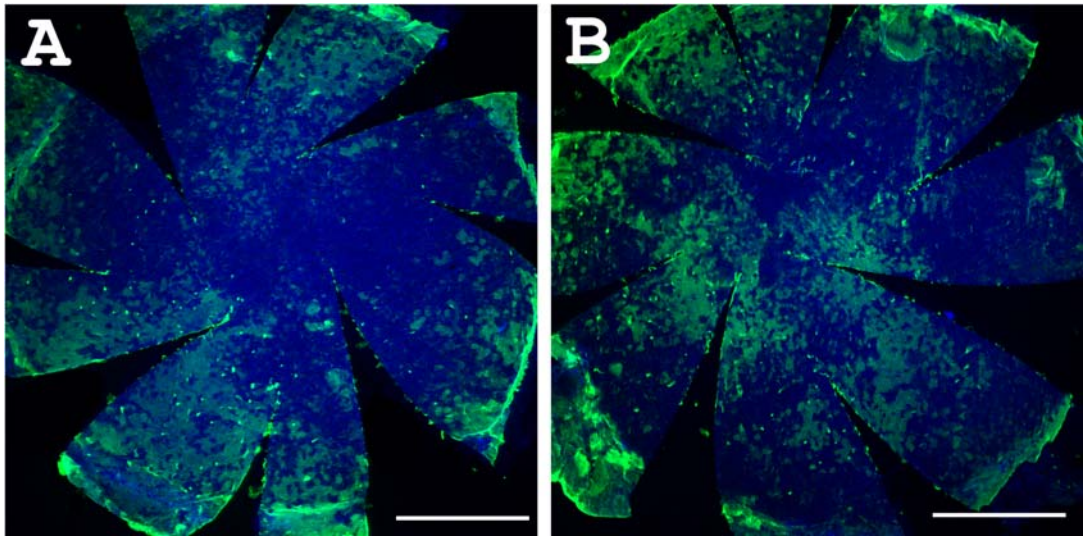

Figure 6.1 Immunohistochemical detection of keratin 5 in the ocular surface of wild type mice. Whole-mount flattened murine eyes at 15 weeks (A) and 30 weeks (B). No evident reduction of keratin 5 protein could be detected at 30 weeks of age eyes when compared to 15 weeks old, and rather there may be a small increase. Green: Keratin 5; Blue: TO-PRO3 iodide counterstain. Scale bars are 1 mm.

RNA in situ hybridisation was performed on whole-mount albino eyes using cDNA probes designed from sequence BC108361 obtained from the Entrez Nucleotide database (Fig. 2.2). In situ hybridisation performed on E12.5 embryos as positive controls showed the staining pattern expected from published results (Byrne et al., 1994) for the *Krt5* promoter activity, confirming the specificity of the probe (Fig 6.2). Briefly, *Krt5* mRNA is present at the whisker pad and laterally along the body but it is reduced ventrally and dorsally. In the wild-type adult mouse eye, *Krt5* mRNA could be detected in the conjunctiva and limbus but not in the corneal epithelium (Fig. 6.3 A - C). There was some patchy staining in the $Pax6^{Sey/+}$ corneas, which was more obvious in whole mounts than in the sections (Fig. 6.3 D - F) and negative controls (eyes without antibody for digoxigenin) were clear. Thus, although *Krt5* mRNA could not be detected in the wild-type corneal epithelium, K5 protein was detected by immunohistochemistry. These results are consistent with the hypothesis that the *Krt5* gene is expressed in the conjunctiva and limbus but not the cornea and that K5 protein persists in some corneal epithelial cells that are derived from LSCs that express *Krt5*. The weak and patchy staining of the *Krt5* mRNA in the $Pax6^{Sey/+}$ corneas may reflect the presence of conjunctival cells in the cornea.

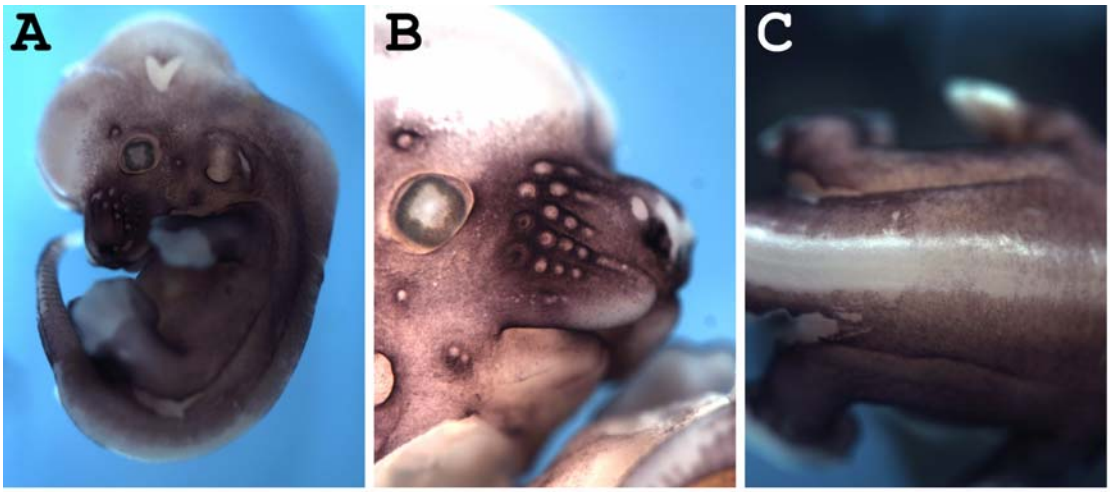

Figure 6.2 Keratin 5 mRNA in situ hybridization on an E12.5 mouse embryo. (A) Lateral view of the stained embryo. (B) Higher magnification photo of the embryo shown in A. Krt5 mRNA is present at the whisker pad. (C) Dorsal view of the embryo in (A) demonstrating that Krt5 mRNA is reduced at the middle of the dorsal axis. The colour is produced by the reaction of alkaline phosphatase that was conjugated to the antibody with BM purple.

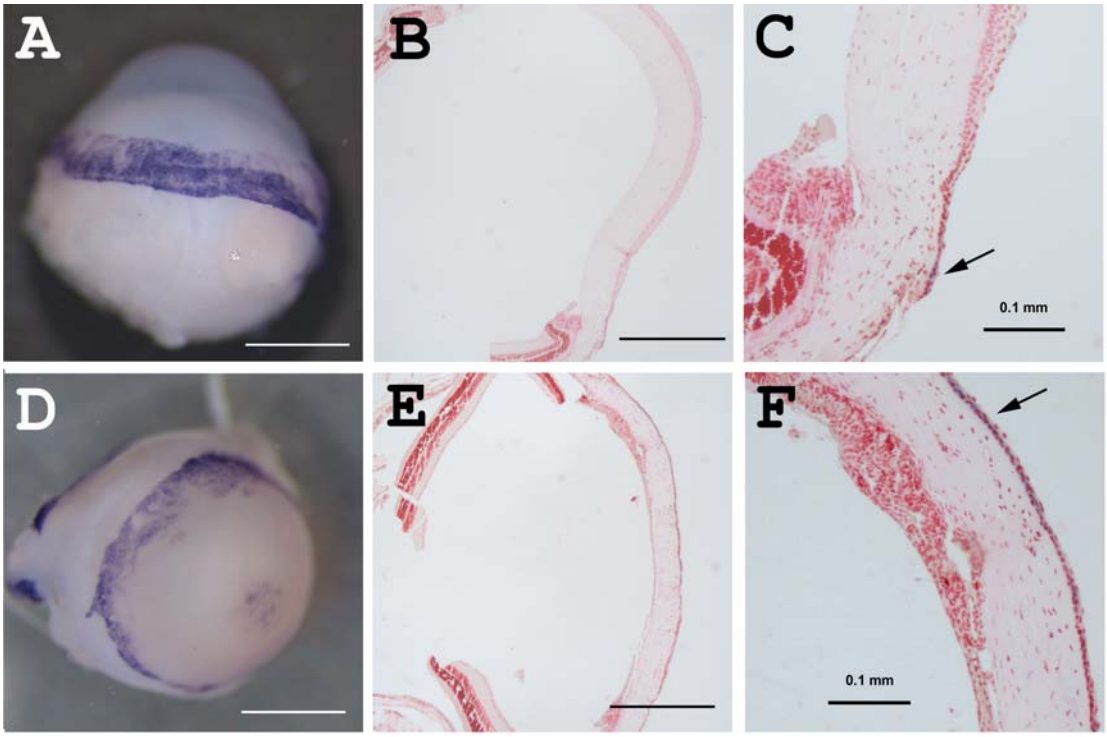

Figure 6.3 Keratin 5 mRNA in situ hybridization on the ocular surface of wild-type (A - C) and *Pax6*$^{+/-}$ (D - F) albino eyes. Whole-mount photos (A & D) show absence of staining in the corneal epithelium of wild-type eyes (A). (C & F) Higher magnification photos of sections in (B & E) respectively. Sections were counterstained with eosin and neutral red. Arrows indicate stained areas. Scale bars are 1 mm (A & D), 0.5 mm (B & D) and 0.1 mm (C & F).

6.3.2 β-gal staining in the ocular surface of *Krt5-LacZ/-* mice

Krt5-LacZ mice carry β-gal gene under the control of the human *KRT5* promoter and so all cells actively expressing *Krt5* should also be positive for β-gal. The eyes of *Krt5-LacZ/-* hemizygotes appeared normal by gross morphology and histology (Fig. 6.4 A & B). Eyes from eight 15-week old and nine 30-week old *Krt5-LacZ/-* hemizygotes were stained with X-gal as described in the Materials and Methods section (see chapter 2). β-gal positive cells were identified in the conjunctiva, limbus and cornea. Only a proportion of conjunctival and limbal cells were β-gal positive (Fig. 6.4 C - D) and these were grouped in patches scattered throughout the tissue. This mosaic pattern of *Krt5-LacZ* expression in the conjunctiva and limbus differed from the more uniform expression of K5 protein identified by immunohistochemistry (Fig. 6.1).

In the cornea, cells carrying the reporter gene were also present but occurred much less frequently than in the conjunctiva or the limbus. Only 9 of 34 *Krt5-LacZ/-* eyes showed β-gal positive cells in the cornea whilst patches in the conjunctiva were seen in all 26 eyes which had conjunctival tissue attached around the whole circumference of the cornea. Most of the β-gal positive cells in the cornea were arranged as radial stripes of various lengths (Fig. 6.4 E - L). The longest stripes extended from the limbus to the central cornea (Fig. 6.4 E - J), whereas small patches of β-gal positive cells could be found anywhere on the cornea (Fig. 6.4 L). Histological sections of the stained whole mounts showed that the β-gal staining in the cornea was confined to the epithelium (Fig. 6.4 A - C).

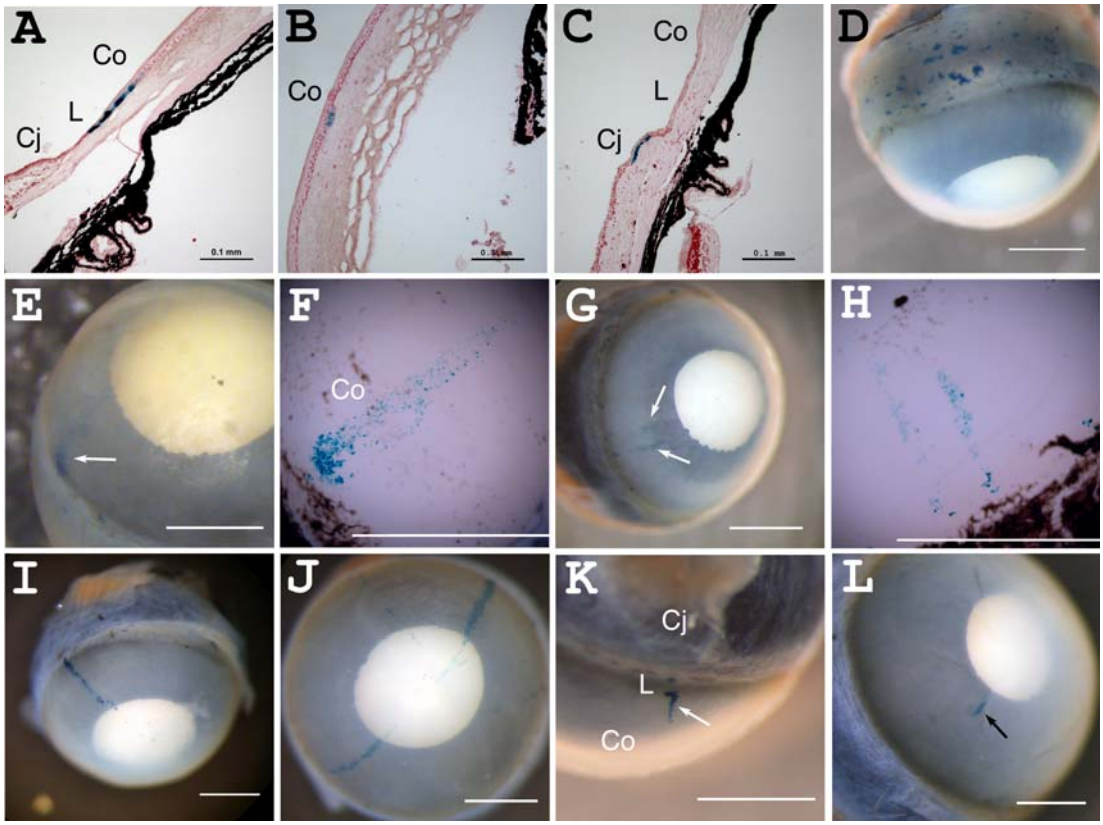

Figure 6.4 Corneal stripes and conjunctival patches in wild-type *Krt5-LacZ* mouse eyes. (A – C) Sections of corneas showing a limbal-corneal (LC) stripe (A), a central corneal patch (B) and a conjunctival patch (C). (D) Whole mount eye showing patches of β-gal positive cells in the conjunctiva. (E) Cornea with a single long stripe of β-gal positive cells in the limbus and the cornea. (F) Flattened preparation of eye in E. (G) Cornea with long limbal- corneal (LC) stripes. (H) Flattened preparation of eye in G. (I) Cornea with a long LC stripe from a 30-week old mouse. (J) Cornea with two long LC stripes. (K) A small stripe of cells starting from the limbus. (L) A small patch of β-gal positive cells in the cornea. Blue indicates the X-gal endpoint. In some cases the pigmented iris is visible through the cornea and obscures some of the β-gal staining. White arrows indicate corneal stripes; black arrows show small patches in the cornea. Co: Cornea; Cj: Conjunctiva; L: Limbus. Scale bars are 1 mm unless otherwise stated.

6.3.3 Analysis of β-gal positive patches and stripes in the *Krt5-LacZ/-* corneal epithelium

For experiments discussed later, hemizygous *Krt5-LacZ/-* mice were produced by crossing *Krt5-LacZ/- mice* with either heterozygous *Pax6*$^{Sey\text{-}Neu/+}$ or heterozygous *Pax6*^{Sey} mice. Each cross produced some *Krt5-LacZ/-* mice that were wild-type for *Pax6* and so genetically equivalent to the hemizygous *Krt5-LacZ/-* mice in the main colony. The sizes and distributions of β-gal positive patches and stripes in the corneal epithelium of eyes from wild-type *Krt5-LacZ/-* mice from all three crosses were analysed. Only β-gal positive regions larger than 50 μm in diameter were included and these all appeared as radial stripes. The results are summarised in figure 6.5. Most of the stripes analysed (35/52 = 67%) had a peripheral end at the limbus and a more central end in the cornea (LC stripes) and the others had both peripheral and central ends in the cornea (CC stripes). Inspection of the LC stripes showed that they extended into the limbus itself (Fig. 6.4 A & K).

If β-gal positive stripes were produced by LSCs they might vary in length if β-gal positive LSCs cycled through phases of activity and inactivity. Thus, the LC stripes could reflect stripes produced by LSCs that were in their active phase when the mouse was killed whereas the CC stripes could have been produced by LSCs that had subsequently become inactive. Although, on average, the central end of the CC stripes was further from the limbus than the LC stripes (1075±87 μm versus 783±59 μm from the limbus; $P = 0.007$ by t-test), CC stripes were significantly shorter than the LC stripes (391±60 μm versus 783±59 μm; $P = 0.002$ by t-test). Both observations are consistent with the suggestion that CC stripes were incomplete remnants of stripes produced earlier which had extended centripetally and were being eroded from the periphery by β-gal negative cells following behind.

As mentioned in Chapter 1, a recently proposed alternative to the LSC hypothesis suggested that stem cells were scattered throughout the cornea and cells were more

likely to move centrifugally than centripetally. If stem cells were distributed randomly over the area of the cornea and for simplicity this is considered to be a flattened circle, the geometry implies there should be more stem cells close to the limbus than close to the centre because the area close to the limbus is larger. The most central location for the end of a stripe was approximately 1650 μm from the limbus and the radius was approximately 1800 μm (these measurements were taken from 2-dimensional images of 3-dimensional whole-mount corneas and so are imprecise but they provide an adequate comparison of the sizes and locations of different stripes). If 1800 μm is taken as the radius and divided into three 600-μm lengths this will divide the area into three regions which are respectively 55.56%, 33.33% and 11.11% of the total area (from periphery to centre of the cornea). Thus, if rare stripes arose stochastically from stem cells distributed randomly throughout the corneal epithelium and extended towards the limbus, 55.56% of the stripes would be predicted to have their more central ends in the outer area (within 600 μm of the limbus), 33.33% should be in the middle (600-1200 μm from the limbus) and 11% should be in the inner area (1200-1800 μm from the limbus). The observed frequencies of the anterior ends of all the stripes in these three regions were 14 in the outer area: 29 in the middle area: 9 in the inner area. (Stripes that ended at 600 or 1200 μm were counted as being in the inner or middle group respectively.) This is significantly different from the predicted distributions ($\chi^2 = 17.32$; $P = 0.00017$). If only the LC stripes (with one end at the limbus) are considered, the frequency distributions are 12:20:3 ($\chi^2 = 9.05$; $P = 0.011$). These results do not support this interpretation of the stripe formation.

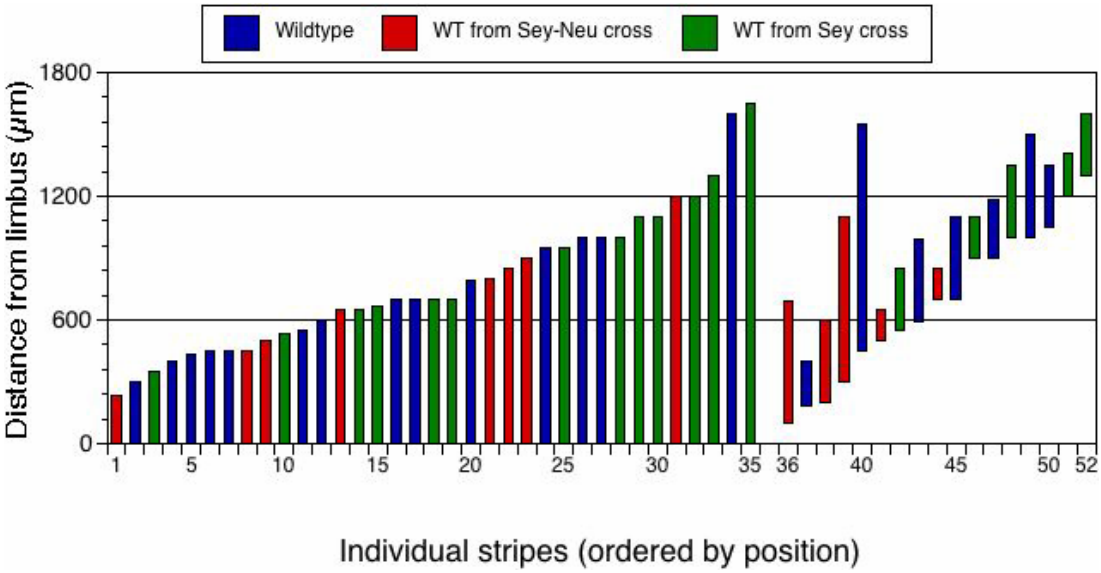

Figure 6.5 Distribution of β-galactosidase-positive stripes in the corneal epithelium of *Krt5-LacZ/-* mice. The positions and lengths of 52 stripes in the corneal epithelia of 29 eyes from 15-week old 'wild-type *Krt5-LacZ/-*' mice from three different crosses are shown. The length of the bars shows the length of the stripes (µm) and the ends of the bars indicate the distance from the limbus to the ends of the stripes (µm). Thirty-five corneal stripes have one end at the limbus and are called LC (limbus-cornea) stripes in the text; 17 stripes have both ends at the cornea are called CC (cornea-cornea) stripes. The individual stripes are grouped as LC or CC stripes and ordered by position.

6.3.4 Age-related reduction of β-gal positive stripes in *Krt5-LacZ/-* corneal epithelia

Previous studies showed that corneal epithelial stripe numbers declined with age in mouse chimaeras and X-inactivation mosaics (Collinson et al., 2002; Mort et al., 2009) so it was tested whether the same was true of the β-gal positive stripes in wild-type *Krt5-LacZ/-* mice at 15 and 30 weeks. Eight of the 16 eyes from the 15-week old *Krt5-LacZ/-* mice had at least 1 stripe and altogether there were 18 stripes (Fig. 6.6 A). Most of these (12/18) were LC stripes, extending from the limbus towards the centre but some (6/18) were CC stripes, extending from the peripheral cornea to the centre (Fig. 6.5). In contrast, only 1 (Fig. 6.4 I) out of the 18 eyes from the 30 week old mice had a stripe, so the mean stripe number per eye was significantly lower than at 15 weeks (Mann-Whitney U test; P=0.003; Fig. 6.6 B). This reduction in β-gal positive stripe numbers in wild-type *Krt5-LacZ/-* mice is unlikely to mirror any age-related change in endogenous *Krt5* promoter activity as immunohistochemistry showed similar patterns of K5 staining at 15 and 30 weeks (Fig. 6.1). Furthermore, a generalised down-regulation of the *Krt5-LacZ* transgene between 15 and 30 weeks is also unlikely because neither the frequency of β-gal positive patches in the conjunctiva nor the mean number of patches differed significantly between the two ages (Mann Whitney U test P=0.194; Fig. 6.6 C & D). This is an inexact statistical comparison, because the area of conjunctival tissue dissected out was not constant among eyes. However, differences in the sizes of the conjunctiva tissue were small and, visually, the frequencies of conjunctival patches appeared more similar at the two ages. Since neither the endogenous K5 protein nor the *Krt5-LacZ* transgene shows a generalised down-regulation with age, the observed difference in frequency of corneal stripe formation is presumably specific to the limbus and/or cornea.

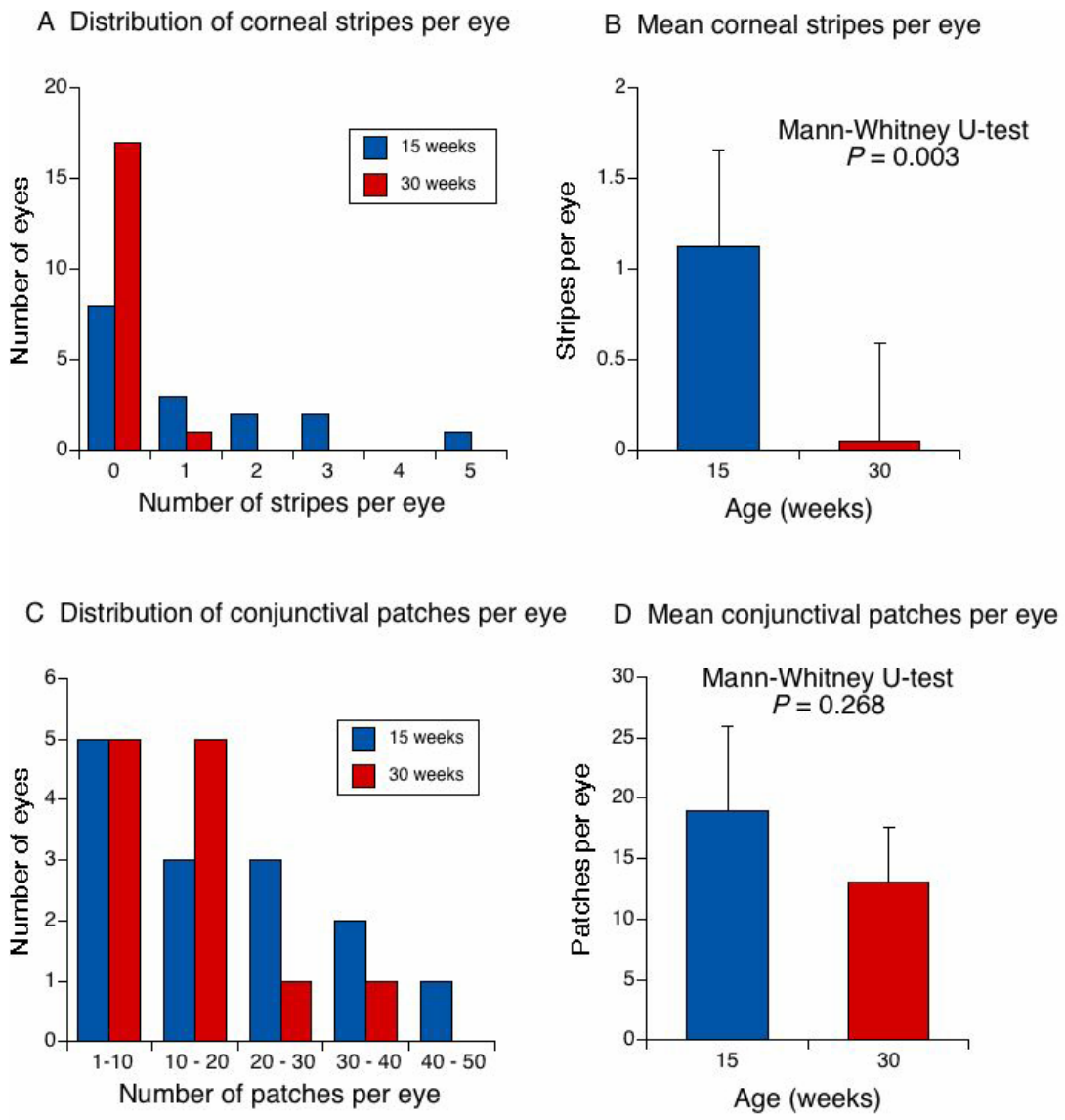

Figure 6.6 Comparison of stripes in the cornea (A & B) and patches in the conjunctiva (C & D) between 15 and 30 weeks old mice. (A) Frequency distribution of corneal stripes per eye at 15 and 30 weeks. (B) Mean number of corneal stripes per eye at 15 and 30 weeks. (C) Frequency distribution of conjunctival patches per eye at 15 and 30 weeks. (D) Mean number of conjunctival patches per eye at 15 and 30 weeks. Conjunctival patches were only counted for eyes, which had the conjunctiva attached around the whole circumference.

6.3.5 Effect of *Pax6* genotype on β-gal positive stripes in *Krt5-LacZ/-* corneal epithelia

To test whether the number of β-gal positive stripes in *Krt5-LacZ/-* corneal epithelia was reduced in $Pax6^{+/-}$ mice *Krt5-LacZ/-* mice were crossed to mice from two $Pax6^{+/-}$ stocks ($Pax6^{Sey/+}$ on a mixed genetic background and $Pax6^{Sey\text{-}Neu/+}$ congenic on an inbred CBA/Ca genetic background) in separate experiments (section 6.2.1). Skin from the ears of wild-type, *Krt5-LacZ/-* and $Pax6^{+/-}$, *Krt5-LacZ/-* mice was collected and stained for β-gal activity. Skin patterns of β-gal positive cells appeared to have similar patchy distributions between the two genotypes (Fig. 6.7). However, this was not the case for the mosaic patterns produced in the corneal epithelium of wild-type and $Pax6^{+/-}$ mice.

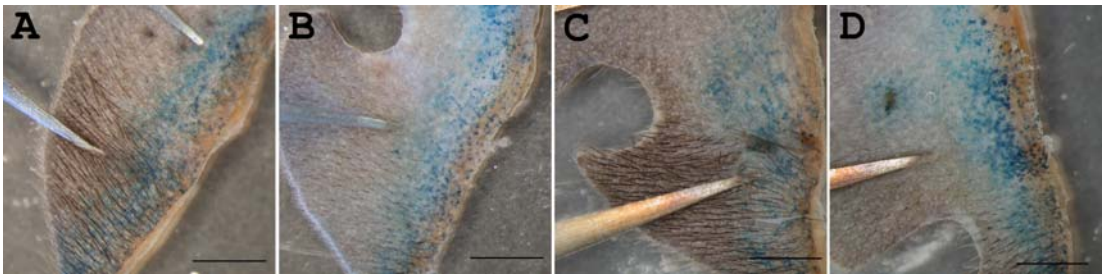

Figure 6.7 Patches of β-gal positive cells in the skin of *Krt5-LacZ/-* mice.
Whole-mounts of skin from the outermost, right ear of wild-type (A & B) and $Pax6^{+/-}$ (C & D) *Krt5-LacZ/-* mice, stained with X-gal. Scale bars are 2 mm.

In the first *Pax6*$^{+/-}$ experiment, eyes from 11 *Krt5-LacZ/-*, *Pax6*$^{Sey/+}$ mice were stained for β-gal at 15 weeks, along with 16 wild-type *Krt5-LacZ/-*, *Pax6*$^{+/+}$ littermates. 12 out of the 32 wild-type stained eyes showed at least one stripe in the cornea. The eyes of the *Krt5-LacZ/-*, *Pax6*$^{Sey/+}$ mice were small and highly abnormal (Fig. 6.8 E & F) with many features that have been reported previously for this genotype on an outbred background (Kanakubo et al., 2006). β-galactosidase positive patches in the *Krt5-LacZ/-*, *Pax6*$^{Sey/+}$ corneas were usually small, clustered and in most cases localized at the peripheral cornea (Fig. 6.8 E & F). Interestingly, these patches resembled the conjunctival patches seen in the wild-type eyes (Fig. 6.4 D) and may have resulted from incursion of the conjunctiva into the cornea. Because the small patches in the *Pax6*$^{Sey/+}$, *Krt5-LacZ/-* corneas were not comparable to the stripes seen in the wild-type, *Krt5-LacZ/-* corneas they were not quantified.

In the second *Pax6*$^{+/-}$ experiment, eyes from 10 *Krt5-LacZ/-*, *Pax6*$^{Sey\text{-}Neu/+}$ mice were dissected and stained for β-gal at 15 weeks, along with 22 wild-type *Krt5-LacZ/-*, *Pax6*$^{+/+}$ littermates. One of the 44 wild-type *Krt5-LacZ/-*, *Pax6*$^{+/+}$ eyes had 3 stripes, 2 had 2 stripes and another 6 had 1 stripe. The corneas of the *Krt5-LacZ/-*, *Pax6*$^{Sey\text{-}Neu/+}$ mice were less severely affected than those of the *Krt5-LacZ/-*, *Pax6*$^{Sey/+}$ mice (Fig. 6.8), which were on a different genetic background. One of the *Krt5-LacZ/-*, *Pax6*$^{Sey\text{-}Neu/+}$ eyes showed a stripe equivalent to the stripes from the wild-type animals (Fig. 6.8 A). However, other eyes appeared similar to those seen in the *Krt5-LacZ/-*, *Pax6*$^{Sey/+}$ eyes and showed small patches of clustered β-gal positive cells, which were mostly localized in the periphery of the cornea (Fig. 6.8 B – D).

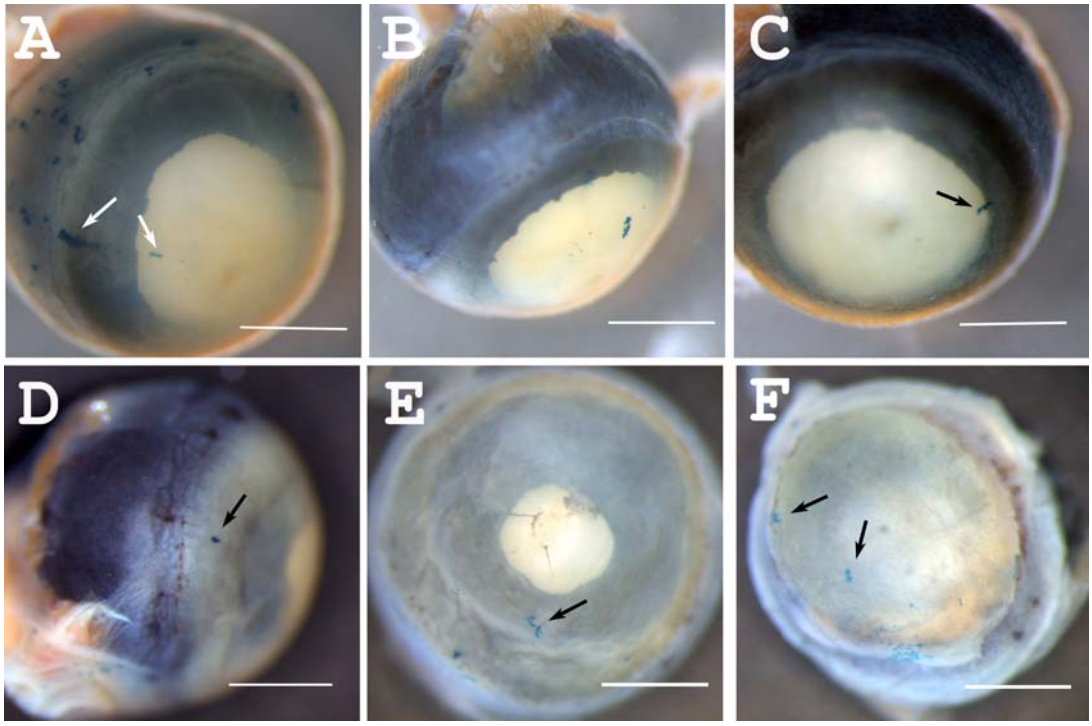

Figure 6.8 Patches of β-gal positive cells in the ocular surface of *Pax6*$^{+/-}$ *Krt5-LacZ/-* mice. (A) A long but discontinuous limbus-cornea stripe in a *Pax6*$^{Sey\text{-}Neu/+}$ *Krt5-LacZ/-* cornea. (B - D) Small patches of β-gal positive cells in *Pax6*$^{Sey\text{-}Neu/+}$ *Krt5-LacZ/-* corneas. (E & F) Whole mounts of *Pax6*$^{Sey/+}$ *Krt5-LacZ/-* eyes showing small patches of β-gal positive cells and abnormal eye morphology. White arrows indicate corneal stripes; black arrows show small patches in the cornea. Scale bars are 1 mm.

6.4 DISCUSSION

6.4.1 Expression of *Krt5* in the ocular surface

Although (Lu et al., 2006) reported the detection of both K5 protein, by immunohistochemistry, and *Krt5* RNA, by RT-PCR, in the mouse cornea, the RT-PCR results were not illustrated and I was unable to confirm the presence of RNA in wild-type corneas by *in situ* hybridization. Experiments detected *Krt5* mRNA in the conjunctiva and limbus but not the corneal epithelium whereas K5 protein was detected by immunohistochemistry in the conjunctiva, limbus and many corneal epithelial cells. A similar dichotomy of K5 protein in the absence of *Krt5-LacZ* reporter staining was explained by a combination of the extreme stability of the intermediate filaments and the conventional LSC hypothesis of corneal epithelial maintenance (Byrne and Fuchs, 1993). If the *Krt5* gene is expressed in the LSCs, the presented results indicate it is inactivated in the corneal epithelial cells, which the LSCs produce, but K5 protein can persist for longer. On the other hand, the differences in *Krt5* expression pattern in the ocular surface of mice found with different methods could be explained by low levels of *Krt5* mRNA in the peripheral cornea. If *Krt5* mRNA is absent from the central cornea and the mRNA levels at the peripheral corneal epithelium are really low, *in situ* hybridization may fail to demonstrate their existence. However, a more sensitive technique, like RT-PCR, may be able to detect them, but since RT-PCR cannot provide information about the exact location of the mRNA, Lu et. al might have simply concluded that the cornea is positive for *Krt5* mRNA.

6.4.2 Distribution of rare β-gal positive clones in the *Krt5-LacZ/-* corneal epithelium

The *KRT5* promoter should only drive expression of the *LacZ* reporter transgene in tissues where the endogenous *Krt5* gene is expressed, so it is not a permanent lineage marker. Thus, *Krt5-LacZ* transgene expression was expected in the conjunctiva and

limbus but not the cornea. *Krt5-LacZ* mice showed a mosaic pattern of expression in the conjunctiva and limbus, unlike the more uniform expression of the endogenous *Krt5* gene, suggesting that the transgene undergoes stochastic inactivation, which may be attributable to position effect variegation (Dobie et al., 1997). *Krt5-LacZ* expression in the corneal epithelium was not predicted on the basis of endogenous *Krt5* expression yet radial β-gal positive stripes were produced. The most likely explanation is that the rare β-gal positive stripes are derived from individual stem cells located in the limbus. If a small proportion of these cells produce transient amplifying cells in the cornea in which the *Krt5-LacZ* expression is maintained, the result will be the emergence of rare β-gal positive stripes in the corneal epithelium. However, this hypothesis has not been investigated.

6.4.3 β-gal positive patches in relation to age and *Pax6* genotype

Previous work of the laboratory using chimaeras and X-chromosome inactivation mosaics (Collinson et al., 2004b) revealed that older animals have fewer stripes of cells marked with a *LacZ* reporter gene on their corneas. This means that there are fewer functional LSC clones but it does not necessarily mean fewer numbers of functional LSCs because LSCs may be randomly distributed or clustered in clonal units, variables that could be changing with age or genotype. Consistent with these analyses, the present results show that the frequency of β-gal positive clones is significantly lower in wild-type, *Krt5-LacZ/-* mice at 30 weeks than at 15 weeks. If the rare β-gal positive stripes are derived from individual stem cells their frequency will depend on the number of active LSCs. On the other hand, the observed reduction could reflect an age-related mechanism for down-regulation of either the endogenous *Krt5* or the transgene. Neither could be confirmed as comparison of K5 protein at 15 and 30 weeks old corneas or β-gal positive patches in an independent, *Krt5* expressing tissue like the conjunctiva at the same age could not demonstrate any reduction. Thus, LSCs function seems to be reduced with age. Such a reduced functionality will have an impact on normal homeostasis of the cornea, which can be

demonstrated by the various age-related visual conditions.

This is not the first time that a reduction of stem cell function with age is reported. In fact, adult stem cells are known to reside in most if not all the mammalian tissues contributing to normal homeostasis and repair. This, in conjunction with the age-related reduction in normal cell turnover and regeneration observed in almost every tissue that has been studied, suggests an age-related decline in stem cell function. Two of the most well examined stem cell populations where the effects of aging have been extensively studied are skeletal muscle and haematopoietic stem cells reviewed elsewhere (Rando, 2006). In these systems, age-related loss of normal function can be attributed to either intrinsic aging of the cells (e.g. due to mutation accumulation) or to reversible changes (e.g. epigenetic modifications) dictated by the aged environment or niche.

In the case of *Pax6* genotype, comparison of the frequency of rare β-gal positive clones in *Pax6*$^{+/-}$ and wild-type *Krt5-LacZ/-* corneal epithelia was not possible because most of the clones produced by the *Pax6*$^{+/-}$ mice were small patches and were mainly in the peripheral cornea. This could demonstrate a defect of the *Pax6*$^{+/-}$ cells in processes like migration, cell-cell and cell-stroma adhesion etc. Similar observations have also been previously reported (Collinson et al., 2004a) in X-inactivation mosaics where stripes in the *Pax6*$^{+/-}$ were disorganized showing diversion from normal centripetal migration, an effect that was corrected in the *Pax6*$^{+/-}$, *LacZ*$^{+}$↔*Pax6*$^{+/+}$, *LacZ*$^{-}$ chimaeras, probably due to the correct migration of the wild-type cells on the cornea of these mice. Furthermore, some of these patches may have resulted from invasion of the conjunctiva into the cornea (one of the *Pax6*$^{+/-}$ eye-abnormalities; also see chapter 4 and Fig. 4.2). Indeed β-gal positive patches in the *Pax6*$^{+/-}$ corneas resembled those found in the conjunctiva of wild-type *Krt5-LacZ/-* eyes. The presence of conjunctival cells expressing the *Krt5-LacZ* transgene in the cornea would have undermined any numerical comparison. However the difference in the morphology of the β-gal positive clones confirmed that corneal epithelial maintenance is highly abnormal in *Pax6*$^{+/-}$ mice.

6.4.4 Location of stem cells maintaining the corneal epithelium

The analysis of the stripes found in wild-type *Krt5-LacZ* mice, also provided interesting results concerning the hypotheses about the location of stem cells maintaining the corneal epithelium. Specifically, the frequency of the stripes and their location on the corneal epithelium are more consistent with the conventional view suggesting that the limbus is the niche of the stem cells responsible for maintaining the cornea during normal homeostasis. This issue is discussed in more detail in chapter 7.

6.4.5 Conclusions

Krt5-LacZ mice produced rare β-gal positive radial stripes in the corneal epithelium. Stripe distributions suggested they extended centripetally from the limbus, representing clonal LSC-derivatives and providing a lineage marker for LSC activity. The decline in stripe frequency with age is consistent with the hypothesis that LSC function declines with age. *Pax6*$^{+/-}$*, Krt5-LacZ* corneas had small patches rather than stripes and this may represent incursion of transgene-expressing conjunctival cells into the abnormal *Pax6*$^{+/-}$ cornea.

Chapter 7
General Discussion

The first part of the General Discussion (7.1) considers to what extent the experiments reported in the thesis have met the original aims. The second part (7.2) then, considers whether the results obtained can help evaluate a recently published alternative to the conventional limbal stem cell hypothesis. Finally, the third part (7.3) deals with future research directions.

7.1 EFFECTS OF AGE AND GENOTYPE ON THE MOUSE CORNEAL EPITHELIUM AND LSC FUNCTION

The aims of the investigations reported in this thesis were to evaluate two hypotheses that were developed from results produced previously by the laboratory concerning the stem cells that maintain the corneal epithelium, their progeny and migration. Sections 7.1.1-7.1.4 discuss the specific results of these investigations whilst sections 7.1.5 and 7.1.6 discuss the effects of age and *Pax6* genotype on stem cell function respectively.

7.1.1 Effects of Pax6 genotype on cell mixing during corneal epithelial development

As mentioned in detail in section 3.1, $LacZ^{+} \leftrightarrow LacZ^{-}$ chimaeras and X-inactivation mosaic mice had corneal epithelia that showed speckled, mosaic patterns of randomly oriented patches until the age of 5 weeks. At this age, the first β-gal positive patches that were organized in stripes were identified at the periphery of the cornea. The original pattern was resolved to stripes spanning the whole radius of the corneal epithelium by the age of about 8 weeks but the boundaries between the

stripes continued to sharpen for several more weeks (Collinson et al., 2002; Mort et al., 2009).

Analysis of the stripe numbers in wild-type mosaics showed that the corrected mean number of β-gal positive stripes in the corneal epithelium was lower in older mice. Although the corneal epithelium of *Pax6*$^{+/-}$ animals younger than 5 weeks showed an equivalent speckled mosaic pattern to that seen in wild-type mice, in older *Pax6*$^{+/-}$ mice the corrected mean stripe number was lower than in wild-type corneas and the stripes were broader. Together these results suggest that age and *Pax6* heterozygosity probably result in a reduction in the numbers of coherent clones of LSCs and/or in their function (Collinson et al., 2004a; Collinson et al., 2002; Mort et al., 2009). In addition, the contribution of *Pax6*$^{+/-}$ cells to the corneal epithelium of *Pax6*$^{+/-}$↔wild-type chimaeras was lower than the global contribution to other tissues in adults but not in foetal stages, suggesting that *Pax6*$^{+/-}$ LSC may be deficient (Collinson et al., 2001).

On the other hand, as mentioned before, a lower number of functional LSC clones is not the same as a lower number of LSCs in these systems. So, the main objective of this thesis was to test if the number of active LSCs maintaining the corneal epithelium is affected in older and in *Pax6*$^{+/-}$ mice, as the previous results suggested. This was investigated by comparing wild-type and *Pax6*$^{+/-}$ mice at different ages.

The previously found deficiency in the corrected mean number of stripes in the adult *Pax6*$^{+/-}$ corneal epithelium when compared to wild-type could also be explained by an alternative hypothesis (Fig. 3.1). If there was less cell mixing in the original, randomly oriented, speckled pattern seen in young *Pax6*$^{+/-}$animals (<5 weeks old) than that at the ocular surface of wild-type mice, a more coarse-grained mosaic pattern would be identified. If LSCs are defined according to this original mosaic pattern, clones of corneal epithelial cells produced by clonally related LSCs would be more likely to be adjacent to each other, producing fewer stripes in the adult corneal epithelium of *Pax6*$^{+/-}$ mice. According to results reported in this thesis, this alternative hypothesis should be rejected. Analysis of X-inactivation mosaics at 3

weeks of age showed that the patches in the corneal epithelium of wild-type mice were larger than those in the *Pax6*$^{+/-}$ cornea. This means that the pattern in the wild-type rather than *Pax6*$^{+/-}$ mice is more coarse-grained, which would mean that if this hypothesis was correct, adult wild-type mice should have fewer stripes than their *Pax6*$^{+/-}$ counterparts, which is not the case (see chapter 3). Thus, the previously identified reduction in the corrected mean number of stripes in the adult *Pax6*$^{+/-}$ corneal epithelium is probably due to fewer active clones of LSCs maintaining the corneal surface of these mice compared to wild-type littermates, rather than clumping of cells into larger coherent clones during development of the surface ectoderm in *Pax6*$^{+/-}$ X-inactivation mosaics.

7.1.2 Identification of the limbus in the adult ocular surface

In general, work reported in this thesis was successful in identifying the border between limbus and cornea in the eyes of mice with immunolocalisation of at least two independent markers, keratin 19 and a marker of blood vessels (CD31). According to published work, both proteins are present in the conjunctiva and the limbus but they are absent from the corneal epithelium of the mouse (Yoshida et al., 2006). Immunolocalisation of these markers also resulted in the identification of a hallmark in flattened whole-mount corneas that aids the identification of limbus without the need for additional markers. This same ridge in whole-mount corneas has also been suggested by Pajoohesh-Ganji et al., (2004) as the border between cornea and limbus. Alternatively, a recent report suggests that the boundary between limbus and cornea can be identified based on the morphology of the nuclei of the cells occupying these areas after nuclear counterstain with DAPI (Zhao et al., 2009). However, in the experiments presented herein, a different fluorescent counterstain was used (namely TO-PRO3) and the morphological differences distinguishing limbal from corneal epithelial cells could not be confirmed.

7.1.3 BrdU Label-retaining cells

The hypotheses from chimaeras and X-inactivation mosaics that age and *Pax6* haploinsufficiency affect the number of functional LSCs that maintain the corneal epithelium were investigated using a LRC technique with the thymidine analogue BrdU. This failed to confirm either of the hypotheses tested. There was no significant reduction in the number LRCs (putative stem cells) in the limbus of either older or *Pax6*$^{+/-}$ mice. Also, in most cases there was a trend for the limbus of *Pax6*$^{+/-}$ mice to harbour more LRCs than the wild-type one. These results suggest either the original hypotheses are incorrect and have to be rejected or the technique used was not appropriate for quantifying the number of putative active LSCs.

Actually, there are several reports warning that results from experiments with thymidine analogues have to be interpreted cautiously because of the possibility that the label is transferred from cell to cell (Burns et al., 2006; Coyne et al., 2006). The exact mechanism of this transfer is not yet clear but presumably it involves the death of a labelled cell and the incorporation of the labelled oligonucleosides by neighbouring cells undergoing DNA repair or replication. Furthermore, it has been reported that activated macrophages can label themselves by phagocytosing the remnants of labelled cells, especially in environments where inflammation and angiogenesis are taking place (Pawelczyk et al., 2009). Such an environment is probably created in *Pax6*$^{+/-}$ mice since their corneas are fragile, leading to a chronic wound-healing state (Ou et al., 2008), and are invaded by newly formed blood vessels (Davis et al., 2003; Ramaesh et al., 2003). Additional evidence suggesting that LRCs do not specifically identify putative stem cells in *Pax6*$^{+/-}$ eyes comes from the following findings: a) BrdU positive particles were identified outside the nucleus of cells only in the corneal epithelium of *Pax6*$^{+/-}$ mice, which could suggest that LRCs do release their labelled parts in the surrounding environment after death and b) there were a lot of LRCs in the more central cornea in *Pax6*$^{+/-}$ mice and in most cases these cells were found to be on top or adjacent to blood vessels implying that some LRCs may not be stem cells but rather cells from the developing blood vessels that were dividing when the blood vessels were formed and then they differentiated.

Thus, results from the LRC technique are difficult to interpret, especially for the *Pax6*$^{+/-}$ mice.

Additionally, the LRC approach was also applied to *Mp*/+ mice. These mice were used as controls for the small size of *Pax6*$^{+/-}$ eyes. They were chosen as controls because the *Mp* mutation did not map to the same chromosome as the *Pax6* gene and histological examination showed a normal corneal epithelium (although other eye-abnormalities including the lens and the retina were evident). Analysis of LRCs in the eyes of these mice showed that there are significantly more LRCs in the limbal region of these mice compared to wild-type littermates. If the LRC technique is indeed able to reveal putative stem cells, this result might indicate that in *Mp* mice there is a problem in differentiating corneal epithelial cells, which would result in more stem cells in the limbal region. In support of this notion, unpublished data on X-inactivation mosaics with the *Mp*/+ genotype showed normal numbers of stripes although they have a smaller circumference (Dr. Richard L. Mort, MRC Human Genetics Unit, Edinburgh, personal communication). So, if the number of stripes is indicative of the number of active LSC clones, *Mp*/+ mice seem to have more stem cell clones per circumference length.

Interestingly, *Mp*/+ mice have several abnormalities in the lens, which appears to deteriorate with age (data not shown). The role of the lens in development of the whole eye is vital. This structure has been reported to provide the essential signals for the differentiation of the anterior ocular mesenchyme (Cvekl and Tamm, 2004) as well as for the development of other structures in the eye including the cornea, ciliary body, iris and the anterior chamber (Beebe and Coats, 2000; Davis-Silberman and Ashery-Padan, 2008). One possibility is that in *Mp*/+ mice potential abnormalities in the corneal epithelium and its maintenance arise as a result of abnormalities in other eye tissues. In conclusion, further work is essential to characterise aspects of corneal epithelial maintenance (cell proliferation and apoptosis) in *Mp*/+ mice before the LRC results can be interpreted correctly.

Abnormal homeostasis of the corneal epithelium has also been suggested for another mutant mouse line called *Dstn*^{corn1} (Zhang et al., 2008). These mice are deficient for destrin (an actin binding protein) and they demonstrate stromal vascularisation and epithelial hyperplasia in the cornea (Smith et al., 1996). Corneal epithelial cells in adult *Dstn*^{corn1} mice do not show any movement and LRCs have been identified throughout the cornea, mimicking the maintenance of the conjunctival epithelium (Zhang et al., 2008). These findings led the authors to suggest that there are stem cells in the corneal epithelium of these mice, although they did not stain for blood vessels in these hyperplastic corneas. However, an interesting possibility was raised by this report, coupling the cell movement of the corneal epithelium to the stromal vascularisation. A normal avascular cornea demonstrates centripetal migration of corneal epithelial cells, whilst *Dstn*^{corn1} and *Pax6*$^{+/-}$ show disturbed migration and have corneal vasculogenesis. Based on these observations, the authors suggested that epithelial cell movement may be required for corneal avascularity and blood vessels may be triggered by lack of epithelial movement. However, the reciprocal effect, that blood vessel-ingrowth might disrupt corneal epithelial movement by providing different stimuli to the overlying epithelium may also be true. Observations on *Mp/+* mice are also consistent with this relationship between these two processes as they do not show vascularisation of the cornea and, at least in X-inactivation mosaics, they can form stripes indicating that there is movement in their corneal epithelia.

The extent of cell movement has not been examined adequately for *Pax6*$^{+/-}$ corneas but if the *Dstn*^{corn1} conclusion was extended to include *Pax6*$^{+/-}$ eyes, this would imply that the LRCs identified in the cornea could be stem cells rather than differentiating cells. While this seems unlikely, based on the evidence discussed elsewhere in this thesis, the possibility could not be ruled out.

7.1.4 Lineage analysis

Several lineage analysis approaches were used to evaluate the hypotheses that age and *Pax6* genotype affect the number of functional LSCs that maintain the corneal epithelium. The first lineage tracing experiment attempted to label rare clones of corneal epithelial cells, derived from individual stem cells marked with a reporter transgene. Various mouse strains with cells carrying a reporter gene downstream of a floxed STOP cassette (or equivalent) were used. In order to induce expression of the transgene, a Cre recombinase that had been rendered cell-permeable by the fusion of small peptides (namely a His-tag, a HIV-TAT and an NLS) as PTDs was used topically in the form of eye drops. The protein was expressed in bacterial cultures after plasmid transformation and was isolated and purified. Although, recombination of *LoxP* sites proved successful in an *in vitro* assay, the cell-permeable Cre failed to induce such recombination in live animals. At first, it was believed that *LoxP* site specific recombination could not be observed because the cell-permeable Cre solution was not able to penetrate the tear film of the cornea. After all, one of the main roles of the cornea is to protect the eye from the hostile environment. However, even after the application of a topical anaesthetic that would presumably dry the cornea, overcoming the tear film barrier, and reduce the intercellular barriers (Prof. J. Ambati, personal communication) expression of the reporter gene could not be detected. It is worth noting that in the literature, recombination of *LoxP* sites with a cell-permeable Cre has been achieved in the cornea (Ambati et al., 2006). This was performed on mouse eyes that had been treated with a topical anaesthetic but the Cre recombinase they used did not have the HIV-TAT domain. Although this peptide has been reported to maximise cellular uptake in cell culture, it might not be appropriate for applications on the cornea.

Reporter mice were then crossed to mice expressing Cre, which becomes localised to the nucleus only after the administration of tamoxifen, since Cre recombinase is coupled to a modified oestrogen receptor (Cre/ER^{TM}). Published reports have indicated that in this system there is some leaky reporter gene activity in the absence of tamoxifen (Hayashi and McMahon, 2002). Although this “leakiness” of the

system could, in principle, be used for clonal analysis, since the frequency of this event is low, no reporter gene expression could be detected in the ocular surface without administration of tamoxifen. On the other hand, leaky reporter gene expression was detected in some other tissues like liver, kidney and small intestine of these mice.

Administration of tamoxifen resulted in reporter gene activation in the eye. However, the cells marked with the reporter were not organised in stripes. Although the amount of the induced reporter activity of the cornea depended on the concentration of the tamoxifen, the age of the mouse and the chase period, only patches of cells (rather than stripes) could be identified in the corneal epithelium, irrespective of the wide variation of these factors. Only in one eye out of the 38 checked was a stripe detected. This was a long stripe of cells, positive for the reporter gene that extended between the limbus and central cornea.

However, since a wide variety of conditions was used unsuccessfully on adults in an attempt to recapitulate this result, this stripe is more likely to have been produced by spontaneous *LoxP* recombination during development rather than by Cre-dependent recombination. This hypothesis is also supported by the fact that the animal that demonstrated the stripe of cells in the corneal epithelium had a chase period of only a few days. However, according to published reports, the rate of centripetal movement in the corneal epithelium of the adult mouse has been estimated around 17 – 26 μm/day during normal corneal maintenance (Buck, 1985; Nagasaki and Zhao, 2003). Based on these figures, it would take about 40 days for a stripe to reach the centre of the cornea (around 1 mm). Even the newly formed stripes in young X-inactivation mosaics were shown to take 3 weeks to reach the centre of the corneal epithelium (Collinson et al., 2002).

So far, no corneal epithelial stripes have been produced by labelling adult stem cells and where stripes have been produced, the lineage markers may have labelled stem cell progenitor cells before individual stem cells were formed. In chimaeras, the two cell populations are combined during the preimplantation stage of development. In

X-inactivation mosaics, the β-gal positive and β-gal negative cell populations become distinguishable at the time of X-chromosome inactivation, early in development. Additionally, although not reported yet, the LaacZ system (Bonnerot and Nicolas, 1993; Nicolas et al., 1996) produces long stripes of β-gal positive cells in the corneal epithelium (Dr. Valerie Wilson, MRC Centre for Regenerative Medicine, Edinburgh, personal communication). In this system, the intra-chromosomal recombination that activates the expression of the *LacZ* can take place at any point during development. Stripes of GFP positive cells were also identified recently in the corneal epithelium after gene transfer using a lentiviral vector allowing constitutive expression of GFP under the regulation of the human CMV promoter (Endo et al., 2007). In this report, the delivery of the transgene was performed via injection in the amnion of embryos at E8 – E18 developmental stages and the authors reported that gene expression in the ocular surface was dependent on the developmental stage of the embryo. Thus, it is possible that adult LSCs that represent a very small proportion of cells in the ocular surface are labelled less frequently than stem cell precursors earlier in development.

In the next experiment, a transgenic mouse (termed K5-*LacZ*) that carries a β-gal reporter gene under the control of the human keratin 5 promoter was used. This mouse showed a mosaic distribution of labelled cells, probably due to position effect variegation of the transgene, in tissues where all cells were actively expressing keratin 5 (i.e. skin and conjunctiva; Byrne and Fuchs, 1993; Byrne et al., 1994). Different lengths of stripes of cells marked with β-gal could be identified in various places in the corneal epithelium. In principle, if stripes arise stochastically, the probability of a stripe occurring in the corneal epithelium should be related to the number of active stem cells, since other cells in the cornea that might be marked will differentiate and will eventually be lost from the ocular surface. Analysis of the frequency of stripes in the corneal epithelium of 15 and 30 weeks old K5-*LacZ* mice revealed significantly more stripes in the younger adult mice. The reduced stripe numbers in older mice appeared not to be due to progressive down-regulation of endogenous keratin 5 or the transgene and this result fits well with the hypothesis

that functional LSCs decline with age.

Attempts to compare the frequency of K5-*LacZ* stripes *Pax6*$^{+/-}$ mice and their wild-type littermates were less successful. Both *Pax6*$^{+/-}$ mouse strains used had corneal epithelial abnormalities, as reported previously (Collinson et al., 2004a; Davis et al., 2003; Ramaesh et al., 2003) and these abnormalities probably prevented proper stripe formation. In almost all the cases where β-gal positive cells could be identified in the ocular surface of the *Pax6*$^{+/-}$ mice, they were organized in small patches, rather than elongated radial stripes. These patches were reminiscent of the conjunctival patches observed in the K5-*LacZ* mice. Thus, direct comparison of stripe frequency (and hence active LSC numbers) could not be performed. This is not the first time that abnormal migration in the corneal epithelium of *Pax6*$^{+/-}$ eyes has been observed. Collinson et al., reported that in *Pax6*$^{+/-}$ X-inactivation mosaics, the stripe pattern was disorganised (Collinson et al., 2004a). Additionally, *Pax6*$^{+/-}$ eyes have been shown to also have abnormal migration during wound-healing (Ramaesh et al., 2005), providing additional support for abnormal corneal migration in these mice. Actually, since several adhesion molecules are targets of *Pax6*, it has been suggested that *Pax6*$^{+/-}$ mutant cells of the corneal epithelium have abnormal adhesion properties probably affecting cell migration (Collinson et al., 2000; Davis et al., 2003; Ramaesh et al., 2003).

The main drawback of the stripe analysis in the K5-*LacZ* mice is the inability to fully explain or understand why and how stripes are formed in the corneal epithelium under the keratin 5 promoter. It seems likely that each stripe demonstrates the marked progeny of a β-gal positive LSC, since the limbus showed mosaic expression of the transgene. According to the *in situ* results for keratin 5, this gene is not expressed in the corneal epithelium. At least, it is not expressed in levels detectable by in situ hybridisation, although the protein has been detected in the corneal epithelium. This means that the keratin 5 promoter is probably down-regulated in the corneal epithelium. Additionally, as mentioned above, the time required for a long stripe (around 1 mm) to be formed due to centripetal migration is at least 3 weeks (Buck, 1985; Collinson et al., 2002; Nagasaki and Zhao, 2003). This means that the

daughter cells of a β-gal expressing LSC should continue to be β-gal positive for at least 3 weeks, without *de novo* expression of the reporter gene, which seems unlikely even for an extremely long-lived protein such as the β-gal. One possible explanation is that the stripes detected reflect LSCs that failed to down-regulate the production of keratin 5 in their progeny and so all the corneal epithelial cells produced by this LSC expresses the β-gal transgene. On the other hand, the frequency of the stripes was higher than might be predicted for a genetic error (like one that would allow the progeny of specific stem cells to ectopically express a structural protein without any further abnormalities). Furthermore, these phenomena that cannot be fully explained may have arisen from the location at which the transgene was inserted in the specific line of transgenic animals under examination. For example, if the transgene was inserted in the proximity of a gene expressed in the corneal epithelium, even if the endogenous promoter of the keratin 5 gene was down-regulated, the site of the insertion might allow enough expression of the transgene for it to be detected in the progeny of that cell.

7.1.5 The effects of age on stem cell function

The initial hypotheses, based on previous results of the laboratory, were that the number of functional LSCs declines with age and is reduced in *Pax6*$^{+/-}$ mice. The negative effect of age on functional LSCs was supported by the lineage tracing experiment using the K5-*LacZ* mice but not by the LRC technique. As discussed above, although the way a stripe is formed in the K5-*LacZ* mice is not fully understood, some concerns have been raised about the validity of the LRC technique. However, although the two results seem to be opposing, there is a possibility that both techniques were successful. Maybe the number of slow-cycling cells and thus, stem cells is the same in young and old mice, but stem cells in the older mice are not so effective in maintaining the corneal epithelium. In this case the LRC numbers will not differ significantly between the two mouse populations under examination. However, efficiently active stem cells able to produce progeny continuously,

resulting in a stripe in the K5-*LacZ* corneal epithelium might be scarcer in the older mice. The reduced functionality of LSC could be attributed to niche changes over time or to accumulation of mutations in these cells making them less effective. The concept of a decline in stem cell functionality with age is not new. Reduced functionality of stem cells with age has also been identified in other lineages and has been studied in haematopoietic stem cells and in skeletal muscle satellite cells both *in vivo* and *in vitro* (reviewed by Rando, 2006). However, it is still not clear if age affects the stem cells themselves, the niche that supports the stem cells' function, the tissue environment or a combination of the above (Fig. 7.1). For example, in the haematopoietic lineage, although there is evidence that blood related functions (i.e. oxygen transport and blood coagulation) suffer a gradual decrease due to age (Carmel, 2001), stem cell numbers actually increase (Sudo et al., 2000). However, the cell cycle status of these cells is steady between young and old mice but aged mice have more defective (in terms of lymphoid differentiation) haematopoietic stem cells (Sudo et al., 2000). Furthermore, reduced regenerative capacity has been reported for the satellite cells of the skeletal muscles from aged mice (Conboy and Rando, 2005). However, the regeneration capacity of aged satellite cells was highly effective when transplanted in young animals (Carlson and Faulkner, 1989) and when exposed to an environment of a young animal as in parabiotic pairings of young and aged mice, they could repair muscle fibres almost as effective as young satellite cells (Conboy et al., 2005). Thus, the decline of the regeneration potential of the aged satellite cells seems to be due to effects of the aged environment or niche on the function of stem cells.

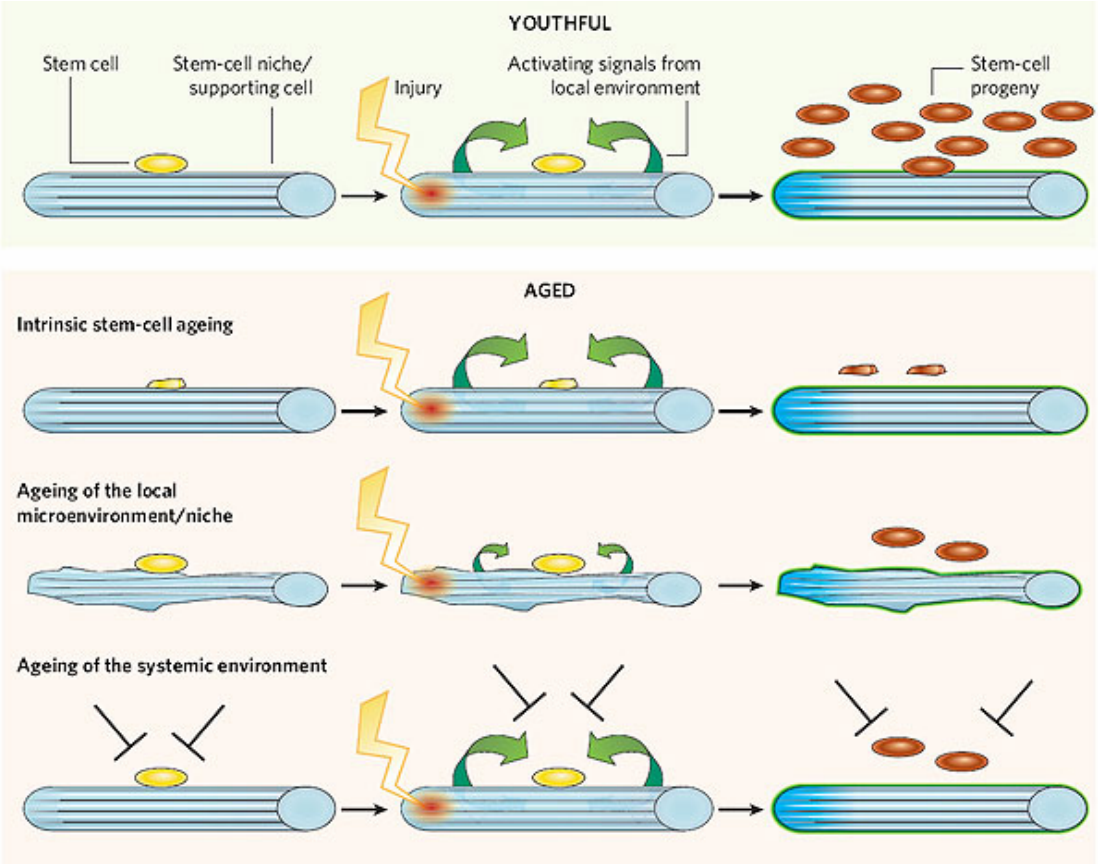

Figure 7.1 Decline in stem cell functionality with age. In response to tissue injury the satellite cell is induced to proliferate. The age-related changes can be in the satellite cell itself, in the niche or in the environment that result in reduced functionality as manifested by the inability to produce sufficient functional progeny. The figure shows a skeletal muscle fibre with a satellite cell as a model (Rando, 2006).

7.1.6 The effects of *Pax6* genotype on stem cell function

The hypothesis concerning a deficiency in the number of active stem cells maintaining the corneal epithelium of *Pax6*$^{+/-}$ mice could not be evaluated adequately. This was mainly because of the known abnormalities in the corneal epithelium of these mice that probably interfered with all the techniques that were used and hence, direct comparison with their wild-type littermates could not be performed.

Although the experiments reported in this thesis failed to identify a LSC defect in *Pax6*$^{+/-}$ mice there is circumstantial clinical evidence suggesting that the human *PAX6*$^{+/-}$ genotype in aniridia patients may be associated with LSC deficiency. This includes the occurrence of goblet cells in the corneal epithelium, which has been attributed to an invasion of conjunctival cells into a corneal epithelium that is not adequately maintained because of LSC deficiency (Mackman et al., 1979; Nishida et al., 1995). Also, surgical transplantation of healthy limbal tissue or ex-vivo expanded LSC grafts have been shown to be effective treatment for corneal abnormalities in aniridia patients (Holland et al., 2003) as described in the Introduction.

Some results presented in this thesis also provide circumstantial evidence for invasion of the conjunctiva into the corneal epithelium, equivalent to that suggested for aniridia patients. This intrusion of conjunctiva has been previously documented in *Pax6*$^{+/-}$ eyes and has been speculated that is taking place because the limbus can no longer provide an efficient barrier (Daniels et al., 2001; Davis et al., 2003; Ramaesh et al., 2003). Keratin 19 is expressed in the conjunctiva, the limbus and the cornea in humans, but it is absent from the corneal epithelium in mice (Yoshida et al., 2006). Immunolocalisation of this keratin showed it was only identifiable in the conjunctiva and the limbus of wild-type eyes but the cornea was also positive in *Pax6*$^{+/-}$ eyes. Additionally, when *Pax6*$^{+/-}$ mice were crossed to K5-*LacZ*, the patches that were detected in the corneal epithelium resembled the conjunctival patches seen on wild-type eyes. These patches were small and usually occupied the peripheral cornea. This might be considered as another line of evidence for an incursion of

conjunctival cells into the corneal epithelium in the mouse model of aniridia.

7.2 EVALUATION OF TWO HYPOTHESES OF CORNEAL EPITHELIAL MAINTENANCE

As mentioned in the introduction (section 1.1.3), the conventional view of corneal epithelial maintenance by centripetal cell movement of stem cell progeny migrating from the limbus has been recently challenged (Majo et al., 2008). These authors transplanted limbal tissue from mice ubiquitously expressing a reporter gene, to the limbal area of immunocompromised mice but migration of transplanted cells towards the centre of the corneal epithelium could not be observed, unless the corneal epithelium was wounded. The absence of cell movement from the transplanted limbal tissue during normal homeostasis was interpreted by the authors as evidence that the limbus does not contribute to normal corneal maintenance, but rather to corneal wound repair. Then, they transplanted central corneal tissue to either the limbal or the central epithelium and, after wounding the cornea, cells from the transplant migrated centripetally or centrifugally respectively. Serial transplantation of central cornea tissue to the limbus of mice resulted in transplanted cells that migrated to both the conjunctiva and the cornea, when both tissues were wounded. Thus, the authors concluded that central cornea of the mouse contains stem cells that can restore both the cornea and conjunctival epithelium. To extend these findings to other species, they then cultured cells from different parts of the ocular surface of several species including humans and rats (but not mice, probably because of the inability to culture corneal murine cells). Holoclones were produced from the central cornea of many species, suggesting high proliferative potential. These findings led the authors to propose a unifying model where, during normal homeostasis, epithelial stem cells of equal potency are distributed throughout the ocular surface (Fig. 7.2 A) and conjunctival and corneal epithelia are continuously expanding in opposite directions towards each other (Fig. 7.2 B).

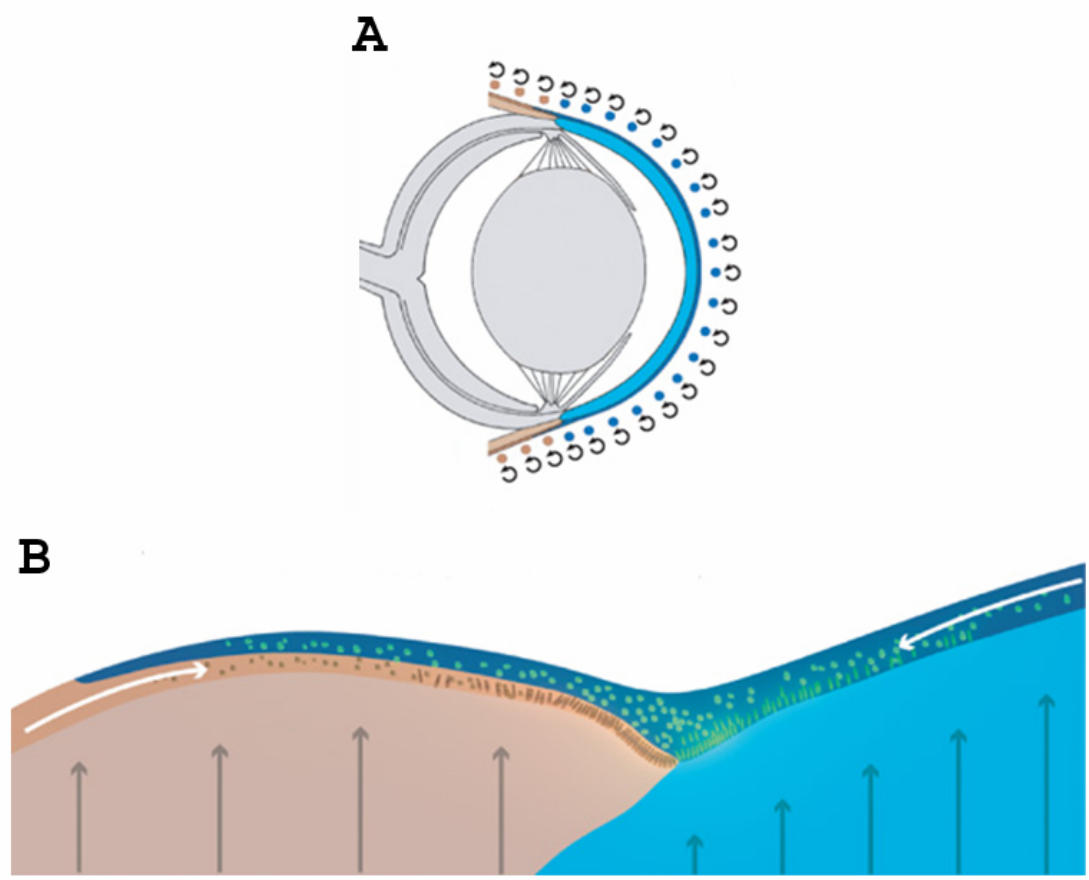

Figure 7.2 The alternative hypothesis for the maintenance of the ocular surface. (A) Schematic representation of the stem cells of equal potency distributed throughout the whole ocular surface. (B) Model of the opposing forces (white arrows) between the corneal and the conjunctival epithelium that confront at the limbus (Majo et al., 2008).

One of the main drawbacks of the above work is that the authors are claiming a model of corneal maintenance during normal homeostasis while all their methods involved serious interventions to the tissue like implantations and wounding. Such manipulations lead to stress and provide extrinsic stimuli that can alter the way cells behave under normal circumstances. Specifically for the surgical transplantation experiments, even the sutures that were used to stabilise the transplanted tissue have been reported to have a major impact on the ocular surface involving blood-vessel in-growth and rearrangement of neurons underlying the corneal epithelium (Streilein et al., 1996). Additionally, at least in the rabbit, it has been reported that transplanted limbal tissue can successfully colonise an unwounded corneal epithelium (Bradshaw et al., 1999). And this was not the only published work the authors failed to mention. If fact, they disregarded convincing evidence from over 30 years of research indicating that, during normal maintenance of the cornea, stem cells able to renew the corneal epithelium are located at the limbus and corneal epithelial cells migrate centripetally and not centrifugally. Several lines of evidence that are based on the physiology of the limbus, experimental as well as clinical observations along with compelling evidence about the centripetal migration of the corneal epithelial stem cells are detailed in section 1.1.3.

Some of the results presented in this thesis are also relevant to the issue of whether the corneal epithelium is maintained by LSCs or by stem cells distributed throughout the ocular surface.

First in the analysis of the X-inactivation mosaics at 3, 6 & 10 weeks old mice revealed that the mean number of patches decreased with age, a finding consistent with the emergence of stripes in the corneal epithelium that displace the original random, speckled pattern of patches. Moreover, when the number of patches in the periphery of the corneal epithelium was compared to those at the centre across ages, the peripheral corneal epithelium showed a significant reduction in the mean number of patches between 3 and 6 weeks old corneas. The mean number was reduced further and it was also significant between 3 and 10 weeks old corneas. On the other hand, for patches in the central corneal epithelium, a significant decline in the mean

number of patches could only be detected at 10 weeks old corneas. Since the decline indicates the initiation of stripes, the results indicate that stripes emerge first at the periphery and then they are extending towards the central cornea, supporting the centripetal migration of corneal epithelial cells. If the migration of cells was centrifugal, the decline in mean number of patches should have been detected first at the centre and later in the periphery of the cornea.

Then, the LRC technique confirmed that slow-cycling cells and thus, putative stem cells, can be identified in the limbal region of the eye. These cells could not be observed in the peripheral or central corneal epithelium. If the entire ocular surface was occupied by stem cells of equal potency, LRCs should have been identified in the corneal epithelium as well, since both limbus and conjunctiva have been reported to harbour slow-cycling cells (Cotsarelis et al., 1989; Lehrer et al., 1998; Nagasaki and Zhao, 2005; Pajoohesh-Ganji et al., 2006; Zhao et al., 2009).

Also, stripes of marked cells were observed in the corneal epithelium of K5-*LacZ* mice at different frequencies and locations. Analysis of these stripes suggests that stem cells are not randomly distributed throughout the corneal epithelium. If this was true, based on geometrical measurements, more than 50% of the stripes should have their more centrally located ends within the outer third of the corneal radius, since this third occupies more that 50% of the surface area. The observed distribution of corneal stripes was significantly different from the predicted one, providing one more line of evidence that the alternative hypothesis for the maintenance of the corneal epithelium is not valid.

7.3 FUTURE DIRECTIONS

Conditional expression of a reporter gene in the normal corneal epithelium under steady-state maintenance conditions may provide useful insights about issues like migration of epithelial cells and timing of stem cell specification, where knowing the exact timing of reporter gene expression would be advantageous. High levels of induction of the reporter were possible using tamoxifen and issues of toxicity were tackled by splitting the dose of tamoxifen over a period of three days. The next goal should be the detection of cells positive for the reporter gene that are organised in stripes. This would provide evidence that the reporter gene expression could be induced in stem cells. In order to accomplish that, a specific time point in development has to be identified before the specification of LSC, which, according to research on X-inactivation mosaics, should be before the age of 5 weeks in the mouse (Collinson et al., 2002). Gene delivery via lentiviral vectors has shown that gene expression can be found in the cornea following gene delivery at E8 – E15 during development (Endo et al., 2007). However, such a window of opportunity may also exist in newborn mice since in this species the development of the cornea continues afterbirth (Collinson et al., 2002). If induction of stem cells results in the appearance of stripes in the corneal epithelium, this technique could then be used to compare the number of LSCs in young and old mice. In this case, the mechanism of stripe formation would be understood and the timing of stripe emergence will be controlled by the time of tamoxifen administration.

Furthermore, the kinetics of the corneal epithelial maintenance in young and old mice should be studied further. This would provide information about the frequency of corneal epithelial renewal and if this differs between young and old animals, it would probably reflect the activity of the stem cells maintaining this tissue. However, this might still not provide enough evidences for corneal stem cell functionality. As in the case of haematopoietic stem cells (mentioned above), these cells might circulate at normal rate and even self-renew but they might still be defective (Sudo et al., 2000). The ultimate test for the activity of the stem cells should be their ability to reconstitute the whole corneal epithelium after

transplantation in mice where the limbus has been surgically or chemically removed. This test could also be used to compare the reconstitution abilities of cells from the limbus of *Pax6*$^{+/-}$ and wild-type animals. If *Pax6*$^{+/-}$ mice have limbal stem cell deficiency, transplantation of cells from these mice should demonstrate reduced ability to produce a normal corneal epithelium.

Furthermore, the most reliable way to identify LRCs seems to be the use of the H2B-GFP mouse. In this system, the transfer of labels should be minimal since the labelled agent is a protein and not nucleoside. This technique offers more advantages as well, since the labelled cells are still alive. So, they could be isolated with FACS based on their fluorescence and then they could either be analysed to identify a unique combination of markers that would allow easier identification, or they could be transplanted in disease models (like in the *Pax6*$^{+/-}$) in order to confirm that they are indeed stem cells or to show stem cell deficiency of the model.

The development of a culturing technique of murine LSCs or corneal epithelial cells would also provide one more valuable analytical tool for in the eye-scientist. By culturing putative LSCs, it will be possible to evaluate their stem cell characteristics by investigating their colony forming efficiency and measuring their capacity for population doublings. The results from these experiments could then be used to compare these properties of putative LSCs from *Pax6*$^{+/-}$ and wild-type mice or even between young and old animals. Additionally, when in culture, several differentiation protocols could be used to investigate if these relatively accessible cells can be differentiated to any other cell type.

It is clear that there is great need to find a marker or a combination of markers that exclusively identify LSCs. Use of such marker would easily prove if age affects the number of stem cells or if the observed reduced activity of LSCs from older mice is the consequence of an aged niche. It would also prove beyond any doubt whether *Pax6*$^{+/-}$ mice have LSC deficiency and, if so, help establish whether the abnormalities observed are due to the reduced number of LSCs or whether they are the secondary consequence of other abnormalities in the eye.

Bibliography

Abremski, K., and Hoess, R. (1984). Bacteriophage P1 site-specific recombination. Purification and properties of the Cre recombinase protein. J Biol Chem *259*, 1509-1514.

Ambati, B. K., Nozaki, M., Singh, N., Takeda, A., Jani, P. D., Suthar, T., Albuquerque, R. J., Richter, E., Sakurai, E., Newcomb, M. T., *et al.* (2006). Corneal avascularity is due to soluble VEGF receptor-1. Nature *443*, 993-997.

Baader, S. L., Schilling, M. L., Rosengarten, B., Pretsch, W., Teutsch, H. F., Oberdick, J., and Schilling, K. (1996). Purkinje cell lineage and the topographic organization of the cerebellar cortex: a view from X inactivation mosaics. Dev Biol *174*, 393-406.

Badea, T. C., Wang, Y., and Nathans, J. (2003). A noninvasive genetic/pharmacologic strategy for visualizing cell morphology and clonal relationships in the mouse. J Neurosci *23*, 2314-2322.

Bard, J. B., Hay, E. D., and Meller, S. M. (1975). Formation of the endothelium of the avian cornea: a study of cell movement in vivo. Dev Biol *42*, 334-361.

Barker, N., van de Wetering, M., and Clevers, H. (2008). The intestinal stem cell. Genes Dev *22*, 1856-1864.

Barker, N., van Es, J. H., Kuipers, J., Kujala, P., van den Born, M., Cozijnsen, M., Haegebarth, A., Korving, J., Begthel, H., Peters, P. J., and Clevers, H. (2007). Identification of stem cells in small intestine and colon by marker gene Lgr5. Nature *449*, 1003-1007.

Barrandon, Y., and Green, H. (1987). Three clonal types of keratinocyte with different capacities for multiplication. Proc Natl Acad Sci U S A *84*, 2302-2306.

Beebe, D. C., and Coats, J. M. (2000). The lens organizes the anterior segment: specification of neural crest cell differentiation in the avian eye. Dev Biol *220*, 424-431.

Beebe, D. C., and Masters, B. R. (1996). Cell lineage and the differentiation of corneal epithelial cells. Invest Ophthalmol Vis Sci *37*, 1815-1825.

Bickenbach, J. R. (1981). Identification and behavior of label-retaining cells in oral mucosa and skin. J Dent Res *60 Spec No C*, 1611-1620.

Bickenbach, J. R., McCutecheon, J., and Mackenzie, I. C. (1986). Rate of loss of tritiated thymidine label in basal cells in mouse epithelial tissues. Cell Tissue Kinet

19, 325-333.

Bonnerot, C., and Nicolas, J. F. (1993). Clonal analysis in the intact mouse embryo by intragenic homologous recombination. C R Acad Sci III *316*, 1207-1217.

Bopp, D., Burri, M., Baumgartner, S., Frigerio, G., and Noll, M. (1986). Conservation of a large protein domain in the segmentation gene paired and in functionally related genes of Drosophila. Cell *47*, 1033-1040.

Boulton, M., and Albon, J. (2004). Stem cells in the eye. Int J Biochem Cell Biol *36*, 643-657.

Bradshaw, J. J., Obritsch, W. F., Cho, B. J., Gregerson, D. S., and Holland, E. J. (1999). Ex vivo transduction of corneal epithelial progenitor cells using a retroviral vector. Invest Ophthalmol Vis Sci *40*, 230-235.

Braun, K. M., Niemann, C., Jensen, U. B., Sundberg, J. P., Silva-Vargas, V., and Watt, F. M. (2003). Manipulation of stem cell proliferation and lineage commitment: visualisation of label-retaining cells in wholemounts of mouse epidermis. Development *130*, 5241-5255.

Braun, K. M., and Watt, F. M. (2004). Epidermal label-retaining cells: background and recent applications. J Investig Dermatol Symp Proc *9*, 196-201.

Buck, R. C. (1985). Measurement of centripetal migration of normal corneal epithelial cells in the mouse. Invest Ophthalmol Vis Sci *26*, 1296-1299.

Buck, S. B., Bradford, J., Gee, K. R., Agnew, B. J., Clarke, S. T., and Salic, A. (2008). Detection of S-phase cell cycle progression using 5-ethynyl-2'-deoxyuridine incorporation with click chemistry, an alternative to using 5-bromo-2'-deoxyuridine antibodies. Biotechniques *44*, 927-929.

Budak, M. T., Alpdogan, O. S., Zhou, M., Lavker, R. M., Akinci, M. A., and Wolosin, J. M. (2005). Ocular surface epithelia contain ABCG2-dependent side population cells exhibiting features associated with stem cells. J Cell Sci *118*, 1715-1724.

Burns, T. C., Ortiz-Gonzalez, X. R., Gutierrez-Perez, M., Keene, C. D., Sharda, R., Demorest, Z. L., Jiang, Y., Nelson-Holte, M., Soriano, M., Nakagawa, Y.*, et al.* (2006). Thymidine analogs are transferred from prelabeled donor to host cells in the central nervous system after transplantation: a word of caution. Stem Cells *24*, 1121-1127.

Byrne, C., and Fuchs, E. (1993). Probing keratinocyte and differentiation specificity of the human K5 promoter in vitro and in transgenic mice. Mol Cell Biol *13*, 3176-3190.

Byrne, C., Tainsky, M., and Fuchs, E. (1994). Programming gene expression in developing epidermis. Development *120*, 2369-2383.

Caric, D., Gooday, D., Hill, R. E., McConnell, S. K., and Price, D. J. (1997). Determination of the migratory capacity of embryonic cortical cells lacking the transcription factor Pax-6. Development *124*, 5087-5096.

Carlson, B. M., and Faulkner, J. A. (1989). Muscle transplantation between young and old rats: age of host determines recovery. Am J Physiol *256*, C1262-1266.

Carmel, R. (2001). Anemia and aging: an overview of clinical, diagnostic and biological issues. Blood Rev *15*, 9-18.

Chaloin-Dufau, C., Pavitt, I., Delorme, P., and Dhouailly, D. (1993). Identification of keratins 3 and 12 in corneal epithelium of vertebrates. Epithelial Cell Biol *2*, 120-125.

Chaloin-Dufau, C., Sun, T. T., and Dhouailly, D. (1990). Appearance of the keratin pair K3/K12 during embryonic and adult corneal epithelial differentiation in the chick and in the rabbit. Cell Differ Dev *32*, 97-108.

Chan, R. W., and Gargett, C. E. (2006). Identification of label-retaining cells in mouse endometrium. Stem Cells *24*, 1529-1538.

Chen, W., Hara, K., Tian, Q., Zhao, K., and Yoshitomi, T. (2007). Existence of small slow-cycling Langerhans cells in the limbal basal epithelium that express ABCG2. Exp Eye Res *84*, 626-634.

Chen, W., Ishikawa, M., Yamaki, K., and Sakuragi, S. (2003). Wistar rat palpebral conjunctiva contains more slow-cycling stem cells that have larger proliferative capacity: implication for conjunctival epithelial homeostasis. Jpn J Ophthalmol *47*, 119-128.

Chen, Z., de Paiva, C. S., Luo, L., Kretzer, F. L., Pflugfelder, S. C., and Li, D. Q. (2004). Characterization of putative stem cell phenotype in human limbal epithelia. Stem Cells *22*, 355-366.

Chow, R. L., Altmann, C. R., Lang, R. A., and Hemmati-Brivanlou, A. (1999). Pax6

induces ectopic eyes in a vertebrate. Development *126*, 4213-4222.

Christiansen, J. H., Dennis, C. L., Wicking, C. A., Monkley, S. J., Wilkinson, D. G., and Wainwright, B. J. (1995). Murine Wnt-11 and Wnt-12 have temporally and spatially restricted expression patterns during embryonic development. Mech Dev *51*, 341-350.

Chung, E. H., Bukusoglu, G., and Zieske, J. D. (1992). Localization of corneal epithelial stem cells in the developing rat. Invest Ophthalmol Vis Sci *33*, 2199-2206.

Civin, C. I. (1992). Identification and positive selection of human progenitor/stem cells for bone marrow transplantation. Prog Clin Biol Res *377*, 461-472; discussion 473.

Clements, J., Lu, Z., Gehring, W. J., Meinertzhagen, I. A., and Callaerts, P. (2008). Central projections of photoreceptor axons originating from ectopic eyes in Drosophila. Proc Natl Acad Sci U S A *105*, 8968-8973.

Collinson, J. M., Chanas, S. A., Hill, R. E., and West, J. D. (2004a). Corneal development, limbal stem cell function, and corneal epithelial cell migration in the Pax6(+/-) mouse. Invest Ophthalmol Vis Sci *45*, 1101-1108.

Collinson, J. M., Hill, R. E., and West, J. D. (2000). Different roles for Pax6 in the optic vesicle and facial epithelium mediate early morphogenesis of the murine eye. Development *127*, 945-956.

Collinson, J. M., Hill, R. E., and West, J. D. (2004b). Analysis of mouse eye development with chimeras and mosaics. Int J Dev Biol *48*, 793-804.

Collinson, J. M., Morris, L., Reid, A. I., Ramaesh, T., Keighren, M. A., Flockhart, J. H., Hill, R. E., Tan, S. S., Ramaesh, K., Dhillon, B., and West, J. D. (2002). Clonal analysis of patterns of growth, stem cell activity, and cell movement during the development and maintenance of the murine corneal epithelium. Dev Dyn *224*, 432-440.

Collinson, J. M., Quinn, J. C., Buchanan, M. A., Kaufman, M. H., Wedden, S. E., West, J. D., and Hill, R. E. (2001). Primary defects in the lens underlie complex anterior segment abnormalities of the Pax6 heterozygous eye. Proc Natl Acad Sci U S A *98*, 9688-9693.

Conboy, I. M., Conboy, M. J., Wagers, A. J., Girma, E. R., Weissman, I. L., and Rando, T. A. (2005). Rejuvenation of aged progenitor cells by exposure to a young systemic environment. Nature *433*, 760-764.

Conboy, I. M., and Rando, T. A. (2005). Aging, stem cells and tissue regeneration: lessons from muscle. Cell Cycle *4*, 407-410.

Cotsarelis, G., Cheng, S. Z., Dong, G., Sun, T. T., and Lavker, R. M. (1989). Existence of slow-cycling limbal epithelial basal cells that can be preferentially stimulated to proliferate: implications on epithelial stem cells. Cell *57*, 201-209.

Cotsarelis, G., Sun, T. T., and Lavker, R. M. (1990). Label-retaining cells reside in the bulge area of pilosebaceous unit: implications for follicular stem cells, hair cycle, and skin carcinogenesis. Cell *61*, 1329-1337.

Coyne, T. M., Marcus, A. J., Woodbury, D., and Black, I. B. (2006). Marrow stromal cells transplanted to the adult brain are rejected by an inflammatory response and transfer donor labels to host neurons and glia. Stem Cells *24*, 2483-2492.

Cvekl, A., and Piatigorsky, J. (1996). Lens development and crystallin gene expression: many roles for Pax-6. Bioessays *18*, 621-630.

Cvekl, A., and Tamm, E. R. (2004). Anterior eye development and ocular mesenchyme: new insights from mouse models and human diseases. Bioessays *26*, 374-386.

Danielian, P. S., Muccino, D., Rowitch, D. H., Michael, S. K., and McMahon, A. P. (1998). Modification of gene activity in mouse embryos in utero by a tamoxifen-inducible form of Cre recombinase. Curr Biol *8*, 1323-1326.

Danielian, P. S., White, R., Hoare, S. A., Fawell, S. E., and Parker, M. G. (1993). Identification of residues in the estrogen receptor that confer differential sensitivity to estrogen and hydroxytamoxifen. Mol Endocrinol *7*, 232-240.

Daniels, J. T., Dart, J. K., Tuft, S. J., and Khaw, P. T. (2001). Corneal stem cells in review. Wound Repair Regen *9*, 483-494.

Davanger, M., and Evensen, A. (1971). Role of the pericorneal papillary structure in renewal of corneal epithelium. Nature *229*, 560-561.

Davis, J., Duncan, M. K., Robison, W. G., Jr., and Piatigorsky, J. (2003). Requirement for Pax6 in corneal morphogenesis: a role in adhesion. J Cell Sci *116*, 2157-2167.

Davis-Silberman, N., and Ashery-Padan, R. (2008). Iris development in vertebrates; genetic and molecular considerations. Brain Res *1192*, 17-28.

de Paiva, C. S., Chen, Z., Corrales, R. M., Pflugfelder, S. C., and Li, D. Q. (2005). ABCG2 transporter identifies a population of clonogenic human limbal epithelial cells. Stem Cells *23*, 63-73.

Di Iorio, E., Barbaro, V., Ruzza, A., Ponzin, D., Pellegrini, G., and De Luca, M. (2005). Isoforms of DeltaNp63 and the migration of ocular limbal cells in human corneal regeneration. Proc Natl Acad Sci U S A *102*, 9523-9528.

Diamond, I., Owolabi, T., Marco, M., Lam, C., and Glick, A. (2000). Conditional gene expression in the epidermis of transgenic mice using the tetracycline-regulated transactivators tTA and rTA linked to the keratin 5 promoter. J Invest Dermatol *115*, 788-794.

Dobie, K., Mehtali, M., McClenaghan, M., and Lathe, R. (1997). Variegated gene expression in mice. Trends Genet *13*, 127-130.

Dua, H. S., Joseph, A., Shanmuganathan, V. A., and Jones, R. E. (2003). Stem cell differentiation and the effects of deficiency. Eye (Lond) *17*, 877-885.

Dua, H. S., Shanmuganathan, V. A., Powell-Richards, A. O., Tighe, P. J., and Joseph, A. (2005). Limbal epithelial crypts: a novel anatomical structure and a putative limbal stem cell niche. Br J Ophthalmol *89*, 529-532.

Ebato, B., Friend, J., and Thoft, R. A. (1988). Comparison of limbal and peripheral human corneal epithelium in tissue culture. Invest Ophthalmol Vis Sci *29*, 1533-1537.

Endo, M., Zoltick, P. W., Chung, D. C., Bennett, J., Radu, A., Muvarak, N., and Flake, A. W. (2007). Gene transfer to ocular stem cells by early gestational intraamniotic injection of lentiviral vector. Mol Ther *15*, 579-587.

Favor, J., and Neuhauser-Klaus, A. (2000). Saturation mutagenesis for dominant eye morphological defects in the mouse Mus musculus. Mamm Genome *11*, 520-525.

Fellous, T. G., McDonald, S. A., Burkert, J., Humphries, A., Islam, S., De-Alwis, N. M., Gutierrez-Gonzalez, L., Tadrous, P. J., Elia, G., Kocher, H. M., *et al.* (2009). A methodological approach to tracing cell lineage in human epithelial tissues. Stem Cells *27*, 1410-1420.

Fitch, J., Fini, M. E., Beebe, D. C., and Linsenmayer, T. F. (1998). Collagen type IX and developmentally regulated swelling of the avian primary corneal stroma. Dev Dyn *212*, 27-37.

Francesconi, C. M., Hutcheon, A. E., Chung, E. H., Dalbone, A. C., Joyce, N. C., and Zieske, J. D. (2000). Expression patterns of retinoblastoma and E2F family proteins during corneal development. Invest Ophthalmol Vis Sci *41*, 1054-1062.

Frank, E., and Sanes, J. R. (1991). Lineage of neurons and glia in chick dorsal root ganglia: analysis in vivo with a recombinant retrovirus. Development *111*, 895-908.

Friend, J., and Kenyon, K. R. (1987). Physiology of the conjunctiva: metabolism and biochemistry (Little Brown, Boston).

Gao, F., Toriyama, K., Ma, H., and Nagata, T. (1993). Light microscopic radioautographic study on DNA synthesis in aging mice corneas. Cell Mol Biol (Noisy-le-grand) *39*, 435-441.

Gehring, W. J. (2005). New perspectives on eye development and the evolution of eyes and photoreceptors. J Hered *96*, 171-184.

Glaser, T., Walton, D. S., and Maas, R. L. (1992). Genomic structure, evolutionary conservation and aniridia mutations in the human PAX6 gene. Nat Genet *2*, 232-239.

Golmohammadi, M. G., Blackmore, D. G., Large, B., Azari, H., Esfandiary, E., Paxinos, G., Franklin, K. B., Reynolds, B. A., and Rietze, R. L. (2008). Comparative analysis of the frequency and distribution of stem and progenitor cells in the adult mouse brain. Stem Cells *26*, 979-987.

Goodell, M. A., Brose, K., Paradis, G., Conner, A. S., and Mulligan, R. C. (1996). Isolation and functional properties of murine hematopoietic stem cells that are replicating in vivo. J Exp Med *183*, 1797-1806.

Gossen, M., and Bujard, H. (1992). Tight control of gene expression in mammalian cells by tetracycline-responsive promoters. Proc Natl Acad Sci U S A *89*, 5547-5551.

Gossen, M., Freundlieb, S., Bender, G., Muller, G., Hillen, W., and Bujard, H. (1995). Transcriptional activation by tetracyclines in mammalian cells. Science *268*, 1766-1769.

Goverdhana, S., Puntel, M., Xiong, W., Zirger, J. M., Barcia, C., Curtin, J. F., Soffer, E. B., Mondkar, S., King, G. D., Hu, J.*, et al.* (2005). Regulatable gene expression systems for gene therapy applications: progress and future challenges. Mol Ther *12*, 189-211.

Grindley, J. C., Davidson, D. R., and Hill, R. E. (1995). The role of Pax-6 in eye and

nasal development. Development *121*, 1433-1442.

Halder, G., Callaerts, P., and Gehring, W. J. (1995). Induction of ectopic eyes by targeted expression of the eyeless gene in Drosophila. Science *267*, 1788-1792.

Haskjold, E., Bjerknes, R., and Bjerknes, E. (1989). Migration of cells in the rat corneal epithelium. Acta Ophthalmol (Copenh) *67*, 91-96.

Haustein, J. (1983). On the ultrastructure of the developing and adult mouse corneal stroma. Anat Embryol (Berl) *168*, 291-305.

Hawiger, J. (1999). Noninvasive intracellular delivery of functional peptides and proteins. Curr Opin Chem Biol *3*, 89-94.

Hay, E. D. (1979). Development of the vertebrate cornea. Int Rev Cytol *63*, 263-322.

Hayashi, R., Yamato, M., Sugiyama, H., Sumide, T., Yang, J., Okano, T., Tano, Y., and Nishida, K. (2007). N-Cadherin is expressed by putative stem/progenitor cells and melanocytes in the human limbal epithelial stem cell niche. Stem Cells *25*, 289-296.

Hayashi, S., and McMahon, A. P. (2002). Efficient recombination in diverse tissues by a tamoxifen-inducible form of Cre: a tool for temporally regulated gene activation/inactivation in the mouse. Dev Biol *244*, 305-318.

Hazlett, L., Masinick, S., Mezger, B., Barrett, R., Kurpakus, M., and Garrett, M. (1996). Ultrastructural, immunohistological and biochemical characterization of cultured mouse corneal epithelial cells. Ophthalmic Res *28*, 50-56.

Hesse, M., Zimek, A., Weber, K., and Magin, T. M. (2004). Comprehensive analysis of keratin gene clusters in humans and rodents. Eur J Cell Biol *83*, 19-26.

Hill, R. E., Favor, J., Hogan, B. L., Ton, C. C., Saunders, G. F., Hanson, I. M., Prosser, J., Jordan, T., Hastie, N. D., and van Heyningen, V. (1991). Mouse small eye results from mutations in a paired-like homeobox-containing gene. Nature *354*, 522-525.

Hogan, B. L., Hirst, E. M., Horsburgh, G., and Hetherington, C. M. (1988). Small eye (Sey): a mouse model for the genetic analysis of craniofacial abnormalities. Development *103 Suppl*, 115-119.

Hogan, B. L., Horsburgh, G., Cohen, J., Hetherington, C. M., Fisher, G., and Lyon,

M. F. (1986). Small eyes (Sey): a homozygous lethal mutation on chromosome 2 which affects the differentiation of both lens and nasal placodes in the mouse. J Embryol Exp Morphol *97*, 95-110.

Holland, E. J., Djalilian, A. R., and Schwartz, G. S. (2003). Management of aniridic keratopathy with keratolimbal allograft: a limbal stem cell transplantation technique. Ophthalmology *110*, 125-130.

Huang, A. J., and Tseng, S. C. (1991). Corneal epithelial wound healing in the absence of limbal epithelium. Invest Ophthalmol Vis Sci *32*, 96-105.

Jaks, V., Barker, N., Kasper, M., van Es, J. H., Snippert, H. J., Clevers, H., and Toftgard, R. (2008). Lgr5 marks cycling, yet long-lived, hair follicle stem cells. Nat Genet *40*, 1291-1299.

Jecker, P., Beuleke, A., Dressendorfer, I., Pabst, R., and Westermann, J. (1997). Long-term oral application of 5-bromo-2-deoxyuridine does not reliably label proliferating immune cells in the LEW rat. J Histochem Cytochem *45*, 393-401.

Jo, D., Nashabi, A., Doxsee, C., Lin, Q., Unutmaz, D., Chen, J., and Ruley, H. E. (2001). Epigenetic regulation of gene structure and function with a cell-permeable Cre recombinase. Nat Biotechnol *19*, 929-933.

Jordan, T., Hanson, I., Zaletayev, D., Hodgson, S., Prosser, J., Seawright, A., Hastie, N., and van Heyningen, V. (1992). The human PAX6 gene is mutated in two patients with aniridia. Nat Genet *1*, 328-332.

Kanakubo, S., Nomura, T., Yamamura, K., Miyazaki, J., Tamai, M., and Osumi, N. (2006). Abnormal migration and distribution of neural crest cells in Pax6 heterozygous mutant eye, a model for human eye diseases. Genes Cells *11*, 919-933.

Kanda, T., Sullivan, K. F., and Wahl, G. M. (1998). Histone-GFP fusion protein enables sensitive analysis of chromosome dynamics in living mammalian cells. Curr Biol *8*, 377-385.

Kawakita, T., Shimmura, S., Higa, K., Espana, E. M., He, H., Shimazaki, J., Tsubota, K., and Tseng, S. C. (2009). Greater growth potential of p63-positive epithelial cell clusters maintained in human limbal epithelial sheets. Invest Ophthalmol Vis Sci *50*, 4611-4617.

Kawakita, T., Shimmura, S., Hornia, A., Higa, K., and Tseng, S. C. (2008). Stratified epithelial sheets engineered from a single adult murine corneal/limbal progenitor cell. J Cell Mol Med *12*, 1303-1316.

Kenyon, K. R., and Tseng, S. C. (1989). Limbal autograft transplantation for ocular surface disorders. Ophthalmology *96*, 709-722; discussion 722-703.

Kiel, M. J., Yilmaz, O. H., Iwashita, T., Terhorst, C., and Morrison, S. J. (2005). SLAM family receptors distinguish hematopoietic stem and progenitor cells and reveal endothelial niches for stem cells. Cell *121*, 1109-1121.

Kim, H. J., Gatz, C., Hillen, W., and Jones, T. R. (1995). Tetracycline repressor-regulated gene repression in recombinant human cytomegalovirus. J Virol *69*, 2565-2573.

Kim, H. S., Jun Song, X., de Paiva, C. S., Chen, Z., Pflugfelder, S. C., and Li, D. Q. (2004). Phenotypic characterization of human corneal epithelial cells expanded ex vivo from limbal explant and single cell cultures. Exp Eye Res *79*, 41-49.

Kinoshita, S., Friend, J., and Thoft, R. A. (1981). Sex chromatin of donor corneal epithelium in rabbits. Invest Ophthalmol Vis Sci *21*, 434-441.

Kobayashi, T., Yoshioka, R., Shiraishi, A., and Ohashi, Y. (2009). New technique for culturing corneal epithelial cells of normal mice. Mol Vis *15*, 1589-1593.

Koroma, B. M., Yang, J. M., and Sundin, O. H. (1997). The Pax-6 homeobox gene is expressed throughout the corneal and conjunctival epithelia. Invest Ophthalmol Vis Sci *38*, 108-120.

Kruse, F. E., Chen, J. J., Tsai, R. J., and Tseng, S. C. (1990). Conjunctival transdifferentiation is due to the incomplete removal of limbal basal epithelium. Invest Ophthalmol Vis Sci *31*, 1903-1913.

Kuhlman, R. E., and Resnik, R. A. (1958). Quantitative histochemical changes in the development of the rat lens and cornea. Am J Ophthalmol *46*, 47-55.

Kurpakus, M. A., Maniaci, M. T., and Esco, M. (1994). Expression of keratins K12, K4 and K14 during development of ocular surface epithelium. Curr Eye Res *13*, 805-814.

Kurpakus, M. A., Stock, E. L., and Jones, J. C. (1990). Expression of the 55-kD/64-kD corneal keratins in ocular surface epithelium. Invest Ophthalmol Vis Sci *31*, 448-456.

Lakshmipathy, U., and Verfaillie, C. (2005). Stem cell plasticity. Blood Rev *19*, 29-38.

Le Douarin, N., and Kalcheim, C. (1999). The neural crest (Cambridge, Cambridge university press).

Lehrer, M. S., Sun, T. T., and Lavker, R. M. (1998). Strategies of epithelial repair: modulation of stem cell and transit amplifying cell proliferation. J Cell Sci *111 (Pt 19)*, 2867-2875.

Lersch, R., Stellmach, V., Stocks, C., Giudice, G., and Fuchs, E. (1989). Isolation, sequence, and expression of a human keratin K5 gene: transcriptional regulation of keratins and insights into pairwise control. Mol Cell Biol *9*, 3685-3697.

Li, F., Lu, L., and Lu, J. (2009). Identification and location of label retaining cells in mouse liver. J Gastroenterol.

Lin, G., Huang, Y. C., Shindel, A. W., Banie, L., Wang, G., Lue, T. F., and Lin, C. S. (2009). Labeling and tracking of mesenchymal stromal cells with EdU. Cytotherapy *11*, 864-873.

Lin, H. (2002). The stem-cell niche theory: lessons from flies. Nat Rev Genet *3*, 931-940.

Lin, Q., Jo, D., Gebre-Amlak, K. D., and Ruley, H. E. (2004). Enhanced cell-permeant Cre protein for site-specific recombination in cultured cells. BMC Biotechnol *4*, 25.

Lobe, C. G., Koop, K. E., Kreppner, W., Lomeli, H., Gertsenstein, M., and Nagy, A. (1999). Z/AP, a double reporter for cre-mediated recombination. Dev Biol *208*, 281-292.

Lu, H., Zimek, A., Chen, J., Hesse, M., Bussow, H., Weber, K., and Magin, T. M. (2006). Keratin 5 knockout mice reveal plasticity of keratin expression in the corneal epithelium. Eur J Cell Biol *85*, 803-811.

Lyon, M. F. (1961). Gene action in the X-chromosome of the mouse (Mus musculus L.). Nature *190*, 372-373.

Ma, X., Shimmura, S., Miyashita, H., Yoshida, S., Kubota, M., Kawakita, T., and Tsubota, K. (2009). Long-term culture and growth kinetics of murine corneal epithelial cells expanded from single corneas. Invest Ophthalmol Vis Sci *50*, 2716-2721.

Mackman, G., Brightbill, F. S., and Optiz, J. M. (1979). Corneal changes in aniridia.

Am J Ophthalmol *87*, 497-502.

Maeshima, A., Yamashita, S., and Nojima, Y. (2003). Identification of renal progenitor-like tubular cells that participate in the regeneration processes of the kidney. J Am Soc Nephrol *14*, 3138-3146.

Majo, F., Rochat, A., Nicolas, M., Jaoude, G. A., and Barrandon, Y. (2008). Oligopotent stem cells are distributed throughout the mammalian ocular surface. Nature *456*, 250-254.

Margo, C. E. (1983). Congenital aniridia: a histopathologic study of the anterior segment in children. J Pediatr Ophthalmol Strabismus *20*, 192-198.

Mathis, L., and Nicolas, J. F. (2000). Different clonal dispersion in the rostral and caudal mouse central nervous system. Development *127*, 1277-1290.

Mathis, L., and Nicolas, J. F. (2003). Progressive restriction of cell fates in relation to neuroepithelial cell mingling in the mouse cerebellum. Dev Biol *258*, 20-31.

Matic, M., Petrov, I. N., Chen, S., Wang, C., Dimitrijevich, S. D., and Wolosin, J. M. (1997). Stem cells of the corneal epithelium lack connexins and metabolite transfer capacity. Differentiation *61*, 251-260.

Mattioni, T., Louvion, J. F., and Picard, D. (1994). Regulation of protein activities by fusion to steroid binding domains. Methods Cell Biol *43 Pt A*, 335-352.

Merkle, F. T., Tramontin, A. D., Garcia-Verdugo, J. M., and Alvarez-Buylla, A. (2004). Radial glia give rise to adult neural stem cells in the subventricular zone. Proc Natl Acad Sci U S A *101*, 17528-17532.

Moore, J. E., McMullen, C. B., Mahon, G., and Adamis, A. P. (2002). The corneal epithelial stem cell. DNA Cell Biol *21*, 443-451.

Morley, S. D., Chang, S. P., Tan, S. S., and West, J. D. (2004). Validity of the 21-OH/LacZ transgenic mouse as a model for studying adrenocortical cell lineage. Endocr Res *30*, 513-519.

Mort, R. L., Ramaesh, T., Kleinjan, D. A., Morley, S. D., and West, J. D. (2009). Mosaic analysis of stem cell function and wound healing in the mouse corneal epithelium. BMC Dev Biol *9*, 4.

Murayama, A., Matsuzaki, Y., Kawaguchi, A., Shimazaki, T., and Okano, H. (2002).

Flow cytometric analysis of neural stem cells in the developing and adult mouse brain. J Neurosci Res *69*, 837-847.

Nagasaki, T., and Zhao, J. (2003). Centripetal movement of corneal epithelial cells in the normal adult mouse. Invest Ophthalmol Vis Sci *44*, 558-566.

Nagasaki, T., and Zhao, J. (2005). Uniform distribution of epithelial stem cells in the bulbar conjunctiva. Invest Ophthalmol Vis Sci *46*, 126-132.

Nakamura, T., Ohtsuka, T., Sekiyama, E., Cooper, L. J., Kokubu, H., Fullwood, N. J., Barrandon, Y., Kageyama, R., and Kinoshita, S. (2008). Hes1 regulates corneal development and the function of corneal epithelial stem/progenitor cells. Stem Cells *26*, 1265-1274.

Nelson, J. D., and Cameron, J. D. (1997). The conjunctiva. Fundamentals of cornea and external disease (Mosby, St Louis).

Nelson, L. B., Spaeth, G. L., Nowinski, T. S., Margo, C. E., and Jackson, L. (1984). Aniridia. A review. Surv Ophthalmol *28*, 621-642.

Nelson, W. G., and Sun, T. T. (1983). The 50- and 58-kdalton keratin classes as molecular markers for stratified squamous epithelia: cell culture studies. J Cell Biol *97*, 244-251.

Nicolas, J. F., Mathis, L., Bonnerot, C., and Saurin, W. (1996). Evidence in the mouse for self-renewing stem cells in the formation of a segmented longitudinal structure, the myotome. Development *122*, 2933-2946.

Nishida, K., Kinoshita, S., Ohashi, Y., Kuwayama, Y., and Yamamoto, S. (1995). Ocular surface abnormalities in aniridia. Am J Ophthalmol *120*, 368-375.

Niwa, H., Toyooka, Y., Shimosato, D., Strumpf, D., Takahashi, K., Yagi, R., and Rossant, J. (2005). Interaction between Oct3/4 and Cdx2 determines trophectoderm differentiation. Cell *123*, 917-929.

No, D., Yao, T. P., and Evans, R. M. (1996). Ecdysone-inducible gene expression in mammalian cells and transgenic mice. Proc Natl Acad Sci U S A *93*, 3346-3351.

Onuma, Y., Takahashi, S., Asashima, M., Kurata, S., and Gehring, W. J. (2002). Conservation of Pax 6 function and upstream activation by Notch signaling in eye development of frogs and flies. Proc Natl Acad Sci U S A *99*, 2020-2025.

Ou, J., Walczysko, P., Kucerova, R., Rajnicek, A. M., McCaig, C. D., Zhao, M., and Collinson, J. M. (2008). Chronic wound state exacerbated by oxidative stress in Pax6+/- aniridia-related keratopathy. J Pathol *215*, 421-430.

Pajoohesh-Ganji, A., Ghosh, S. P., and Stepp, M. A. (2004). Regional distribution of alpha9beta1 integrin within the limbus of the mouse ocular surface. Dev Dyn *230*, 518-528.

Pajoohesh-Ganji, A., Pal-Ghosh, S., Simmens, S. J., and Stepp, M. A. (2006). Integrins in slow-cycling corneal epithelial cells at the limbus in the mouse. Stem Cells *24*, 1075-1086.

Pajoohesh-Ganji, A., and Stepp, M. A. (2005). In search of markers for the stem cells of the corneal epithelium. Biol Cell *97*, 265-276.

Pal-Ghosh, S., Pajoohesh-Ganji, A., Brown, M., and Stepp, M. A. (2004). A mouse model for the study of recurrent corneal epithelial erosions: alpha9beta1 integrin implicated in progression of the disease. Invest Ophthalmol Vis Sci *45*, 1775-1788.

Pawelczyk, E., Arbab, A. S., Chaudhry, A., Balakumaran, A., Robey, P. G., and Frank, J. A. (2008). In vitro model of bromodeoxyuridine or iron oxide nanoparticle uptake by activated macrophages from labeled stem cells: implications for cellular therapy. Stem Cells *26*, 1366-1375.

Pawelczyk, E., Jordan, E. K., Balakumaran, A., Chaudhry, A., Gormley, N., Smith, M., Lewis, B. K., Childs, R., Robey, P. G., and Frank, J. A. (2009). In vivo transfer of intracellular labels from locally implanted bone marrow stromal cells to resident tissue macrophages. PLoS One *4*, e6712.

Peitz, M., Pfannkuche, K., Rajewsky, K., and Edenhofer, F. (2002). Ability of the hydrophobic FGF and basic TAT peptides to promote cellular uptake of recombinant Cre recombinase: a tool for efficient genetic engineering of mammalian genomes. Proc Natl Acad Sci U S A *99*, 4489-4494.

Pellegrini, G., Dellambra, E., Golisano, O., Martinelli, E., Fantozzi, I., Bondanza, S., Ponzin, D., McKeon, F., and De Luca, M. (2001). p63 identifies keratinocyte stem cells. Proc Natl Acad Sci U S A *98*, 3156-3161.

Pellegrini, G., Golisano, O., Paterna, P., Lambiase, A., Bonini, S., Rama, P., and De Luca, M. (1999). Location and clonal analysis of stem cells and their differentiated progeny in the human ocular surface. J Cell Biol *145*, 769-782.

Phipps, K. D., and Sullenger, D. B. (1964). Plutonium Dioxide: Preparation of Single

Crystals. Science *145*, 1048-1049.

Potten, C. S., and Morris, R. J. (1988). Epithelial stem cells in vivo. J Cell Sci Suppl *10*, 45-62.

Potten, C. S., Owen, G., and Booth, D. (2002). Intestinal stem cells protect their genome by selective segregation of template DNA strands. J Cell Sci *115*, 2381-2388.

Quinn, J. C., West, J. D., and Hill, R. E. (1996). Multiple functions for Pax6 in mouse eye and nasal development. Genes Dev *10*, 435-446.

Quinn, J. C., West, J. D., and Kaufman, M. H. (1997). Genetic background effects on dental and other craniofacial abnormalities in homozygous small eye (Pax6Sey/Pax6Sey) mice. Anat Embryol (Berl) *196*, 311-321.

Quiring, R., Walldorf, U., Kloter, U., and Gehring, W. J. (1994). Homology of the eyeless gene of Drosophila to the Small eye gene in mice and Aniridia in humans. Science *265*, 785-789.

Ramaesh, T., Collinson, J. M., Ramaesh, K., Kaufman, M. H., West, J. D., and Dhillon, B. (2003). Corneal abnormalities in Pax6+/- small eye mice mimic human aniridia-related keratopathy. Invest Ophthalmol Vis Sci *44*, 1871-1878.

Ramaesh, T., Ramaesh, K., Martin Collinson, J., Chanas, S. A., Dhillon, B., and West, J. D. (2005). Developmental and cellular factors underlying corneal epithelial dysgenesis in the Pax6+/- mouse model of aniridia. Exp Eye Res *81*, 224-235.

Rando, T. A. (2006). Stem cells, ageing and the quest for immortality. Nature *441*, 1080-1086.

Reese, B. E., Necessary, B. D., Tam, P. P., Faulkner-Jones, B., and Tan, S. S. (1999). Clonal expansion and cell dispersion in the developing mouse retina. Eur J Neurosci *11*, 2965-2978.

Reya, T., Morrison, S. J., Clarke, M. F., and Weissman, I. L. (2001). Stem cells, cancer, and cancer stem cells. Nature *414*, 105-111.

Roach, S. A. (1968). The Theory of Random Clumping (London, Methuen).

Roberts, R. C. (1967). Small eyes - a new dominant eye mutant in the mouse. Genet Res *9*, 121-122.

Romano, A. C., Espana, E. M., Yoo, S. H., Budak, M. T., Wolosin, J. M., and Tseng, S. C. (2003). Different cell sizes in human limbal and central corneal basal epithelia measured by confocal microscopy and flow cytometry. Invest Ophthalmol Vis Sci *44*, 5125-5129.

Romano, G. (2004). Systems for regulated or tissue-specific gene expression. Drug News Perspect *17*, 85-90.

Sadek, S., and Bell, S. C. (1996). The effects of the antihormones RU486 and tamoxifen on fetoplacental development and placental bed vascularisation in the rat: a model for intrauterine fetal growth retardation. Br J Obstet Gynaecol *103*, 630-641.

Salic, A., and Mitchison, T. J. (2008). A chemical method for fast and sensitive detection of DNA synthesis in vivo. Proc Natl Acad Sci U S A *105*, 2415-2420.

Schedl, A., Ross, A., Lee, M., Engelkamp, D., Rashbass, P., van Heyningen, V., and Hastie, N. D. (1996). Influence of PAX6 gene dosage on development: overexpression causes severe eye abnormalities. Cell *86*, 71-82.

Schermer, A., Galvin, S., and Sun, T. T. (1986). Differentiation-related expression of a major 64K corneal keratin in vivo and in culture suggests limbal location of corneal epithelial stem cells. J Cell Biol *103*, 49-62.

Schlotzer-Schrehardt, U., and Kruse, F. E. (2005). Identification and characterization of limbal stem cells. Exp Eye Res *81*, 247-264.

Schmidt, G. H., Wilkinson, M. M., and Ponder, B. A. (1986). Non-random spatial arrangement of clone sizes in chimaeric retinal pigment epithelium. J Embryol Exp Morphol *91*, 197-208.

Schwarze, S. R., Ho, A., Vocero-Akbani, A., and Dowdy, S. F. (1999). In vivo protein transduction: delivery of a biologically active protein into the mouse. Science *285*, 1569-1572.

Sevel, D., and Isaacs, R. (1988). A re-evaluation of corneal development. Trans Am Ophthalmol Soc *86*, 178-207.

Shen, Q., Goderie, S. K., Jin, L., Karanth, N., Sun, Y., Abramova, N., Vincent, P., Pumiglia, K., and Temple, S. (2004). Endothelial cells stimulate self-renewal and expand neurogenesis of neural stem cells. Science *304*, 1338-1340.

Shi, S., and Gronthos, S. (2003). Perivascular niche of postnatal mesenchymal stem

cells in human bone marrow and dental pulp. J Bone Miner Res *18*, 696-704.

Silvestri, F., Banavali, S., Baccarani, M., and Preisler, H. D. (1992). The CD34 hemopoietic progenitor cell associated antigen: biology and clinical applications. Haematologica *77*, 265-273.

Simpson, T. I., and Price, D. J. (2002). Pax6; a pleiotropic player in development. Bioessays *24*, 1041-1051.

Smith, A. (2006). A glossary for stem-cell biology. Nature *441*, 1060.

Smith, R. S., Hawes, N. L., Kuhlmann, S. D., Heckenlively, J. R., Chang, B., Roderick, T. H., and Sundberg, J. P. (1996). Corn1: a mouse model for corneal surface disease and neovascularization. Invest Ophthalmol Vis Sci *37*, 397-404.

Soriano, P. (1999). Generalized lacZ expression with the ROSA26 Cre reporter strain. Nat Genet *21*, 70-71.

Srinivas, S., Watanabe, T., Lin, C. S., William, C. M., Tanabe, Y., Jessell, T. M., and Costantini, F. (2001). Cre reporter strains produced by targeted insertion of EYFP and ECFP into the ROSA26 locus. BMC Dev Biol *1*, 4.

Staszkiewicz, J., Gimble, J., Cain, C., Dietrich, M., Burk, D., Kirk-Ballard, H., and Gawronska-Kozak, B. (2009). Flow cytometric and immunohistochemical detection of in vivo BrdU-labeled cells in mouse fat depots. Biochem Biophys Res Commun *378*, 539-544.

Sternberg, N., and Hamilton, D. (1981). Bacteriophage P1 site-specific recombination. I. Recombination between loxP sites. J Mol Biol *150*, 467-486.

Streilein, J. W., Bradley, D., Sano, Y., and Sonoda, Y. (1996). Immunosuppressive properties of tissues obtained from eyes with experimentally manipulated corneas. Invest Ophthalmol Vis Sci *37*, 413-424.

Sudo, K., Ema, H., Morita, Y., and Nakauchi, H. (2000). Age-associated characteristics of murine hematopoietic stem cells. J Exp Med *192*, 1273-1280.

Summer, R., Kotton, D. N., Sun, X., Ma, B., Fitzsimmons, K., and Fine, A. (2003). Side population cells and Bcrp1 expression in lung. Am J Physiol Lung Cell Mol Physiol *285*, L97-104.

Tam, P. P., and Tan, S. S. (1992). The somitogenetic potential of cells in the

primitive streak and the tail bud of the organogenesis-stage mouse embryo. Development *115*, 703-715.

Tan, S. S., Faulkner-Jones, B., Breen, S. J., Walsh, M., Bertram, J. F., and Reese, B. E. (1995). Cell dispersion patterns in different cortical regions studied with an X-inactivated transgenic marker. Development *121*, 1029-1039.

Tan, S. S., Williams, E. A., and Tam, P. P. (1993). X-chromosome inactivation occurs at different times in different tissues of the post-implantation mouse embryo. Nat Genet *3*, 170-174.

Thoft, R. A., and Friend, J. (1983). The X, Y, Z hypothesis of corneal epithelial maintenance. Invest Ophthalmol Vis Sci *24*, 1442-1443.

Ton, C. C., Hirvonen, H., Miwa, H., Weil, M. M., Monaghan, P., Jordan, T., van Heyningen, V., Hastie, N. D., Meijers-Heijboer, H., Drechsler, M., and et al. (1991). Positional cloning and characterization of a paired box- and homeobox-containing gene from the aniridia region. Cell *67*, 1059-1074.

Tseng, S. C. (1989). Concept and application of limbal stem cells. Eye (Lond) *3 (Pt 2)*, 141-157.

Tumbar, T., Guasch, G., Greco, V., Blanpain, C., Lowry, W. E., Rendl, M., and Fuchs, E. (2004). Defining the epithelial stem cell niche in skin. Science *303*, 359-363.

Turner, H. C., Budak, M. T., Akinci, M. A., and Wolosin, J. M. (2007). Comparative analysis of human conjunctival and corneal epithelial gene expression with oligonucleotide microarrays. Invest Ophthalmol Vis Sci *48*, 2050-2061.

van der Wath, R. C., Wilson, A., Laurenti, E., Trumpp, A., and Lio, P. (2009). Estimating dormant and active hematopoietic stem cell kinetics through extensive modeling of bromodeoxyuridine label-retaining cell dynamics. PLoS One *4*, e6972.

Walther, C., and Gruss, P. (1991). Pax-6, a murine paired box gene, is expressed in the developing CNS. Development *113*, 1435-1449.

Warren, N., and Price, D. J. (1997). Roles of Pax-6 in murine diencephalic development. Development *124*, 1573-1582.

Wei, Z. G., Cotsarelis, G., Sun, T. T., and Lavker, R. M. (1995). Label-retaining cells are preferentially located in fornical epithelium: implications on conjunctival

epithelial homeostasis. Invest Ophthalmol Vis Sci *36*, 236-246.

Weissman, I. L. (2000). Translating stem and progenitor cell biology to the clinic: barriers and opportunities. Science *287*, 1442-1446.

West, J. D. (1976). Clonal development of the retinal epithelium in mouse chimaeras and X-inactivation mosaics. J Embryol Exp Morphol *35*, 445-461.

West, J. D., Hodson, B. A., and Keighren, M. A. (1997). Quantitative and spatial information on the composition of chimaeric fetal mouse eyes from single histological sections. Dev Growth Differ *39*, 305-317.

Whikehart, D. R., Parikh, C. H., Vaughn, A. V., Mishler, K., and Edelhauser, H. F. (2005). Evidence suggesting the existence of stem cells for the human corneal endothelium. Mol Vis *11*, 816-824.

Wilkie, A. L., Jordan, S. A., and Jackson, I. J. (2002). Neural crest progenitors of the melanocyte lineage: coat colour patterns revisited. Development *129*, 3349-3357.

Yang, A., Schweitzer, R., Sun, D., Kaghad, M., Walker, N., Bronson, R. T., Tabin, C., Sharpe, A., Caput, D., Crum, C., and McKeon, F. (1999). p63 is essential for regenerative proliferation in limb, craniofacial and epithelial development. Nature *398*, 714-718.

Yao, T. P., Forman, B. M., Jiang, Z., Cherbas, L., Chen, J. D., McKeown, M., Cherbas, P., and Evans, R. M. (1993). Functional ecdysone receptor is the product of EcR and Ultraspiracle genes. Nature *366*, 476-479.

Yoshida, S., Shimmura, S., Kawakita, T., Miyashita, H., Den, S., Shimazaki, J., and Tsubota, K. (2006). Cytokeratin 15 can be used to identify the limbal phenotype in normal and diseased ocular surfaces. Invest Ophthalmol Vis Sci *47*, 4780-4786.

Zhang, W., Zhao, J., Chen, L., Urbanowicz, M. M., and Nagasaki, T. (2008). Abnormal epithelial homeostasis in the cornea of mice with a destrin deletion. Mol Vis *14*, 1929-1939.

Zhao, B., Allinson, S. L., Ma, A., Bentley, A. J., Martin, F. L., and Fullwood, N. J. (2008). Targeted cornea limbal stem/progenitor cell transfection in an organ culture model. Invest Ophthalmol Vis Sci *49*, 3395-3401.

Zhao, J., Mo, V., and Nagasaki, T. (2009). Distribution of label-retaining cells in the limbal epithelium of a mouse eye. J Histochem Cytochem *57*, 177-185.

Zhou, S., Schuetz, J. D., Bunting, K. D., Colapietro, A. M., Sampath, J., Morris, J. J., Lagutina, I., Grosveld, G. C., Osawa, M., Nakauchi, H., and Sorrentino, B. P. (2001). The ABC transporter Bcrp1/ABCG2 is expressed in a wide variety of stem cells and is a molecular determinant of the side-population phenotype. Nat Med *7*, 1028-1034.

Zhu, Z., Zheng, T., Lee, C. G., Homer, R. J., and Elias, J. A. (2002). Tetracycline-controlled transcriptional regulation systems: advances and application in transgenic animal modeling. Semin Cell Dev Biol *13*, 121-128.